THE PHOTOGENERATION OF CHARGED INTERMEDIATES IN ORGANIC PHOTOCHEMISTRY: The Effect of an Internal Cyclic Array of p-Orbitals.

By

Erik Krogh
B.Sc., University of Toronto, 1986

ACCEPTED
FACULTY OF GRADUATE STUDIES

DEAN

DATE 1991-01-21

A Dissertation Submitted In Partial Fulfilment of the Requirements for the Degree of

DOCTOR OF PHILOSOPHY

in the Department of Chemistry

We accept this dissertation as conforming to the required standard

Dr. P. Wan, Supervisor (Department of Chemistry)

Dr. A.D. Kirk, Department Member (Department of Chemistry)

Dr. T. Dinale, Department Member (Department of Chemistry)

Dr. A. Fischer, Department Member (Department of Chemistry)

Dr. P. Romaniuk, Outside Member (Department of Biochemistry and Microbiology)

Dr. K. Yates, External Examiner (University of Toronto)

University of Victoria

Supervisor: Dr. P. Wan

Abstract

A series of structurally related compounds has been prepared to investigate how the number of cyclically conjugated π electrons affect photochemical reaction rates. To this end, photosolvolysis and photodecarboxylation reactions have been extended to a series of bridged diaryl methanol and diaryl acetic acid derivatives. Product studies have been carried out in a number of solvent systems and demonstrate that charged intermediates are involved in these reactions. Mechanistic probes, such as solvent, pH and substituent effects, support a mechanism involving heterolytic bond cleavage of the S_1 state as the primary photochemical event. The bridging unit in the series of structurally related compounds has been varied to affect the number of π electrons in the internal cyclic array (ICA) of these photogenerated intermediates. Product quantum yields and fluorescence lifetimes were measured for all members of the series. The combined data were used to establish the rates of the excited state bond cleavage. The most photosolvolytically reactive system, 9-fluorenol, involves a *4n* π electron *carbocation* intermediate, the 9-fluorenylium ion. The rate constant for excited state bond cleavage has been calculated to be $k_s \approx 5 \times 10^9\ s^{-1}$, which was at least 500 times greater than that of 5-suberenol, which involves a *4n+2* π electron intermediate. The most reactive system towards photodecarboxylation was 5-suberenecarboxylic acid, ($k_{dc} \approx 6 \times 10^9\ s^{-1}$), which involves a *4n* π electron *carbanion* intermediate, the 5-suberenyl anion. Here again, the rate constant for

fluorenecarboxylic acid, a *4n+2* π electron precursor. Thus, the charged intermediates most favoured in these photochemical reactions, (i.e. *4n* systems), are those that are the most elusive in the ground state because of their formally antiaromatic character. The present study clearly shows a reversal of the ground state reactivity trends for both solvolysis and decarboxylation reactions upon photoactivation. Rate constants for all members of the series will be presented and the origin of the special structure-reactivity effects will be discussed.

Examiners:

Dr. P. Wan, Supervisor (Department of Chemistry)

Dr. A.D. Kirk, Department Member (Department of Chemistry)

Dr. T. Dingle, Department Member (Department of Chemistry)

Dr. A. Fischer, Department Member (Department of Chemistry)

Dr. P. Romaniuk, Outside Member (Department of Biochemistry and Microbiology)

Dr. K. Yates, External Examiner (University of Toronto)

Table of Contents

PRELIMINARY PAGES

CHAPTER ONE - INTRODUCTION

CHAPTER TWO - RESULTS PHOTODEHYDROXYLATION

List of Tables

List of Figures

List of Abbreviations

ACN - acetonitrile
aq - aqueous
BDE - bond dissociation energy
CB - cyclobutadiene
CH - cycloheptatrienyl
CI - chemical ionization
CP - cyclopentadienyl
d - doublet
DBCH - dibenzocycloheptatrienyl
DBCP - dibenzocyclopentadienyl
E_T - triplet state energy
EI - electron impact
ET - electron transfer
GC - gas chromatography
HFIP - hexafloroisopropyl alcohol
HHPW - half height pulse width
HOMO - highest occupied molecular orbital
IC - internal conversion
ICA - internal cyclic array
IR - infrared
IRF - instrument response function
ISC - intersystem crossing
LUMO lowest unoccupied molecular orbital
m - multiplet
MCA - multichannel analyzer
MS - mass spectrometry
NMR - nuclear magnetic resonance
PMT - photomultiplier tube
s - singlet
S_0 - singlet ground state
S_1 - first excited singlet state
SCF - self consistent field
SPC - single photon counter
t - triplet
T_1 - first excited triplet state
TAC - time-to-amplitude converter
TLC - thin layer chromatography

Acknowledgements

I must first extend my gratitude and thanks to my supervisor Dr. Peter Wan. He deserves much credit for his early contribution to this project. His enthusiasm and generosity are gratefully acknowledged. I would also like to thank the group of individuals that I truly have had the pleasure of working with: Murali, Mike, Iain, Barb, Deepak, Dave, Huang, Xigen, Marion and Pin. They have made my stay here thoughtful, educational and enjoyable. A word of appreciation to my teachers, Dr. T. Fyles, Dr. A. Kirk, and Dr. P. West. The kind assistance of Dr. D. Holden and Dr. S. Atherton who are responsible for guiding my early forays into single photon counting is also gratefully acknowledged.

Finally it remains for me to thank my wife, Jane Armstrong, for her unique qualities and guidance as an editor/typist/lover, although not necessarily in that order.

Dedication

To Jeremy's Grandparents:

My father, who taught me how to ask the right questions, and my mother, who taught me the right questions to ask. I'm still asking.

CHAPTER ONE

INTRODUCTION

1.1 General

The absorption of light by an organic molecule occurs with the promotion of an electron to a higher energy level, thus producing an electronically excited state. By definition, excited states have excess energy which may in principle be dissipated via a number of processes and reaction pathways. Because excited states are inherently short lived, unimolecular processes, such as bond fragmentation, are common. Since this report deals extensively with excited state bond cleavage, a description of the possible mechanisms involved is appropriate.

In general, there are only a limited number of ways in which excited state bond cleavage can occur. Three of these are relevant to the current discussion and may be classified as follows: homolysis, where the bonding electron pair is equally apportioned between the departing fragments; heterolysis, where the bonding electron pair remains with one fragment, thus forming an ion pair; and mesolytic cleavage,* which involves the fragmentation of radical ions, generated as the result of electron transfer or charge transfer. The particular pathway followed by a given molecule is governed by a number of factors, but can be strongly influenced by the reaction medium in which it is carried out.

---

* This term has been introduced to describe the cleavage of radical ions which may be viewed as homolytic or heterolytic depending on the electron apportionment in the fragments.[1]

Much of the early work in organic photochemistry was restricted to poorly solvating media, reflecting the fact that it evolved from the subdisciplines of gas phase photochemistry and classical organic solution chemistry. As a result, the majority of the mechanisms reported in the literature involved homolytic bond fragmentation and radical intermediates.[2,3,4] Until relatively recently, the suggestion of heterolytic bond cleavages and ion pair intermediates had been met with a certain degree of skepticism. Interestingly, quite the reverse situation appears to be true in the field of co-ordination metal photochemistry, where aqueous solvent systems and charged reaction intermediates are ubiquitous.[5]

That heterolysis had not, in general, been observed in organic photochemistry is not surprising; especially given that normal photochemical activation involves an energy expenditure of 50-100 kcal mol^{-1}. It has been estimated[6] that, in the absence of stabilizing solvation effects, heterolysis of a carbon chlorine bond requires ≈ 170 kcal mol^{-1}, whereas the analogous homolytic bond dissociation energy is about 80 kcal mol^{-1}. The situation, however, changes dramatically if solvation effects are taken into account. In strongly solvating media ion pairs are highly stabilized, so that heterolytic fragmentation may become the more energetically favourable process. Since many organic compounds can be studied in polar, and even aqueous solution, the investigation of their attendant photochemistry has opened up a new domain in organic photochemistry.

1.2 Photosolvolysis

One of the earliest examples of heterolytic bond cleavage in organic photochemistry was reported in 1919.[7] Irradiation of the triarylmethyl leuco dye (I) resulted in the efficient loss of cyanide ion and the formation of the extremely stable triarylmethyl cation (II) (eq 1.1). These reactions were initially carried out in ethanol and the triarylmethyl ethyl ether was shown to be one of the final products. Thus, this reaction constituted photosolvolysis. The photoheterolysis process was later shown to be very solvent dependent, requiring polar solvents to promote production of the cation.[8]

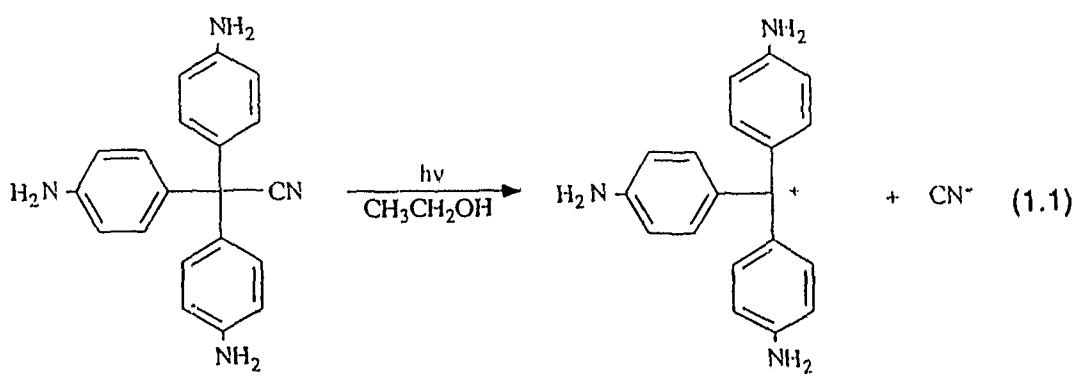

I II (1.1)

Although the early work on the photoproduction of the triarylmethyl cation II generated considerable interest, it was not until many years later that photosolvolysis reactions, *per se*, were extended to other systems and studied in more detail. Over the past three decades, a great deal of work has been published in this area.[9] In general, photosolvolysis refers to any reaction in which

the net process involves the photoactivated displacement of a leaving group (or nucleofuge) by a solvent molecule. Thus photosolvolysis has come to encompass a wide range of reactions, which operate through a variety of mechanisms.[9] Those substrates which have been investigated include: benzyl derivatives, substituted phenoxy esters and ethers, β-arylethyl derivatives, allylic halides with proximal aromatic rings, some substituted carbonyl compounds, and certain alkyl halides. The list of leaving groups has been extended from cyanide to include: halides, acetates, alkoxides, phenoxides, trialkylammonium salts, dialkylsulfonium salts and even hydroxide.[9] The majority of these studies have concentrated on substituent, solvent and leaving group effects. In addition, many investigators have focused on the mechanism of photosolvolysis; particularly as it pertains to the multiplicity, that is the electron spin state, of the excited state and the details of the bond cleavage step. Within the context of the following discussion, an examination of a few of these contributions is worthwhile.

In 1973 Kropp reported that, in polar solvents, the photolysis of certain alkyl iodides and bromides resulted in products which were derived from carbocation intermediates.[10] These results were intriguing because all of the preceding studies of alkyl halides had indicated that photolysis resulted in homolytic cleavage and radical intermediates. When 1-iodonorborane (**III**) was irradiated in methanol, both the methyl ether (**IV**) and the photoreduced product norbornane (**V**) were produced (eq 1.2). Photolysis of **III** in aqueous solution led to the formation of 1-norbornol. In general, products derived from both homolysis and heterolysis were

obtained. In subsequent papers, considerable evidence for the intermediacy of carbocations was presented, including trapping by a variety of nucleophilic solvents, and isolation of products arising from carbocation rearrangements. Noting that excitation of the C-X chromophore (n-σ^*) leads to a polarization opposite to that required for heterolytic cleavage, the authors proposed a mechanism involving initial bond homolysis followed by electron transfer (ET) to yield the carbocation (eq 1.3).[11]

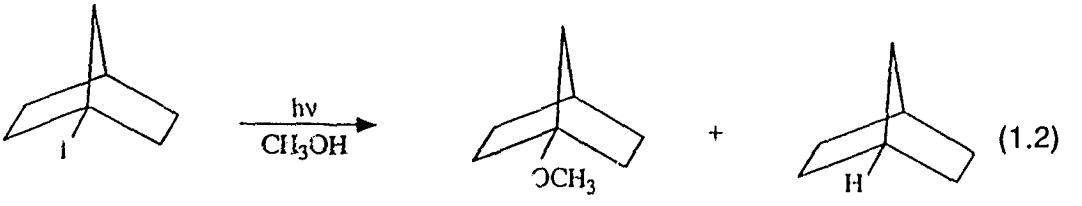

III IV V (1.2)

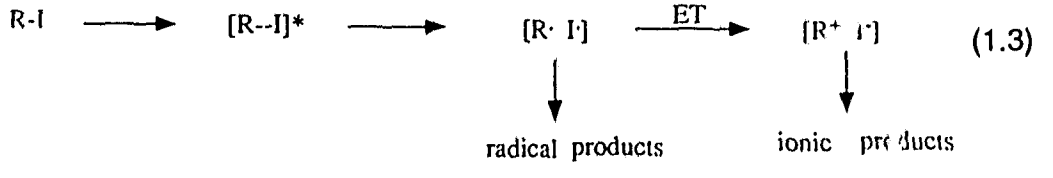

(1.3)

Another intriguing photosolvolysis reaction, first reported by Jaeger[12], involves β-arylethyl derivatives. When the homobenzylic system 2-(3',5'-dimethoxyphenyl)ethyl methanesulfonate (**VI**) was photolyzed in 50% aqueous methanol, the corresponding alcohol, **VII**, and methyl ether, **VIII**, were obtained in

good yields (eq 1.4). The photoreduced product 3,5-dimethoxyphenyl ethane was also obtained in small amounts. The results of a deuterium scrambling experiment provided convincing evidence that the bridged phenonium ion intermediate, **IX**, was a precursor to the solvolyzed products. It was reasoned that the aromatic ring is the chromophore and that the excited state must be somehow activating the methanesulfonate group.[12]

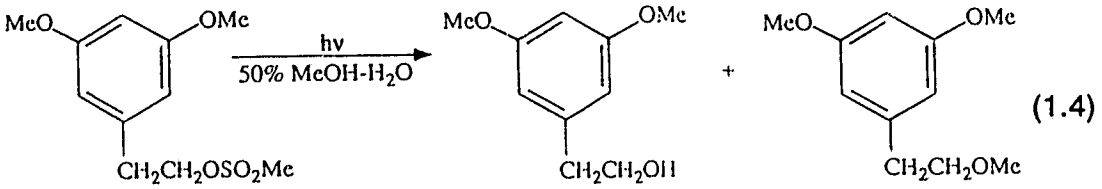

VI VII VIII (1.4)

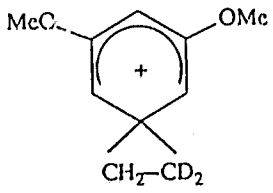

IX

A considerable amount of research by the Cristol[13] and Morrison[14] groups has involved elucidating the mechanism of this intramolecular excitation transfer process. Much of the work has concentrated on a systematic investigation of benzo and dibenzo bicyclic systems, such as **X** and **XI**. In addition to solvolysis products, Wagner-Meerwein rearrangement products have been observed,

providing further support for carbocation intermediates.[13]

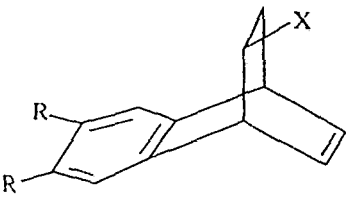

X

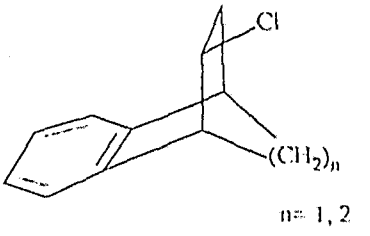

XI

As a result of a great deal of work directed towards understanding the stereochemical requirements of both nucleofugal and migrating groups, Cristol[13] has proposed a mechanism (eq 1.5) that involves initial electron transfer from the aromatic ring to the remote leaving group, which yields a zwitterionic biradical species. Loss of the nucleofuge then leads to a biradical cation, which may then decay to the bridged phenonium ion or undergo rearrangement. A similar type of mechanism may be operating in the photosolvolysis reactions of epoxides, reported by Sonawane and co-workers.[15] In fact, Chow and co-workers have recently reported evidence for an intermolecular electron transfer mechanism, leading to the photosolvolysis of cyclohexene and styrene oxides.[16]

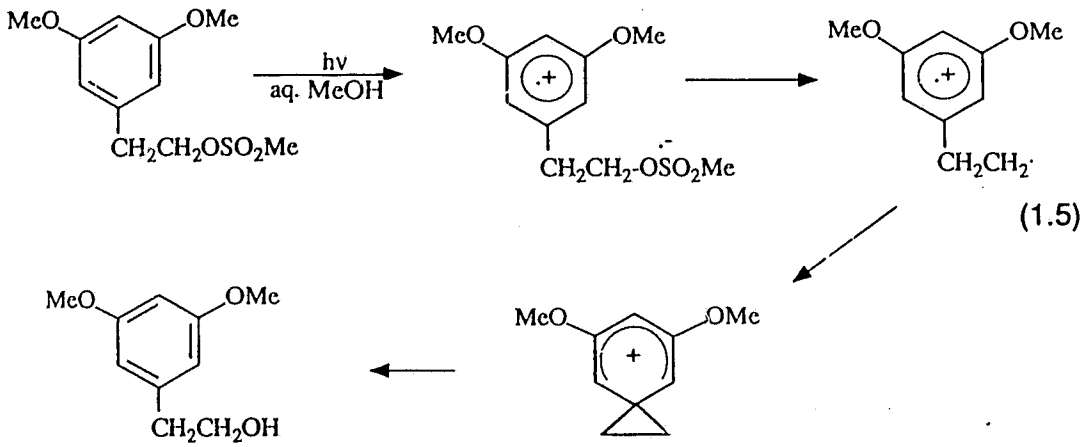

(1.5)

Photosolvolysis of benzyl derivatives is of particular interest because of their structural similarity to the compounds in the current investigation. To date, numerous studies have appeared in the literature that involve benzyl systems. This is undoubtedly due to the inherent simplicity of these systems and the significant contribution made by Zimmerman and co-workers in the early sixties.[17,18] These workers studied the photosolvolysis of methoxy-substituted benzyl acetates in an effort to elucidate the electronic nature of the excited states and to probe the structure-reactivity relationships of these states. In a landmark paper,[17] Zimmerman and Sandel correctly predicted the enhanced photoreactivity of meta-methoxybenzyl acetate (**XII**) (versus the para derivative) by calculating the electron density distributions for the first excited singlet state. The meta isomer, which is the most resistant to thermal solvolysis, has a quantum yield for photosolvolysis nearly ten times that of the para isomer, clearly indicating a reversal of the ground state reactivity. The authors explained this so-called "meta

electron transmission" with the aid of the non-Kekulé valence structure **XIII** (eq 1.6).

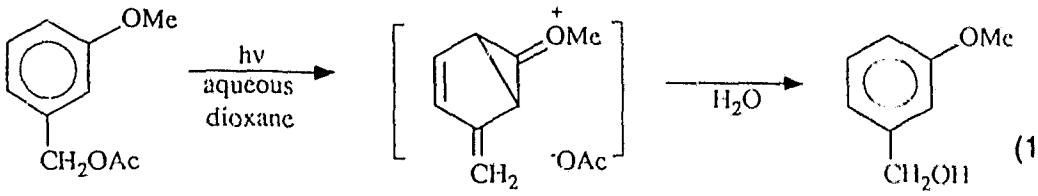

(1.6)

XII XIII

Radical derived products, generated from the homolysis of the benzylic C-OAc bond, were also noted in these photohydrolysis reactions. The authors further reported that meta-methoxybenzyl chloride (**XIV**) and meta-(N,N-dimethylamino)benzyl acetate (**XV**) also underwent photohydrolysis, whereas meta-methoxybenzyl methyl ether (**XVI**) and meta-methoxyphenylacetonitrile (**XVII**) did not, presumably due to their poorer leaving group abilities.

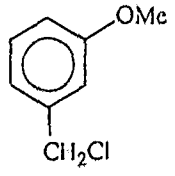

XIV

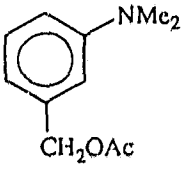

XV

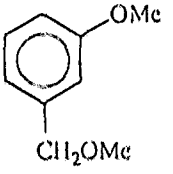

XVI

XVII

The involvement of carbocations in the photosolvolysis of a number benzyl compounds has been supported by several investigations and is now generally accepted. For instance, Cristol and co-workers[19] have reported on the formation of a rearranged product, produced in the photosolvolysis of the labelled

bromohomotriptycene **XVIII**. The formation of **XIX** is envisioned to arise from an aryl migration of the initially formed carbocation (a Wagner-Meerwein carbocation rearrangement) followed by solvolysis with water.

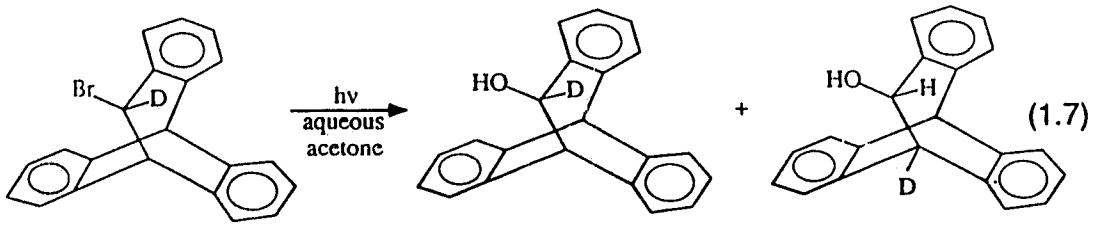

(1.7)

XVIII **XIX**

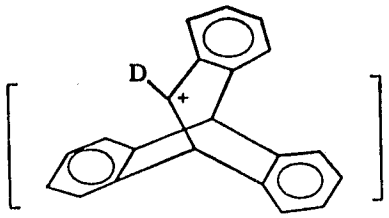

When optically active benzyl derivatives were irradiated, McKenna[20] and others[21] observed racemization in the photosolvolysis products. For instance, when (-)-(1-phenylethyl)trimethylammonium iodide (**XX**) was photolyzed in water, the solvolysis product, 1-phenylethanol, was largely racemized with some degree of inversion. Interestingly, the recovered starting material showed little loss of optical rotation, thus indicating that internal return, at least of a loose ion pair, was not significant. Similar results were obtained by Jaeger[21] on photolysis of (R)-(+)-1-(3',5'-dimethoxyphenyl)ethyl acetate (**XXI**) in 50% (v/v) methanol water. These results are consistent with benzyl cation intermediates.

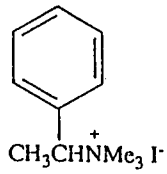

(-) XX

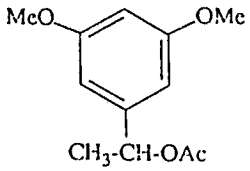

(+) XXI

Ivanov and co-workers[22] provided further evidence for the presence of carbocation intermediates in flash photolysis studies. The transients produced on photolysis of triarylmethyl acetates and triarylacetonitriles had absorption spectra matching those of the ground state cations. More recently, McClelland and Steenken[23,24,25,26] have employed laser flash photolysis techniques to generate a large number of di- and triarylmethyl cations from acetate, cyano, and 4-cyanophenyl ether precursors. The transient cations have been observed by absorption spectroscopy and their decay in nucleophilic solvents monitored by time resolved absorption and conductivity techniques. The photosolvolysis of a number of other benzyl derivatives has been carried out in a variety of solvent systems.[9] In general, products derived from both homolysis and heterolysis are isolated, with the latter being favoured in more polar solvents. Thus yields for solvolysis are typically higher in water or methanol, than in the less polar alcohols. Furthermore, in the flash photolysis work of Ivanov[22] and others,[23-25,27,28] it is generally noted that the yield of cationic intermediates is improved as the water content of solvent is increased.

The multiplicity and mechanistic details of the photosolvolysis of the benzyl

derivatives has not, in general, been observed to be consistent over the wide range of substrates and leaving groups studied. While the photosolvolysis of the benzyl ammonium salts appears to be an exclusively singlet state reaction,[9] reports of both singlet and triplet state reactions have appeared for the aryl acetates and benzyl halides.[9] In addition, no single mechanism appears to accommodate all of the available results. While some authors propose a mechanism involving initial cleavage to generate an ion pair,[17,21-29] others have suggested that the results are consistent with an equilibrating radical pair - ion pair intermediate,[9,20,30] similar, in some respects, to the mechanism proposed by Kropp[11] for norbornyl halides.

1.3 Photodehydroxylation

The first example of a photosolvolysis reaction involving a benzyl alcohol derivative (photodehydroxylation) was described by Ullman and co-workers[31] in 1976. They reported that irradiation of certain bichromophoric benzyl alcohols, **XXII**, resulted in heterolysis of the C-OH bond. The authors further demonstrated that the reaction proceeded only in the presence of good electron donors (not necessarily in the same molecule) and hence proposed a charge transfer mechanism, where hydroxide ion is lost from the radical anion of the benzyl alcohol moiety. Recently, Wan and co-workers[32,33,34,35,36] have shown that in benzyl alcohol derivatives, the hydroxide ion behaves as an exceptionally good leaving group, via an entirely different mechanism.

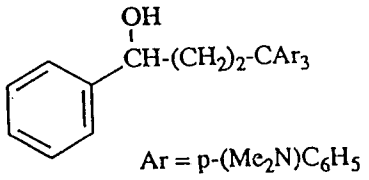

XXII

Several other studies involving photodehydroxylation of triarylmethane derivatives have also appeared. Amino substituted triarylmethanols[37] (leucohydroxides) have been photolyzed to generate the exceptionally stable dye cations, as discussed above, (eq 1.1). Peters and Manning[29] have investigated the dynamics of the photodissociation of various triarylmethanes using picosecond flash photolysis techniques. The results indicated that the first excited singlet state undergoes heterolytic cleavage to yield the ion pair in solution. The rates of the cleavage step were observed to be quite sensitive to the nature of both the solvent and the leaving group. In 1985 Wan and Turro[32] reported that, on excitation to the singlet state, ortho and meta-methoxybenzyl alcohols undergo proton-assisted loss of hydroxide ion to give the corresponding benzyl cations. Furthermore, it was noted that the fluorescence emission was quenched by protons in the same region that photochemical catalysis was observed. Subsequent work[34,36,38] corroborated these initial findings, and a mechanism involving initial C-OH heterolysis in the S_1 state has since been well established. The benzylic cation has been trapped by a variety of alcohol solvents, acetic acid and by added cyanide ion. A systematic investigation of excited state substituent effects, using methoxy, hydroxy, fluoro

and methyl substituted benzyl alcohols, has been carried out and the results corroborate the "meta electron transmission" effects outlined by Zimmerman.[17] Thus, the meta substituted benzyl alcohols were more reactive towards photosolvolysis than the para derivatives. The ortho derivatives were the most reactive of all, with quantum yields generally three times greater than those for the meta derivatives. Combining the fluorescence lifetime data with product quantum yields, Wan reported[36] several hydronium ion and water assisted rate constants for photodehydroxylation. The most reactive system, 2,6-dimethoxybenzyl alcohol (**XXIII**), had a product quantum yield for methyl ether formation of Φ_p = 0.31 in 50% (v/v) MeOH-H_2O.

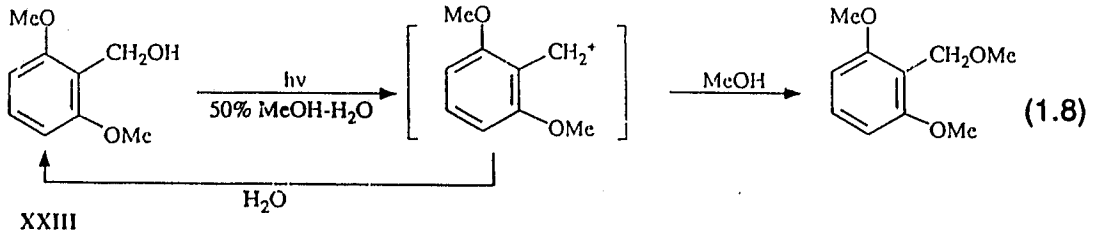

(1.8)

It should be noted that in the absence of the strongly electron donating hydroxy or methoxy substituents, the quantum yields were substantially lower, Φ_p < 0.02. In a study of the structurally rigid benzyl alcohol derivative 9-phenylxanthen-9-ol (**XXIV**), Wan and coworkers reported[33] a very interesting observation. Under steady state photosolvolysis conditions that lead to the formation of the corresponding methyl ether, **XXIV** dehydroxylated to yield the 9-

phenylxanthylium cation (**XXV**) adiabatically* (eq 1.9). That is, the photodehydroxylation step occurred on the excited state potential energy surface, initially producing the excited state carbocation. This was clearly demonstrated by steady state fluorescence studies, which detected fluorescence emission from the cation upon selective excitation of the parent alcohol. The adiabatic nature of photodehydroxylation is significant for a number of reasons. Firstly, adiabatic processes are rare, generally involving either structural isomerization or proton transfer to heteroatoms.[39] Secondly, adiabatic dehydroxylation lends further support to the one step heterolytic bond cleavage mechanism, since the involvement of more than one step would likely prohibit adiabaticity. Finally, it addressed, if not answered, a long standing question about the electronic nature of photogenerated carbocations. Although the appearance of adiabatic fluorescence emission from the cation does not imply that all of the photochemical reaction proceeds via this excited state intermediate, at least some portion of it does. Das[40] and McClelland,[25] in separate studies, have recently re-investigated this system and have suggested, based on the results of kinetic measurements obtained from laser flash photolysis experiments, that the adiabatic pathway contributes only a small percentage to the overall photosolvolysis product yield. This aside, the fact the cation can be produced in the excited state, clearly indicates that the carbocations, initially generated via photodehydroxylation, are not

*For a discussion of adiabaticity in organic photoreactions see ref. 2. For a review of adiabatic photoreactions see ref. 39

identical to the thermally equilibrated ground state cations.

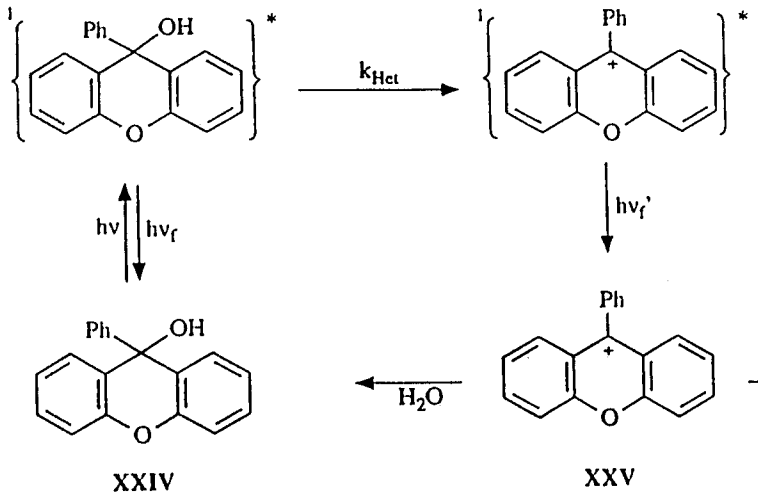

(1.9)

1.4 9-Fluorenol

With reference to Zimmerman's original paper[17], Wan and coworkers[33] discussed the excited state electron donating ability of the ortho oxygen in **XXIV**. They suggested that this effect might indeed be tested by investigating other rigid alcohols, such as the related system 9-phenylfluoren-9-ol (**XXVI**). Pursuing of this suggestion, it was unexpected that this compound efficiently photosolvolyzed.[41]

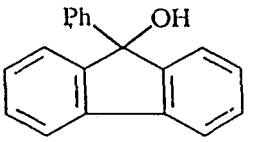

XXVI

It was further observed that the parent compound, 9-fluorenol, also underwent efficient photosolvolysis when irradiated in 50% MeOH-H_2O. This result was of considerable interest, in view of the fact that this benzyl alcohol derivative clearly lacked any of the obvious electron donating substituents that were previously shown to be necessary to promote photosolvolysis.[32-36] It was noted that the photoreactivity of 9-fluorenol is further contrasted to its marked stability towards thermal solvolysis. This thermal behaviour is well known[42] and has been associated with the formally antiaromatic character of cyclopentadienyl cation intermediates (*4n* π electrons). It was therefore postulated that the anomalous photodehydroxylation rates might be associated with the formation of a "stabilized" excited state *4n* π intermediate.[43]

1.5 Aromaticity and the Internal Cyclic Array

It has long been recognized that the extraordinary stability, or aromaticity, of benzene and related compounds is associated with a fully conjugated cyclic array of p-orbitals.[44,45] Although the etymology of the term "aromatic" indicates that these properties were originally associated with a certain fragrance, it is now associated with specific molecular criteria. For instance, Hückel has predicted that

for a planar cyclic array, only systems containing the number of electrons in the series *4n + 2*, where n is zero or a positive integer, will be particularly stable.[46] The experimental criteria for identifying aromaticity are: the presence of a diamagnetic ring current, bond equalization, planarity, chemical stability, and the ability to undergo aromatic electrophilic substitution. Hückel's prediction, which is based on the occupancy of the calculated molecular orbitals, is actually a consequence of Hund's rule and the associated stability of filled molecular orbitals. The molecular orbital energy level diagrams for several carbocyclic systems are shown in Figure 1.1.[46] The first pair of electrons occupy the lowest energy orbital. The next two molecular orbitals constitute a degenerate set and are filled alternately, in accord with Hund's rule. Thus a system containing two or six π electrons will contain a closed shell, whereas a system containing four π electrons will have two unpaired electrons and exist as a diradical. Although remarkably simplified in its approach, the Hückel *4n + 2* aromaticity rule has been experimentally verified for a large number of neutral and charged cyclic systems. Molecules containing benzenoid (6π electrons) moieties are particularly stable and ubiquitous in organic chemistry. On the other hand, experimental attempts to isolate cyclobutadiene (4π electrons) have succeeded only under controlled conditions at very low temperatures due to its extremely unstable nature.[47] Interestingly, many of the synthetic techniques used to generate cyclobutadiene (CB) involve the use of photochemical methods.[47]

The extra delocalization energy associated with a cyclically constructed

polyene, compared to an analogous acyclic polyene, has been taken as a measure of a system's aromatic character.[48] In order to distinguish this behaviour from those polyenes for which cyclic conjugation actually reduces the delocalization energy, Breslow[49] has introduced the term "antiaromatic".

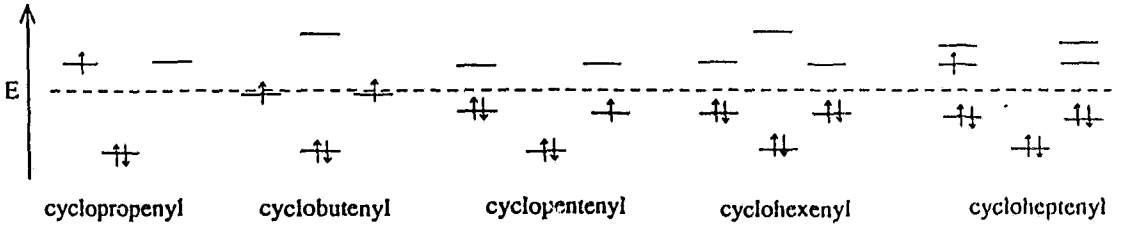

Figure 1.1: Energy Level Diagram for Simple Conjugated Carbocyclic Systems.

Examination of the energy level diagram above, indicates that the removal of one electron from the cyclopropenyl system or from the cycloheptatrienyl system would result in a closed shell (*4n + 2*) cationic species. Similarly, addition of an electron to the cyclopentadienyl system results in a *4n + 2* anionic species. All of these closed shell ions have been prepared and studied in some detail. Each has been shown to have aromatic character.[50,51] Similar results have been obtained for the benzo and dibenzo derivatives, although annelation diminishes these properties to some extent.[51,52] The charged intermediates containing *4n* π electrons, for instance the cyclopropenyl and cycloheptatrienyl anion and the cyclopentadienyl cation, have been the focus of many years of research. Derivatives of some of these ionic species have been observed in controlled

environments as fleeting intermediates,[53] but none of the parent systems have been isolated at ambient conditions, owing to their inherent instability. That these systems are actually antiaromatic has been experimentally borne out.[51] For instance Breslow[54] has studied the thermal solvolysis reaction of both iodocyclopentane (**XXVII**) and iodocyclopentadiene (**XXVIII**) in propionic acid and in the presence of silver perchlorate. Under these conditions **XXVII** readily solvolyzed via the intermediate carbocation, whereas no solvolysis was observed for **XXVIII**. If $C_5H_5^+$ were merely non-aromatic, then the two iodides should solvolyze with similar rates, since $C_5H_9^+$ has *no* resonance stabilization.

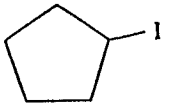

XXVII

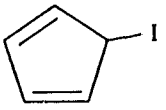

XXVIII

Although Woodward and Hoffman,[55] Zimmerman[56] and Dewar[57] have each developed theoretical treatments for predicting the outcome of ground and excited state pericyclic reactions, these approaches do not deal explicitly with photochemical reactions that generate cyclically conjugated charged intermediates. However, several recent accounts[58,59,60,61,62] have been specifically aimed at investigating S_1 and T_1 states of *4n* and *4n+2* π electron systems.

For instance, Janoschek and co-workers[58] have carried out *ab initio* SCF calculations on the ground and excited states of cyclobutadiene (CB). The strong

alternations in the bond length of CB (weak electron delocalization) and its extremely reactive nature have been taken as indicative of marked antiaromatic character. However, the calculations indicate that on excitation to the S_1 state, these bond length alternations disappear and the π-electrons are evenly delocalized on the four membered ring.[58] The authors further conclude that upon electronic excitation, the aromaticity of benzene decreases whereas that of CB increases. Experimental support for this notion of a reversal of roles in the excited state is suggested by several photochemical observations. CB appears to be relatively photochemically stable, decomposing to acetylene on extended irradiation.[47] On the other hand, the photochemistry of benzene is notably multifarious in contrast to its remarkable thermal stability. Jug and co-workers have preformed extensive calculations on a number of Hückel aromatic and antiaromatic systems at the SINDO1 level,[59] and have examined the aromatic character in the excited states using a bond order approach.[63] They note a marked decrease in the aromatic character of 6 π electron ring systems in the excited S_1 and T_1 states, as indicated by the general elongation of the ring bonds and increased bond alternations.[60] In contrast to these findings, the optimized geometries of the excited states of some *4n* π electron species strongly suggest an increase in aromatic character as indicated by bond equalization. In this work Jug has examined the cyclopentadienyl (CP) cation (particularly relevant to our present investigation), and concludes that it too displays a considerable increase in its aromatic character upon suitable excitation.[61] Jug has explained the reversal

of ground and excited state roles as follows, "the change in the degree of aromatic character accompanying electronic excitation can easily be interpreted by the nodal behaviour of the 'essential orbitals' (i.e., those involved in the electronic transition)". For *4n* π systems, the nodal planes of these "essential orbitals" are such that the regions that are antibonding or nonbonding in the HOMO are bonding in the LUMO and vice versa. (The same cannot be said for the essential orbitals of *4n+2* π systems). Thus, π-π^* excitation will reduce the bond alternations caused by the HOMO in the ground state.[61] Recently, Chak and Dingle[62] have performed PPP π-SCF calculations on the cyclopentadienyl (CP) and cycloheptatrienyl (CH) systems as well as their dibenzo derivatives, DBCP and DBCH respectively. The calculations on the DBCP and DBCH *4n* π systems indicate that the strong alternation in bond length and charge distribution in S_o becomes weaker in S_1. Calculations on the same systems with aromatic electron counts (*4n+2*), showed that they experience extensive electron redistribution in the S_1 state. Whereas the ground state species tended to maximize the CP anion or the CH cation character of the central ring, the S_1 states tended to shift the negative or positive charge to the benzene rings, leaving the CP and CH centres essentially neutral.

The unusually efficient photosolvolysis of 9-fluorenol (**1**) has precipitated the present study, in which we have undertaken to probe the driving force of this reaction and elucidate the necessary structural and/or electronic requirements. The

following diaryl methanol derivatives have formed the basis of this study.

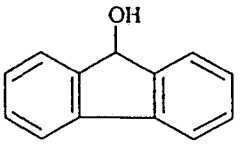

1

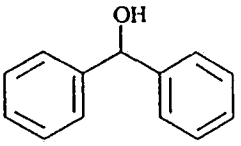

2

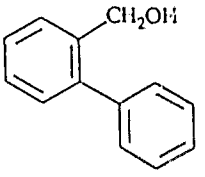

3

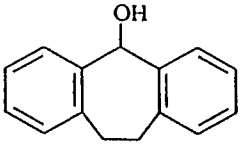

4

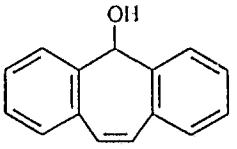

5

Diphenylmethanol (**2**) and 2-phenylbenzyl alcohol (**3**) are closely related to 9-fluorenol, but are without the added structural rigidity and the internal cyclic array (ICA) of π-atoms upon dehydroxylation. Compounds **2** and **3** probe the effect of α-phenyl and ortho-phenyl substitution, respectively, on benzyl alcohol. 5-Suberol (**4**) (5*H*-dibenzo[a,d]cycloheptan-5-ol) regains some of the structural rigidity present in **1**, but is electronically similar to diphenylmethanol because of the insulating effect of the saturated bridging unit (-CH_2-CH_2-). 5-Suberenol (**5**) (5*H*-dibenzo[a,d]cyclohepten-5-ol) contains a conjugating bridging unit, (-CH=CH-), which necessarily adds two π-electrons to the cyclic system. Dehydroxylation of 5-suberenol (**5**) leads to the dibenzotropylium ion, which can be readily generated thermally due to its aromatic character (*4n + 2*) in the ground state. Thus, if the stability of the photogenerated cations has any of the numerical requirements that

have been demonstrated for the ground state species (i.e., *4n + 2*) it should clearly manifest in a difference in the photoreactivity of **1** and **5**. If, on the other hand, the unusual reactivity of **1** is due to the α-phenyl substitution and/or structural rigidity (i.e., a lifetime effect), then **1**, **4** and **5** should display similarly high photosolvolysis efficiencies.

In our efforts to understand the structural and electronic effects that give rise to the remarkable photoreactivity of 9-fluorenol (**1**), we have focused our attention on the effect of the internal cyclic array (ICA), which is generated upon photodehydroxylation (Figure 1.2). Furthermore, we would like to explore the possibility of "excited state aromatic character"[•] for systems which are formally antiaromatic in the ground state.

[•] The term "excited state aromaticity" is employed to imply certain features of the electronic distribution and a relative stability on the excited state potential energy surface. The unusual chemical stability associated with ground state aromatic molecules does not apply to excited states which are necessarily unstable with respect to the ground state. The aromatic character of electronically excited states has been discussed previously in several theoretical treatments.[58,61]

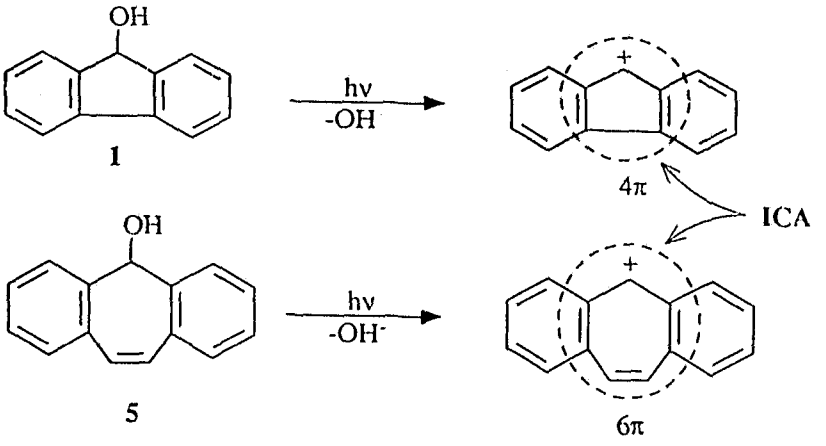

*Figure 1.2: The Internal Cyclic Array Generated for **1** and **5**.*

1.6 Photodecarboxylation.

The bridged diaryl alcohols **1** - **5** provide a means of generating the corresponding carbocations by way of photodehydroxylation. 9-Fluorenol (**1**) and 5-suberenol (**5**) are the progenitors of *4n* and *4n + 2* π electron ICA intermediates, respectively. In this work we have found that the *4n* carbocations derived from **1** were much more efficiently photogenerated than the corresponding *4n + 2* systems, derived from **5**. These results prompted a similar investigation of the photogenerated carbanions. Indeed, it would be desirable to find precursors analogous to **1** - **5** that would provide carbanions rather than carbocations. In this case, the 9-fluorenyl anion (6π) and the 5-suberenyl anion (8π) would be photochemically generated. Of the available methods known to photogenerate carbanions,[64,65,66] photodecarboxylation has proved to be the most attractive for a number of reasons. Compounds **6** - **9** could be readily prepared and preliminary investigations showed that the photodecarboxylations occurred cleanly

and efficiently. Furthermore, all of compounds **6 - 9** show some photoreactivity, so that the rate constants for all members of the series can be directly compared.

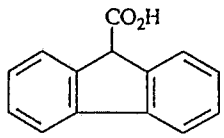

6

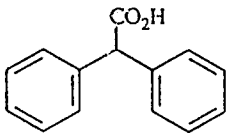

7

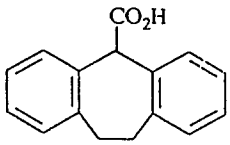

8

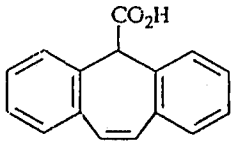

9

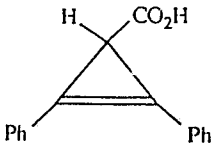

10

Decarboxylation reactions are relatively common in organic chemistry and used frequently in organic synthesis, particularly with malonic acid derivatives.[67] Thermal decarboxylations commonly occur from the carboxylate ion and are accelerated by the presence of electron withdrawing groups, which can stabilize the incipient carbanion.[68,69,70] Mechanistically, decarboxylations can be viewed as the reverse of the addition of carbanions to carbon dioxide. Photodecarboxylations have become widely studied over the past two decades.[71-84] Photodecarboxylation reactions have been observed for a wide variety of substrates, including both alkyl and phenylglyoxylic acids[71,72,73,74] N-acyloxyphthalimides,[75] alkyl acetic acid derivatives,[76] aryl acetic acid derivatives,[77,78,79,80,81,82,83] as well as a number of biologically active carboxylic acids and derivatives.[84] Not surprisingly for such a diverse list of

substrates, a variety of mechanisms have been shown to operate. These mechanisms may be broadly classified as : a) electron transfer induced b) homolytic (proceeding through radicals) or c) heterolytic (giving rise to charged intermediates). While a full discussion of these mechanisisms is clearly beyond the scope of this discussion, it will be useful to briefly examine a few of the closely related systems. Since the carboxylic acids in the present study are all diaryl acetic acid derivatives, only the work on the closely related arylacetic acids will be reviewed here.

The photodecarboxylation of meta and para-nitrophenyl acetates was first reported by Margerum and co-workers[77] in 1969. Since this report a number of studies have been carried out concerning the mechanism, particularly as it pertains to the presence of carbanion intermediates.[64,80] Both isomers undergo efficient photodecarboxylation in aqueous solution (pH > pK_a), yielding the corresponding nitrotoluene and dinitrobibenzyl products, ($\Phi_p \approx 0.6$). In the case of m-nitrophenyl acetate (**XXIX**), the major product was m-nitrotoluene. Steady-state studies[64] and time resolved investigations[80] have provided firm support for a mechanism involving C-C bond heterolysis as the primary photochemical event.

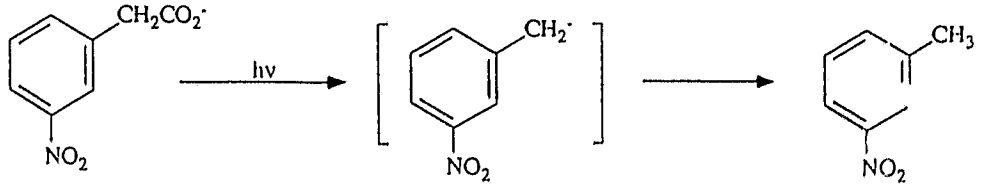

XXIX (1.10)

Efficient photodecarboxylations have also been observed to occur for ortho, meta and para-pyridylacetate ions in aqueous solution ($\Phi_p \approx 0.2$ - 0.5). The authors[78] have suggested carbanion intermediates and a mechanism similar to Margerum,[77] at least for the ortho and meta isomers.

The photochemical decarboxylation of the parent system, phenylacetate, has been investigated by a number of workers.[79,82] Although some doubt remains about the primary photochemical event, the incorporation of deuterium in the photoproduct when the acetate was irradiated in MeOD, implicates the benzyl anion as a reactive intermediate. It should be noted that the quantum yield for this reaction is quite low ($\Phi_p \approx 0.03$). In contrast to the earlier examples, the acid and esterified forms also decarboxylate in hydroxylic solvent with a similar photochemical yield but via a homolytic rather than heterolytic pathway.

1.7 Electronic Spectra and Excited States.

Electronic transitions occur when photons (electromagnetic radiation) of the appropriate energy are absorbed by a molecule. The lowest energy absorptions (longest wavelength) result from the promotion of an electron in the highest occupied molecular orbital, HOMO, to the lowest unoccupied molecular orbital, LUMO. Since most neutral organic molecules are spin paired, that is, they have closed shells of electrons, they exist in the so-called singlet ground state, S_0. The excited state initially produced by the absorption of a photon is generally in a spin

paired, or singlet state, denoted by S_n, where $n \geq 1$.[85] However, since the HOMO and LUMO are now only singly occupied the electrons can also exist with parallel spins. This electronic configuration is referred to as the triplet excited state, T_1. The energy of the absorbed light is governed by the energy difference between the S_1 and S_o states. The spectral distribution of the absorption curve is governed by various structural and environmental factors which influence such things as the shape of the potential energy surfaces, the spacing of vibrational and rotational energy sub-levels, and the Boltzmann distribution of molecules between these sub-levels.[86] The UV absorption spectra of organic molecules in solution phase are generally broad and featureless. This is due to the presence of an ensemble of closely spaced transitions arising from slightly different nuclear geometries which may correspond to the initial and final states.[86] In certain cases, a progression of narrower bands appear in absorption spectra. This vibrational fine structure is due to transitions to higher vibrational sub-levels of a given electronic excited state. It is the lowest energy transitions (S_1 - S_0) which are of primary interest in organic photochemistry, since the vast majority of photochemical reactions and other decay processes occur from S_1.

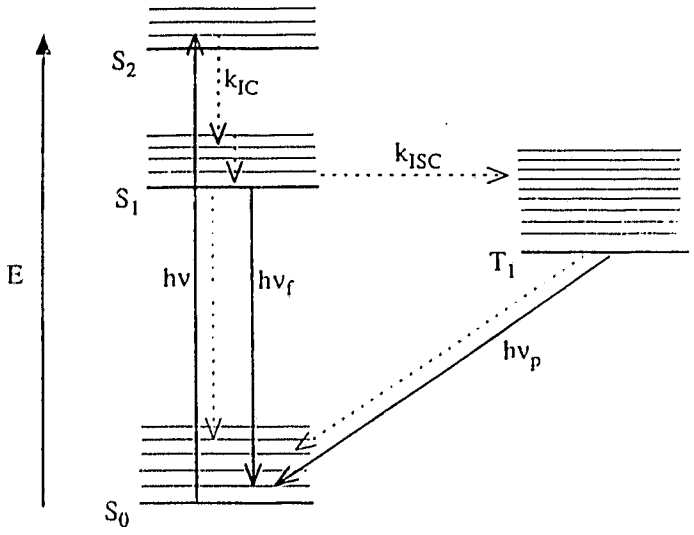

Figure 1.3: Modified Jablonski Diagram.

The first step in a photochemical process necessarily involves an electronic transition from the ground state, S_o, to an electronically excited state, S_n, where $n \geq 1$. Electronically excited states are highly unstable with respect to the ground state, and hence a variety of energy dissipating processes immediately begin to occur. These processes are depicted in Figure 1.3.[87] Molecules that initially find themselves in vibrationally excited ($v' > 0$) or higher excited (S_n; $n \geq 2$) states rapidly relax to the lowest vibrational level of the S_1 state, disposing their excess energy as heat to the surroundings. This process is known as internal conversion (IC), and usually occurs on the time scale of vibrations ($k_{IC} \approx 10^{11}$-10^{13} s^{-1}). Once vibrationally relaxed ($v' = 0$), molecules in S_1 may undergo internal conversion (leading directly to S_o) or intersystem crossing (ISC) to the triplet excited state, T_1.

Internal conversion from S_1 to S_0 is usually much slower than the same process involving higher excited states because of the much larger energy gap associated with the former process. Intersystem crossing to the triplet state is exergonic, but involves a spin change and is therefore formally forbidden by selection rules.[85] Photochemical reactions provide another escape route for the excited state species and may proceed either directly from the S_1 state or from the T_1 state. Finally, if the S_1 state is relatively long-lived, it may radiatively decay to the ground with the emission of a photon, known as fluorescence. Fluorescence emission involves a radiative transition that is allowed by selection rules, and therefore depopulate the excited singlet states of organic molecules on a time scale of 10^{-8}-10^{-9}s. A fluorescence *emission* spectrum is a plot of the emission intensity (I_f) as a function of wavelength (λ) of the emitted light (at fixed excitation wavelength). The key features of the fluorescence process are: a) the spectral shape and distribution, b) the quantum efficiency, Φ_f, and c) the lifetime, τ_f. A fluorescence *excitation* spectrum records the dependence of the emission intensity on the excitation wavelength. For weakly absorbing solutions, the emission intensity is proportional to the molar extinction coefficient, and therefore excitation spectra have the same spectral appearance as absorption spectra. Because emission occurs on a time scale that allows for solvent and conformational adjustments, the energy of emitted photons is often lower than that of the absorbed photons. This phenomenon is manifest in the red-shifting of the fluorescence emission spectra with respect to the absorption (or excitation)

spectra. The fine structure in emission spectra arise from transitions from the relaxed (S_1; v'=0) state to vibrationally excited levels of the ground state (v"≥0) (Figure 1.3). The Stokes loss[88] (or Stokes shift) is a measure of the energy difference in the 0,0 bands between the absorption and emission processes. Hence, the Stokes loss can be used as a measure of the degree of the solvent and/or conformational relaxation.[88]

All of the compounds in the present study contain benzene units and hence have appreciable absorptions in the UV region of the electromagnetic spectrum. In addition, all of the parent hydrocarbon chromophores are reasonably fluorescent ($\Phi_f \geq 0.1$), a property that is particularly useful in directly probing excited states. The diphenylmethane and 5*H*-dibenzo[a,d]cycloheptane (suberane) systems have isolated benzene chromophores which have long wavelength absorption bands at ≈ 265 nm, $\varepsilon_{max} \approx 10^2$ $M^{-1}cm^{-1}$. Fluorene has a very strong absorption at ≈ 265 nm and a weaker absorption band at ≈ 305 nm, ($\varepsilon_{max} \approx 10^4$ and 10^3 $M^{-1}cm^{-1}$, respectively). 5*H*-Dibenzo[a,d]cycloheptene (suberene) also has a very strong absorption band ($\lambda_{max} \approx 285$ nm, $\varepsilon_{max} \approx 10^4$ $M^{-1}cm^{-1}$). The fluorescence emission from diphenylmethane and suberane is relatively weak ($\Phi_f \approx 0.1$) and unstructured. Emission from fluorene, on the other hand, shows some vibrational fine structure, and is not appreciably Stokes shifted. The characteristics of fluorene are consistent with relatively planar ground and excited states structures, which is not unexpected for this rigid system. The fluorescence emission of suberene is very

broad, and appreciably Stokes shifted (≈24 kcal mol^{-1}). This behaviour is indicative of some conformational flexibility, that is expressed in a relaxed excited S_1 state.[88]

An overlay of the fluorescence excitation and emission spectrum for the

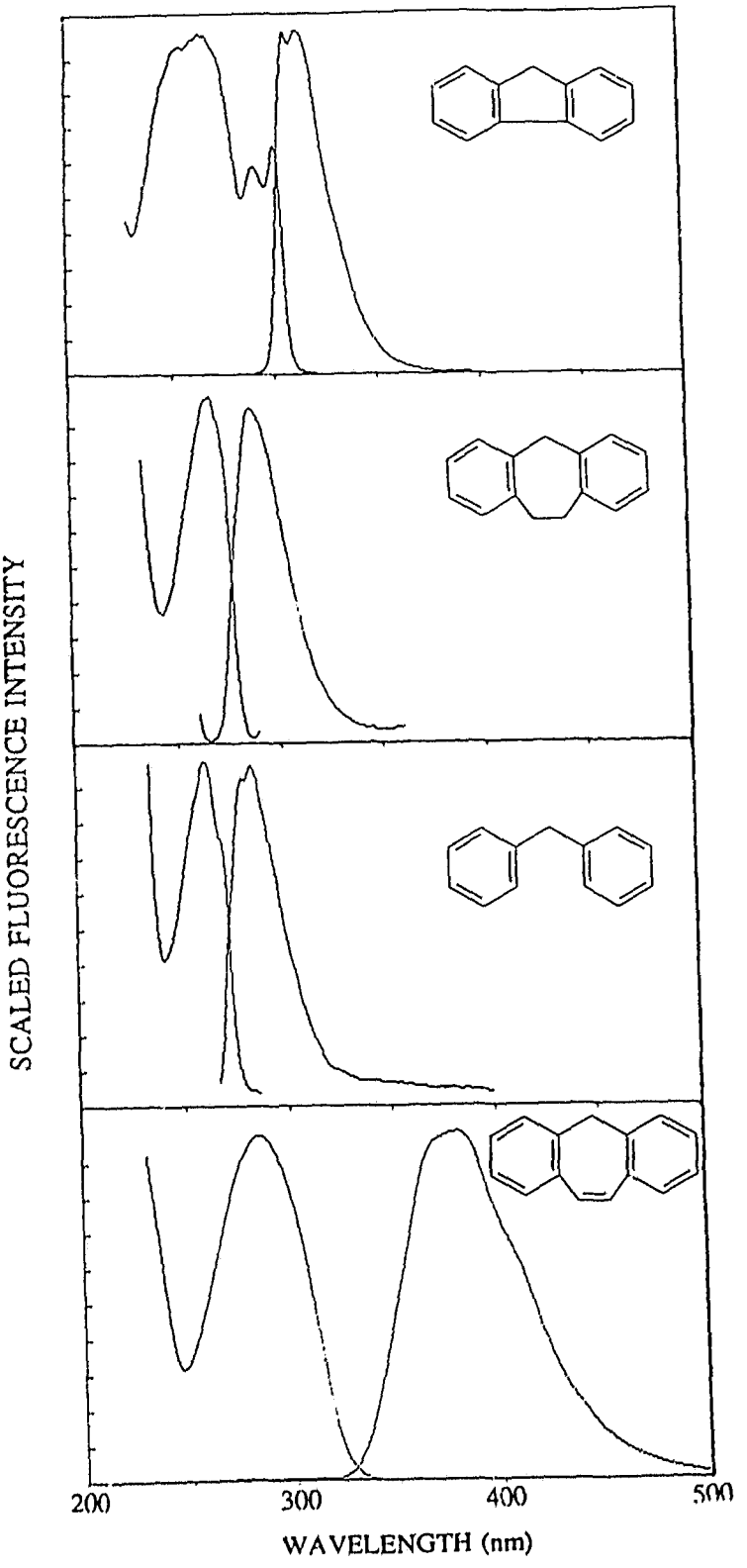

Figure 1.4: Excitation and Emission Spectra of the Parent Hydrocarbons in Cyclohexane.

representative hydrocarbons are shown in Figure 1.4. With few exceptions, the absorption and emission spectra of the alcohols and carboxylic acids, which form the basis of the present investigation, are very similar to those shown here.

Fluorescence behaviour, both steady-state and transient, provides the only available direct probe of the excited singlet state. Steady-state fluorescence measurements record the spectral distributions of the fluorescence emission and excitation spectra. This data can provide information about the nature (structural and temporal) of the excited state. Investigating the effect of the solvent or structural variation of the chromophore can lead to interesting conclusions about the reactivity of the S_1 state. Transient fluorescence measurements record temporal information in the form of a fluorescence lifetime, τ_f. The lifetime of an excited state is governed by the efficiency of the various deactivational modes available to it (Figure 1.2). If the loss of a fluorescent species can be described by a series of unimolecular or pseudo-first order processes, then the lifetime τ_f (the time required for the concentration to reach 1/e of its original value) is given by,

$$\tau_f = \frac{1}{k_{obs}} = \frac{1}{\Sigma k_d} \qquad (1.11)$$

where Σk_d represents the sum of the rate constants leading to the depletion of the excited state. The excited state reactivity then, has a direct influence on the fluorescence lifetime. An excited state that undergoes efficient chemical reaction will necessarily have an additional deactivational pathway, k_r, and the excited state

lifetime will necessarily be diminished. Since the product quantum yield is a function of both the rate constant, k_r, and the lifetime, τ_f, measurement of the latter is necessary in evaluating excited state reactivity, k_r.

1.8 Experimental Approach.

In the present study, the excited state reactivity of a series of structurally related compounds has been compared. By varying the number of π electrons in, or the connectivity of, the central ring, this investigation becomes, in essence, a structure-reactivity study. It is the rate of reaction of the various excited states either towards dehydroxylation or decarboxylation, that is of primary interest. However, these rate constants are not themselves directly measurable. Instead, use is made of directly measurable parameters, viz., the product quantum yield, Φ_p, and the fluorescence lifetime, τ_f. The product quantum yield (Φ_p) is a measure of the efficiency of product formation, with respect to the number of photons absorbed, as given in eq 1.12. Expressed another way, it is the ratio of the rate constant for reaction, k_r, to the sum total of all other rate constants that lead to the depletion of the excited state, Σk_d, (eq 1.13).

$$\Phi_p = \frac{\textit{moles of product}}{\textit{moles of photons}} \qquad (1.12)$$

Since the fluorescence lifetime, τ_f, is defined as the inverse of the sum of all the

$$\Phi_p = \frac{k_r}{\Sigma k_d} \qquad (1.13)$$

depletion rate constants, as given in eq 1.11, the product quantum yield can be expressed simply as,

$$\Phi_p = k_r \tau_f \qquad (1.14)$$

Thus, for a simple photochemical reaction, where the excited singlet state undergoes unimolecular fragmentation, the rate constant, k_r, can be expressed as,

$$k_r = \frac{\Phi_p}{\tau_f} \qquad (1.15)$$

The results presented in this dissertation (Chapters 2 and 3) follow the systematic breakdown outlined as follows. Initially, evidence for a working mechanism are accumulated. This comes largely from product studies, where the major photoproducts are identified and characterized by NMR, UV and GC-MS. The effect of solvent and structural variation, including isotope effects, proved useful as mechanistic probes. Steady-state fluorescence studies also aided in this regard. Next, the product quantum yields, Φ_p, are determined by measuring the efficiency of product formation with respect to the number of photons required. The amount of photoproduct produced was quantified by GC analysis or occasionally by ^{1}H NMR integrations (in larger scale reactions). The light intensity

of a given irradiation was monitored using chemical actinometry and quantified by either UV absorption spectroscopy (potassium ferrioxalate) or GC/^{1}H NMR (secondary photochemical actinometers). Finally, the fluorescence lifetimes, τ_f, are measured by a method known as single photon counting.[89] This technique measures the time delay between an incident flash and the emission of the first photon from the sample, via a time to amplitude converter which transforms the temporal information into a voltage signal. Using a flash frequency of about 20 kHz this measurement can be repeated at rates up to 1000 times per second. The individual voltage signals are sorted according to their amplitude and counted. The data is accumulated in a histogram and a decay curve is generated in this fashion.

Derivatives **1** - **10** have been prepared and studied in this investigation. In addition, compounds **11** - **32** were also studied for various mechanistic reasons. The structures of **11** - **32** are shown in Figure 1.5.

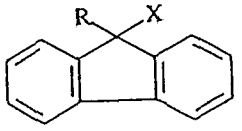

R=D	X=OH	11
R=CH_3	X=OH	12
R=$CH{=}CH_2$	X=OH	13
R=$CH(CH_3)_2$	X=OH	14
R=$C(CH_3)_3$	X=OH	15
R=Ph	X=OH	16
R=H	X=OMe	17
R=H	X=Br	18
R=H	X=OAc	19

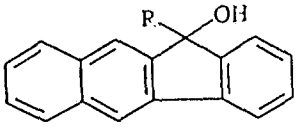

R=H 20
R=CH_3 21

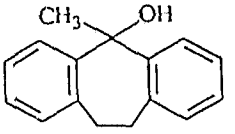

24

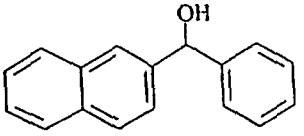

22

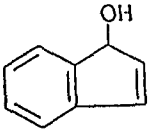

23

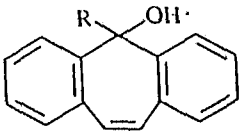

R=D	25
R=CH_3	26
R=$CH{=}CH_2$	27

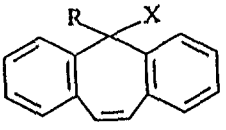

R=D	X=CO_2H	28
R=H	X=CO_2Et	29
R=CH_3	X=CO_2H	30
R=CH_3	X=CO_2Et	31

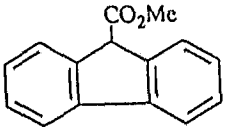

32

Figure 1.5: List of Additional Substrates Studied in this Investigation.

CHAPTER TWO

RESULTS - PHOTODEHYDROXYLATION

2.1 PRODUCT STUDIES

Photodehydroxylation of the diaryl alcohols **1 - 5**, **11 - 16** and **20 - 27** was carried out in aq MeOH solutions (typically 50% (v/v) MeOH-H_2O). On photolysis, many of these alcohols were converted to their corresponding methyl ethers, thus the overall process is photosolvolysis. Many of the methyl ethers produced in this way are themselves photochemically reactive, producing secondary photoproducts, particulary at higher conversions. Certain alcohols (**12** and **14**) were also photolyzed in aq CH_3CN (ACN), where dehydroxylation was followed by loss of a proton, leading overall to a photodehydration reaction.

2.1.1 Photolysis of 9-Fluorenol (1). Exploratory studies had indicated that 9-fluorenol (**1**) was unusually reactive towards solvolysis when photolyzed in 50% (v/v) MeOH-H_2O. This is in sharp contrast to its thermal stability towards solvolytic displacement reactions, which has been ascribed to the formally antiaromatic character of the dibenzocyclopentadienyl cation.[42] To investigate the photoreaction further and explore a variety of mechanistic probes, such as solvent, substituent and isotope effects, **1** and a number of related compounds were photolyzed under a variety of conditions.

2.1.1.1 Photosolvolysis of 1 in aqueous methanol. The photolysis of 9-

fluorenol (**1**) in 50% MeOH-H_2O resulted in an efficient solvolysis process, producing 9-methoxyfluorene (**17**) after short irradiation times. For instance, when 50 mg of **1** was irradiated for 2 min in 100 mL of argon saturated solution, 15% of the starting alcohol was converted to **17**, (eq 2.1).

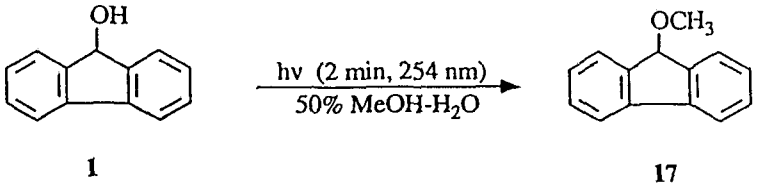

1 **17** (2.1)

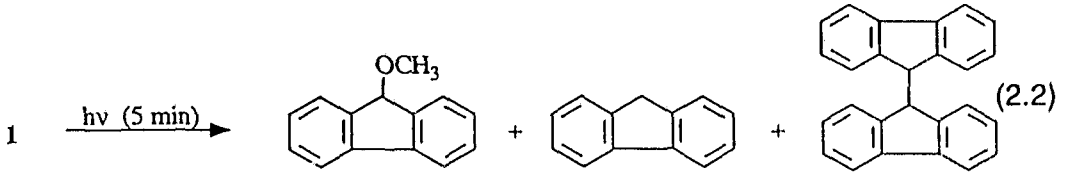

17 (32%) **33** (26%) **34** (≈ 5%) (2.2)

Photolysis of **1** for 5 min in this solvent resulted in the formation of **17**, fluorene (**33**) and a small amount of 9,9'-bifluorene (**34**) (the remaining portion being due to recovered starting material), (eq 2.2). Extended photolysis gave **33** (90%) and **34** (10%) as the only major products. The distribution of photoproducts was followed as a function of time and the results are plotted in Figure 2.1.

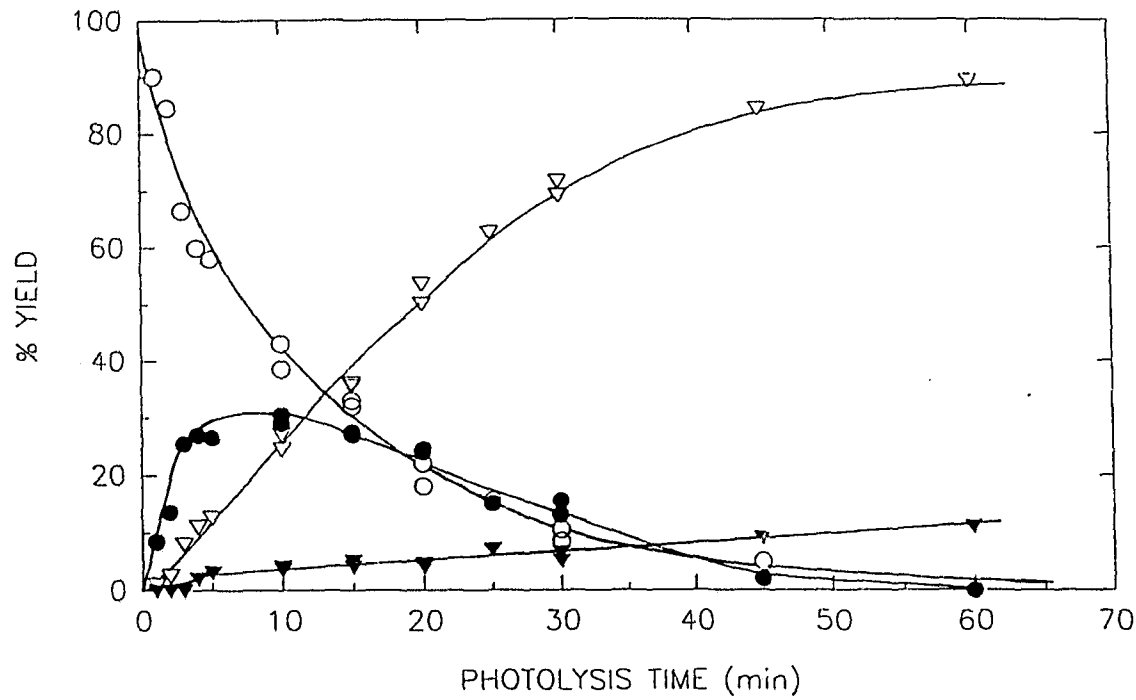

*Figure 2.1: Time Dependent Product Distribution on Photolysis of **1** in 50% MeOH-H_2O. Photolysis of 2.7 m**M** argon purged solutions; analysis by ^1H NMR and GC, (**1** hollow circles; **17** solid circles; **33** hollow triangles; **34** solid triangles).*

The results suggest that 9-methoxyfluorene (**17**) is itself photochemically reactive to give the hydrocarbon products **33** and **34**. The nature of these secondary photoproducts indicates that homolytic, rather than heterolytic cleavage, is the dominate pathway for **17**, (eq 2.3). This behaviour is explored further below (*vide infra*).

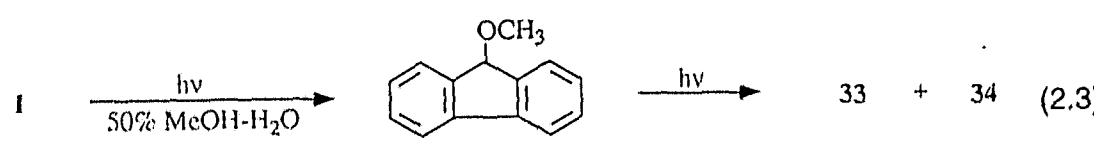

(2.3)

The photosolvolysis of 9-fluorenol (**1**) was carried out in a number of aq methanol mixtures ranging from 40% (v/v) MeOH-H_2O to 100% MeOH. Photolysis in pure methanol led to relatively low yields of the methyl ether and resulted in the formation of a new photoproduct, 9-fluorenylmethanol (**35**); presumably arising from initial homolytic cleavage of 9-fluorenol (**1**), followed by abstraction of a hydrogen from the solvent and then the combination of the hydroxymethyl radical with another 9-fluorenyl radical.

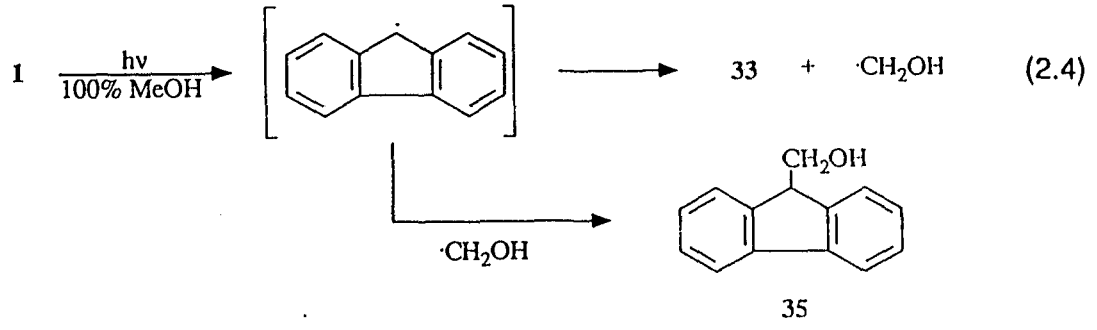

(2.4)

The distribution of the photoproducts was followed as a function of time. Figure 2.2 indicates that the radical derived products are present even at short photolysis times.

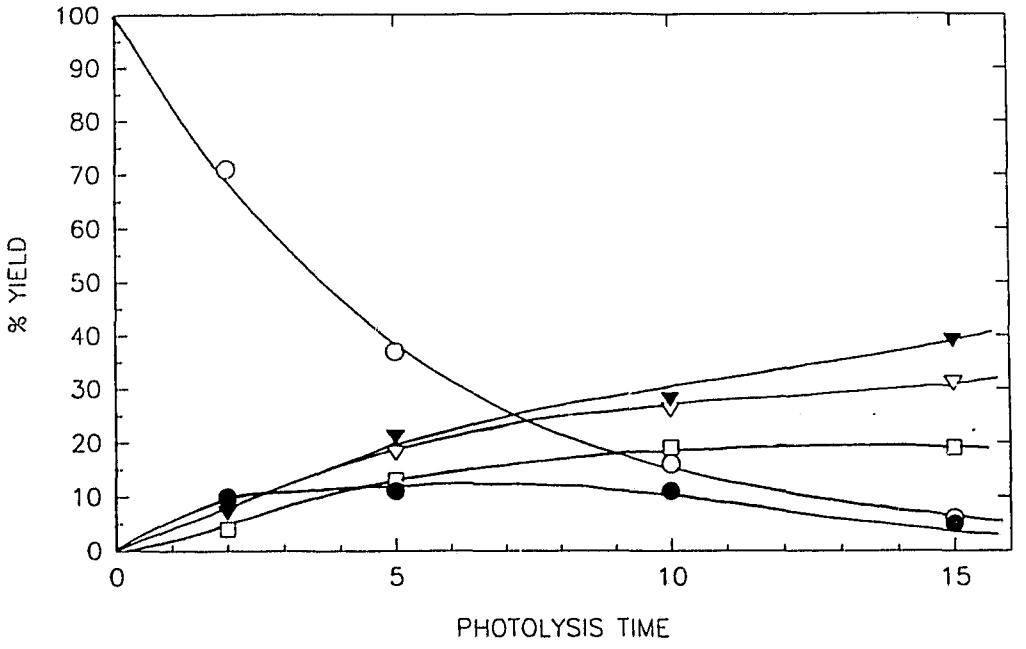

*Figure 2.2: Time Dependent Product Distribution on Photolysis of **1** in 100% MeOH. Photolysis of 2.7 m**M** argon purged solutions; analysis by ^1H NMR, (**1** hollow circles; **17** solid circles; **33** solid triangles; **34** hollow squares; **35** hollow triangles).*

This behaviour contrasts the situation presented in Figure 2.1, when 50% (v/v) MeOH-H_2O was employed as the solvent. Thus in pure methanol it appears that the excited state of **1** is partitioned between homolytic and heterolytic pathways. In general, the heterolytic process was favoured as the proportion of H_2O in the solvent mixture increased. At 60% (v/v) MeOH-H_2O only traces of **35** were formed. It was found that 50% (v/v) MeOH-H_2O was the most convenient for photosolvolysis studies in terms of promoting dehydroxylation on the one hand and providing a medium in which organic substrates can be readily dissolved, on the other.

Acid catalysis has been observed in other photodehydroxylations[32,34,35,38] and has been used to support heterolytic cleavage as the primary photochemical event. To investigate the effect of pH on the photosolvolysis of **1**, photochemical reactions were carried out in 50% MeOH-H_2O solutions, where the aqueous portion was replaced by aq NaOH or H_2SO_4 solutions. Preparative photolysis of **1** at pH 12, 6, and 1 resulted in similar conversions and product distributions. Hence, no acid catalysis was observed in this pH range, which contrasts the behaviour of a number of substituted benzyl alcohol derivatives previously studied.[32,34,35,38] However, when **1** was irradiated using 5%, 10%, and 30% H_2SO_4 as the aqueous portions, the conversions to methyl ether gradually increased (Table 2.1). Dark reactions carried out in 30% H_2SO_4 indicated that no methyl ether was formed under these conditions (another material, probably a sulfonated 9-fluorenol derivative, was produced in small amounts). This dark reaction could result in loss of starting material, giving rise to an apparent increase in the conversion to photoproducts, but this would have an inflationary effect on both the photoproducts, whereas the data indicate the amount of **33** remains relatively low throughout. Although some caution must be exercised in the interpretation of this data, particularly at such high acid strengths, it appears that some degree of acid catalysis does occur.

Table 2.1: Conversions and Product Distributions in the Photosolvolysis of 1 in Acidic Aqueous Methanol Solutions.

Acidity of H_2O	Conversion[a]	Product Distribution[b]	
		17	**33**
pH ≈ 6	29%	19%	10%
5% H_2SO_4	33%	26%	7%
10% H_2SO_4	52%	41%	11%
30% H_2SO_4	62%	51%	11%

[a] Substrate was 2.7 **mM** in 50% (v/v) MeOH-H_2O, photolyzed for 5 min at 254 nm.
[b] Analyzed by ^1H NMR only.

A similar, but less dramatic trend was observed in GC scale product studies, which showed that the conversion to methyl ether gradually increased from 9% to 11% and to 16% on changing the aqueous portion of the solvent mixture from H_2O (pH 6) to 0.12 **M** $HClO_4$ and to 1.2 **M** $HClO_4$, respectively. The distribution of the photoproducts in Table 2.1 reveal another interesting trend. The ratio of **17** to **33** increases notably at higher acidities. This trend would be expected if the first photochemical reaction, that is, formation of methyl ether, was acid catalyzed, and the second photochemical reaction, homolysis of **17**, was unaffected by acid.

In the photosolvolysis reactions carried out in 50% MeOH-H_2O, the yield of methyl ether is only a lower limit of the yield of carbocation formation because a certain portion of these intermediates will be trapped by H_2O and therefore regenerate the starting material, as illustrated in eq 2.5.

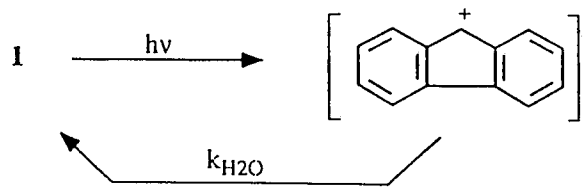

(2.5)

To establish the yield of carbocation generated in these reactions, it is necessary to quantify the partitioning of the intermediate between attack by MeOH and H_2O. In an effort to establish the relative rates or capture ratio (k_{MeOH}/k_{H_2O}) in this mixed solvent environment, it was necessary to quantify the amount of starting material that was regenerated by reaction of the incipient cation with water. To this end, ^{18}O labelled 9-fluorenol (20 atom %) was photolyzed in 50% (v/v) MeOH-H_2O. Thus, using gas chromatography (GC) to measure the conversion to methyl ether and mass spectroscopy (MS) to determine the extent of ^{18}O loss in the starting material, k_{MeOH}/k_{H_2O} was evaluated. The data from a series of photolysis runs are presented in Table 2.2.

Table 2.2: Conversions to Methyl Ether and Loss of Isotope Label in the Photolysis of 9-Fluorenol-(^{18}O) in 50% MeOH-H_2O.

Photolysis Time (min)[a]	% Loss ^{18}O [b]	% Conversion[c]
2	10.9	10.0
4	20.7	22.3
6	23.5	28.3
10	28.9	38.9

[a] Substrate was 2.5 x 10^{-4} M in UV cuvettes.
[b] From analysis of MS data, values quoted have estimated relative errors of ± 10%.
[c] From corrected GC analysis.

The data clearly shows that as the conversion to methyl ether increases, the extent of ^{18}O loss increases as well. An expression for the capture ratio, k_{MeOH}/k_{H_2O}, is based on the scheme presented in eq 2.5. The quantum yield for methyl ether formation, Φ_{FlOMe}, and unlabelled 9-fluorenol, Φ_{FlOH}, are given by,

$$\Phi_{FlOMe} = \Phi_{Fl^+} \times \frac{k_{MeOH}[MeOH]}{k_{MeOH}[MeOH] + k_{H_2O}[H_2O]} \qquad (2.6)$$

and,

$$\Phi_{FlOH} = \Phi_{Fl^+} \times \frac{k_{H_2O}[H_2O]}{k_{H_2O}[H_2O] + k_{MeOH}[MeOH]} \qquad (2.7)$$

where, Φ_{Fl^+} represents the quantum yield for carbocation formation. Thus, the ratio of rate constants is given by,

$$\frac{k_{MeOH}}{k_{H_2O}} = \frac{\Phi_{FlOMe}}{\Phi_{FlOH}} \times \frac{[H_2O]}{[MeOH]} \qquad (2.8)$$

But since,

$$\frac{\Phi_{FlOMe}}{\Phi_{FlOH}} = \frac{\%\ Conversion\ FlOMe}{\%\ Loss^{18}O} \qquad (2.9)$$

the ratio of rate constants can be written as,

$$\frac{k_{MeOH}}{k_{H_2O}} = \frac{\%\ Conversion\ FlOMe}{\%\ Loss^{18}O} \times \frac{[H_2O]}{[MeOH]} \qquad (2.10)$$

Since the ratio $[H_2O]/[MeOH]$ in 50% (v/v) MeOH-H_2O is equal to 2.23, the relative rates of attack by the two nucleophiles can be calculated from the data given in Table 2.2. Using the first two entries, which are at conversions of less than 30%, $k_{MeOH}/k_{H_2O} = 2.2 \pm 0.2$.

2.1.1.2 Photolysis of 1 in other alcohol solvents. When 9-fluorenol (**1**) was photolyzed in other aqueous-alcohol solvents it efficiently solvolyzes to yield the corresponding ethers (eq 2.11). The ethyl, isopropyl and tert-butyl ethers were prepared in this way and were identical to authentic materials that were synthesized from 9-bromofluorene (**18**) via thermal solvolysis in the appropriate alcohol. The results of several preparative runs are summarized in Table 2.3.

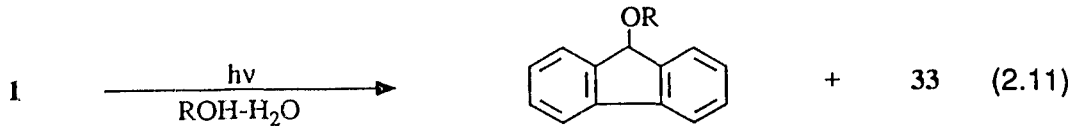

(2.11)

Table 2.3: Conversions and Product Distribution in the Photolysis of 9-Fluorenol (1) in Various Alcohol Solvents.

Solvent System[a] (v/v)	Mole Fraction of ROH (χ)	Conversion[b]	Product Distribution		
			FIOR	**33**	**34**
50% MeOH-H_2O	0.31	45%	25%	16%	<5%
50% EtOH-H_2O	0.24	38%	17%	16%	5%
50% (*i*-PrOH)-H_2O	0.19	27%	24%	<5%	-
50% (*t*-BuOH)-H_2O	0.16	25%	18%	<5%	-[c]
65% (*i*-PrOH)-H_2O	0.31	25%	22%	<5%	-
70% (*t*-BuOH)-H_2O	0.31	32%	23%	<5%	-[c]

[a] Substrate was 2.7 **mM** in argon saturated solution.
[b] Conversions and distributions on the basis of ^1H NMR and GC analysis.
[c] An unidentified product was also present ≈ 5%.

Based on the conversions in Table 2.3, 50% MeOH-H_2O appears to be the most efficiently solvolyzing medium. When the volume fraction was held constant, at 50%, the conversion to the other ethers decreased with the increasing steric bulk of the alcohol. However, when these reactions were carried out at constant mole fraction (χ ≈ 0.31) this trend was not observed. Because there are large variations in the dielectric constants, which are known to have pronounced effects

on the efficiency of carbocation generation,[107] it is difficult to comment further on the relative efficiencies in this series. The results do indicate that the methyl and ethyl ethers are more prone to undergo subsequent photochemistry than their isopropyl and tert-butyl analogues. The relative stability of the isopropyl ether was unexpected, since homolysis of the C_9-O bond followed by disproportionation would yield the stable molecules **33** and acetone. The tert-butyl ether is the only one in the present series that cannot undergo this process, as there are no β-hydrogens on the incipient t-butyloxy radical. Secondary photoheterolysis of any of the ethers (FlOR) would not be detected, since this would simply regenerate starting material.

2.1.1.3 Photolysis of 1 with triplet sensitizers and triplet quenchers. In order to determine the multiplicity of the excited state responsible for the photodehydroxylation, 9-fluorenol (**1**) was photolyzed in the presence of a triplet sensitizer. In a triplet sensitization experiment, one attempts to selectively populate the triplet state of the substrate without populating the excited singlet state. This is accomplished by exclusively exciting a triplet sensitizer, which efficiently intersystem crosses to its triplet state and can then undergo an energy transfer step to yield the substrate triplet. To avoid direct excitation of the substrate, the sensitizer must absorb light in a region where the substrate has only a weak absorption. In order to ensure that the energy transfer step is energetically favourable, the triplet state energy (E_T) of the sensitizer must be higher than that

of the substrate. The only direct probe that the energy transfer step is actually occurring comes from quenching of the sensitizer phosphorescence or the sensitization of the substrate phosphorescence. In general, this evidence is very difficult to obtain, because solution phosphorescence is rare for organic molecules. Generally, energy transfer is assumed to occur at, or near, the diffusion limit, provided the thermodynamics are favourable. When the photoproducts in a triplet sensitized reaction are the same as those obtained upon direct photolysis of the substrate, the triplet state is strongly implicated as a reactive intermediate. If, on the other hand, no photoproducts or different photoproducts are isolated, the triplet state is not involved in the direct photochemistry. Sodium 4-acetylbenzene sulfonate (**36**), which is a water soluble derivative of acetophenone ($E_T \approx 74$ kcal mol^{-1}; $\Phi_{ISC} \approx 1$)[90], was employed as a triplet sensitizer in this study.

When a solution of 9-fluorenol (**1**) ($E_T \approx 68$ kcal mol^{-1})[90] was photolyzed in 50% (v/v) MeOH-H_2O containing 3.0 g of **36**, no methyl ether formation was observed. Small amounts of the radical derived products **33** and **35** were detected. We have also photolyzed **1** in the presence of the triplet quencher disodium 1,3-cyclohexadiene-5,6-dicarboxylate (**37**) ($E_T \approx 52$ kcal mol^{-1}),[90] and found it to have little effect on the outcome of the photosolvolysis reaction. Both the triplet sensitization and quenching studies strongly implicate the involvement of an excited singlet state in the photosolvolysis reactions of 9-fluorenol (**1**). This result is in agreement with earlier findings that have shown that photodehydroxylation occurs from the S_1 state.[32-35]

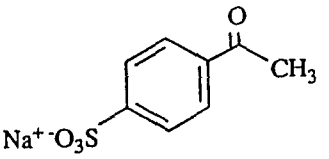

36

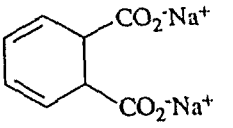

37

2.1.1.4 Photolysis of 1 with external nucleophiles. In order to substantiate the intermediate 9-fluorenyl cation, attempts were made to trap it using nucleophiles other than those present in the solvent cage. Previous studies in our laboratory have shown that cyanide ion (0.25 **M** NaCN in aq CH_3CN (ACN)) is capable of trapping the incipient cation generated in the photolysis of 2,6-dimethoxybenzyl alcohol.[35] However, repeated attempts to trap the 9-fluorenyl cation (irradiation times ranging from 5 - 60 min) failed to yield 9-cyanofluorene (**38**). Thus, when 50 mg of **1** was photolyzed in 40% ACN-H_2O (0.3 **M** NaCN) for 10 min, the starting material was recovered in > 80% yield. Some photodecomposition to **33**, **34** and rearranged fluorenols does occur at longer irradiation times. This photodecomposition is due to residual reaction with the solvent or isomerization of the substrate, and occurs in the absence of NaCN. The major reaction pathway in this solvent presumably involves formation of the cation followed by rapid trapping by water to regenerate the starting alcohol. To check that this was indeed occurring, 9-fluorenol labelled with ^{18}O was photolyzed in 30% (v/v) ACN-H_2O. After a 5 min irradiation, only 55% of the original label remained in the recovered starting material. A 10 min photolysis resulted in 70% loss of the ^{18}O label. Similar photolysis (20 - 60 min, 0.25 **M** NaCN) of 9-bromofluorene (**18**), a system

shown to be efficiently solvolyzed in 40% ACN-H_2O (*vide infra*), also failed to yield the cyanide trapped product. The major photoproduct in these reactions was 9-fluorenol (**1**). In order to check the trapping methodology directly, 9-xanthenol (**39**) was photolyzed under identical conditions. This alcohol had been previously shown to photodehydroxylate and yield the corresponding methyl ether when photolyzed in aq methanol.[91] The intermediate 9-xanthenyl cation is relatively stable in the ground state and hence expected to be much longer lived than 9-fluorenyl cation. Two cyanide trapped products, 9-cyanoxanthene (**40**) and a ring substituted cyanoxanthene (**41**) were isolated after a 15 min photolysis.

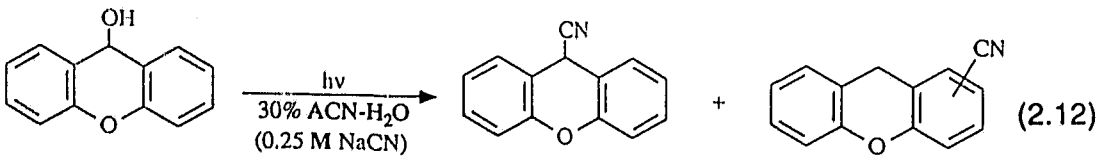

39 **40** **41** (2.12)

2.1.1.5 Photolysis of 1 in acetonitrile. Acetonitrile (ACN) is widely used as a co-solvent in these studies and although it is generally considered a relatively inert solvent, the preparative trapping studies and preliminary fluorescence work has led us to briefly investigate the photodecomposition of **1** in pure ACN and ACN-water mixtures. When 50 mg of **1** was irradiated in 100% ACN for 15 min, extensive decomposition occurred (≈ 50% by loss of starting material). The products were analyzed by ^{1}H NMR and GC-MS and are depicted in eq 2.13.

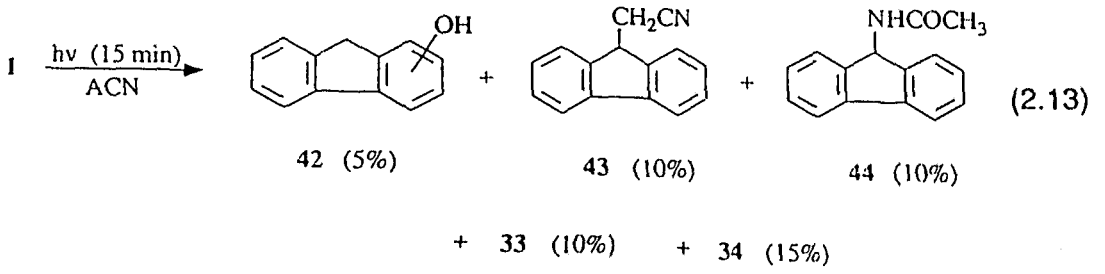

(2.13)

The products appear, for the most part, to be derived from the 9-fluorenyl radical. Initial C-OH homolysis followed by recombination of the radical pair can give back **1** or the hydroxyfluorenes (**42**; presumed to be a mixture of isomers). Abstraction of a hydrogen from ACN by the 9-fluorenyl radical gives fluorene (**33**) and the cyanomethyl radical, which on recombination with another 9-fluorenyl radical yields the substituted acetonitrile product **43**. Escape and recombination of two 9-fluorenyl radicals leads to the dimer **34**. Heterolysis of the C-OH bond, followed by trapping of the 9-fluorenyl cation by ACN and subsequent hydrolysis by residual water, gives the acetamide product **44**. Photolysis in 50% ACN-H_2O for the same time resulted in much less photodecomposition (≈ 15%), consistent with an increased tendency towards heterolysis followed by solvolysis with water. In 80% ACN-H_2O the homolytic pathway is suppressed even further and starting material is recovered in > 90% yield.

2.1.2 Photolysis of 9-Methoxyfluorene (17). In order to confirm that fluorene (**33**) and 9,9'-bifluorene (**34**) are indeed the result of a secondary photochemical reaction of the initially formed methyl ether, **17** was independently photolyzed.

When **17** was irradiated in 50% MeOH-H_2O for 10 min it was almost completely converted to fluorene (**33**). Small amounts of **34** and **35** were also detected. Surprisingly, **1** was not observed in this reaction, indicating that photoheterolysis does not occur for this substrate. Thus, it appears that the leaving group has a marked effect on the outcome of photolysis.

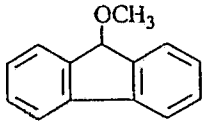

17

$$\xrightarrow[50\%\ MeOH\text{-}H_2O]{h\nu} \quad \begin{matrix} \mathbf{33}\ (75\%) + \mathbf{34}\ (\approx 10\%) \\ + \mathbf{35}\ (\approx 5\%) \end{matrix} \qquad (2.14)$$

9-Methoxyfluorene (**17**) displayed essentially the same reactivity in 30% ACN-H_2O, indicating there is no marked solvent effect. This observation suggests that fluorene (**33**) arises via disproportionation of the initially formed radical pair, as opposed to abstraction of a hydrogen atom from the solvent. Such a mechanism has been reported by Tomioka and co-workers for the photolysis of 9-fluorenyl ethers in aerated alcohol solvents.[92] This mechanism was indeed confirmed in the present study by photolysis of 9-(trideuteriomethoxy)fluorene in aqueous MeOH or ACN solutions. 9-Deuteriofluorene (**33**-d) was the exclusive photoreduction product in these photolysis (eq 2.15).

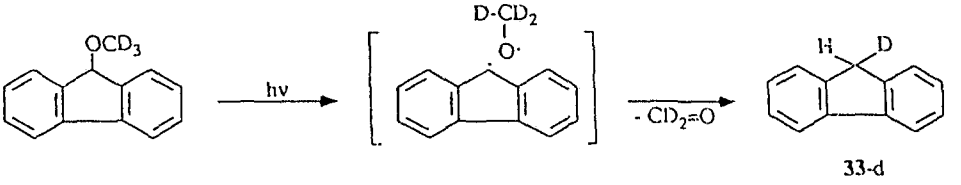

33-d (2.15)

2.1.3 Photolysis of 9-Substituted-9-Fluorenols 12-16. A variety of substituted 9-fluorenols have been prepared and photolyzed in aq MeOH. All gave the corresponding methyl ethers with efficiencies similar to or greater than that observed for 9-fluorenol (**1**). On extended photolysis many of the initially formed ether products underwent subsequent photochemistry to yield the hydrocarbon products **33** and **34**. Substituted fluorenols bearing β-hydrogens often underwent E1 elimination, thus yielding an alkene product (overall photodehydration). The photodehydration reaction contrasts the photosolvolysis transformation in that the chromophore of the product differs from that of the starting material, and hence these reactions can be followed by UV absorption spectroscopy (*vide infra*).

2.1.3.1. Photolysis of 9-methyl-9-fluorenol (12). Preparative photosolvolysis experiments of 9-methyl-9-fluorenol (**12**) lead to the normal distribution of solvolysis products and an additional product, 9-methylenefluorene (**45**). For instance, photolysis of **12** in 50% MeOH-H_2O (100 mg in 200 mL of argon saturated solution) for 10 min gave the expected methyl ether **46** (40%), the hydrocarbon **47** (15%) and the photodehydration product **45** (≈ 10%). Shorter irradiation times led only to the 9-methoxy-9-methylfluorene (**46**) indicating that the hydrocarbon

arises from the subsequent photolysis of **46** (analogous to 9-methoxyfluorene).

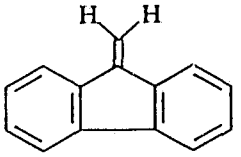

45

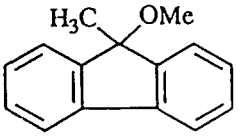

46

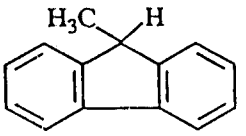

47

Products **46** and **47** were easily characterized but, due to the inherent instability of 9-methylenefluorene (**45**), we were unable to isolate and characterize it in a pure form (see Experimental). When **12** was photolyzed in aq ACN the only photoproduct observed was **45**. Considerable amounts of a insoluble white material are usually present in the crude reaction mixtures (**45** is known to be unstable towards polymerization[93]). The amount of 9-methylenefluorene (**45**) in proportion to starting material did not increase beyond about 15% with longer irradiation times. However, increased amounts of the insoluble polymer were observed on longer photolysis. The table below summarizes the results of several photolysis. Photosolvolysis appears to be considerably more efficient than the photodehydration for **12**, but the actual yields for the latter process are difficult to establish because of the undetermined amounts of polymer produced.

Table 2.4: Summary of Preparative Photolysis of 9-Methyl-9-Fluorenol (12).

Substrate Conc. (x 10^{-3} M)	Solvent System	Photolysis Time (min)[a]	Conversion	Product Distribution		
				44	**45**	**43**
2.5	50% MeOH-H_2O	10	62%	40%	15%	8%
1.2	50% ACN-H_2O	10	15%[b]	-	-	15%
2.5	50% ACN-H_2O	15	12%[b]	-	-	12%
2.5	50% ACN-H_2O	20	12%[b]	-	-	12%
2.5	25% ACN-H_2O	20	10%[b,c]	-	-	10%

[a] Irradiation carried out at λ_{ex} = 254 nm in argon saturated solution.
[b] Amount of **45** in proportion to starting material by ^{1}H NMR, insoluble material also present in crude mixture.
[c] Cleaner reaction in this solvent system.

The nature and distribution of the photoproducts suggest that loss of a proton from the incipient cation competes favourably with nucleophilic attack by solvent.

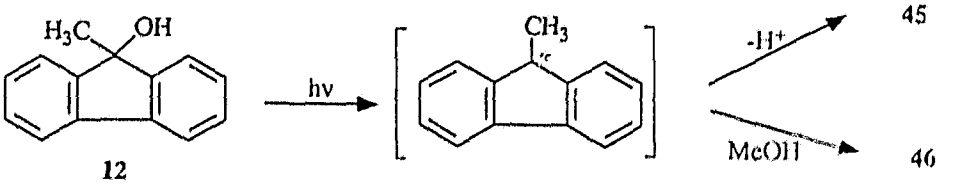

12 (2.16)

2.1.3.2 Photolysis of 9-vinyl-9-fluorenol (13). This 9-fluorenol derivative was photolyzed in aqueous acetonitrile to probe the possibility of a photorearrangement reaction. The incipient 9-vinyl-9-fluorenyl cation is expected to be resonance stabilized, and hence should undergo nucleophilic trapping by solvent at two positions. When H_2O is the only nucleophile, the reaction appears to be a photorearrangement as hydroxide is lost from the 9-position and water attacks the terminal carbon of the vinyl substituent, generating an α-hydroxymethyl dibenzofulvene. Thus, when 50 mg of **13** was photolyzed in 100 mL of 50% (v/v) ACN-H_2O for 5 min the rearranged alcohol, **48**, was the exclusive photoproduct, produced in 35% yield.

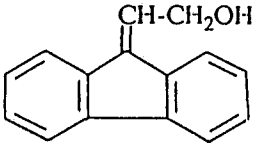

48

When **13** was photolyzed for 15 min in 50%(v/v) MeOH-H_2O solution, three products were obtained in roughly equal proportion. In addition to the rearranged alcohol, **48**, two methyl ethers were produced as well, **49** and **50**.

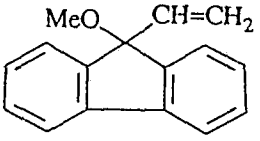

49

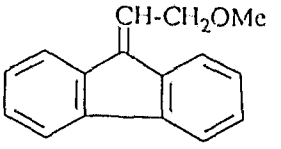

50

The following equation illustrates the importance of the resonance stabilized allylic cation in the formation of the dibenzofulvene derivatives.

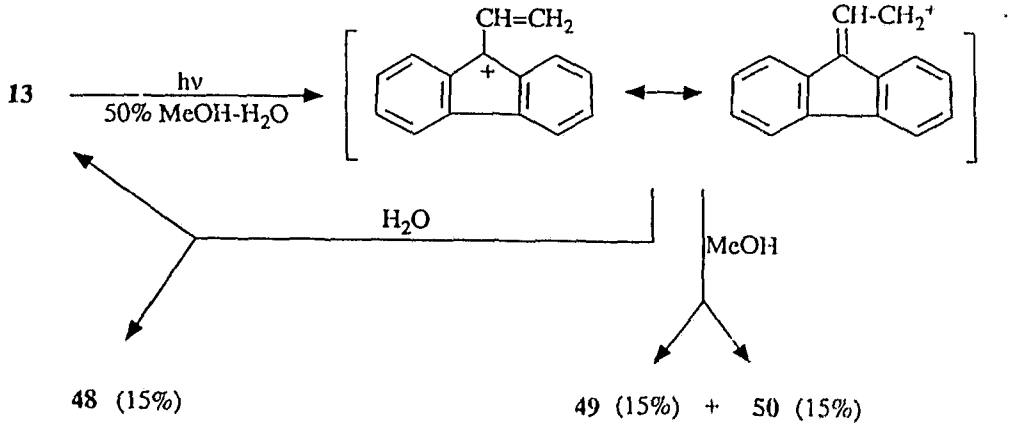

(2.17)

2.1.3.3 Photolysis of 9-*i*-propyl-9-fluorenol (14). The *iso*propyl derivative is related to **12**, in that both contain β-hydrogens can be lost (via E1 elimination) following an initial photodehydroxylation step. Thus in 50% MeOH-H_2O **14** was expected to undergo, in addition to photosolvolysis, efficient photodehydration, leading to 6,6'-dimethyldibenzofulvene (**51**). Photodehydration did indeed occur but with a markedly lower efficiency than 9-methyl-9-fluorenol (**12**). When **14** was photolyzed in 30% (v/v) ACN-H_2O (100 mg in 200 mL argon saturated solution) for 5 min, the starting material was almost entirely recovered. Only a trace (< 5%) of the dehydrated product was observed. Photolysis for 20 min in the same solvent

environment resulted in a mere 5% conversion to **51**. No other photodecomposition was apparent at this conversion.

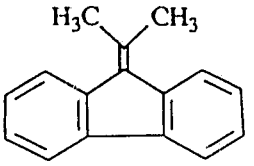

51

When **14** was photolyzed in 60% (v/v) MeOH-H_2O the expected methyl ether product, **52**, was observed in conversions similar to those for 9-fluorenol (**1**). Therefore, the suppressed rate of formation of the alkene is not due to a less efficient photodehydroxylation step. It is proposed that the orthogonality of the β C-H bond to the vacant p-orbital on C_9 retards the rate of elimination. Thus in aq ACN, nucleophilic attack of the incipient cation favourably competes, and the starting alcohol is regenerated in this fashion. Table 2.5 summarizes the results of several preparative photolysis of **14**.

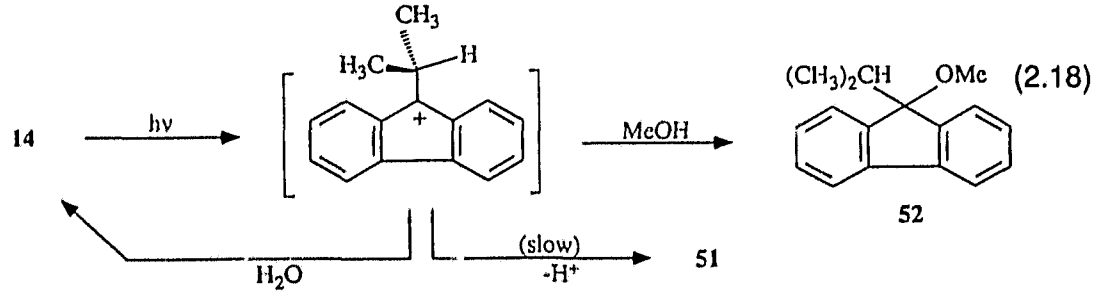

(2.18)

Table 2.5: Summary of Preparative Photolysis of 9-*i*-Propyl-9-Fluorenol (14).

Substrate Conc. (x 10^{-3} **M**)	Solvent System; Ar (g)	Photolysis Time (min); λ_{ex}=254 nm	Conversion[a]	Product
3	60% MeOH-H_2O	2	25%	**50**
2	30% ACN-H_2O	5	< 5%	**49**
2	30% ACN-H_2O	20	≈ 5%	**49**

[a] Conversions were measured by ^{1}H NMR.

2.1.3.4 Photolysis of 9-*t*-butyl-9-fluorenol (15). This 9-fluorenol derivative was photolyzed in aq acetonitrile to investigate the possibility of a 1,2-methyl shift of the incipient 9-*t*-butyl-9-fluorenyl cation (eq 2.19). However, when **15** was photolyzed in 50% ACN-H_2O or 100% ACN (50 mg in 100 mL of argon saturated solution) for 10 min the starting material was recovered. Photolysis for 30 min in 50% (v/v) ACN-H_2O lead to some photodecomposition, but no evidence for the rearranged alcohol **53** was obtained.

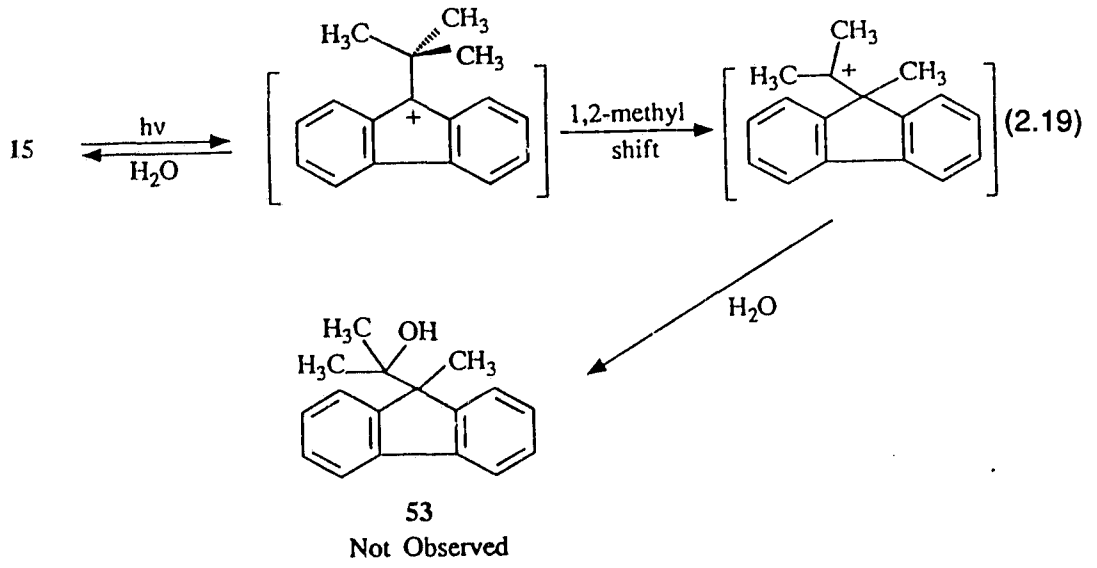

Photolysis of **15** in 50% MeOH-H_2O (50 mg, 100 mL argon saturated solution) for 10 min did lead to the expected solvolysis product 9-*t*-butyl-9-methoxyfluorene (**54**) and the hydrocarbon 9-*t*-butylfluorene (**55**) (eq 2.20). The ^{1}H NMR indicated that no other methoxy signal was present, again suggesting that no rearrangement of the initially formed carbocation had occurred.

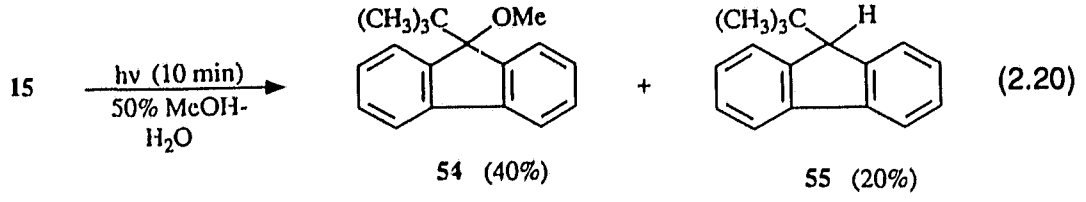

2.1.3.5 Photolysis of 9-phenyl-9-fluorenol (16). When **16** was photolyzed in 60% (v/v) MeOH-H_2O (70 mg in 100 mL of argon saturated solution) for 5 min, 70% of the starting material was converted to a mixture of the methyl ether **56**,

and the hydrocarbon **57**. Under otherwise identical conditions, shorter irradiations of this substrate lead to **56** (30%) and **57** (≤ 5%). The ratio of methyl ether to hydrocarbon markedly increased at lower conversion indicating that, like the other 9-fluorenyl ethers, **56** is also photochemically labile towards homolytic cleavage.

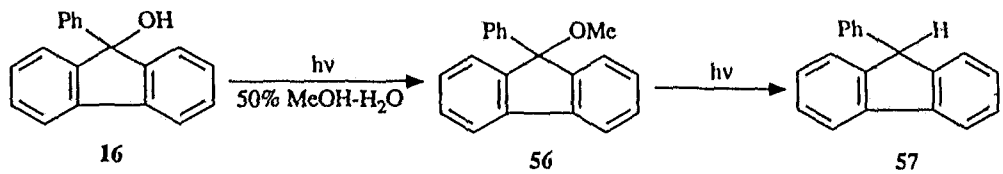

16 *56* *57* (2.21)

2.1.4 Photolysis of Diphenylmethanol (2) and 2-Phenylbenzyl Alcohol (3).

To probe the structural dependence of the unusually reactive 9-fluorenol system, two model compounds were investigated. Diphenylmethanol (**2**) and 2-phenylbenzyl alcohol (**3**) represent structural analogues to 9-fluorenol (**1**), in which the internal cyclic array (ICA) has been disrupted. Removing the C_{10}-C_{11} (aryl-aryl) bond of 9-fluorenol (**1**) yields diphenylmethanol (**2**) (benzhydrol), whereas removal of the C_9-C_{10} bond gives 2-phenylbenzyl alcohol (**3**). When **2** was photolyzed in 50% MeOH-H_2O the starting material was recovered, even after prolonged irradiations (60 min). Irradiation of **3** indicated that it too was unreactive towards photosolvolysis in 50% MeOH-H_2O. Under conditions that lead to the complete loss of 9-fluorenol (**1**), greater than 90% of the starting alcohol was recovered. On

longer irradiations, **3** isomerized to 3-phenylbenzyl alcohol.[94] Hence it is clear that removing the internal ring has a profound effect on the propensity of these benzyl alcohol derivatives to undergo photosolvolysis.

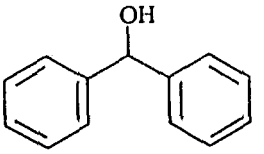

2

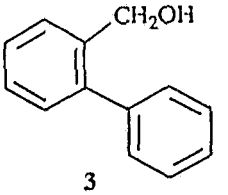

3

2.1.5 Photolysis of 5-Suberols. To probe the effect of removing the conjugation from the ICA that is present in the cationic intermediate generated from **1**, while at the same time preserving some degree of structural rigidity (provided by the central ring), the aryl-aryl bond was replaced by a bridging -CH_2CH_2- unit. This structural feature was expected to increase the excited state lifetime of **4**, compared to **2** and **3**.

2.1.5.1 Photolysis of 5-suberol (4) in aqueous methanol. When 5-suberol (**4**) was photolyzed in 50% MeOH-H_2O under conditions which lead to the extensive solvolysis of 9-fluorenol, little or no reaction occurred. However, on longer irradiation, 5-methoxysuberane (**58**) was produced as the major product. This methyl ether could be obtained in higher chemical yields than **17** (> 50%) because of the reduced tendency of the former to undergo secondary photochemical

reaction. Small amounts of the hydrocarbon suberane (**59**) did appear at higher conversions, presumably from the secondary photochemistry of the initially formed methyl ether.

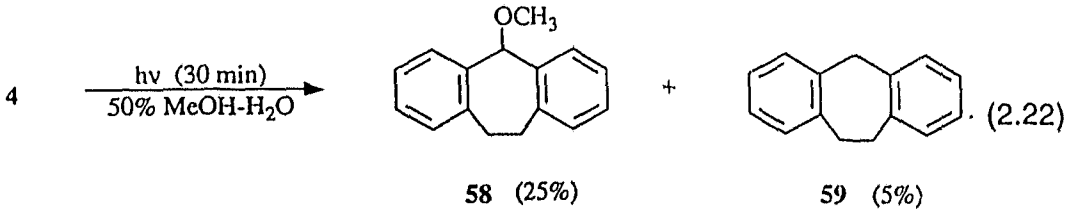

(2.22)

58 (25%) **59** (5%)

Table 2.6 summarizes some typical photolysis conditions and conversions to product. When **4** was photolyzed in 30% ACN-H_2O (0.25 **M** NaCN), the corresponding cyanosuberane (**60**) was obtained in low yields (< 10%).[95] Because the acid catalyzed thermal solvolysis of 5-suberol (**4**) becomes sufficiently rapid below pH ≈ 3, investigation of excited state acid catalysis was not carried out.

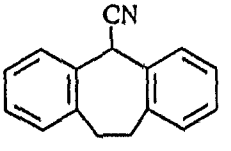

60

Table 2.6: Typical Photosolvolysis Reactions of 5-Suberol (4) in 50% MeOH-H_2O.

Substrate Conc. (x 10_{-3} M)	Photolysis Time (min)[a]	Conversion[b]	Product Distribution	
			58	**59**
2.4	5	≈ 5%	≈5%	-
4.8	30	30%	25%	5%
2.4	60	43%	32%	11%

[a] Argon saturated solutions were irradiated at λ_{ex}=254 nm.
[b] Conversions and product distributions were determined by ^{1}H NMR.

2.1.5.2 Photolysis of 5-methyl-5-suberol (24). Although the photosolvolysis of 5-suberol (**4**) was less efficient than 9-fluorenol (**1**), it did react to give the methyl ether in good yields on longer photolysis. It was therefore expected that the photodehydration reaction that was observed for 9-methyl-9-fluorenol (**12**), could be extended to **24**. Surprisingly, photolysis of **24** in 40% (v/v) ACN-H_2O for up to 60 min gave no trace of the expected 5-methylenesuberane (**61**).

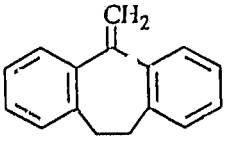

61

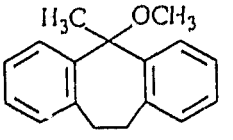

62

Alcohol **24** was photolyzed under a variety of conditions, including 50%

MeOH-H_2O. In each case the starting material was completely recovered. Both the methyl ether **62** and the alkene **61** could be prepared by thermal reactions at pH ≈ 2. The dramatic substituent effect that caused the complete lack of photoreactivity of **24** is still under investigation. It is thought that the conformational behaviour of dibenzocycloheptane derivatives can result in a dramatic decrease in reactivity as a result of stereoelectronic effects. The observation of dynamic ^{1}H NMR behaviour for this and some related compounds has lead us to investigate the ground state conformations (see below). Force field calculations (MMX)* indicated the presence of two potential energy minima for 5-substituted dibenzocycloheptane and dibenzocycloheptene derivatives. In the case of the alcohols **4** and **24**, the leaving group can adopt either a pseudo-equatorial or pseudo-axial orientation with respect to the seven membered ring. Overlap of the developing p-orbital, with the existing π-system of the phenyl rings is favoured only for the axial alcohols.

---

* Minimized structure input using PCMODEL3 (Serena Software). Full calculations including pi-atoms preformed using MMX (Serena Software).

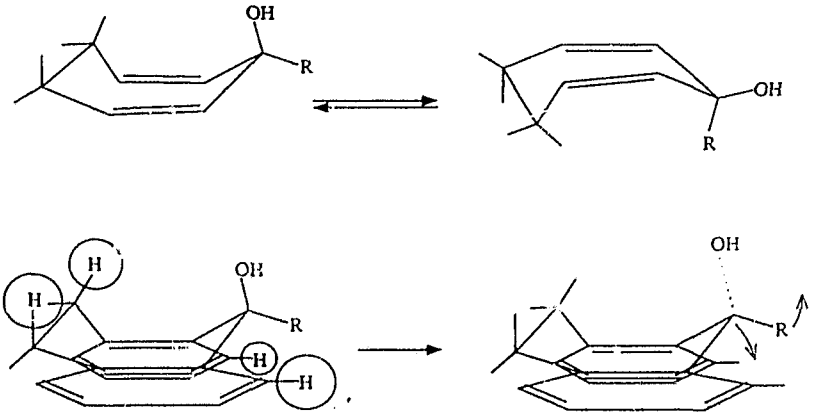

2.1.6 Photolysis of 5-Suberenols. On dehydroxylation, the suberenol derivatives **5** and **26** are precursors to dibenzotropylium ions. These alcohols will therefore readily solvolyze in the ground state in aq methanol solutions at pH ≤ 4. At neutral pH they are thermally stable.

2.1.6.1 Photolysis of 5-suberenol (5). When **5** was irradiated in 60% (v/v) MeOH-H_2O (pH ≥ 8) for 60 min, the starting material was almost completely recovered. Trace amounts of the **63**, **64**, and **65** were detected (≈ 5% each). Therefore, dehydroxylation appears to be only a very minor process for the excited state at this pH.

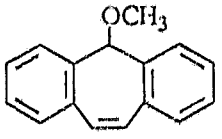

63

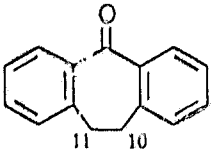

64

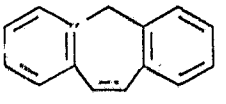

65

Extended photolysis of **5** in 30% (v/v) ACN-H_2O gave only dibenzosuberone (**64**) as the major photoproduct. When **5** was photolyzed in 30% (v/v) ACN-D_2O, **64** had incorporated deuterium at the 10 and 11 positions.[96] The mechanism of this reaction was elucidated further by the photolysis of 5-deuterio-5-suberenol (**25**) in aq ACN, which lead to small amounts of unlabelled **5** (via C_5-H heterolysis and exchange with the solvent), in addition to the ketone. Hence, the formation of **64** is thought to result from an initial C-H heterolysis followed by protonation of the carbanion at the 10-position and ketonization, as shown in eq 2.23.[96] This unusual C-H heterolysis, leading to an 8π electron intermediate carbanion, is an example of excited state carbon acid behaviour. A similar process has been observed and extensively studied for other dibenzosuberene compounds.[97,98]

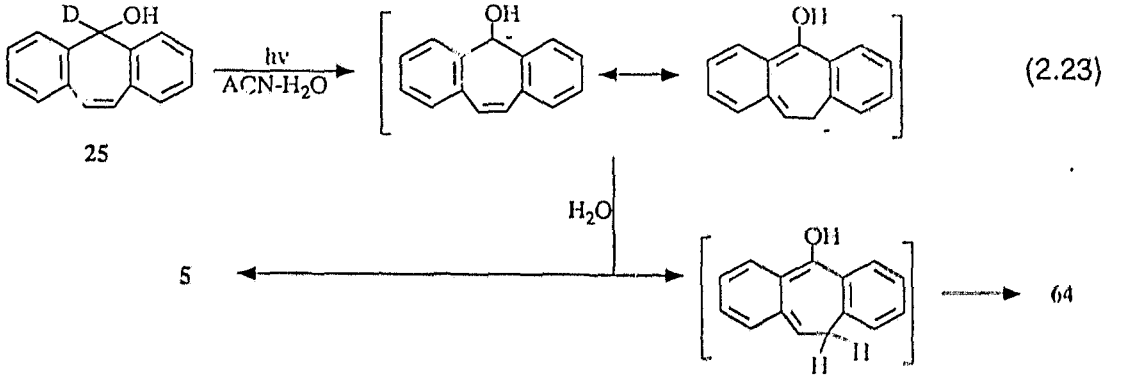

(2.23)

2.1.6.2 Photolysis of 5-methyl-5-suberenol (26). Photolysis of **26** in 60% (v/v) MeOH-H_2O (pH ≥ 8) for 60 min resulted in complete recovery of starting material. Neither the methyl ether **66**, nor the 5-methylene compound **67** were detected, even in trace amounts. Hence, the photodehydroxylation step does not appear to

occur at all at these pH's. For comparative purposes, both **66** and **67** were readily prepared under thermal conditions. That the ketone **64** is not observed is not surprising, given that the labile C_5-H bond has been replaced by a C_5-Me moiety. This behaviour is also reflected in the fluorescence behaviour of **5** and **26** (*vide infra*).

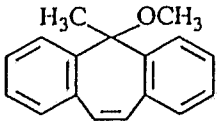

66

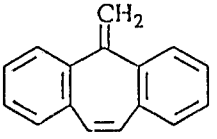

67

2.1.7 Photolysis of 11*H*-Benzo[b]fluoren-11-ol (20) and related systems. The very weak fluorescence emission of 9-fluorenol (**1**) and its derivatives resulted in our inability to probe the excited state directly. This lead us to search for more fluorescent 9-fluorenol analogues. The 2,3-benzannelated derivative of 9-fluorenol, **20**, provides another example of a *4n* π ICA system which is generated upon dehydroxylation. It is strongly fluorescent and has an excited state lifetime on the order of 20 ns in non-reactive solvents, making it ideal for steady-state and transient fluorescence measurements.

2.1.7.1 Photolysis of 11*H*-benzo[b]fluoren-11-ol (20). The photolysis of **20** in 60% MeOH-H_2O for 2 min resulted in a 50% conversion to the corresponding methyl ether, **68** (eq 2.24).

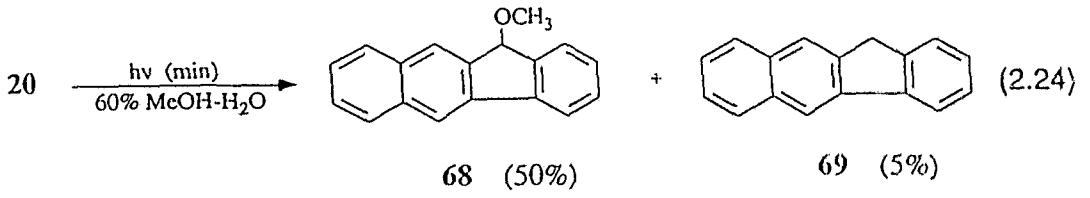

(2.24)

68 (50%) **69** (5%)

Photolysis of **1** under the same conditions resulted in only 20% conversion, indicating that the quantum yield of **20** is substantially higher. At higher conversions (> 50%) substantial amounts of the photoreduced product, 11*H*-benzo[b]fluorene (**69**), was also detected. Here again, independent photolysis of authentic **68,** and analysis of its time dependent product distribution (Figure 2.3), have shown that the initially formed methyl ether undergoes homolysis to yield the hydrocarbon.

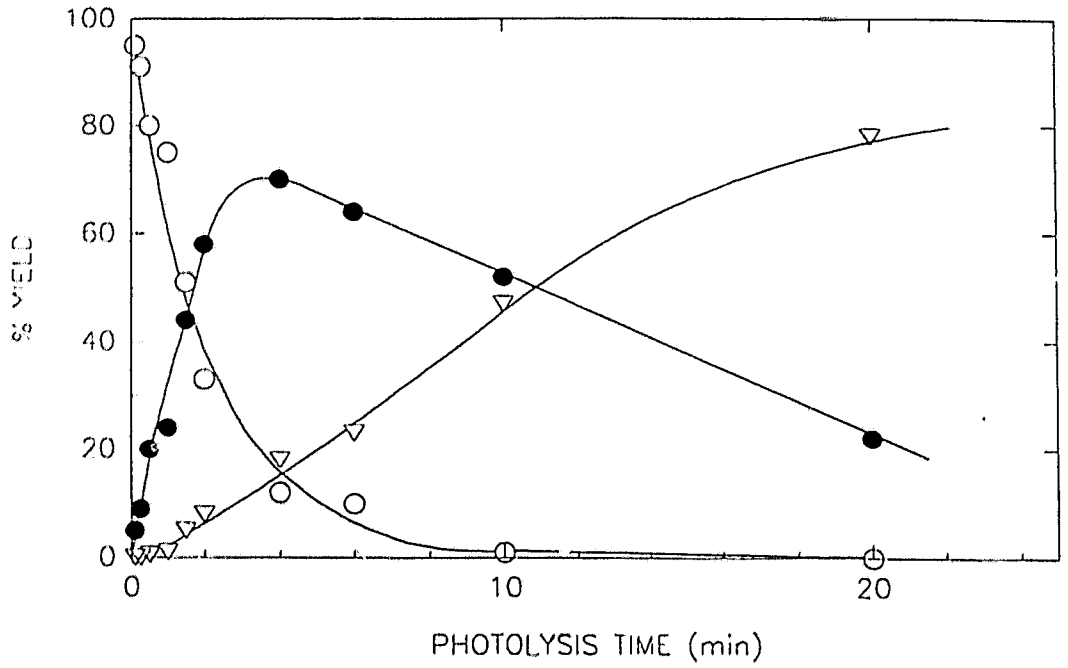

*Figure 2.3: Time Dependent Product Distribution on Photolysis of **20** in 50% MeOH-H_2O. Photolysis of 1 m**M** argon purged solutions in UV cuvettes; analysis by GC, (**20** hollow circles; **68** solid circles; **69** hollow triangles).*

Preparatory photosolvolysis in acidic aq MeOH solutions resulted in an increase in the conversion to the methyl ether, as indicated by the results shown in Table 2.7. Hence, acid catalysis of photosolvolysis of a fluorenol derivative has been firmly established.

Table 2.7: Conversions to Methyl Ether in the Photolysis of 11*H*-benzo[b]fluoren-11-ol (20) in 50% MeOH-H_2O under Acidic Conditions.

Acidity of Aqueous Portion[a]	Conversion
pH ≈ 6	19%
0.5 M H_2SO_4	28%
10% H_2SO_4	35%
30% H_2SO_4	50%[b]

[a] Argon purged solutions, (2.2 mM), were irradiated for 1.5 min.
[b] Dark reaction begins to make a minor contribution at this acidity.

11*H*-Benzo[b]fluoren-11-ol (**20**) was also photolyzed in other mixed alcohol-water solvents and the corresponding ethers have been isolated and characterized by ^{1}H NMR. Table 2.8 summarizes the preparative scale results. As observed for **1**, MeOH-H_2O solutions appear to favour ether formation to a greater extent than the other alcohol-water solvent systems. This is presumably due to a combination of factors, including the higher dielectric constant of methanol-water, which favours carbocation formation, as well as the more nucleophilic character of MeOH as compared to the other alcohols.

Table 2.8: Conversions and Product Distributions in the Photosolvolysis of 11*H*-Benzo[b]fluorenol (20) in Various Alcohol Solvents.

Solvent System[a] (vol/vol)	Mole Fraction of ROH (χ)	Conversion[b]	Product Distribution[c]	
			BFIOR	**69**
60% MeOH-H_2O	0.40	80%	65%	15%
60% EtOH-H_2O	0.32	48%	34%	14%
60% (*n*-PrOH)-H_2O	0.27	35%	26%	9%
60% (*i*-PrOH)-H_2O	0.26	32%	24%	8%

[a] Dearated solutions, (2.2 m**M** in substrate), were irradiated for 4 min.
[b] Conversions were determined by integration of ^{1}H NMR.
[c] Distributions were measured by GC analysis. BFIOR represents the appropriate ether product.

The excited state responsible for the heterolytic bond cleavage of **20** has been probed by carrying out triplet sensitization experiments. When **20** ($E_T \approx 57$ kcal mol^{-1})[90] was photolyzed in the presence of 2.5 g of sodium 2-benzoylbenzoate (**70**; $E_T \approx 69$ kcal mol^{-1})[90] at 350 nm and under conditions that would otherwise lead to extensive formation of the methyl ether, only trace amounts of **68** were produced. Upon longer irradiations the methyl ether was detected, but the UV absorption characteristics of the substrate/sensitizer solution indicated that the residual product formation may be due to light absorption by the substrate. This conclusion was supported by the fact that when the amount of sensitizer was reduced, the conversion to methyl ether increased. The difficulty in carrying out these experiments arises from the fact that the substrate has a long wavelength

absorption band at 340 nm and the sensitizer has only a weak, tailing absorption at 350 nm.

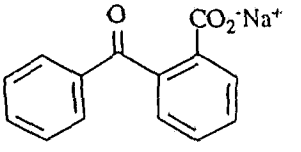

70

A number of attempts have been made to trap the incipient cation with added nucleophiles by photolyzing **20** in 50% (v/v) ACN-H_2O (0.25 **M** Br^- or CN^-). However, as was the case for the 9-fluorenyl system, no Br^- or CN^- substituted products were isolated.

2.1.7.2 Photolysis of α-(phenyl)-naphthalenemethanol (22). The alcohol 22, which does not contain an internal cyclic array upon dehydroxylation, was prepared as an analogue of 11*H*-benzo[b]fluoren-11-ol (**20**). When **22** was photolyzed in 50% MeOH-H_2O for 20 min (conditions more than sufficient to lead to the complete loss of **20**), it failed to react. In fact, the starting material was recovered in greater than 90% yield, even after a 60 min irradiation in this solvent. Hence **22** appears to be completely inert to photosolvolysis at neutral pH. However, when **22** was irradiated in a 50% MeOH-H_2O (0.1 **M** H_2SO_4) solution for 20 min, the corresponding methyl ether, **71**, was formed in 25% yield (eq 2.25). Dark control

reactions indicated that thermal solvolysis occurs too slowly at this acidity to account for the methyl ether formation in this photolysis.

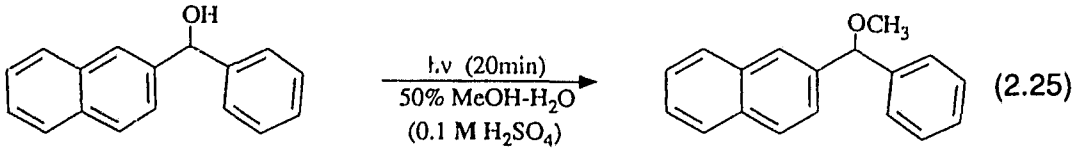

22 71 (25%) (2.25)

2.1.7.3 Photolysis of 11-methyl-11*H*-benzo[b]fluoren-11-ol (21). In an effort to extend the generality of the photodehydration reaction, which was first noted for **12**, preliminary studies were carried out on **21**. Photolysis in 60% MeOH-H_2O yielded the expected methyl ether **72** in high yield. However, when **21** was irradiated in 40% (v/v) ACN-H_2O for up to 20 min, the ^1H NMR indicated that only starting material was present. The failure of **21** to produce substantial amounts of benzo[b]dibenzofulvene was subsequently supported by a similar lack of reactivity, as monitored by UV absorption spectroscopy.

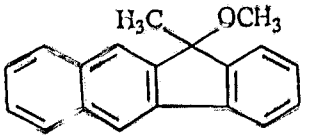

72

2.1.8 Photolysis of Other 9-Substituted Fluorenes 17-19. The product studies of 9-fluorenol (**1**) have indicated that both heterolytic and homolytic cleavage

pathways are accessible to the excited state. The results have clearly shown that the solvent plays an influential role in determining the outcome. Furthermore, the studies of 9-methoxyfluorene (**17**) indicate that the leaving group may also dramatically affect the mode of bond cleavage. To investigate these leaving group effects further several additional compounds have been photolyzed. The results of the photolysis of 9-bromo (**18**), 9-acetoxy (**19**) and 9-methoxy (**17**) fluorenes in 50% (v/v) ACN-H_2O are summarized in Table 2.9. The nature of the photoproducts is taken as indicative of the cleavage pathway followed. Whereas **17** undergoes predominantly homolytic cleavage, 9-bromofluorene (**18**) appears to solvolyze rapidly via a heterolytic pathway. The acetate **19** is less reactive than the other two, and probably undergoes both homolytic and heterolytic processes concurrently.

Table 2.9: Conversions and Product Distributions in the Photolysis of 9-Substituted Fluorenes in 50% ACN-H_2O.

Compound[a]	Conversion	Product Distribution[c]		
		1	**33**	**34**
17	65%	~ 2%	58%	5%
18	62%	58%	< 2%	~ 3%
19	26%	16%	5%	5%

[a] Each solution contained 100 mg of substrate in 120 mL of deaerated solvent and was irradiated for 10 min at 254 nm.
[b] Product distribution analyzed by ^1H NMR and GC.

9-Bromofluorene (**18**) was also photolyzed in 50% (v/v) MeOH-H_2O to determine the extent to which methanol and water compete as nucleophiles for the incipient cation.

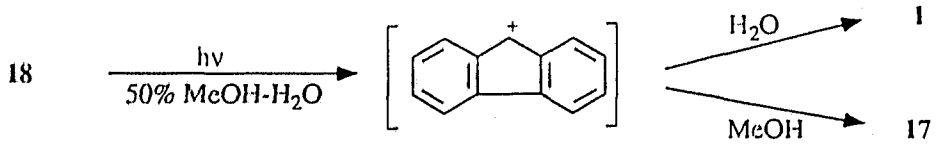

(2.26)

When **18** was irradiated in 50% (v/v) MeOH-H_2O the two solvolysis products, **1** and **17**, were produced in 20 and 40% yields respectively. The product ratio, together with the molar ratio of the two nucleophiles, yields k_{MeOH}/k_{H_2O}, according to equation 2.27.

$$\frac{k_{MeOH}}{k_{H_2O}} = \frac{\%\ Conversion\ 17}{\%\ Conversion\ 1} \times \frac{[H_2O]}{[MeOH]} \qquad (2.27)$$

A value of $k_{MeOH}/k_{H2O} = 4.5 \pm 0.4$ was calculated, which is a factor of two greater than the capture ratio determined for **1** (*vide supra*). The thermal and photochemical solvolysis reactions gave similar product ratios, indicating there was little difference in selectivity of the photochemical and thermal processes.

2.2 QUANTUM YIELDS

The product quantum yields for methyl ether formation have been measured

in 50% (v/v) MeOH-H_2O. The quantum yield of 9-fluorenol (**1**), $\Phi_p = 0.139 \pm .007$, has been accurately measured at pH 7 and used as a secondary reference for quantum yield determinations of several of the other compounds. The quantum yield of 11*H*-benzo[b]fluoren-11-ol (**20**), the most photosolvolytically efficient compound in the series, has also been accurately determined, $\Phi_p = 0.56 \pm .01$. In addition to quantifying the yields at pH 7, the effect of pH on the efficiency of photosolvolysis has also been investigated. Solvent isotope effects have been measured for the most reactive systems.

2.2.1 Quantum Yields in 50% MeOH-H_2O. The quantum yields for 9-fluorenol (**1**) and 11-benzo[b]fluorenol (**20**) have been measured using a 200 W Hg lamp light source and a monochromator (λ_{ex} = 280 nm, 5 nm slits) on an optical bench. Potassium ferrioxalate actinometery was employed to monitor the light intensity, (see appendix B). Both the substrate and the actinometer solutions were purged with a stream of argon prior to and during the photolysis to effect dearation and stirring. Three independent determinations were made for each compound and the standard deviation within each set has been quoted as the error associated with each quantum yield. The values obtained were reproducible to better than ±5% of the quoted value.

Table 2.10: Product Quantum Yields, (Φ_p), of Methyl Ether Formation for 1 and 20.

Φ_p	
1	**20**
0.139 ± .007	0.55_5 ± .01

The product quantum yield of 9-fluorenol (**1**) was employed as a secondary chemical actinometer for a number of the 9-substituted-9-fluorenols. These determinations were made by simultaneously irradiating equal molar solutions of each compound in UV cuvettes using a merry-go-round apparatus in a RPR photochemical reactor,(λ_{ex} = 254 nm). The conversions were monitored by GC and the results are summarized in Table 2.11. The methyl and isopropyl substituted 9-fluorenol derivatives have quantum yields marginally higher than **1** itself. On the other hand, the quantum yields for the t-butyl and phenyl derivatives are substantially greater than that for **1**. The effect of replacing the α-hydrogen with a deuterium is shown in the first entry of Table 2.11. The slightly reduced yield for this compound reflects a secondary isotope effect, $\Phi_{\alpha\text{-}H}/\Phi_{\alpha\text{-}D} = 1.17 \pm 0.09$.

Table 2.11: Product Quantum Yields (Φ_p) of Methyl Ether Formation for Substituted 9-Fluorenols.

Compound	Φ_p [a]
11	0.12 ± .01
12	0.16 ± .02
14	0.17 ± .02
15	0.25 ± .03
16	0.26 ± .03

[a] Measured using **1** as a secondary actinometer. Conversions were determined by GC. Photolysis carried out in 50% MeOH-H_2O (pH 7).

The product quantum yields of the other diaryl alcohols in the series are tabulated in Table 2.12. Because of difficulties encountered in the GC analysis of some derivatives, the conversions in larger scale photolysis were used to estimate the quantum yields. The photosolvolysis of **1** was employed for comparison purposes, and the conversions determined ^{1}H NMR integration.

Table 2.12: Product Quantum Yields of Methyl Ether Formation for 2 - 5 and Several Derivatives.

Compound	Φ_p[a]
2	<0.002[b]
3	<0.002[b]
4	≈0.07[c]
5	≈0.01[c]
22	<0.002[b]
24	<0.002[b]
26	<0.002[b]

[a] Using **1** and/or 3,5-dimethoxybenzyl alcohol as secondary actinometers. Photolysis carried out in 50% MeOH-H_2O (pH ≥ 7).
[b] Estimated upper limit.
[c] Based on ^1H NMR integration.

2.2.2 Quantum Yields as a Function of pH. Since acid catalysis has been used as an important criterion for a heterolytic bond cleavage step in other photodehydroxylations, the yield of methyl ether has been monitored as a function of pH. Initial studies were carried out on 9-fluorenol (**1**) over a range of acidities in which other substituted benzyl alcohol systems had displayed rate accelerations (pH 1 - pH 12).[32,34,35] However, the quantum yield for the production of 9-methoxyfluorene (**17**) was invariant over this entire pH range. Subsequent preparative photosolvolysis (*vide supra*) did indicate that acid catalysis occurred in stronger acid solutions (i.e., 5% H_2SO_4, H_o = 0.04). Using the optical bench apparatus, the quantum yield was measured in 50% MeOH-H_2O (0.5 **M** H_2SO_4, H_o

= 0.06) and found to be 0.162 ± .008. This modest increase, compared to neutral solution, appears to be the beginning of an acid catalyzed region. In contrast to the behaviour of **1**, 11-benzo[b]fluorenol (**20**) displayed acid catalysis at pH ≈ 2. The quantum yield increased dramatically between pH 2 and pH 1, reaching a maximal value close to unity at pH ≤ 1. The quantum yield determined in 50% (v/v) MeOH-H_2O (0.25 **M** H_2SO_4, H_o = 0.45) was measured to be 0.98 ± .08. A plot of Φ_p as a function of the pH (or H_o) of the aqueous portion is shown in Figure 2.4. The quantum yield of the related compound **22**, which showed no reactivity in neutral solution, was determined to be Φ_p = 0.018 in 50% MeOH-H_2O (pH 1).

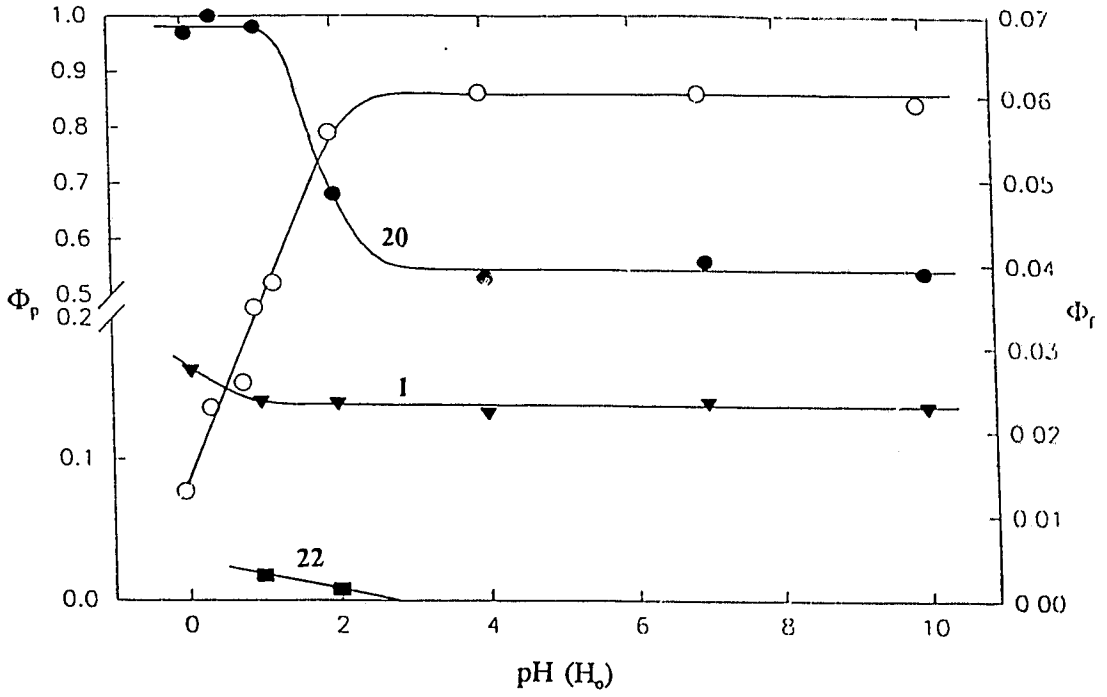

*Figure 2.4: Plot of Product Quantum Yield for Methyl Ether Formation as a Function of pH (H_o). (Product quantum yields shown for: **1** solid squares, **20** solid circles, and **22** solid triangles. Also included are the fluorescence quantum yields for **20**, open circles).*

2.2.3 Solvent Isotope Effects. To probe solvent isotope effects, **1** and **20** were photolyzed in 50% (v/v) MeOD-D_2O. The observed effects were not large, but are reproducible (Table 2.13). They are greater than unity in each case, indicating a positive isotope effect.

Table 2.13: Product Quantum Yield (Φ_p) in MeOD-D_2O and Solvent Isotope Effect (Φ_{H_2O}/Φ_{D_2O}) of Methyl Ether Formation for 1 and 20.

Compound	$\Phi_{MeOD\text{-}D_2O}$[a]	Φ_{H_2O}/Φ_{D_2O}
1	0.128 ± 0.006[b]	1.09 ± 0.05
20	0.52_6 ± 0.01[c]	1.06 ± 0.03

[a] Conversions were measured by GC.
[b] Two determinations.
[c] Four determinations.

2.2.4 Quantum Yields in Other Solvents. The reactivity of **1** and **20** has been monitored in a number of solvents other than 50% MeOH-H_2O, (Table 2.14). For instance the quantum yield for methyl ether formation in 100% MeOH is 0.07 and 0.27 for **1** and **20**, respectively. Thus the efficiency of photosolvolysis is reduced, by roughly 50% on changing to pure methanol. This is presumably a reflection of the reduced ability of the medium to promote heterolysis. The photodecomposition of **1** in pure ACN is a very efficient process, with an estimated quantum yield of ≈ 0.25. A number of products were identified in this reaction, as shown in eq 2.12. This reactivity accounts for the rapid changes in the fluorescence spectrum of **1** in this solvent (*vide infra*). The quantum yields for the formation of the various ethers, generated by photosolvolysis in other alcohol-water solvents, are also listed in Table 2.14.

Table 2.14: Quantum Yields for 1 and 20 in Other Solvents.

Solvent	Φ_p	
	1	**20**
100% MeOH	0.07 ± 0.02[a]	0.27 ± 0.03[a]
100% ACN	≈0.25[b]	-
50% EtOH-H_2O	0.12 ± 0.03[c]	0.32 ± 0.05[c]
50% 1-PrOH-H_2O	-	0.26 ± 0.04[c]
50% 2-PrOH-H_2O	0.09 ± 0.03[c]	0.22 ± 0.04[c]

[a] For methyl ether formation as determined by GC.
[b] For loss of substrate as monitored by ^{1}H NMR.
[c] For ether formation as monitored by ^{1}H NMR.

2.3 FLUORESCENCE AND UV ABSORPTION STUDIES

Steady-state and transient fluorescence measurements can provide crucial information about excited singlet states. In addition to fluorescence lifetimes, which are necessary for a comparison of the excited state reactivities, a number of dramatic solvent and structural effects have been observed in the steady state fluorescence work. The possibility of an adiabatic photodehydroxylation step has been investigated and observed for at least one of the alcohols in the series. The photodehydration reaction, which was observed for 9-substituted-9-fluorenols bearing a β-hydrogen, was accompanied by a dramatic change in the UV absorption spectrum.

2.3.1 Spectral Characteristics. The absorption and fluorescence emission

spectral characteristics of alcohols **1** - **5** and **11** - **27** are largely governed by their parent hydrocarbon chromophores. The fluorescence excitation and emission spectra for the unsubstituted compounds **1**, **4**, and **5** (in ACN) are shown in Figure 2.5. The spectral distributions of the alcohols are similar to the corresponding hydrocarbons, but the fluorescence emission intensity varies widely, and is particularly sensitive to the nature of the solvent. The fluorescence properties of 9-fluorenol (**1**) are dramatically different from those of fluorene itself. The latter, which derives its name from its strongly fluorescent properties, has a fluorescence quantum yield of ≈ 0.80.[99] On the other hand, 9-fluorenol (**1**) appears to be remarkably weakly fluorescent in ACN, $\Phi_f < 0.01$. Furthermore, the fluorescence properties of **1** are highly variable since significant photodecomposition occurs during spectral acquisition (*vide infra*). Unfortunately, **11** - **16** and **23** behave similarly. For this reason, the spectrum shown in Figure 2.5 (panel a) needs to be regarded with some degree of caution. The fluorescence excitation spectrum, obtained from a fresh sample, shows a strong resemblance to the UV absorption spectrum, which has a relatively strong absorption at 305 nm ($\varepsilon \approx 10^3$ M^{-1} cm^{-1}). The lowest energy band in the excitation spectrum nearly overlaps the high energy emission band, indicative of a negligible Stokes loss. The absorption spectra of suberols **4** and **24** are similar to one another, with long wavelength absorption bands at $\lambda_{max} \approx 266$ nm ($\varepsilon \approx 10^2$ M^{-1} cm^{-1}); this is consistent with the excitation spectrum shown in panel b of Figure 2.5. The emission occurs over a relatively narrow range with a $\lambda_{max} \approx 288$ nm, which is only moderately Stokes shifted (≈ 8

kcal mol^{-1}). The electronic transitions of the suberenols (**5** and **26**)are red-shifted, relative to the suberols, due to their increased conjugation. The broad structureless absorption, $\lambda_{max} \approx 285$ nm ($\varepsilon \approx 10^4$ **M**$^{-1}$ cm^{-1}), is also reflected in a broad excitation spectrum. The emission is similarly broadened ($\lambda_{max} \approx 370$nm) and appreciably Stokes shifted ($\approx$ 22 kcal mol^{-1}). The broad, featureless characteristics are indicative of a structurally non-rigid system.

The absorption spectra of **20** and **69** are similar, with a long wavelength band at $\lambda_{max} \approx 340$ nm. Compound **22** does not possess this longer wavelength absorption; its absorption spectrum resembles that of naphthalene. The fluorescence excitation and corrected emission spectra of **20**, **22**, **69** are shown in Figure 2.6.

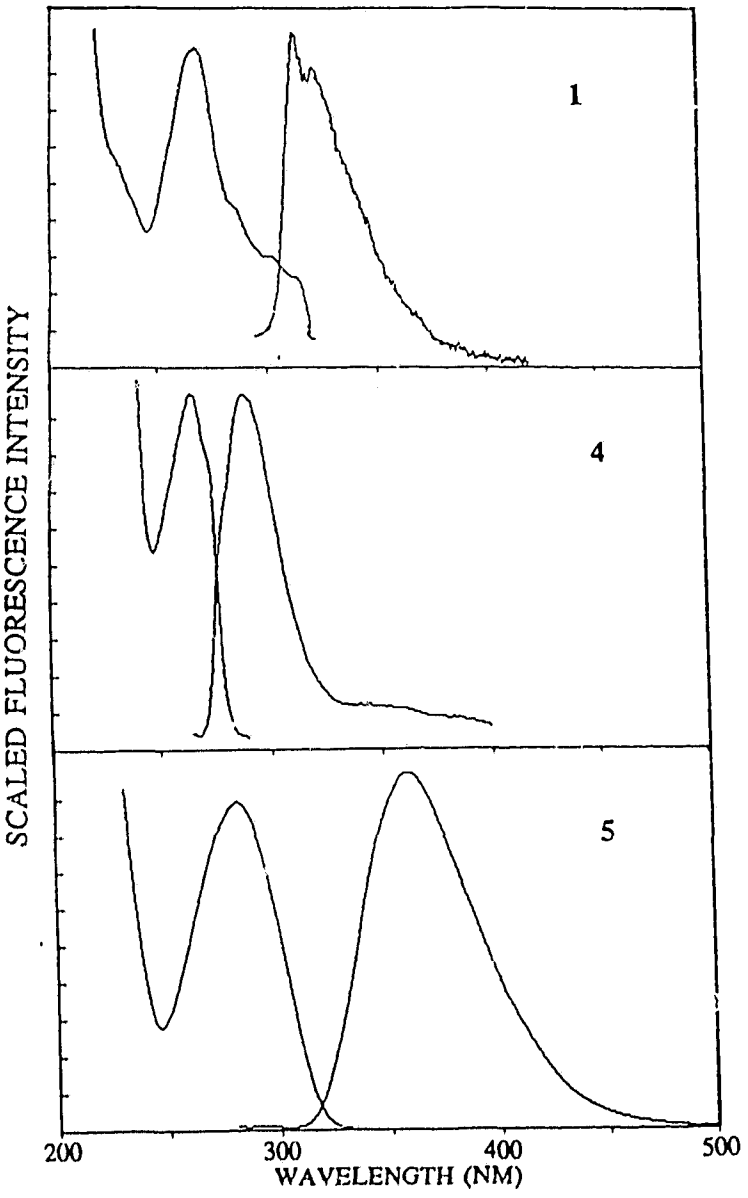

*Figure 2.5: Excitation and Emission Spectra of **1**, **4** and **5** in ACN.*

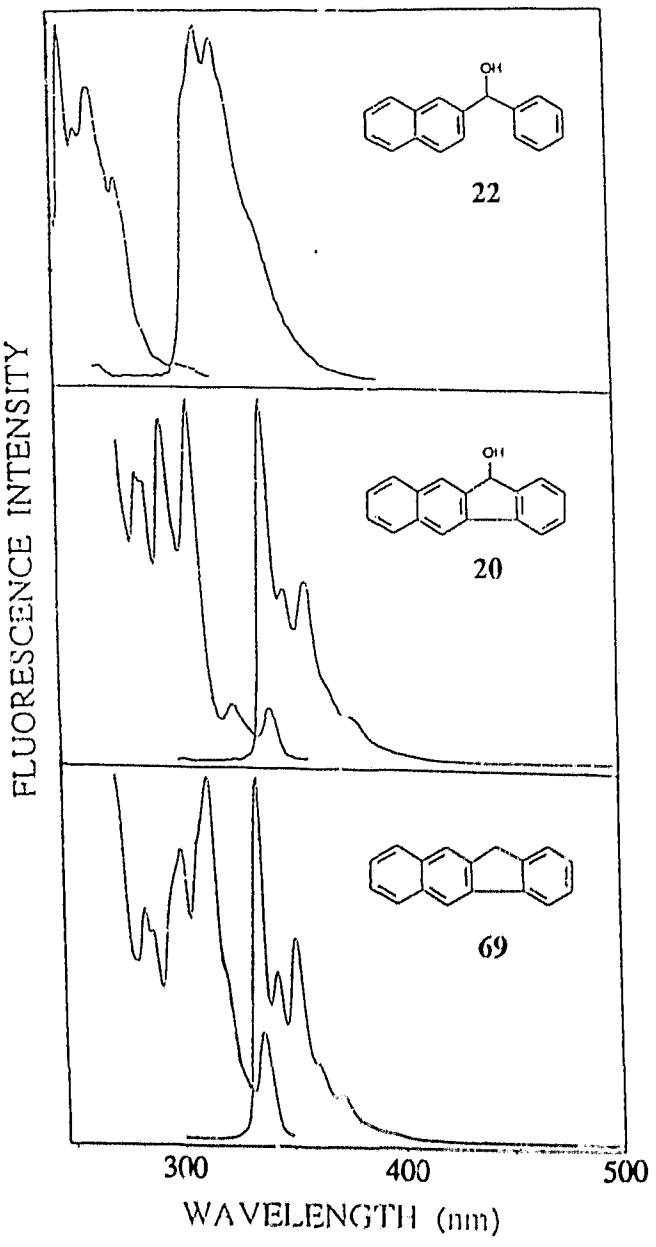

*Figure 2.6: Excitation and Emission Spectra of **20**, **22**, and **69** in ACN.*

Fluorescence quantum yields have been measured for **20**, **22** and **69** in ACN and in 50% MeOH-H_2O (Table 2.15). The hydrocarbon **69** is an intensely fluorescent compound, $\Phi_f \approx 0.84$. The emissive properties of the related alcohol, **20**, are reduced considerably in ACN ($\Phi_f = 0.26$) and even further in MeOH-H_2O ($\Phi_f = 0.06$). Compound **22** ($\Phi_f = 0.10$) is considerably less fluorescent than naphthalene ($\Phi_f = 0.23$),[143] presumably due to the added complexity and internal degrees of freedom introduced by the pendant benzyl alcohol group. The fluorescence quantum of **22** is identical in these two solvents, consistent with the observation that it is unreactive at neutral pH.

Table 2.15: Fluorescence Quantum Yields (Φ_f) for 20, 22, and 69.

Solvent	Φ_f[a]		
	20[b]	**22**[c]	**69**[b]
ACN	0.26 ± 0.03	0.10 ± 0.01	0.82 ± 0.06
50% MeOH-H_2O	0.06 ± 0.01	0.10 ± 0.01	0.85 ± 0.06

[a] Determined by comparing the integrated emission areas of absorbance matched solutions with recommended standards.[143]
[b] Secondary standard was 2-aminopryidine in 0.05 **M** H_2SO_4, $\Phi_f = 0.60$.
[c] Secondary standard was naphthalene in cyclohexane, $\Phi_f = 0.23$.

Steady-state fluorescence spectroscopy provides the only available means of probing whether or not a photochemical reaction proceeds on the excited state

surface, that is *adiabatically*. If fluorescence emission of an intermediate or photoproduct is observed under conditions where only the substrate molecules are being excited, then direct evidence for an adiabatic reaction is provided. Although the photodehydroxylation of 9-phenyl-9-xanthenol (**XXIV**) has been shown to occur, at least to some extent, via an adiabatic process,[33] similar evidence for the present series of alcohols has not, in general, been obtained. Aside from the aforementioned problems associated with obtaining fluorescence spectra of 9-fluorenol derivatives, the estimated energy gap between the ground and excited state 9-fluorenyl cations may be on the order of only 25-35 kcal mol^{-1}, which would mean that the emission from the cation, if it occurred, would be in the near IR region (λ_{max} > 800 nm), making detection a problem using available equipment. Unfortunately, the formally antiaromatic 9-fluorenyl cation has not been unambiguously characterized (spectroscopically) in the ground state.[100] Thus the characteristics of the absorption and emission spectra have not been clearly established. The only system for which adiabatic fluorescence from the cation has been observed is 5-suberenol (**5**). A very weak emission was observed at λ_{max} = 556 nm (Figure 2.7, spectrum a) which matches the emission from the authentic cation (Figure 2.8, spectrum b). Moreover, the excitation spectrum of the 556 nm emission band is identical to that of the parent alcohol (Figure 2.8, spectrum c). Although it is clearly a minor process, **5** has thus been shown to undergo adiabatic photodehydroxylation.

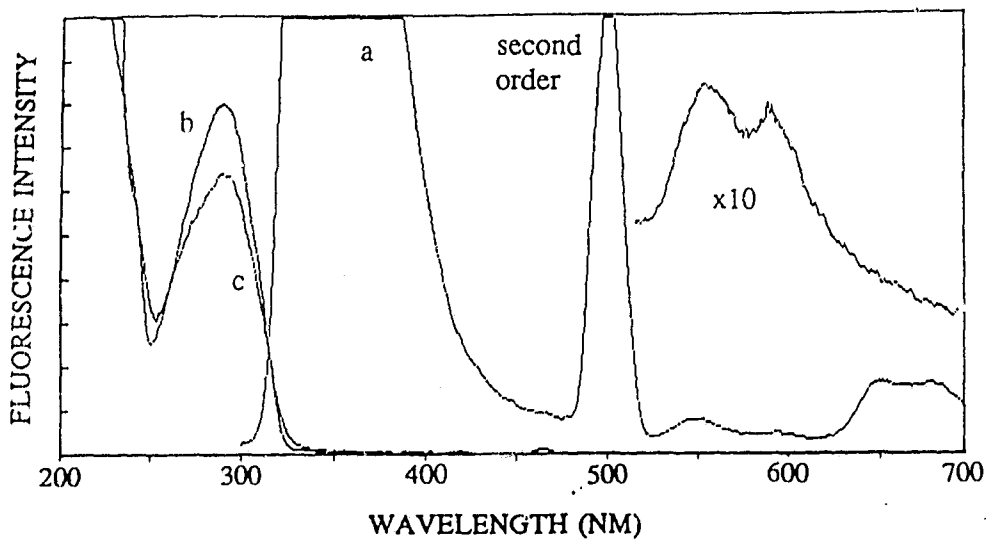

*Figure 2.7: Excitation and Emission Spectra of **5** in H_2O (pH 7). (a) emission scan using 250 nm excitation, substrate emission band offscale at 380 nm; (b) excitation scan monitored at 380 nm; (c) excitation monitored at 550 nm.*

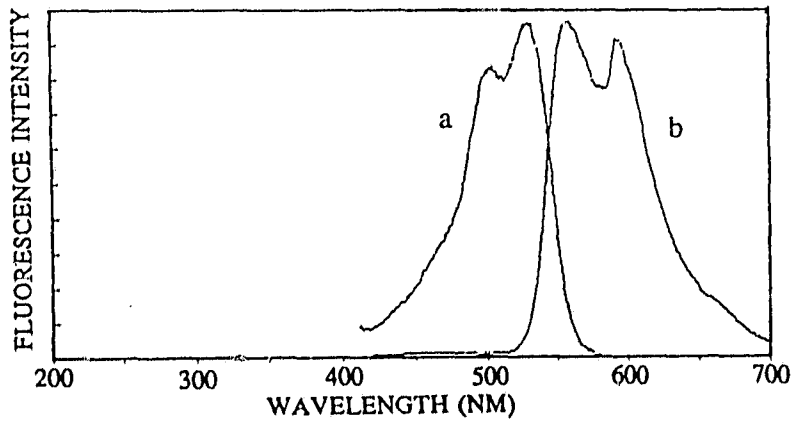

*Figure 2.8: Excitation and Emission Spectra of **5** in 40% H_2SO_4. (a) excitation scan monitored at 600 nm; (b) emission scan using 400 nm excitation.*

2.3.2 Solvent and pH Effects. Solvent and pH dependence of the emission intensity of a substrate can provide useful information. If, for instance, the

fluorescence emission is quenched on going to a solvent where the substrate is known to react photochemically, then the singlet excited state is implicated as the reactive state. The fluorescence of **4**, which is only marginally reactive towards photosolvolysis in aqueous solution, shows only a slight quenching effect on the addition of water. The methyl derivative **24**, which appeared completely unreactive in preparative studies, displayed no solvent effect. Similar behaviour was also observed for the non-reactive suberenol systems, **26** and **27**. Therefore it was unexpected that 5-suberenol (**5**), which was essentially unreactive towards photosolvolysis at pH $\geq$ 7, displayed a dramatic solvent effect. On changing the solvent from ACN to H_2O, the fluorescence emission was quenched 50% and the spectral distribution was slightly blue shifted. Comparing the fluorescence properties of **26** and **27** with those of **5**, it would appear that the unusual behaviour of **5** are associated with the C_5-H substituent. This is consistent with the observation that **5** undergoes C_5-H photoexchange with D_2O and reacts to yield the ketone, **64**, in aqueous solvents. An overlay of the emission spectrum of **5** in ACN, H_2O and D_2O are shown in Figure 2.9.

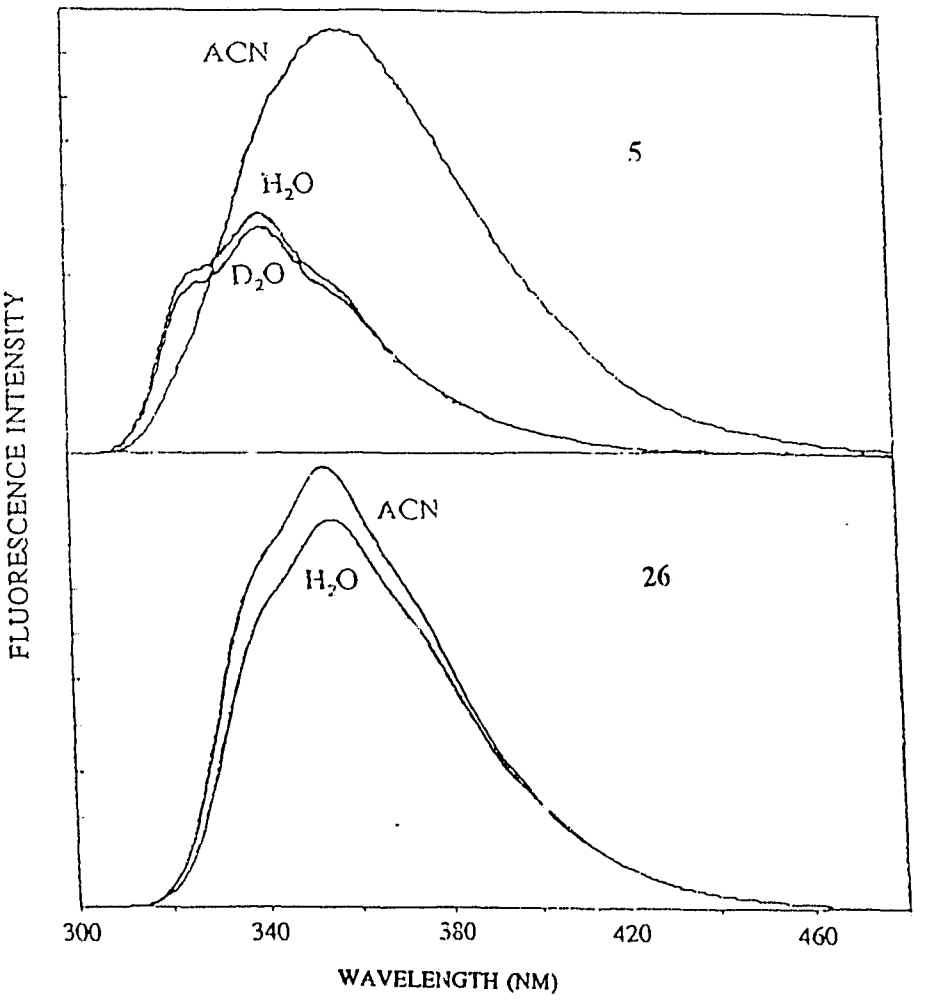

*Figure 2.9: Fluorescence Spectra of **5** and **26** in Various Solvents. (10^{-5} **M** solutions were argon saturated and excited at 280 nm.)*

Similar solvent affects were observed in the solvent dependent fluorescence lifetimes of **5**, **26**, **27** and **65** (Table 2.16), and have subsequently been associated with a C_5-H heterolytic bond cleavage process (excited state carbon acid behaviour). An even more dramatic solvent effect has been observed for the parent hydrocarbon, dibenzosuberene (**65**). The fluorescence emission of this compound was almost completely quenched in H_2O, as shown in Figure 2.10.

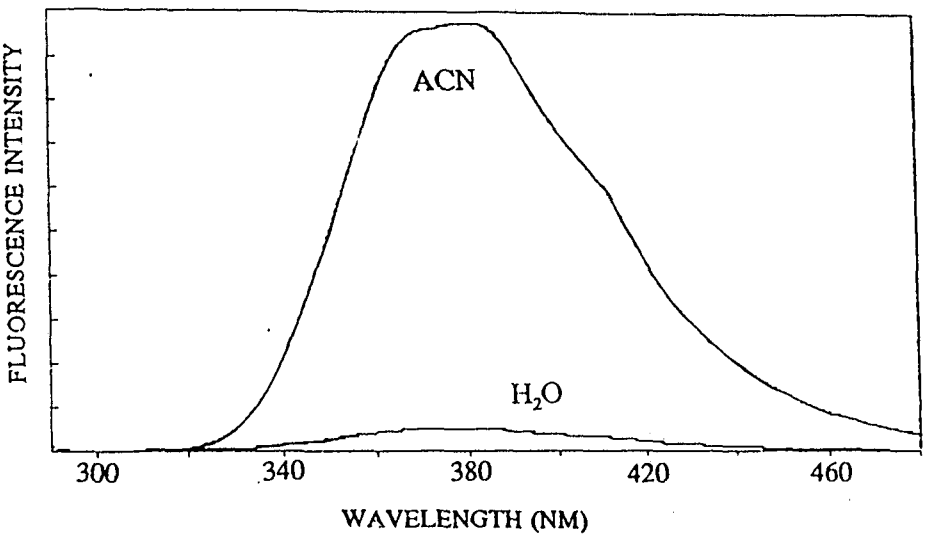

*Figure 2.10: Fluorescence Spectra of **65** in ACN and H_2O. (10^{-5} **M** solutions were argon saturated and excited at 280 nm.)*

Unfortunately, fluorescence studies of the 9-fluorenol derivatives have proved difficult. The placement of a hydroxyl group in the 9-position has a remarkable quenching effect on the emissive properties of fluorene. The unusually weak fluorescence behaviour is further complicated by our inability to obtain reproducible spectra. The spectra obtained are very time dependent because the fluorescence intensity increases rapidly with exposure of the sample to the excitation beam of the spectrofluorimeter. Apparently, the rapid photochemical production of intensely fluorescent chromophores occurs in the spectrofluorimeter during the time required to obtain a scan of the emission wavelengths. Similar behaviour was observed for the other 9-substituted-9-fluorenols, as well as 1-indenol (**23**). The very weak emission of 9-fluorenol (**1**) has therefore been monitored as a function of time in a number of solvents. On exposure to the light source in MeOH-H_2O, the initially weak and structureless emission at $\lambda_{max} \approx 315$

nm begins to resemble the more structured emission band of fluorene ($\lambda_{max} \approx 305$ nm).

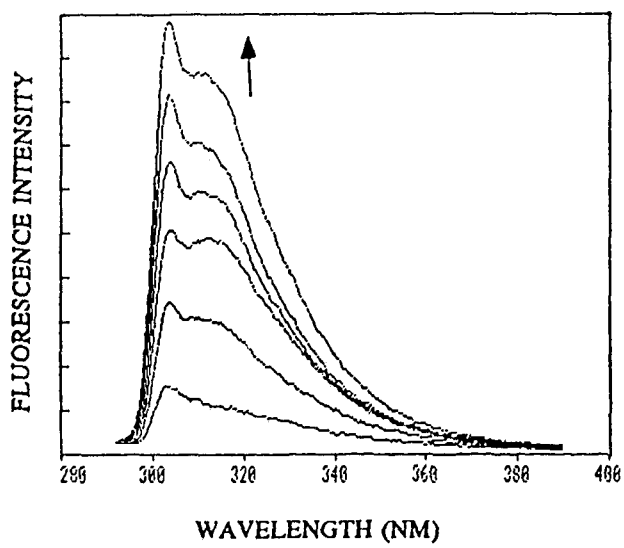

Figure 2.11: Successive Fluorescence Spectra of **1** *in 50% MeOH-H_2O. (Argon saturated solution were excited at 260 nm with 4 nm slits, Δt = 1 min)*

This behaviour is consistent with our present understanding of this system. The extremely weak emission of **1** is rapidly masked by minute amounts of the much more fluorescent product fluorene (**33**). It has been shown (*vide supra*) that in this solvent system the production of fluorene (**33**) promptly follows photosolvolysis, via the secondary photolysis of 9-methoxyfluorene (**17**). That such affects mask the original spectrum in such a short time can be understood when one considers that the photoproduct is probably three orders of magnitude more fluorescent than 9-fluorenol (**1**) itself. Samples of **1** are more "fluorescence stable"

in 100% H_2O, but decompose on longer exposures, as shown in Figure 2.12. A different photodecompostion pathway, probably a rearrangement to a ring substituted hydroxyfluorene, gives rise to the new emission in this solvent.

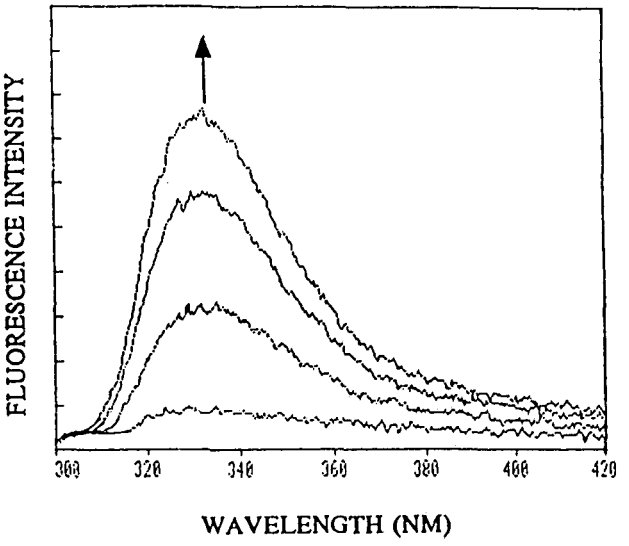

Figure 2.12: Successive Fluorescence Spectra of **1** *in H_2O. (Argon saturated solution were excited at 260 nm with 5 nm slits, Δt = 5 min)*

The fluorescence intensity of **1** has been monitored as a function of time in ACN, H_2O and CH_3OH and extrapolated to zero time. When this is done, it appears that 9-fluorenol (**1**) has a residual fluorescence only in ACN. In the other two solvents, **1** appears to be essentially non-fluorescent. That this time dependent behaviour exists in ACN is consistent with the fact that 9-fluorenol (**1**) undergoes photochemical decomposition in this solvent as well (*vide supra*).

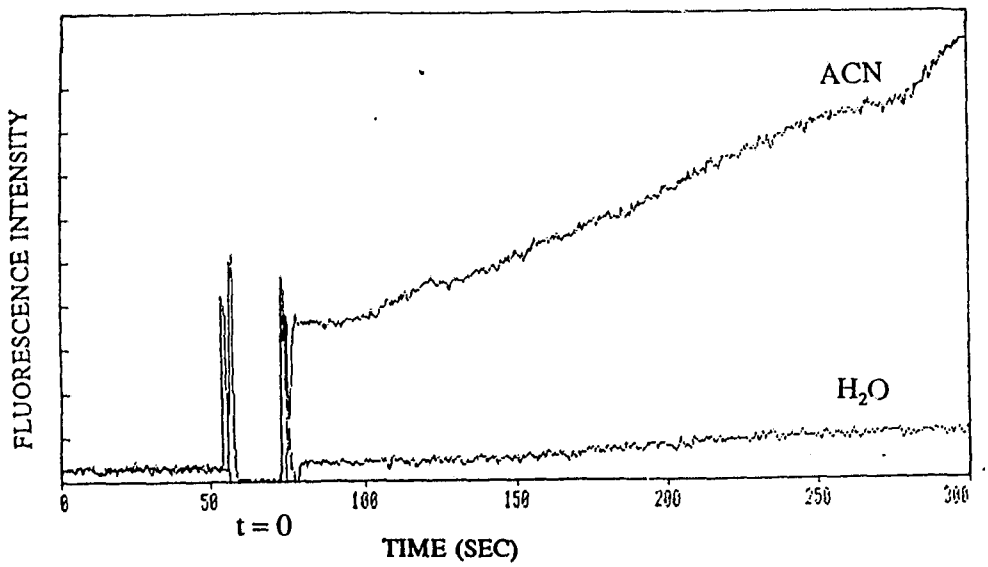

*Figure 2.13: Time Dependent Fluorescence Intensity of **1** in ACN and H_2O. (Argon saturated solutions were excited at 260 nm, monitoring emission at 320 nm with 5 nm slits)*

As a result of the extremely weak and time dependent fluorescence properties of **1**, the 2,3-benzannelated derivative, **20**, was studied. This compound proved to be much more convenient for fluorescence work. The emission intensity of **20** showed a marked solvent dependence, whereas the intensity of the hydrocarbon **69** was invariant with a change in solvent, consistent with a similar trend in the fluorescence lifetimes (*vide infra*). The reference alcohol **22** displayed a reduced emission intensity only in acidic solutions, pH < 1, concurrent with its increased reactivity in acidic solution. The relatively intense fluorescence of 11*H*-benzo[b]fluoren-11-ol (**20**) in ACN (Φ_f = 0.26) was quenched considerably in H_2O (Φ_f = 0.06), consistent with its increased reactivity in this solvent. The emission was further quenched at acidities below pH ≈ 2, consistent with the observed acid

catalysis for methyl ether formation in aq methanol (*vide supra*). The fluorescence quantum yields (Φ_f) for 11*H*-benzo[b]fluorenol (**20**) have been plotted in Figure 2.4 (open circles). The complementary behaviour of the acid catalyzed photosolvolysis reaction and the acid quenching of the fluorescence provide further support for a reactive singlet excited state.

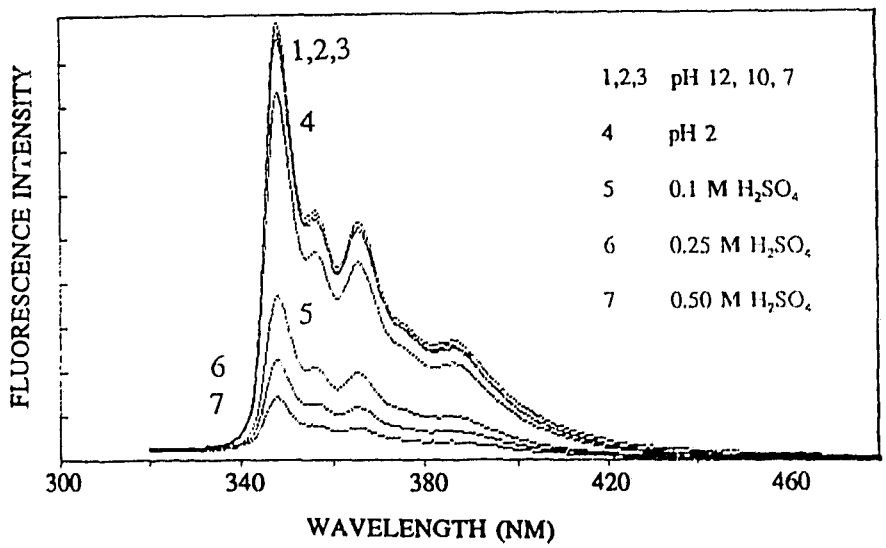

*Figure 2.14: Fluorescence Emission of **20** at Different pH's (or H_o). (10^{-5} **M** solutions were argon saturated and excited at 300 nm; 20% ACN used as a co-solvent, acidity refers to aqueous portion.)*

The fluorescence quenching occurs in the same pH range that acid catalysis was observed, and therefore provides further evidence that the rate associated with bond cleavage is accelerated by protons. The Stern-Volmer relation, arises from the treatment of a simple kinetic scheme in which the excited singlet

$$\frac{\Phi_f^o}{\Phi_f} = 1 + k_q\tau_f[Q] \qquad (2.28)$$

state is depleted by the bimolecular interaction with a quencher, Q. The slope of a plot of Φ_f^o/Φ_f versus [Q] yields $k_q\tau_f$. Thus, provided the lifetime in the absence of the quencher is known, the quenching rate constant, k_q, can be evaluated. A Stern-Volmer treatment of the data for **20** yields a straight line with a slope of 11.9 M^{-1} (Figure 2.15). The slope provides a measure of k_q, which can be equated with the acid catalyzed rate coefficient, k_H. Using a value of τ_f = 3.8 ns in 20% ACN-H_2O (pH 7), k_H is calculated to be 3.1 ± 0.2 x 10^9 M^{-1} s^{-1} in this solvent.

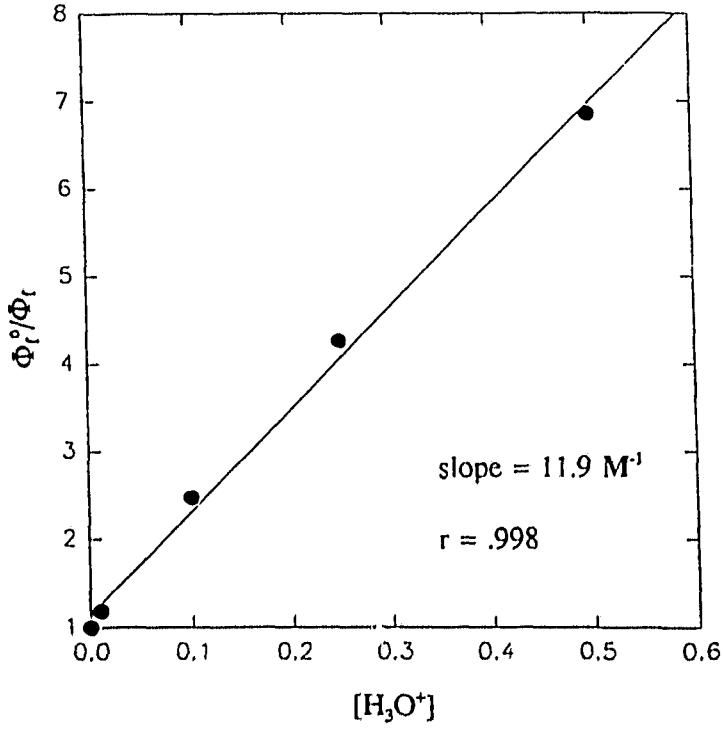

*Figure 2.15: Stern-Volmer plot of Φ_f^o/Φ_f versus $[H_3O^+]$ for **20**.*

2.3.3 Fluorescence Lifetimes. Knowledge of the fluorescence lifetime of a compound is essential in determining its excited state reactivity. The rate constant for reaction of an excited state is given by the ratio $k_r = \Phi_p/\tau_f$. Ideally, the fluorescence lifetimes should be determined in the solvent for which the product quantum yields have been measured, in this case 50% MeOH-H_2O. However, it proved difficult to obtain good lifetime data in this solvent because many of the methyl ethers photodecompose to the corresponding hydrocarbons, which are often much more fluorescent. For convenience, many of the lifetimes have been measured in 20% ACN-H_2O instead. Although this implies that we cannot directly evaluate the absolute rate constants for reaction in 50% MeOH-H_2O, it is of little consequence in determining the relative reactivities among a series of compounds. In general, we find that the singlet lifetimes in 20% ACN-H_2O are comparable with those in 50% MeOH-H_2O.

Fluorescence lifetimes were measured by a technique known as time correlated single photon counting, (see appendix A). The decay curves were fitted to single exponential equations, unless otherwise noted. Occasionally, the fit was markedly improved by including a minor contribution from a second exponential component, particularly for those lifetimes measured in 50% MeOH-H_2O. This usually had little effect on the lifetime of the major component, but improved the mathematical fit considerably. A few typical decay curves for **20** are shown in

Figure 2.16. Note that the ordinate is logarithmic such that the single exponential functions give rise to a straight line. The lifetime is generated by a mathematical deconvolution procedure that separates the lamp profile from the exponential decay function. The best arithmetic fit is generated by an iterative procedure. Note that the calculated curve fits the data over the rising edge of the lamp profile as well as the decay portion. The value of chi squared (χ_r^2), a measure of the agreement between the calculated line and the experimental data, approaches unity as the correspondence between the two improves. Generally, χ_r^2 values of less than 1.2 were obtained, but data with values < 1.4 were occasionally deemed acceptable. The weighted residuals and the autocorrelation functions are also useful in judging the quality of the calculated curve, and are included in Figure 2.16.

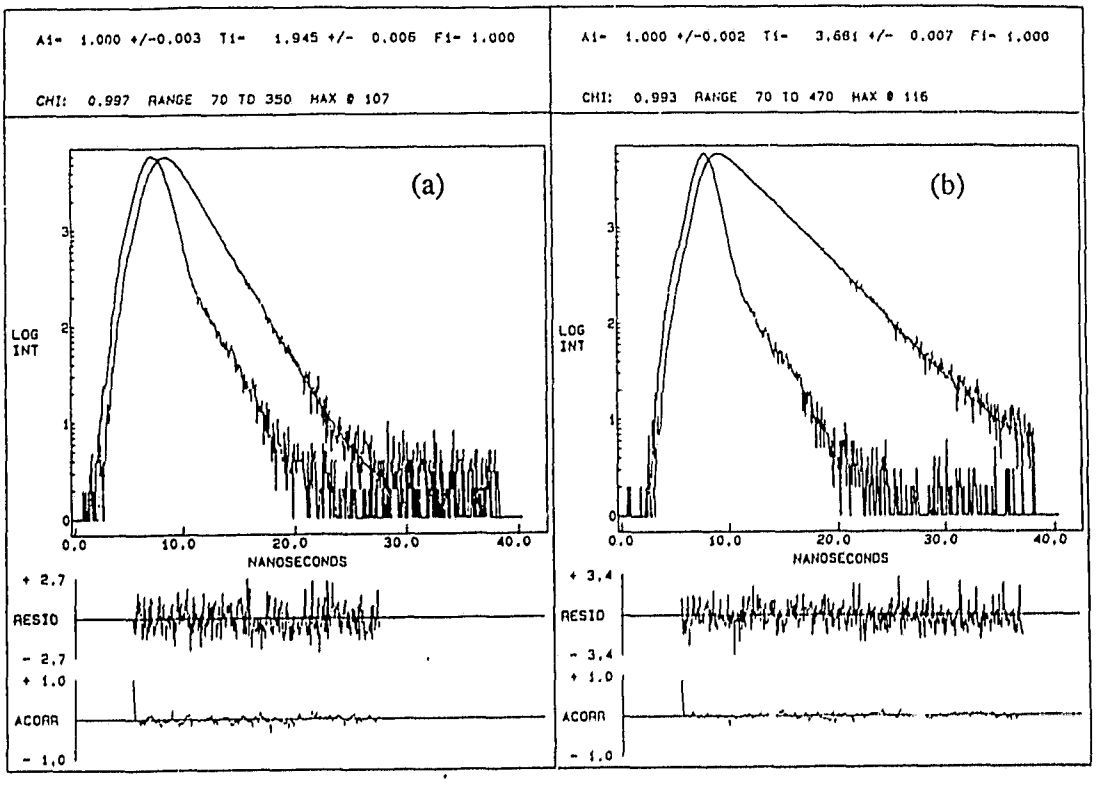

Figure 2.16: Typical Fluorescence Lifetime Decay Curves Generated by Single Photon Counting. Decays shown for ***20*** *in argon saturated solution using 20% ACN as a co-solvent, (a) 0.05* ***M*** *H_2SO_4, τ = 2.0 ns; (b) pH 7, τ = 3.7 ns.*

In this study, the fluorescence lifetimes of many of the diaryl alcohols, and some related compounds, have been measured in pure ACN and 20% ACN-H_2O (see Table 2.16). Unfortunately, the extremely weak fluorescent behaviour of 9-fluorenol (**1**), combined with its inherent photolability, has made fluorescence lifetime measurements very difficult, and this has led to some confusion in the literature.[28]

Table 2.16: Fluorescence Lifetimes (τ_f) of Diaryl Alcohols.

Compound	τ_f (10^{-9} s)[a]	
	ACN	H_2O[b]
1	≈0.3[c]	<0.1[c]
2	20	12
3	< 1	< 1
4	≈9.5[d]	≈2.0[d]
5	2.3	0.92[c]
12	≈0.3[c]	<0.1[c]
16	≈0.3[c]	<0.1[c]
20	19	3.8
22	39	36
23	<0.1[c]	-
24	-	-
25	2.2	0.94[c]
26	2.2	2.1
27	2.3	2.2
33	6.8	5.6
65	4.4	≈0.2[c]

[a] Errors are estimated to be less than ±4% of the quoted value, except for lifetimes less than 1 ns, where it may be larger.
[b] 20% ACN used as a co-solvent.
[c] Picosecond laser pulse as the excitation source.
[d] Data fits double exponential decay, major component reported.

The fluorescence lifetime of **1** was measurable in ACN using a picosecond laser excitation source and found to be ≈ 0.3 ns. However, in H_2O the lifetime is

too short for our instrumental capabilities and an upper limit of 0.1 ns was estimated. It has been noted that the fluorescence of **1** is at least 10 more intense in ACN than in H_2O. Therefore, assuming the k_f remains constant in these solvents, τ_f can be estimated to be ≈ 30 ps in H_2O.

The fluorescence lifetimes of **20**, **22** and **69** have been measured in a number of other solvent systems as well, (Table 2.17). The lifetime of the hydrocarbon **69** remains virtually unchanged in the different solvents, showing only a slight decline in 20% H_2SO_4 solutions. The fluorescence lifetime of the alcohol **22** was unaffected by the solvent, except in moderately acidic solution. This is consistent with the photosolvolytic reactivity of **22**, which produced the methyl ether only in acidic methanol-water solutions. In contrast, the fluorescence lifetime of **20** was very sensitive to solvent changes, consistent with the very reactive nature of this compound.

Table 2.17: Fluorescence Lifetimes (τ_f) for 20, 22 and 69 in Various Solvents.

Solvent System	τ_f (10^{-9} s)[a]		
	20	**22**	**69**
100% MeOH	13	36	27
10% MeOH-H_2O	1.5	36	26
50% MeOH-H_2O	4.6	36	26
50% MeOD-D_2O	5.7	36	26
20% ACN-D_2O	4.7	36	26
50% MeOH-H_2O (pH 1)	2.6	35	26
50% MeOH-H_2O ($H_o \approx -1$)	0.25	26	24

[a] Errors are estimated to be less than ±4% of the quoted value, except for lifetimes less than 1 ns where it may be larger.

The fluorescence lifetime of **20** was particularly sensitive to the presence of water, as illustrated by the drop in the lifetime from 13 ns in pure methanol to 4.6 ns in 50% MeOH-H_2O and 1.5 ns in 10% MeOH-H_2O. Whereas the lifetimes of **22** and **69** were unaffected by replacing the hydroxylic solvents with their deuterated analogues, the lifetime of **20** displayed a significant solvent isotope effect. Using the lifetimes given in Table 2.16 and 2.17, solvent isotope effects, τ_{D_2O}/τ_{H_2O}, were calculated to be 1.24 ± 0.04 and 1.21 ± 0.04 for 20% ACN-L_2O and 50% MeOL-L_2O, respectively. These values can be used in conjunction with the quantum yield data, Φ_{H2O}/Φ_{D2O}, to evaluate the kinetic solvent isotope effect, k_{H2O}/k_{D2O}, for the excited state bond cleavage steps (*vide infra*).

The fluorescence lifetimes of **20** were also measured as a function of the proton concentration in two solvent systems, and the results are presented in Table 2.18.

Table 2.18: Fluorescence Lifetimes (τ_f) of 20 in Acidic Solutions.

Acidity of Aqueous Portion[a]	τ_f (10^{-9} s)[b]	
	20% ACN-H_2O	50% MeOH-H_2O
pH 10	3.7	4.5
pH 7	3.8	4.6
pH 2	3.1	4.2
0.025 M	2.7	3.6
0.050 M	1.9	2.8
0.10 M	1.5	2.5
0.13 M	1.4	2.1
0.25 M	0.82	1.6
0.50 M	0.46	0.81

[a] pH solutions are buffered, molar concentrations refer to H_2SO_4 solutions.
[b] Estimated error ±5% of quoted values.

The Stern-Volmer relation, eq 2.28, can be equally applied to fluorescence lifetimes by the expression,

$$\frac{\tau_f^o}{\tau_f} = 1 + k_q \tau_f [Q] \qquad (2.29)$$

Hence plots of τ_f^o/τ_f versus the proton concentration are linear at moderate acid concentrations, and are shown in the Figure 2.17. As before, the slope provides a measure of k_q, the quenching rate constant, which can be equated with k_H, the acid catalyzed rate constant. Using the lifetimes of **20** in neutral solution, k_H was calculated to be $4.0 \pm 0.3 \times 10^9$ $M^{-1}s^{-1}$ and $3.4 \pm 0.4 \times 10^9$ $M^{-1}s^{-1}$ in 20% ACN-H_2O and 50% MeOH-H_2O, respectively. These values are within experimental error, and also in reasonable agreement with the value obtained earlier from a similar treatment of the fluorescence quantum yields ($k_q = 3.1 \pm 0.2 \times 10^9$ $M^{-1}s^{-1}$).

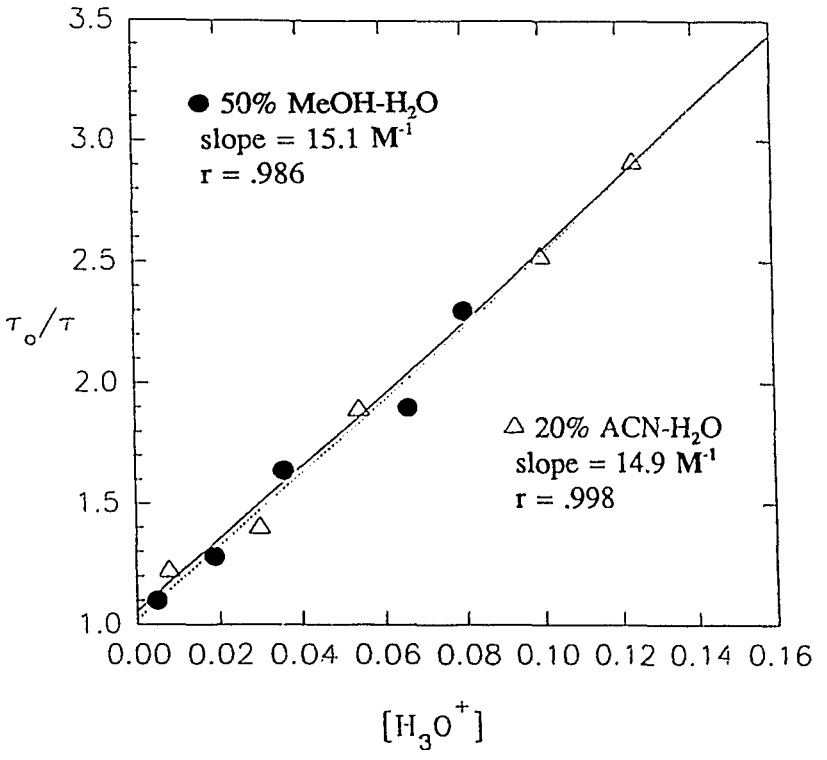

*Figure 2.17: Stern-Volmer Plot for **20** in H_2O and MeOH-H_2O.*

2.3.4 UV Absorption Studies. The photodehydroxylation of **12**, **13**, and **14** was followed by the formation of dibenzofulvene compounds. These photoproducts have distinctly different chromophores, as a result their formation can be easily monitored by UV absorption spectroscopy. Following these reactions by the change in the UV spectrum could, in principle, provide an easy method of monitoring the reactivity of a series of related compounds. After the preparatory photolysis of 9-methyl-9-fluorenol (**12**) in aqueous acetonitrile was shown to yield 9-methylenefluorene (**45**), photolyses were carried out on a UV scale. When dilute aqueous solutions (ca. 10^{-5} **M**) of **12** were photolyzed in quartz cuvettes using the RPR Rayonet reactor (λ_{ex} = 254 nm), the absorption spectrum changed

dramatically. Figure 2.18 displays the overlay of successive UV traces following subsequent 30 sec irradiation intervals. The final spectrum, which has new peaks at 246 and 255 nm, was identical to that of 9-methylenefluorene(**45**), prepared by an independent method (shown in the inset).

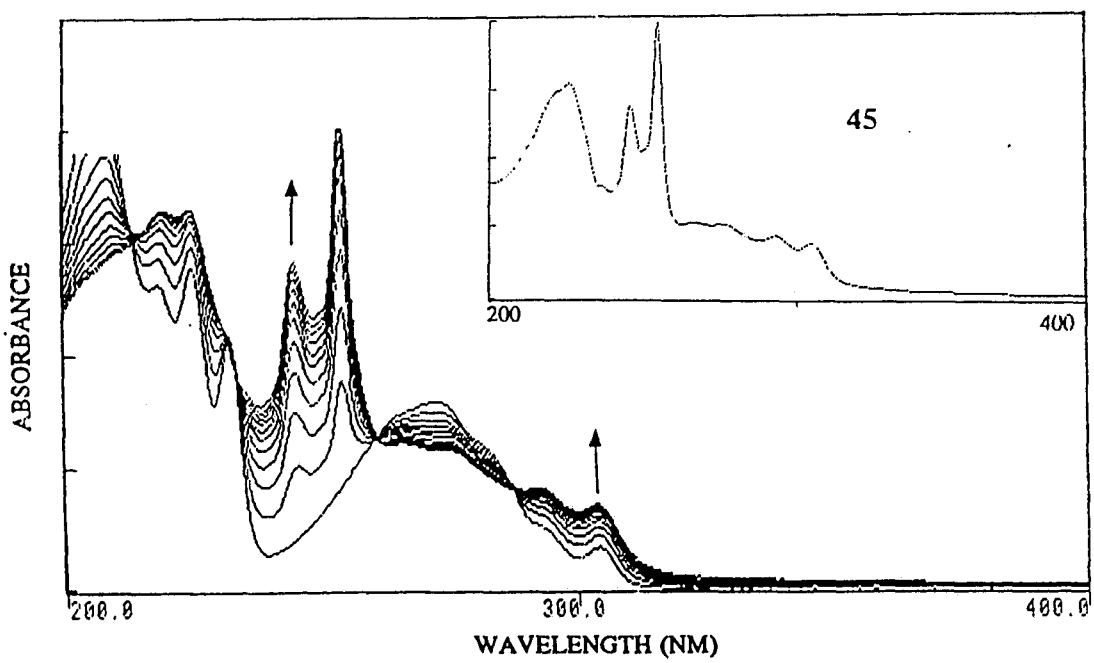

*Figure 2.18: UV Absorption Spectra Upon Photolysis of **12** in H_2O, (Solutions 10^{-5} **M**; photolysis at 254 nm in argon saturated solution; Δt = 30 sec.).*

Initially it was hoped that the other methyl substituted alcohols, **21**, **24** and **26**, would undergo similar photodehydrations and that UV spectroscopy would provide a good quantitative measure of their relative reactivities. Hence the methyl substituted alcohols were prepared. However, preparative photolysis and UV studies have shown that photodehydration is not a general photochemical reaction

among this series. The corresponding thermal reaction occurred readily under acidic conditions to yield the corresponding exocyclic alkenes; **61** and **67** have been prepared in this manner.

Preparative scale photolysis of the isopropyl-substituted fluorenol, **14**, indicated that it did undergo photodehydration, but with a markedly reduced efficiency compared to **12**. These observations were confirmed in UV experiments, where considerably longer irradiation times were required to bring about a substantial change in the UV absorption spectrum. The UV traces in Figure 2.19 were obtained at 2 min irradiation intervals, under conditions otherwise similar to those employed for **12**. The new peaks at 248 and 257 nm are indicative of the presence of the photoproduct 6,6'-dimethyldibenzofulvene (**51**), which was prepared independently and is shown in the inset. However, extended photolysis of these solutions apparently leads to photodecomposition of either the substrate or the photoproduct, as broad structureless features begin to obscure the isosbestic points.

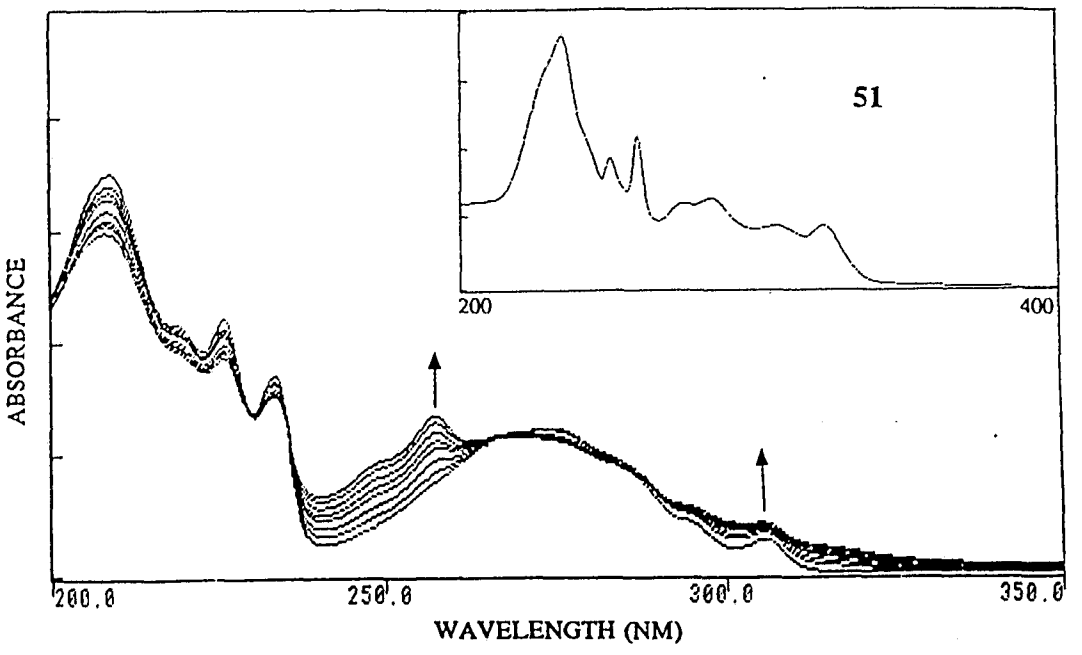

Figure 2.19: UV Absorption Spectra Upon Photolysis of ***14*** *in H_2O, (solutions 10^{-5} **M**; photolysis at 254 nm in argon saturated solution; Δt = 120 sec.).*

The preparative photolysis of 9-vinyl-9-fluorenol (**13**) also gave rise to dibenzofulvene products. When carried out in aqueous solution, the reaction constitutes a photorearrangement of the allylic alcohol. Photolysis of dilute solutions of **13** in UV cuvettes lead to the rapid appearance of new peaks at 246 and 257 nm, as well as a slight shift of the long wavelength band to 310 nm. This matches the UV characteristics of the α-(hydroxymethyl)dibenzofulvene (**48**) that was isolated in product studies (see inset).

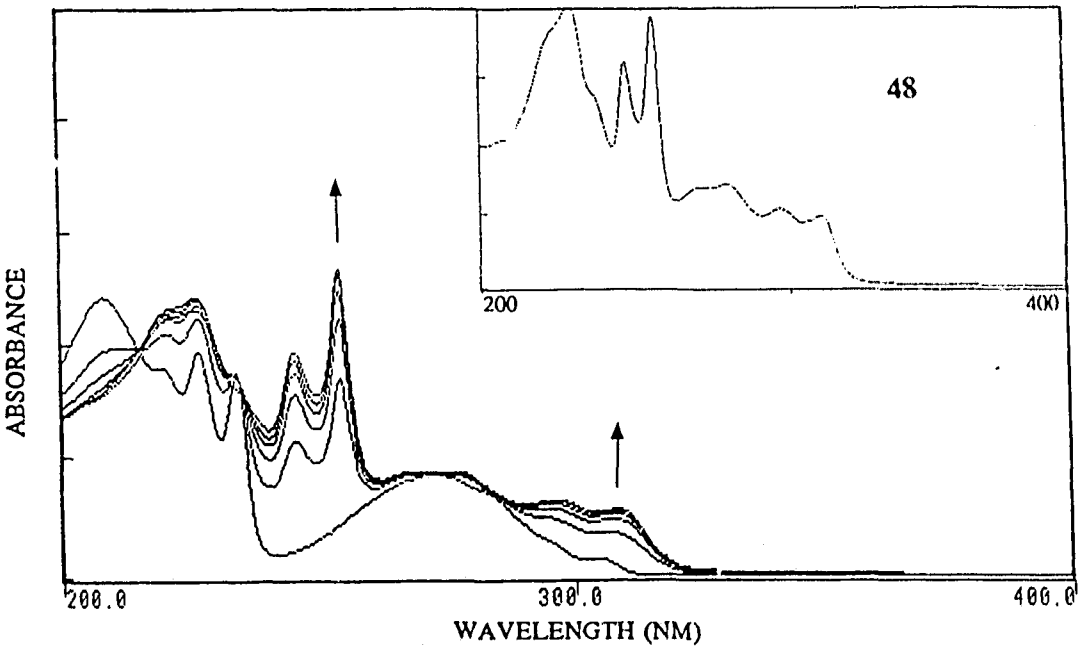

Figure 2.20: UV Absorption Spectra Upon the Photolysis of ***13*** *in H_2O, (solutions 10^{-5}* ***M****; photolysis at 254 nm in argon saturated solution; Δt = 30 sec).*

CHAPTER THREE

RESULTS - PHOTODECARBOXYLATION

3.1 PRODUCT STUDIES

Photodecarboxylations of the diaryl acetic acids were carried out in alkaline aq ACN solutions (typically 40% (v/v) ACN-H_2O; pH ≥ 8). On photolysis, all of **6** - **9** gave exclusively the corresponding hydrocarbons in high yield. In contrast to the photosolvolysis reactions, the photodecarboxylations could be taken to complete conversion without the appearance of competing or secondary photoproducts. Photolysis in ACN-D_2O resulted in the monodeuterated hydrocarbons, whereas photolysis in 100% ACN gave no or very low yields of the hydrocarbons and the starting materials could be recovered. Compounds **6** - **8** were completely unreactive in acidic aq ACN, whereas **9**, the most reactive compound in the series, displayed no measurable pH effect. When the photodecarboxylations were carried out in oxygen saturated solutions the corresponding ketones were produced, in addition to the expected hydrocarbon products.

3.1.1 Photolysis of 9-Fluorene Carboxylic Acid (6). When **6** was photolyzed in aq ACN (pH > 8) for 5 min, conditions that led to the complete decarboxylation of **9**, only 10% conversion to fluorene (**33**) was observed. However, on longer photolysis, **6** underwent complete decarboxylation to yield fluorene (**33**) as the exclusive product in argon saturated solution (eq 3.1). When D_2O was employed

the monodeuterated product 9-deuteriofluorene was isolated (eq 3.2). A dark reaction carried out in 40% ACN-D_2O (pD ≈ 10) for 20 min indicated that no decarboxylation or thermal exchange of the C_9-H bond occurred. The formation of 9-deuteriofluorene is consistent with a heterolytic mechanism that involves abstraction of a deuteron from the solvent by the intermediate 9-fluorenyl anion. Also consistent with this mechanism is the striking lack of reactivity of **6** in either 100% ACN or acidic aq solutions. The reactivity of **6** is quenched at pH < pK_a, indicating that only the carboxylate form is reactive. The results of several preparative photolysis of **6** are presented in Table 3.1.

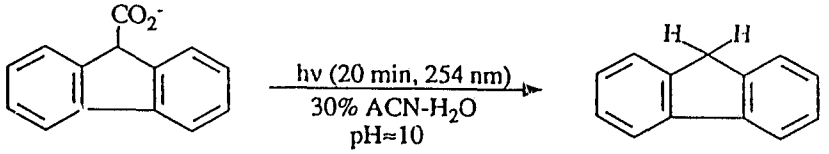

6 **33** (3.1)

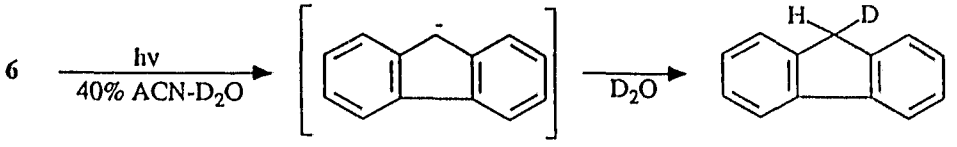

9-fluorenyl anion (3.2)

Table 3.1: Summary of Preparative Photolysis of 9-Fluorene Carboxylic Acid (6).

Substrate Conc. ($\times 10^{-3}$ M)	Solvent System[a]	Irradiation Time (min)[b]	Conversion[c]	Photo-product
2.4	40% ACN-H_2O pH ≈ 10	10	70%	**33**
4.8	40% ACN-D_2O pD ≈ 10	20	70%	**33**-d
2.4	100% ACN	10	<5%	-
2.4	40% ACN-H_2O pH ≈ 1	15	<5%	-
2.4	40% ACN-H_2O pH ≈ 10; O_2	10	68%	**33**: **75** (1.7:1)[d]

[a] Solutions are argon saturated unless otherwise noted.
[b] λ_{ex} = 254 nm.
[c] Determined by integration of ^{1}H NMR.
[d] Determined by GC analysis.

When **6** was photolyzed in oxygen saturated solutions under conditions where extensive decarboxylation occurred, both **33** and 9-fluorenone (**73**) were isolated as photoproducts (eq 3.3). Control experiments where fluorene (**33**) was photolyzed in O_2 saturated aq ACN showed that only trace quantities of the ketone were formed. Thus, photooxygenation of the initially formed photoproduct can be ruled out. Also, photolysis of **6** in oxygen saturated ACN resulted in only trace quantities of **73**. Thus, it appears that the ketone product arises from the bimolecular trapping of the 9-fluorenyl anion by oxygen, leading initially to a

hydroperoxide which is known to break down to yield the ketone,[67] in this case, **73** (eq 3.3). A number of photolysis carried out in 40% ACN-H_2O in the presence of oxygen have consistently lead to a mixture of **33** and **73** that range from 1.5:1 to 1.8:1. This ratio must reflect the partitioning of the intermediate anion between reaction with the protic solvent and the external electrophile, O_2.

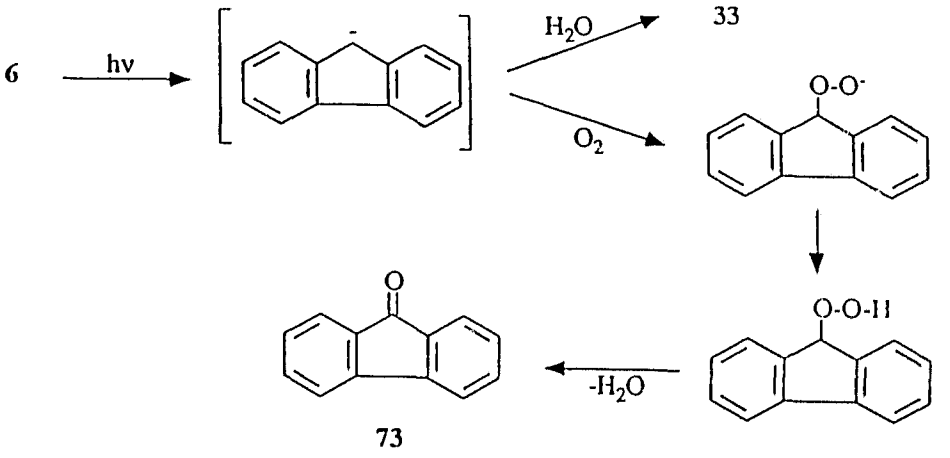

(3.3)

3.1.2 Photolysis of Diphenylacetic Acid (7). Photodecarboxylation also occurred for **7** when it was irradiated in aq ACN solutions, pH > pK_a. The conversions to diphenylmethane (**74**) were similar to those observed in the decarboxylation of 9-fluorenecarboxylic acid (**6**). Once again, the mono-deuterated hydrocarbon was isolated when the reaction was carried out in D_2O. In acidic solution **7** failed to react and the starting material could be recovered. Photolysis of **7** in an oxygen saturated solution of 40% ACN-H_2O (pH ≥ 8), gave a mixture of **74** and benzophenone (**75**). However, the yield of **75** was considerably lower than that observed for **73**. The ratio of diphenylmethane (**74**)

to benzophenone (**75**) was ≈ 2.5:1.

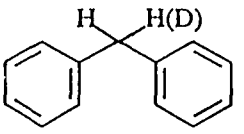

74

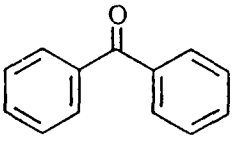

75

3.1.3 Photolysis of 5-Suberane Carboxylic Acid (8). The photolysis of **8** in aq ACN resulted in a clean photodecarboxylation to yieid dibenzosuberane (**59**). The reaction proceeded with conversions intermediate between that of **6** and **9**. Once again, when the reaction was carried out in D_2O the mono-deuterated hydrocarbon was isolated, indicating the intermediacy of the corresponding carbanion.

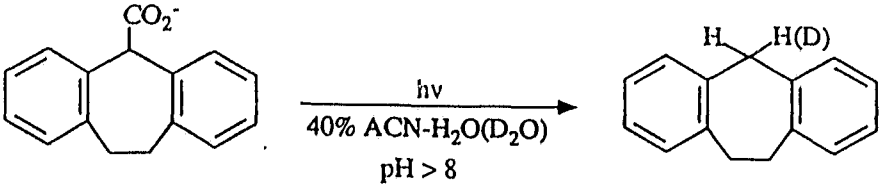

8 **59** (3.4)

When **8** was photolyzed in oxygen saturated aq ACN, **59** was still the major product. However, at 70% conversion, the ketone, **64**, was present in about 5%, indicating that the hydrocarbon to ketone ratio was approximately 15:1.

3.1.4 Photolysis of 5-Suberene Carboxylic Acid (9). The photolysis of **9** lead to the formation of dibenzosuberene (**65**) as the only photoproduct. These

reactions were very efficient and clean, giving no other products by ^1H NMR or GC. For instance, when 50 mg of **9** was photolyzed in 30% ACN-H_2O for 2 min, **65** was produced in 70% yield. When **9** was photolyzed in D_2O the mono-deuterated product, **65**-d, was the exclusive photoproduct. The incorporation of deuterium strongly implicates a carbanion intermediate (eq 3.5).

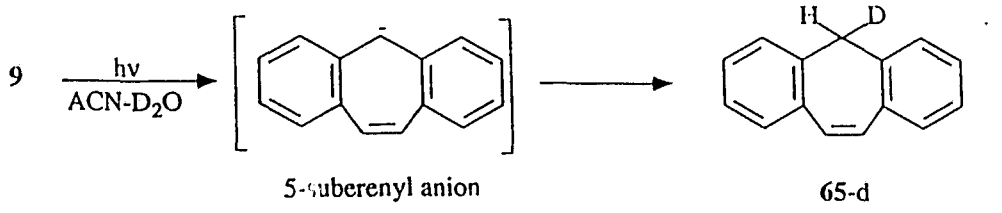

5-suberenyl anion　　65-d　　(3.5)

To rule out that the C_5-H bond is not undergoing photoexchange with the solvent prior to the decarboxylation step, a process that has been observed on longer photolysis of two other suberene derivatives,[97,98] 5-deuterio-5-suberene carboxylic acid (**28**) was photolyzed in ACN-H_2O. The recovered starting material showed no sign of having exchanged at these short irradiation times. The exclusive photoproduct in this case was again **65**-d. Dark reactions in 40% ACN-H_2O (pH ≈ 11) indicated no exchange had occurred after 1 h.

When **9** was photolyzed in 100% ACN under conditions that led to extensive conversion in aqueous solutions, **65** was not observed, and the starting material was recovered. However, on longer irradiations (> 20 min), photodecarboxylation did occur and **65** was obtained in modest yields. When **9** was photolyzed in an oxygen saturated solution, under conditions where extensive photodecarboxylation

occurred, the hydrocarbon **65** was once again the only photoproduct. Dibenzosuberenone (**76**), expected to arise from the trapping of the incipient carbanion by O_2, was not detected by ^1H NMR or GC. This result was reminiscent of our inability to trap the incipient *cation* generated in the photolysis of 9-fluorenol (**1**). Once again, the extreme instability of these ground state anti-aromatic species is thought to give rise to very short-lived intermediates that prohibit bimolecular trapping reactions.

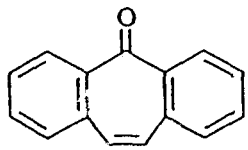

76

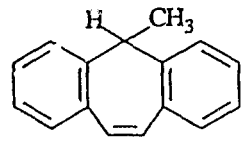

77

In general, both aryl[64,77,101] and diaryl acetic acid derivatives appear to efficiently photodecarboxylate only in their carboxylate form. That is, in aqueous solutions at pH's > pK_a. This behaviour has been observed for **6** - **8** and a number of other substrates studied in our laboratory. However, the preparative photolysis of **9** under acidic conditions indicated that this compound was unique in that it continued to react with the same efficiency Thus, when 50 mg of **9** was photolyzed in 30% ACN-H_2O (20% H_2SO_4) for 2 min the hydrocarbon **65** was produced cleanly in 70% yield. Table 3.2 summarizes the photolysis of **9** under a variety of conditions.

Table 3.2: Summary of Preparative Photolysis of 5-Suberene Carboxylic Acid (9).

Substrate Conc. ($\times 10^{-3}$ **M**)	Solvent System[a]	Irradiation Time (min)[b]	Conversion[c]	Photoproduct[d]
2.1	30% ACN-H_2O pH ≈ 11	2	70%	**65**
4.2	40% ACN-D_2O pD ≈ 10	1.5	20%	**65**-d
2.1	100% ACN	5	≈ 5%	**65**
2.1	30% ACN-H_2O (0.5 **M** H_2SO_4)	2	75%	**65**
2.1	30% ACN-H_2O (20% H_2SO_4)	2	70%	**65**
2.1	30% ACN-H_2O pH≈7; O_2 (g)	2	65%	**65**

[a] Argon saturated solutions unless otherwise noted.
[b] All irradiations carried out at λ_{ex} = 254 nm.
[c] Determined by integration of ^{1}H NMR.
[d] Product mixtures very clean, no other products detected by ^{1}H NMR or GC.

Preparative scale photolysis were also carried out on a related compound, 5-methyl-5-suberene carbcxylic acid (**30**). It was prepared to investigate the effect of the methyl group on the unusual reactivity and fluorescence behaviour of **9**. Replacing the potentially photo-labile C_5-H bond with a carbon-carbon bond was expected to affect the lifetime and the reactivity of the excited state. The

photolysis of **30** in aq ACN (pH > 8) led cleanly to 5-methylsuberene (**77**) in yields slightly lower than those obtained for **9** under identical conditions. The photolysis of **30** was also carried out in acidic solution to investigate acid quenching of the photodecarboxylation. The results are presented in Table 3.3.

Table 3.3: Conversions in the Photodecarboxylation of 30 at Different Acidities.

Acidity of Aqueous Portion	Conversions[a]
pH ≈ 10	55%
pH = 2	40%
0.5 **M** H_2SO_4 (H_o = 0.06)	30%
20% H_2SO_4 (H_o = -1.08)	15%

[a] Determined by integration of ^1H NMR only.

The results indicate that although the methyl derivative shows a definite quenching at acid strengths that led to no change in the reactivity of **9**, the quenching behaviour is still significantly different from that observed for the other diaryl acetic acids in this study (*vide infra*). Whereas, the reactivity of the other acids is effectively quenched below pH 2, the reactivity of **30** has only marginally decreased at this acidity. Even in 20% H_2SO_4, **30** still shows moderate reactivity towards photodecarboxylation.

3.1.5 Photolysis of Related Diarylacetate Esters. The methyl and/or ethyl

esters of **6** and **9** were prepared and photolyzed in ACN and aq ACN solutions. When 5-carboethoxysuberene (**29**) was irradiated for 5 min in 100% ACN, no reaction was observed, and the starting material was completely recovered. Similarly, when **29** was photolyzed in aq ACN no reaction occurred. Photolysis of **9** under these reaction conditions, led to extensive reaction. Thus, although **9** is unusual in that it photodecarboxylates in its protonated form (*vide supra*), the ester is non-reactive. Similarly, the photolysis of the methyl ester of 9-fluorene carboxylic acid (**32**) showed no tendency to photodecarboxylate under conditions that lead to the complete conversion of **6** to the hydrocarbon, **33**.

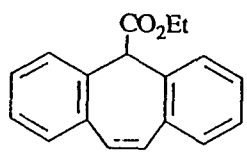

29

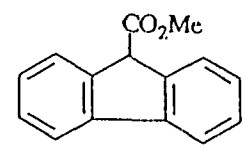

32

3.1.6 Triplet Sensitization. To investigate the importance of the triplet pathway in these photodecarboxylations, triplet sensitization experiments were carried out with 2-benzoylbenzoic acid (**70**) ($E_T \approx 70$ kcal mol^{-1})[90] and sodium 4-acetyl benzenesulfonate (**36**) ($E_T \approx 72$ kcal mol^{-1}) as the water-soluble triplet sensitizers at pH > 7 ($\lambda_{ex} = 350$ nm). When 50 mg of fluorene carboxylic acid (**6**) ($E_T \approx 68$ kcal mol^{-1}) was photolyzed through Pyrex at 350 nm in the presence of 2.0 g of 2-benzoylbenzoic acid, under a photon flux that would otherwise lead to > 80% conversion, only trace amounts (≈ 5% conversion) of fluorene (**33**) were detected. Present also in the product mixture were small amounts of **34**, **43** and **73** as

detected by comparison of their GC retention times with authentic materials. The presence of **34** and **43**, which do not appear in the direct photolysis of **6**, are presumably derived from the fluorenyl radical. Photolysis of suberene carboxylic acid (**9**), ($E_T \approx 57$ kcal mol^{-1}), under similar conditions, yielded small amounts of **65**, **76** and two other unidentified products. The relative inefficiency of these sensitized reactions and the presence of dimeric and other products dramatically contrasts the results obtained upon direct photolysis. These results suggest that the triplet state may undergo a relatively inefficient homolytic cleavage, thus leading to the radical derived products. In the triplet sensitized photolysis of **6**, the fluorenyl radical is strongly implicated as an intermediate by the nature of the photoproducts.

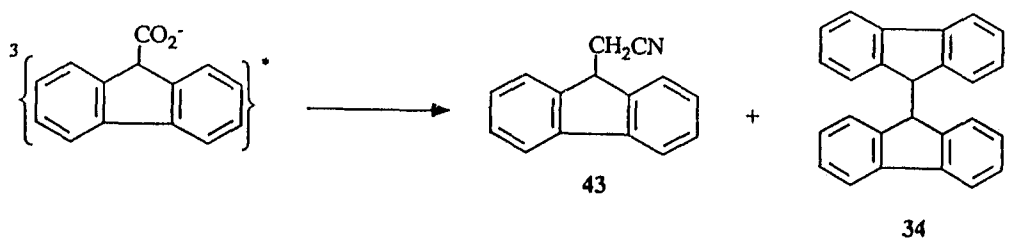

43 34 (3.6)

These products have been characterized in earlier photochemical investigations where the fluorenyl radical has been generated in aq ACN solvents. It appears therefore, that the excited *singlet* state is responsible for the clean and efficient photodecarboxylation processes that occurs via heterolytic cleavage in aqueous solution. To ensure that our triplet sensitizers are indeed capable of energy transfer to these substrates, we have observed that the very weak solution

phosphorescence of sodium 4-acetyl benzenesulfonate ($\lambda_{max} \approx 420$ nm) was quenched by the addition of **6** ($E_T \approx 68$ kcal mol^{-1}), but was unaffected by the addition of **8** ($E_T \approx 80$ kcal mol^{-1}). Unfortunately, preparative experiments using this sensitizer are difficult because of the prohibitively low extinction coefficient of the sensitizer at 350 nm. When 50 mg of **6** was photolyzed at 350 nm in the presence of 2.0 g of **36**, both fluorene and 9,9'-bifluorene were characterized by GC-MS analysis (ca. 12:1 ratio). When suberene carboxylic acid (**9**) was photolyzed under identical conditions both suberene (**65**) and the dimer, 5,5'-bisuberene (**78**) were obtained in about a 6:1 ratio. The relatively high yields of the hydrocarbons obtained with this sensitizer are likely due to some residual light absorption by the substrate. It is significant, however, that in the presence of the sensitizer **36**, both **6** and **9** produced measurable amounts of their corresponding dimers, again suggesting the intermediacy of radicals in the sensitized reactions. No dimeric products were detected in the direct photolysis of any of **6** - **9** in aqueous solution.

3.1.7 Photolysis of 1,2-diphenylcyclopropene-3-carboxylic acid (10). This cyclopropene substituted acetic acid was prepared by the method of Breslow and co-workers,[122] and photolyzed under a variety of conditions. The formally anti-aromatic cyclopropenyl anion has proved to be particulary elusive in the ground state.[49] Therefore, the generation by photochemical means (i.e., photodecarboxylation) would be particularly significant. However, when this

compound was photolyzed (254 or 300 nm) in 30% ACN-H_2O, pH ≥ 8 for 5 min (photolytic conditions which caused extensive photodecarboxylation of **9**), very little decomposition had occurred and the starting material could be completely recovered. On extended photolysis (15 min) in the same solvent, new signals in the ^1H NMR spectrum appeared. However, attempted isolation of this product by preparative thin layer chromatography (TLC) (silica/CH_2Cl_2) yielded a different compound (one that was not present in the crude mixture by ^1H NMR). The α,β unsaturated-γ-lactone, **79**, was assigned on the basis of its ^1H and ^{13}C NMR spectra, as well as MS and IR data.

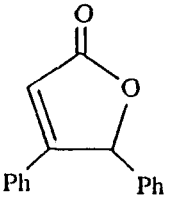

79

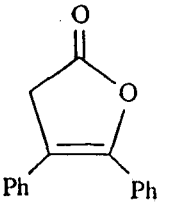

80

When **10** was photolyzed (300 nm) in 40% ACN-H_2O, pH ≈ 1 for 20 min, the main product has been tentatively assigned to the β,γ-unsaturated-γ-lactone, **80**. The same product was obtained when **10** was photolyzed in 100% ACN. However, in neither case was this assignment confirmed by isolation and characterization. When the crude mixtures were separated by TLC (silica/CH_2Cl_2) the only product obtained was the rearranged α,β-unsaturated-γ-lactone **79** described above. Under no conditions was the decarboxylation product, 1,2-diphenylcyclopropene observed. The following table summarizes the results of the photolysis of **10**.

Table 3.4: Summary of Preparative Photolysis of 1,2-Diphenylcyclopropene-3-carboxylic Acid (10).

Substrate Conc. (x 10^{-3} M)	Solvent System	Irradiation Time(min); λ_{ex} (nm)	Conversion (by loss of substrate)	Crude Product[b]	Isolated Product[b]
4	30% ACN-H_2O, pH≈9	5; 254	≈10%	?	-
8	30% ACN-H_2O, pH≈8	20; 300	≈30%	?	**79**
4	40% ACN-H_2O, pH≈1	20; 300	≈80%	**80**	**79**
4	100% ACN	20; 300	≈80%	**80**	**79**

[a] Crude product assignment based only on ^1H NMR of the crude reaction mixture after normal work-up.
[b] Isolated product refers to the major band separated from the crude mixture by preparative TLC (silica/CH_2Cl_2).

3.2 PRODUCT QUANTUM YIELDS.

The photodecarboxylation quantum yields for the acids **6** - **9**, **28** and **30** have been measured in deaerated 20% ACN-H_2O solution at pH 7. The solvent isotope effect and the effect of pH on the photodecarboxylation efficiencies have also been investigated.

3.2.1 Quantum Yields at pH 7. The quantum yield for the formation of the hydrocarbons were measured in pH 7 buffer, using 20% (v/v) ACN as co-solvent.

The measurements for compounds **6**, **9**,and **30** were carried out at λ_{ex} = 280 nm on the optical bench under a fine stream of argon, which served to deaerate and stir the solutions (ca. 1 x 10^{-3} **M**). Potassium ferrioxalate was used to monitor the light intensity, (see appendix B). Deaerated solutions of **7** and **8**, (ca. 5 x 10^{-3} **M**), were photolyzed in the RPR Rayonet reactor using a merry-go-round apparatus and 9-fluorene carboxylic acid (**6**) as a secondary actinometer, $\Phi_p = 0.042 \pm 0.004$. The conversions were determined by GC analysis using a stock solution of 9-fluorenol (**1**) as external standard. The GC results were corrected for differences in the detector response of the standard and the photoproduct in each case. The quantum yields for photodecarboxylation are presented in Table 3.5. The margins of error reflect the standard deviations of repeated measurements. The esters **29** and **32** showed no tendency to decarboxylate under the conditions employed, and an upper limit of $\Phi_p < 0.001$ has been estimated.

Table 3.5: Product Quantum Yields for Photodecarboxylation of the Diaryl Acetic Acids.

Compound	Φ_p[a]		
	H_2O (pH 7)[b]	D_2O (pH > 8)[b]	ACN
6	0.042	0.035	<0.005
7	0.19	0.11	<0.01
8	0.20	0.13	<0.01
9	0.60	0.42	0.055
30	0.38	-	-

[a] The error is ±10% of the quoted value.
[b] 20% ACN was used as a co-solvent.

3.2.2 Solvent and pH Effects. Quantum yields of photodecarboxylation displayed considerable solvent and pH dependence. In general, the reactivity of the acids was quenched on changing to acidic or non-aqueous solutions. The only exception to this trend was with **9**, which displayed no pH effect and remains marginally reactive even in ACN (presumably wet) $\Phi_p \approx 0.05$. The quantum yields for decarboxylation in ACN and in D_2O are included in Table 3.5. To ensure that all the acids are in fact protonated at pH 1, the ground state acidity constants have been measured (Table 3.6). The ground state acid-base behaviour of **6** - **9** are unexceptional. The acidity constants are in the expected range, 10^{-4}-10^{-5}. The pK_a's were measured using dilute aqueous solutions and an automatic titrater.

Endpoints were determined by a curve fitting procedure and the pK_a was simply taken as the pH at half neutralization.

Table 3.6: Ground State pK_a Values for the Diaryl Acetic Acids.

Compound	pK_a[#]
9	5.2
8	5.1
7	4.6
6	4.3

[#] Errors are estimated to be ±0.1. Solutions (ca. 10_{-4} **M**) were titrated with a standardized NaOH solution (0.9950 **M**) under nitrogen purging. A standard glass electrode with an Ag/AgCl reference was employed for the hydronium ion concentrations.

The pH dependence of the product quantum yield is shown in Figure 3.1. The reduction of reactivity for **6** - **8** parallels the protonation of the carboxylates, indicating the importance of the ionized form of the substrate in these photodecarboxylations.

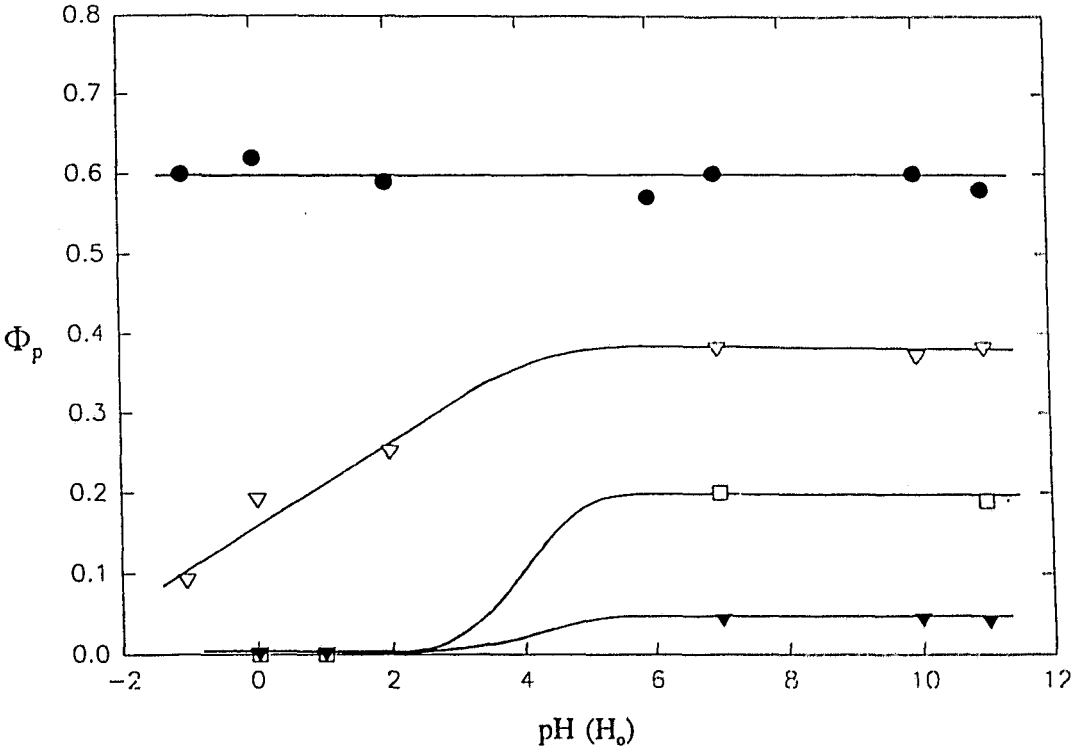

*Figure 3.1: Product Quantum Yields as a Function of pH. Quantum Yields based on Photolysis of 10^{-3} **M** solutions (40% ACN) using ^1H NMR integration, acidity refers to aqueous portion. Solid circles represent **9**, hollow triangles for **30**, hollow squares for **8** and the solid triangles represent **6**.*

3.2.3 Solvent Isotope Effects. The product quantum yields of **6** and **9** were measured in D_2O (20% ACN co-solvent), using the optical bench set-up and potassium ferrioxalate actinometry. The solvent isotope effects for **7** and **8** were measured by comparative photolysis at 254 nm in the RPR Rayonet reactor. In these runs each sample was treated with a stock solution of NaOD to adjust the pD > 8. The solvent isotope effect for photodecarboxylation quantum yield (Φ_{H_2O}/Φ_{D_2O}) are significant, ranging from 1.2 to 1.7, and are presented in Table 3.7.

Table 3.7: Solvent Isotope Effects on the Photodecarboxylation of 6 - 9.

Compound	Φ_{H_2O}/Φ_{D_2O} [a]
6	1.2
7	1.7
8	1.5
9	1.4

[a] Reactions carried out with 20% (v/v) ACN co-solvent at pH 7 or pD ≥ 7; errors are ±14% of the quoted value.

3.3 FLUORESCENCE STUDIES

Steady-state and transient fluorescence measuurements once again provided an invaluable probe of the excited state reactivity. The fluorescence quantum yields have been measured in cyclohexane and aq ACN solutions. The fluorescence lifetimes have been measured in 20% ACN-H_2O, the same solvent system where product quantum yields were measured.

3.3.1 Spectral Characteristics. Overlays of fluorescence excitation and uncorrected emission spectra in cyclohexane are shown in Figure 3.2.

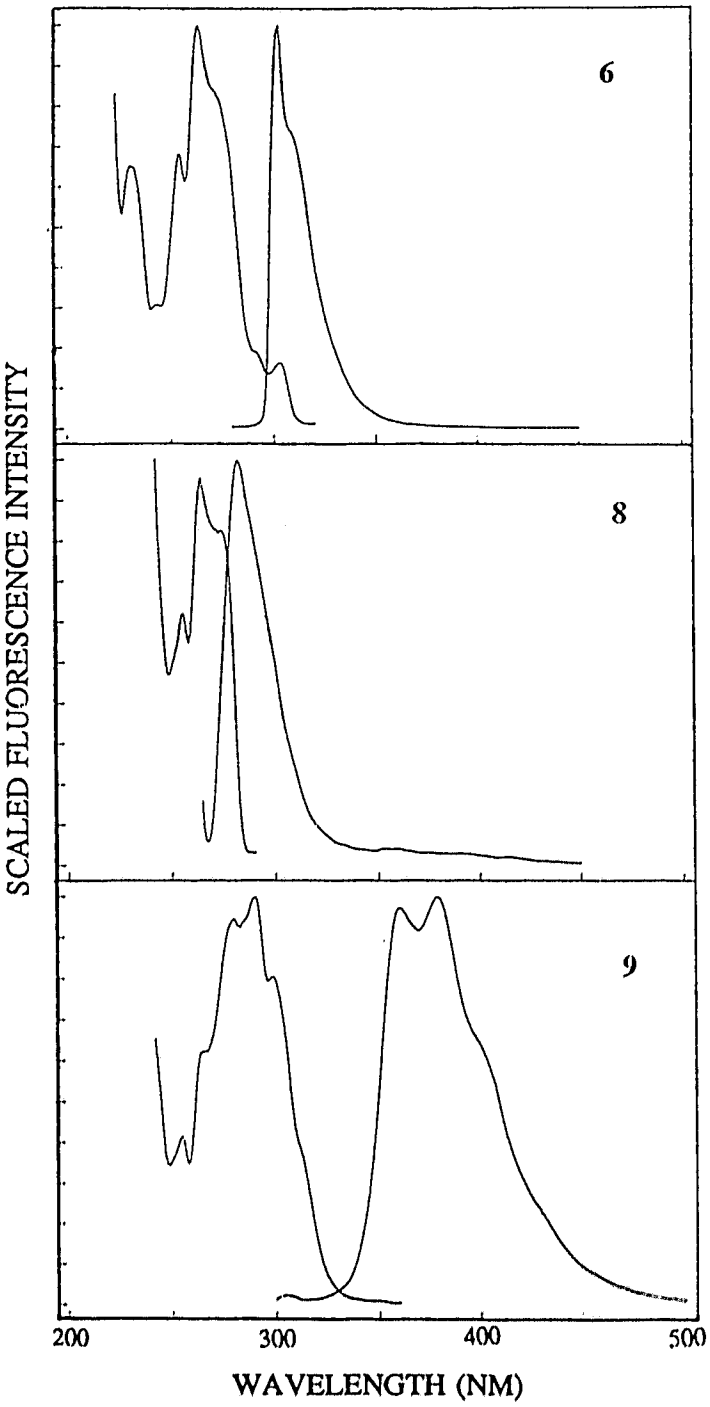

Figure 3.2: Excitation and Emission Spectra of the Diaryl Acetic Acids in Cyclohexane.

The spectral characteristics are similar to those of the corresponding hydrocarbon chromophores. Compounds **6** and **9** have strong UV absorption bands ($\varepsilon_{max} \approx 10^4$ $M^{-1}cm^{-1}$) at 265 and 285 nm, respectively. Compounds **7** and **8** are less conjugated and have weaker absorption bands ($\varepsilon_{max} \approx 10^2$ $M^{-1}cm^{-1}$) at 265 nm. The fluorescence emission spectra of **9** is more structured than that of the corresponding hydrocarbon **65** in the same solvent and somewhat less Stokes shifted, (≈ 22 kcal mol^{-1}). The fluorescence quantum yields of **6** - **9**, **30** and the esters **29** and **32** are presented in Table 3.8.

Table 3.8: Fluorescence Quantum Yields (Φ_f) of Diaryl Acetic Acids and Selected Acid Derivatives in Various Solvents.

Compound	Φ_f[a]			
	C_6H_{12}	ACN	H_2O (pH 7)[b]	H_2O (pH 1)[b]
9[c]	0.54	0.53	<0.001	≈0.01
8[d]	0.068	0.050	0.033	0.044
7[d]	0.030	0.007	0.010	0.011
6[e]	0.38	0.41	0.27	0.030
30[c]	0.45	0.48	<0.001	0.080
29[c]	0.55	0.53	0.54	0.50
32[e]	0.37	0.36	0.015	0.013

[a] Absolute values are ±10% based on the accuracy of the reported fluorescence quantum yields of the secondary standards employed. The relative values within a set are reproducible to ±5%.
[b] Buffered solutions, 20% (v/v) ACN used as a co-solvent.
[c] Versus 2-aminopyridine in 0.1**N** H_2SO_4, $\Phi_f = 0.60 \pm 0.06$, ref.143.
[d] Versus benzene in cyclohexane, $\Phi_f = 0.05 \pm 0.02$, ref.143.
[e] Versus fluorene in cyclohexane, $\Phi_f = 0.80$, ref.90.

3.3.2 Solvent and pH Effects. The fluorescence behaviour of the carboxylic acids was strongly solvent and pH dependent, as the emission spectra in Figure 3.3 illustrate.

The fluorescence intensity of **6** - **9** and **30** was monitored over a range of acid concentrations and are plotted in Figure 3.4 and 3.5. The emission intensity of the esters **29** and **32**, was essentially unaffected by pH, whereas that of the carboxylic acids varied sharply over the range where deprotonation occurred. In

general, it has been observed that the carboxylate forms of aryl-substituted acetic acids are more fluorescent than their protonated counterparts.[102] This behaviour was observed only for **6**, the least reactive of the substrates in this study. The fluorescence quantum yield drops from 0.27 at pH 7 to 0.030 at pH 1. The methyl ester, **32**, whose fluorescence properties should resemble the acid form of **6**, displays a similarly weak emission in aqueous solution, $\Phi_f \approx 0.014$. Most of the carboxylic acids in the present series were more fluorescent at pH's less than their ground state pK_a's, following an opposite trend in their photochemical reactivity. The enhanced reactivity of the ionized forms provides an additional deactivational pathway for the carboxylates, which results in the observation that the protonated forms are more strongly fluorescent.

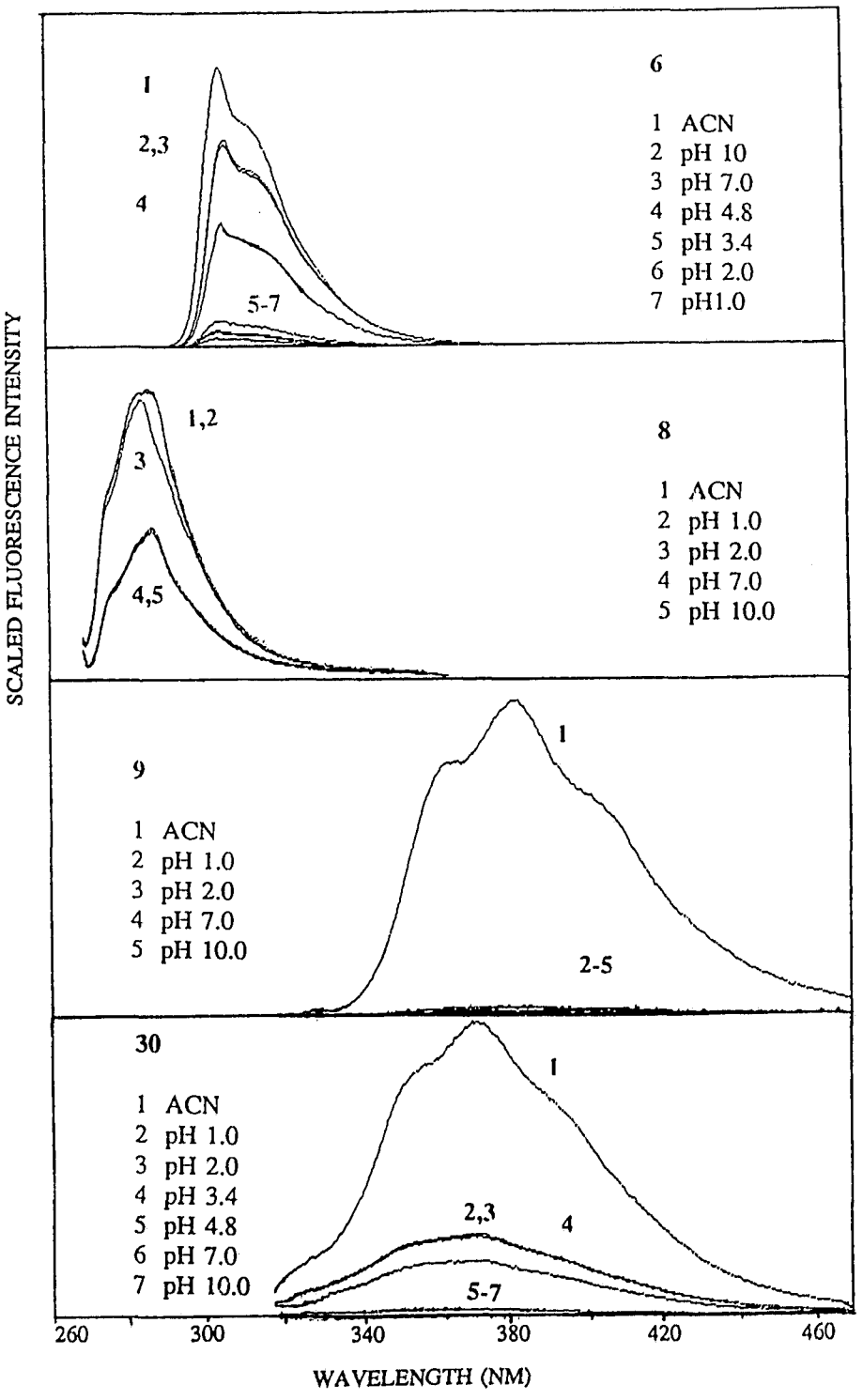

*Figure 3.3: Solvent and pH Dependent Fluorescence Spectra of **6**, **8**, **9** and **30**. All aqueous solutions contain 20% ACN co-solvent.*

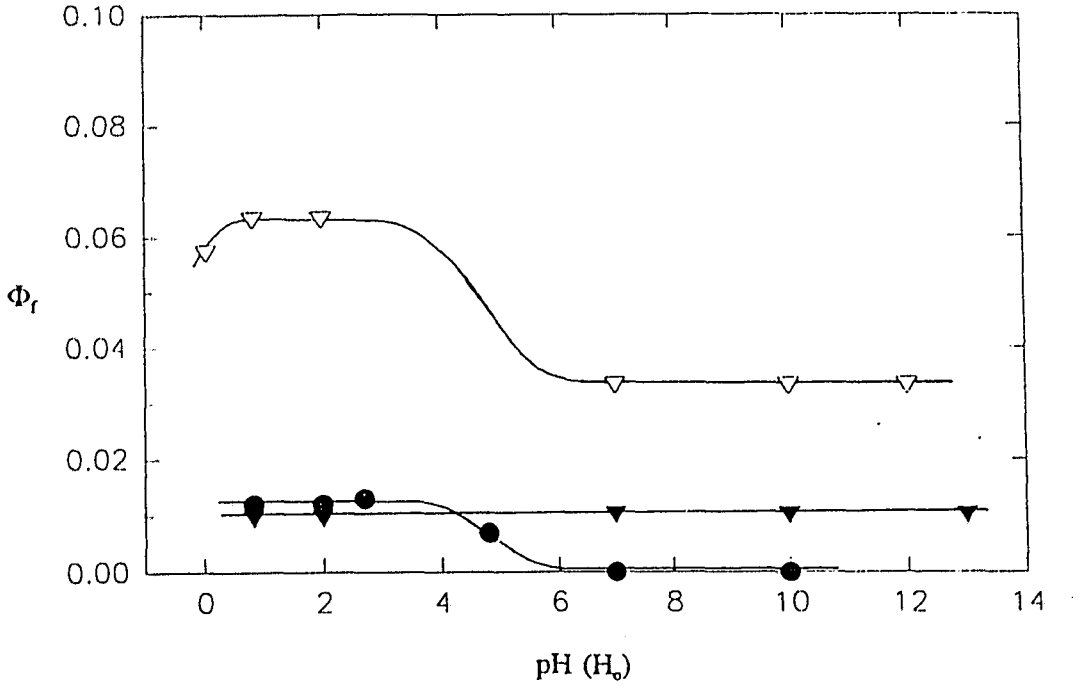

*Figure 3.4: Fluorescence Quantum Yields as a Function of pH for **7** - **9**. Emission was measured in argon saturated solutions using 20% ACN co-solvent for **7** (solid triangles), **8** (hollow triangles), **9** (solid circles).*

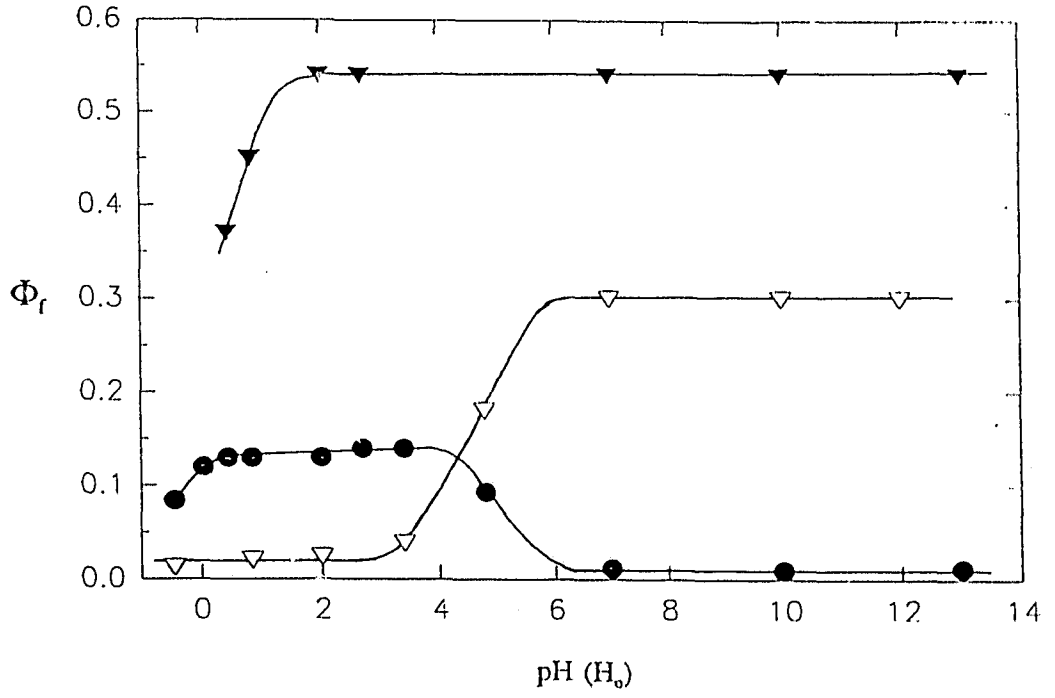

*Figure 3.5: Fluorescence Quantum Yields as a Function of pH for **6**, **29**, and **30**. Emission was measured in argon saturated solution using 20% ACN co-solvent for **6** (hollow triangles), **29** (solid triangles), and **30** (solid circles).*

The most striking solvent effect was observed for 5-suberene carboxylic acid (**9**) which has a fluorescence quantum yield of 0.54 in cyclohexane and ACN, but is essentially non-fluorescent in H_2O (pH 7), a solvent in which it is very photochemically reactive. We have previously noted a similar quenching for the simple hydrocarbon **65** and have reported on the excited state carbon acid behaviour of this compound.[95] To rule out a similar mechanism for the water quenching of **9** (that is, C_5-H heterolysis), the 5-methyl derivative **30** was prepared. The fluorescence quantum yield of **30** drops from 0.48 in ACN, where it is essentially non-reactive, to < 0.001 in H_2O, where it efficiently

photodecarboxylates. This suggests that it is the tendency of these compounds to efficiently photodecarboxylate from S_1 that results in their diminished fluorescence intensity.

3.3.3 Fluorescence Lifetimes. Fluorescence lifetimes of **6 - 9** were measured in ACN and H_2O using time correlated single photon counting (Table 3.9).

Table 3.9: Fluorescence Lifetimes (τ_f) of the Diaryl Acetic Acids and Selected Acid Derivatives in Various Solvents.

Compound	τ_f (10^{-9} s)[a]		
	ACN	H_2O (pH 7)[b]	H_2O (pH 1)[b]
6	9.1	4.8	≈0.5[d]
7	1.6	1.8	2.6
8	5.0[d]	1.6[d]	4.0
9	3.7	<0.15[c]	<0.15[c]
29	4.2	4.5	4.0
30	2.6	<<0.5[e]	0.84
32	9.0	0.4	0.4

[a] All solutions exhaustively purged with a stream of argon prior to measurement, values are accurate to ±5%, except those that are less than 1 ns where the uncertainty may be greater.
[b] Buffered solutions, 20% (v/v) ACN co-solvent.
[c] Picosecond laser pulse excitation source.
[d] Biexponential decay, major component is reported.
[e] Estimated upper limit using a standard hydrogen spark lamp excitation source.

The data (Table 3.9) display the same solvent and pH trends that were noted for the fluorescence quantum yields. The fluorescence lifetimes of the acids were typically shorter in aq solution, consistent with the added deactivational pathway in this solvent (i.e., decarboxylation). The lifetime of the most reactive system, **9**, drops to ≈ 100 ps in H_2O, which is the lower limit of the picosecond single photon counting apparatus that was employed. The unusually short fluorescence lifetimes of **6** at pH 1 and **32** at pH's 1 and 7 (as compared to in ACN) is not understood at this time. The fluorescence lifetime of **9** was very

sensitive to the presence of H_2O. For instance, the prohibitively short lifetime in 100% H_2O (pH 7) increased markedly as the amount of ACN co-solvent was increased, as shown in Table 3.10.

Table 3.10: Fluorescence Lifetimes of 9 in ACN-H_2O Solutions.

Solvent System[a]	τ_f (10^{-9} s)[b]
100% H_2O	<0.10
80% H_2O-ACN	≤0.15
50% H_2O-ACN	0.50
20% H_2O-ACN	0.67
100% ACN	3.7

[a] Aqueous solutions buffered at pH 7.4.
[b] Picosecond laser pulse excitation source used throughout.

The solvent isotope effects, $\tau_f^{D_2O}/\tau_f^{H_2O}$, have been calculated for **6** and **8**. The short lifetime of **9** in aqueous solution prohibited an accurate determination of the same solvent isotope effect for this compound. A small solvent isotope effect was observed for **8**, $\tau_{D_2O}/\tau_{H_2O} = 1.2 \pm 0.1$. However, **6** which was only marginally reactive towards photodecarboxylation, ($\Phi_p \approx 0.04$), showed no measurable solvent isotope effect on its fluorescence lifetime, $\tau_{D_2O}/\tau_{H_2O} \approx 1.0$.

CHAPTER FOUR

DISCUSSION

4.1 PHOTODEHYDROXYLATION

4.1.1 General.

Product Studies. The photolysis of 9-fluorenol (**1**), a number of its derivatives (**11** - **16**), and **20** - **21** in aq methanol solution leads to the efficient production of the corresponding methyl ethers. Prolonged irradiation of these compounds invariably led to homolytic fragmentation of the initially formed ether products. 9-Methyl-9-fluorenol (**12**) and 9-isopropyl-9-fluorenol (**14**) photodehydrated to the corresponding alkenes, **45** and **51**. 5-Suberol (**4**) photosolvolyzed to the methyl ether on longer irradiation at pH 7. The model compounds diphenyl methanol (**2**) and α-phenyl-2-naphthalene methanol (**22**) were completely unreactive towards photosolvolysis at pH 7, but displayed moderate reactivity at pH 1. Acid catalyzed product formation was clearly demonstrated for **20,** concurrent with a complementary fluorescence quenching. In all of the above reactions the isolation of the methyl ether products is consistent with a photodehydroxylation step and formation of ion pair intermediates. The formation of 9-methylenefluorene (**45**) from photolysis of **12** indicates that the elimination of a proton occurs from the ion pair, rather than the radical pair. The latter is known to give rise to several additional side products, as observed in the photolysis of **12** in pure ACN. Similarly, the formation of the dibenzofulvene **48**, as the only photoproduct in the photolysis of 9-vinyl-9-fluorenol (**13**) in aq ACN, is again consistent with ionic

intermediates, since the radical pair is expected to give rise to several additional side products.

Although 5-Suberol (**4**) was moderately reactive toward photosolvolysis, 5-methyl-5-suberol (**24**) was completely unreactive towards photosolvolysis and photodehydration. Photosolvolysis appears to be a minor process for 5-suberenol (**5**) since very low yields of the methyl ether were observed at pH 7. In addition, a competing photoketonization reaction was observed for **5**. Neither the methyl ether nor the dehydrated product were observed in the photolysis of 5-methyl-5-suberenol (**26**).

Upon photodehydroxylation, the initially formed ion pair can either recombine (an internal return process) or separate into free ions. The carbocations thus formed may either lose a β-proton, rearrange, or be quenched by nucleophiles in the system. Since in highly aqueous medium the incipient cations are immediately surrounded by nucleophilic solvent molecules, collapse of the solvent cage, involving either H_2O or MeOH, can occur promptly. This gives rise to the production of the methyl ether or the regenerated alcohol. In experiments with ^{18}O-labelled **1**, it has been demonstrated that exchange with solvent H_2O occurs rapidly. Thus, the quantum yield of methyl ether formation is only a lower limit of the actual yield of carbocation formation.

The photolysis of **1** and **20** should, theoretically, produce an incipient cation which can be trapped with an external nucleophile, such as cyanide ion. Our inability to trap the cation was therefore unexpected. Similar trapping experiments

previously carried out on some simple benzyl alcohol systems[35] and in the present studies on **4** and **39** were successful in that the corresponding cyano products were isolated. However, the trapping reaction is a bimolecular process and requires that a cyanide ion encounter the intermediate cation within its lifetime. That is, the bimolecular mechanism must compete with the pseudo first order solvolysis processes. This will be possible only for carbocations that are relatively long lived. It is thought that the exceedingly reactive nature of the destabilized 9-fluorenyl cation (antiaromatic in the ground state) renders it too short lived to partake in such bimolecular processes. Employing a mechanism that involves attack of the intermediate cation by cyanide ion, the quantum yield expression for the formation 9-cyanofluorene (FlCN) is given by,

$$\Phi_{FlCN} \approx \Phi_{Fl^+}\, \tau_{Fl^+}\, k_d[CN^-] \qquad (4.1)$$

where Φ_{Fl+} is the quantum yield for cation formation, estimated to be ≈ 0.2, τ_{Fl+} is the lifetime of the intermediate cation and k_d is the fastest reported rate of attack for cyanide ion on carbocations, estimated to be ≈ 5×10^9 $M^{-1}s^{-1}$. Rearranging this expression for τ_{Fl+} and assuming that our limit of detection of the cyano product was $\Phi_p \approx 0.01$, an estimate of τ_{Fl+} can be made (eq 4.2).

$$\tau_{Fl^+} \approx \frac{\Phi_{FlCN}}{\Phi_{Fl^+}\, k_d[CN^-]} \qquad (4.2)$$

Thus one explanation for our failure to trap Fl^+ with cyanide ion is that $\tau_{Fl+} \leq 50$ ps. Recent flash photolysis studies in aq MeOH[27] are consistent with this explanation

(*vide infra*). It is worth noting that **4** and **39**, compounds for which the incipient cations have been trapped by an external nucleophile, give rise to relatively stable carbocation intermediates. The dichotomy here is that the most efficient photodehydroxylation reactions occur for those systems which lead to destabilized ground state carbocations (4n π electrons). McClelland[26] has recently employed hexafluoroisopropyl alcohol to stabilize the photogenerated 9-fluorenyl cation, and has observed trapping with relatively non-nucleophilic benzene.

Sensitization Experiments. The photolysis reactions of **1** and **20** were carried out in the presence of triplet sensitizers. In the case of **1**, where the experiment is easier to carry out without residual absorption of the substrate, no photosolvolysis products were observed, even after prolonged photolysis. Extended irradiations did yield small amounts of **33** and **41**, which presumably arise from homolytic cleavage of the triplet state of **1**. When the photosolvolysis of **1** was carried out in the presence of a triplet quencher, the conversion to methyl ether was unaffected. Thus it would appear from these results that the photodehydroxylation process is an exclusively singlet state reaction. Triplet sensitization of **20** also led to the conclusion that the excited singlet state is responsible for heterolytic bond cleavage. This was further supported by the fluorescence behaviour of **20**, which displays significant quenching in aqueous solvents where it is known to react. The observations that photodehydroxylation is a singlet state process is in agreement with earlier studies from this laboratory[32-35] and others.[29] Furthermore, it is

consistent with a simple, unimolecular heterolytic cleavage step for ion pair generation (eq 4.3). Since the ion pair has singlet character, its one step formation from the triplet excited state is formally spin forbidden.

(4.3)

Acid Catalysis. Acid catalysis can be viewed as a general feature of dehydroxylation reactions because the protonation of the hydroxyl oxygen converts the hydroxide ion into a water molecule, which is a much better leaving group. Catalysis is a well known phenomenon in ground state reactions and proton-assisted *photo*dehydroxylations have been documented.[32,34,35] For instance, Wan and Chak have reported that ortho and meta methoxybenzyl alcohols displayed acid catalyzed photosolvolysis below pH ≈ 2.[35] In the present study, the photosolvolysis of **1** was only marginally accelerated at $H_o \approx 0$. Although the conversion to methyl ether increased at higher acidities, the complete lack of fluorescence data for this compound made further interpretation of the observed catalysis difficult.

Acid catalysis was observed for **20** and **22** at considerably lower acid concentrations (pH ≤ 2). Fluorescence quenching and a corresponding decrease in the fluorescence lifetimes at $[H^+] > 0.01$ **M** indicates that depletion of the excited singlet state is accelerated by added hydronium ions. The complementary

behaviour of the increased product quantum yield and the fluorescence quenching of **20** are clearly displayed in Figure 2.4, and lend strong support for a reactive excited singlet state in the photosolvolysis reaction. Since protons are interacting directly with the singlet state to increase the yield of the solvolysis product, the cleavage of the C-OH bond must follow a heterolytic mechanism (eq 4.4).

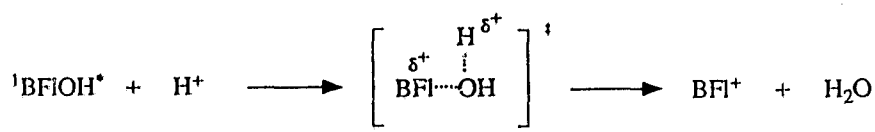

(4.4)

Isotope Effects. The solvent isotope effect for the quantum yield of methyl ether formation in 50% MeOL-L_2O, (where L = H or D) was found to be 1.09 ± 0.05 and 1.06 ± 0.03 for **1** and **20**, respectively. In order to convert this to a kinetic solvent isotope effect the fluorescence lifetimes must be taken into account. Thus,

$$\frac{k_{H_2O}}{k_{D_2O}} \approx \frac{\Phi_{H_2O}}{\Phi_{D_2O}} \frac{\tau_{D_2O}}{\tau_{H_2O}} \qquad (4.5)$$

Although the fluorescence lifetimes of **1** were difficult to ascertain, a value of $\tau_{D_2O}/\tau_{H_2O} = 1.24 \pm 0.04$ was measured for **20** in 50% MeOL-L_2O. Assuming that a secondary isotope effect from nucleophilic attack of the incipient cation by H_2O (vs D_2O) and MeOH (vs MeOD) is negligible, then the kinetic solvent isotope effect can be evaluated as $k_{H_2O}/k_{D_2O} \approx 1.3$. The magnitude of this effect is consistent with a solvent assisted heterolytic C-OH bond cleavage step. Homolytic fragmentation

would be expected to exhibit only a minor secondary isotope effect due to the slight difference in the C-OH and C-OD bond strengths.

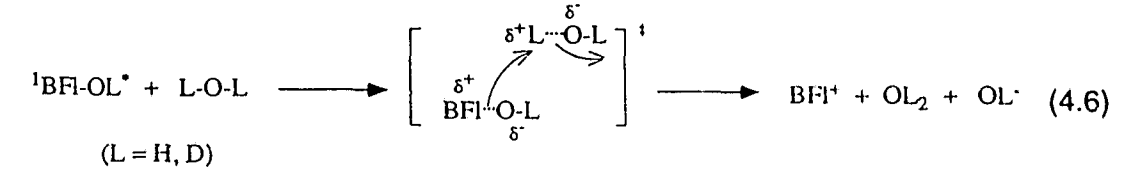

(4.6)

The α-deuterium isotope effect for methyl ether formation ($\Phi_H/\Phi_D = 1.17 \pm 0.9$) was evaluated by comparing the yields of **1** and **11** in 50% MeOH-H_2O. To convert this to a kinetic isotope effect, the fluorescence lifetimes of both substrates must be known. Once again these lifetimes were inaccessible, but it was noted that α-deuterium substitution of **4** and **5** had little effect on the fluorescence lifetimes (within 5%). Thus, taking τ_D/τ_H to be approximately unity for **1** and **11**, the α-secondary kinetic isotope effect is $k_H/k_D \approx 1.2$. A normal secondary α-deuterium kinetic isotope effect in the range of 1.2 - 1.3 is consistent with a dissociative process that involves a change in hybridization (from sp^3 to sp^2) in the transition state.[118] Thus, it appears that at the transition state of the fragmentation step the leaving group-substrate bond is broken prior to association with the nucleophilic solvent. However, since both C-OH heterolysis and homolysis occur with a similar change in hybridization, the observed value of 1.2 is consistent with either process.

Mechanism. The sequence of events that lead up to and immediately follow the bond cleavage step delineate the photoinduced mechanism. As depicted in the equations below, excited state diaryl alcohols (ROH) can give rise to radical and

ion pair intermediates via a number of possible pathways.

$$^1ROH^* \xrightarrow{k_{Het}} R^+ + OH^- \qquad (4.7)$$

$$^1ROH^* \xrightarrow{k_{Hom}} R\cdot + OH\cdot \qquad (4.8)$$

$$^1ROH^* \xrightarrow{k_{ISC}} {}^3ROH^* \xrightarrow{k'_{Hom}} R\cdot + OH\cdot \qquad (4.9)$$

$$(R\cdot, OH\cdot) \underset{}{\overset{k_{ET}}{\rightleftharpoons}} (R^+, OH^-) \qquad (4.10)$$

The excited singlet state may, in principle, fragment to generate either the ion pair intermediates, as in eq 4.7, or the radical pair, as in equation 4.8. The rate constants associated with these steps are given by k_{Het} and k_{Hom}, respectively. It is possible that both heterolysis and homolysis compete, and that the predominate pathway is governed by solvent polarity and the nature of the leaving group. In a third process, intersystem crossing leads to a triplet excited state (^{3}ROH) and the rate of homolytic cleavage is designated k'_{Hom}. It has been shown in the present work that photodehydroxylation (leading to ion pair) occurs from the excited singlet state. The singlet states of the diaryl alcohols are generally 10 - 15 kcal mol $^{-1}$ more energetic than the triplet states, so it is not surprising that heterolytic cleavage is a singlet state process. Furthermore, direct formation of the

ground state ion pair (R^+, OH^-) from ^3ROH is formally spin forbidden. The radical pairs generated in eq 4.8 and 4.9 may give rise to the ion pair via in-cage electron transfer, as depicted in eq 4.10. Electron transfer steps that interconvert radical and ion pairs could complicate the interpretation of product studies since these products (derived ostensibly from ionic intermediates) may have arisen from homolytic fragmentation followed by fast electron transfer (eq 4.11). Such a sequence of steps resemble the mechanism proposed by Kropp[11] for the photosolvolysis of certain alkyl halides.

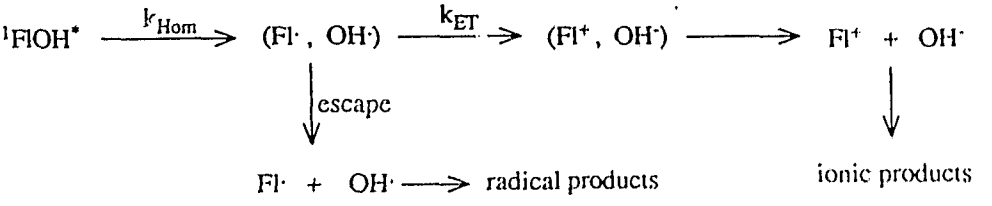

(4.11)

In this mechanism, only one cleavage pathway is followed and the partitioning between ionic and radical derived products is governed by the varying extents of electron transfer, the energetics of which are again influenced by the solvent polarity and the nature of the leaving group. The free energy for the conversion of (Fl· OH·) to (Fl$^+$ OH$^-$) has been estimated to be $\Delta G_{ET} \approx$ -20 kcal mol^{-1} using available electrochemical data.[95] Thus, the two step mechanism shown in eq 4.11 is thermodynamically favourable. However, a number of observations in the present study are inconsistent with the electron transfer (ET) pathway and support a mechanism involving heterolytic bond cleavage as the primary photochemical event. A summary of these observations and their relevance to a heterolytic

cleavage mechanism are outlined below. (1) The fluorescence quenching of S_1 (both steady state and transient measurements) on the addition of water is consistent with the promotion of heterolysis on increasing solvent polarity. In the two-step homolysis - electron transfer mechanism, increasing the solvent polarity will favour electron transfer to the ion pair, but should have little influence on the initial homolytic process. The fluorescence quenching behaviour of **20** demonstrates this effect most dramatically. The fluorescence quantum yield drops from 0.26 in ACN to 0.08 in 50% MeOH-H_2O. (2) The observation of acid catalysis, most convincingly demonstrated for **20** and **22,** is taken as strong evidence for initial heterolysis. The loss of hydroxide is readily accelerated by proton transfer as the hydroxide ion is converted to a water molecule. On the other hand, homolysis and electron transfer steps would be completely unaffected by hydronium ions. (3) On extended photolysis of **1** in aq methanol in the presence of a triplet sensitizer, small amounts of fluorene and rearranged hydroxyfluorenes were observed. While this indicates that the triplet state decomposes via homolytic cleavage, it also suggests that the radical pair thus generated does not appear to undergo electrons transfer. Since this reaction was carried out in the same solvent as the direct irradiations (where the solvolysis product predominates), it appears that ion pair formation does not occur via electron transfer. (4) The solvent isotope effect observed for both **1** and **20** also indicates that a heterolytic cleavage step is the primary photochemical event. In the photosolvolysis of these compounds the yield of methyl ether product was

measurably lower in MeOD-D_2O than MeOH-H_2O. Since homolytic fragmentations are generally unaffected by isotopic substitution of the solvent, this observation provides evidence for a heterolytic mechanism that involves proton assisted loss of the hydroxide ion. Furthermore, no observable solvent isotope effect was measured for the photodecompostion of 9-methoxyfluorene (**17**), the mechanism of which clearly involves homolysis.

SCHEME I

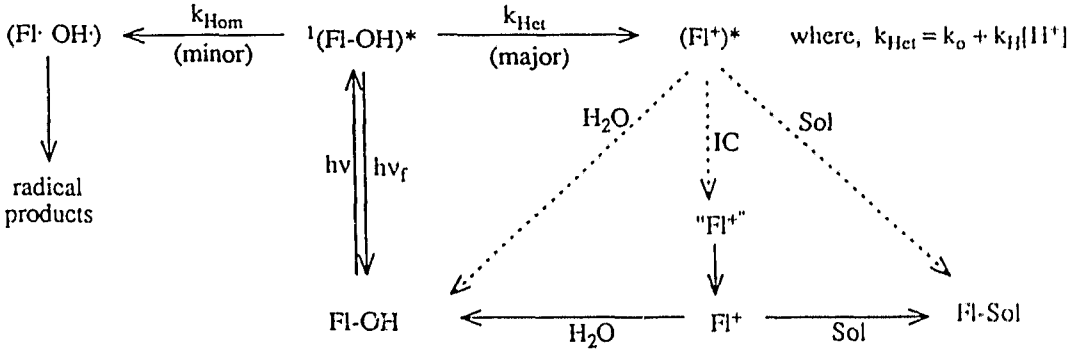

A working mechanism for the photosolvolysis of diaryl alcohols in aqueous solution is shown in Scheme I for **1** (FlOH). Consistent with the above arguments and general results of this study, the primary photochemical event is heterolysis of the C-OH bond (k_{Het}; solvent and proton assisted photodehydroxylation). Although there is a precedent for this process to occur adiabatically, direct evidence for the current series of compounds is unavailable. Thus, it is unclear whether the ion pair is initially formed in the excited state (Fl$^+$)*, a thermally excited

or "hot" ground state ("Fl^{+*}"), or a fully equilibrated ground state (Fl^{+}). The ion pair can recombine in an internal return process. Adiabatic internal return would lead to the formation of $^{1}FlOH^{*}$, which would give rise to non-first order fluorescence decay cuvres. Although this probe could not be used for **1**, no evidence for adiabatic return has been observed in the transient fluorescence behaviour of **20**. The predominate mode of return is presumed to involve capture of Fl^{+} or $Fl^{+\cdot}$ by H_2O, leading to the ground state substrate. The carbocation may also be captured by solvent MeOH which gives rise to the photosolvolysis product. A competing primary pathway from $^{1}FLOH^{*}$ involves C-OH homolysis (k_{Hom}). In ACN, and to a lesser extent in 100% MeOH, this pathway is significant. However, in highly aqueous solvent systems the heterolytic pathway predominates. The initially formed radical pair ($Fl\cdot\ OH\cdot$) probably originates in the ground state, since there is no precedent for adiabatic fragmentations of this sort. Once formed, the radical pair may react via a number of pathways. First, the 9-fluorenyl and hydroxyl radicals may recombine to regenerate the starting material or a rearranged isomer. Secondly, the radicals may react with molecules of the solvent cage, which can lead to several products, such as **35** and **42**. Finally, the radicals may escape the solvent cage and combine to give rise to dimeric products such as **34**.

Flash Photolysis Studies. Three independent researchers have recently carried out flash photolysis studies on 9-fluorenol (**1**). Using nanosecond laser excitation, Fox and co-workers[28] published the first report. They assigned transient

absorptions to the triplet state (^{3}FlOH$^\bullet$), the 9-fluorenyl radical (Fl$^\bullet$), and the 9-fluorenyl cation (Fl$^+$). The radical (λ_{max} = 500 nm) was assigned on the basis of independent generation (via pulsed radiolysis) and comparison to previously reported spectra. A transient absorption at 640 nm, assigned initially to the 9-fluorenyl cation, increased with increasing water concentration at the expense of the absorption due to the radical. This transient had a measured quantum yield of formation of 0.03 and an observed lifetime of several microseconds in 50% aq MeOH. Both the long lifetime and the low quantum yield were inconsistent with our expectations and the interpretation of our steady state experiments. In a subsequent study Hilinski and co-workers[27] suggested that this long lived transient was due to the radical cation of 9-fluorenol (**1**) and not the 9-fluorenyl cation. Further experiments by Fox and Gaillard and McClelland and co-workers[26] now agree with this assignment and have shown that this transient arises from a two photon process. On the basis of picosecond flash photolysis of **1** in 90% aq MeOH, Hilinski[27] assigned the 9-fluorenyl cation to a much shorter lived transient (λ_{max} = 515 nm). This transient appears within the duration of the 30 ps excitation pulse, and decays with a lifetime $\tau < 20$ ps. The same absorption and decay rates were observed in 50% aq MeOH. Solutions of **1** in pure MeOH and ACN gave rise to transient absorptions which were assigned to the 9-fluorenyl radical, and which appeared within 75 ps and persisted for as long as 20 ns. Flash photolysis of 9-chlorofluorene and 9-methyl-9-fluorenol (**12**) in aq methanol also led to transients attributable to the corresponding cations Fl$^+$ and Me-Fl$^+$, respectively. A recent

paper by McClelland and Steenken[26] have substantiated Hilinski's assignments and have increased the lifetime of Fl^+ into the microsecond range using hexafluoroisopropyl alcohol (HFIP) as the solvent.

The flash photolysis experiments have provided a great deal of useful information. In a qualitative sense, the time resolved studies lend support to our mechanistic scheme. The rapid production of Fl^+ in largely aqueous or strongly ionizing solvents, like HFIP, is consistent with a primary photodehydroxylation step. The observed formation of radical intermediates in pure methanol and ACN is also consistent with our product studies. Quantitatively, the prompt formation of the cation (< 30 ps) and its subsequent rapid decay (τ_{Fl+} < 20 ps) is consistent with: (1) the estimate of the fluorescence lifetime of **1** in 4:1 H_2O-ACN, and (2) the failure to trap Fl^+ with external nucleophiles such as 0.3 **M** CN^-. The results of the flash photolysis work have been promising thus far and suggest that much more work in this area is forthcoming.

Capture Ratios. The photogenerated carbocations produced in 50% MeOH-H_2O can be solvolyzed by either of the nucleophilic components of the solvent media. Although Ritchie[103] has reported the relative nucleophilicities of MeOH and H_2O toward several stable carbocations, it is not known if these values can be applied to photogenerated (relatively unstable) carbocations studied in this report. The N^+ values for pure water and MeOH are 0.0 and 0.5, respectively. Since these are log values, a capture ratio of $k_{MeOH}/k_{H_2O} \approx 3.2$ might be expected in our mixed

solvent systems. The ratio measured for **1** in 50% MeOH-H_2O was determined by monitoring the simultaneous conversion to methyl ether and loss of labelled oxygen. A value of $k_{MeOH}/k_{H_2O} \approx 2.2 \pm 0.2$ was obtained. Interestingly, when **18** was photolyzed in the same solvent, the product ratio indicated a capture ratio of about 4.5 ± 0.4. Although the capture ratio was not directly measured for **20**, the product yield, which approaches unity in 50% MeOH-H_2O (pH $\leq$ 1), implies that $k_{MeOH}/k_{H_2O} \geq 20$ in this solvent system!

Although it is unclear why the capture ratios for **1**, **18** and **20** should be so widely different, it is conceivable that the hydrophobic nature of the various substrates pre-arranges the solvent cage to be either depleted or enriched in methanol molecules. Since it is known that the carbocations generated from these substrates are extremely short lived, solvolysis can occur with little more than collapse of the solvent cage. If, for example, the more hydrophobic substrates are associated with more methanol enriched solvent shells, then the observed trend in capture ratios can be explained. Meot-Ner[104] has found that in mixed methanol-water solutions, protons are preferentially solvated by methanol molecules. This result provides an additional explanation for the very high selectivities observed in the photosolvolysis of **20** (in acidic aq methanol), since the hydrophobic substrate molecules are expected to be situated in these methanol clusters as well.

McKenna[20] has studied the photosolvolysis of benzyl trimethylammonium halide derivatives in 50% MeOH-H_2O and reported capture ratios ranging from 1.8

to greater than 20. The authors noted that compounds that yielded stabilized benzyl cations displayed a greater selectivity for methanol. Yates and Anderson[105] have investigated nucleophilic selectivity, k_{ROH}/k_{H_2O}, in the thermal and photochemical addition of alcohol-water mixtures to styrenes. They report that the observed capture ratios are a complex function of several factors, such as the nucleophilicity and solvating ability of the alcohol, the solvent composition, the acid concentration, and the nature of the substrate. Hence, the assumption that capture ratios remain constant over a series of different substrates and proton concentrations would appear to be an oversimplification, albeit a necessary one, until such ratios are determined for each case (*vide infra*).

Solvent Effects. The results have shown that, in the case of **1**, the competition between homolytic and heterolytic cleavage pathways is strongly influenced by the nature of the solvent and the leaving group. Photodehydroxylation is markedly favoured in aqueous solvents. Homolytic cleavage of the C-OH bond often competes with ion pair formation and predominates in less polar solvents. For instance when **1** is photolyzed in 50% MeOH-H_2O, the rapid production of methyl ether indicates that heterolysis predominates. However, when **1** is irradiated in pure MeOH or ACN products derived from 9-fluorenyl radical predominate. The sensitivity of the mode of bond cleavage to the solvent system is expected in such reactions; the energetic arguments are the same as those used to describe similar trends in ground state reactions. The two main factors that determine the outcome

of photoexcitation of **1** are the dielectric constant of the media, and the bond dissociation energy of the weakest C-H bond of the solvent molecules (Table 4.1). That photosolvolysis predominates in aqueous solution is not surprising. The high dielectric constant of water favours ion pair formation and the H-OH bond strength prohibits hydrogen abstraction. On the other hand, the appearance of new photoproducts in the other solvents can be explained by their considerably lower dielectric constants and weaker C-H bond strengths.

Table 4.1: Dielectric Constants and Bond Dissociation Energies (BDE) for Common Solvents.[a]

Solvent	ε (20 °C)	BDE (kcal mol^{-1})
H-OH	80.4	119
H-CH_2OH	33.6	94
H-CH_2CN	37.5[b]	93

[a] Taken from reference 106 unless otherwise noted.
[b] Reference 107.

The situation is represented by the potential energy surface diagram shown in Figure 4.1. The crossing point of the S_1 surface with the potential energy surface of the products depends on the product stability. The activation barrier for cleavage (E_a) then, is a reflection of the product stability as well. Since the stability of the ionic product is greatly influenced by the polarity of the solvent, the

activation barrier for heterolytic cleavage, and thus k_{Het}, will be strongly solvent dependent. The energy surface corresponding to homolytic cleavage will be much less susceptible to solvent changes. Thus in polar solvents the E_a^{Het} is lower than E_a^{Hom}, but the reverse is true in non-polar media. A similar description has been made by Manning and Peters to explain the observed solvent and leaving group effects in the photolysis pathways of a series of triarylmethane derivatives.[29]

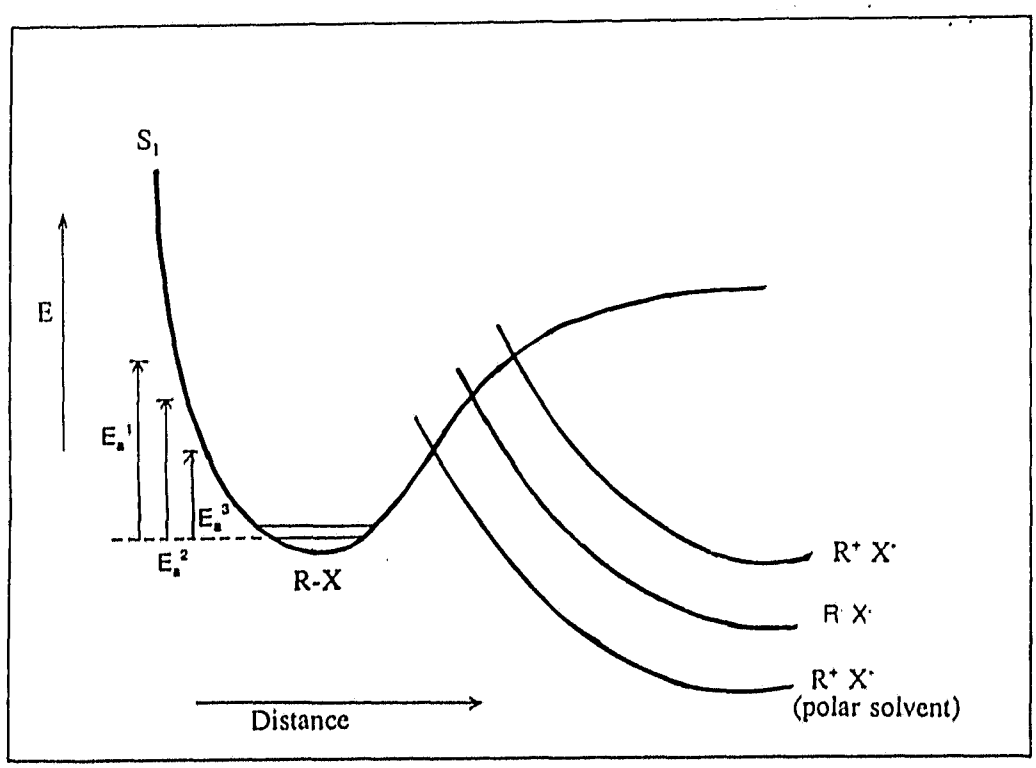

Figure 4.1: Potential Energy Surface Diagram for Cleavage of **1** *from* S_1. E_a^1 = *large barrier for heterolytic cleavage in non-polar solvents,* E_a^2 = *barrier for homolytic cleavage, and* E_a^3 = *small energy barrier for heterolytic cleavage in polar solvent.*

Leaving Group Effects. With respect to photosolvolysis, the results indicate that

hydroxide and bromide ion are good leaving groups. Although hydroxide is a relatively poor leaving group in ground state solvolysis reactions, it has been observed to have an enhanced ability in photoactivated processes.[32,35,36]

Table 4.2: Bond Dissociation Energies (BDE) and Electron Affinities (EA) for Leaving Groups, (X).[a]

X	BDE for $PhCH_2$-X (kcal mol^{-1})	EA for X· (kcal mol^{-1})
OH	78	42.1
OCH_3	69[b]	36.1[b]
OAc	67	-
Br	55	77.4

[a] Taken from reference 106 unless otherwise noted.
[b] Reference 29.

The bond dissociation energies for a variety of substituted benzyl systems are given in Table 4.2. Although these values are expected to differ for the corresponding 9-fluorenyl derivatives, the general trends are likely to remain unchanged. The rates of homolytic bond cleavage are expected to correlate with the bond dissociation energies. Hence, k_{Hom} ought to follow the trend Br > OAc ≈ OCH_3 > OH. On the other hand, the overall energies involved in heterolytic cleavage could be estimated if the electrochemical couples for the various radical pairs, in the appropriate solvents, were known. This information being unavailable, the electron affinities of the radical and the ion solvation energies may be used as

criteria for predicting heterolytic vs homolytic dissociations. The electron affinities for the various leaving fragments have been listed in Table 4.2. That heterolysis predominates for **1** and **18** is probably a reflection of the greater electron affinities of the Br and OH· groups and the greater solvation energy expected for OH^- in aqueous solution. In the case of **17**, the more stable methoxy radical favours homolytic cleavage. The behaviour has been observed by Tomioka,[92] who has studied a series of 9-alkoxyfluorenes that undergo photohomolysis of the C-O bond. The low photosolvolysis yield for **19** in 50% ACN-H_2O is probably due to competing homolysis, which regenerates the starting substrate on recombination. Small amounts of **34** are indicative of some radical cage escape. Unlike the situation with **17**, the radical pair cannot disproportionate leading to stable products. It can only recombine or escape the solvent cage.

Adiabaticity. Although the photodehydroxylation step for 9-xanthenols[33] and 5-suberenol[108] has been convincingly shown to occur, at least in part, on the excited state surface (generating the carbocations in S_1), direct evidence for the other alcohols investigated in this study is lacking. It is possible that further work in this area will reveal additional examples of adiabatic fluorescence emission, but for the present it seems that this feature is not a general one. It should be noted that in addition to the difficultly encountered in the fluorescence experiments of **1** (and its derivatives), spectroscopic assignment of the thermally generated 9-fluorenyl cation remains ambiguous.[109,110]

It is interesting to note that those systems which display adiabatic cation emission are the same ones that generate stabilized ground state cations. Thus, it is the formally 6 π electron xanthylium and suberenylium ions which display fluorescence emission upon excitation of their alcohol precursors. Perhaps this condition is not merely fortuitous, but one that is imposed by the energetics of the S_1 surface. Recent studies in our laboratory have indicated that several thioxanthylium ion derivatives also display adiabatic emission.[111]

Although relatively little is known about the nature of the excited state potential energy surface, it is reasonable to imagine that the S_0 and S_1 surfaces will come into closer contact for ground state antiaromatic systems, where large potential energy barriers are present in S_0. Since the probability of non-radiative diabatic processes, such as internal conversion, varies inversely with the S_0 - S_1 energy gap, only ground state aromatic systems display adiabatic bond fragmentation followed by emission (see Figure 4.4).

Förster Cycle Calculations. An equilibrium treatment of dehydroxylation reactions leads to an expression for the pK_{R+}, a measure of the pseudo acid behaviour of the carbocation (eq 4.12). Ground state pK_{R+} values have been measured for a number of thermally accessible carbocations.[112]

$$R^+ + H_2O \rightleftharpoons R\text{-}OH + H^+ \qquad (4.12)$$

An estimate of the excited state dissociation constant can be made using the Förster cycle.[113] The difference between S_o and S_1 dissociation enthalpies is given by the transition energies of the precursor and the ionized forms, as shown in Figure 4.2.

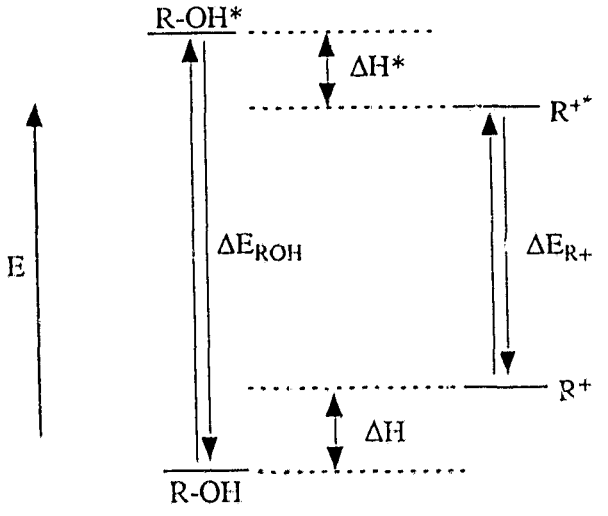

Figure 4.2: Förster Cycle for Ground and Excited State Dissociations.

Using the spectroscopic 0,0 energies for ROH (ΔE_{ROH}) and R^+ (ΔE_{R+}), the enthalpy change for ionization in S_1 (ΔH^*) can be calculated. Assuming identical entropies of reaction in the ground and excited states, the expression for the pK_{R+} (S_1) is given by,

Since it is generally observed that aryl methyl cations absorb at much longer

$$pK_{R^{\cdot}}(S_1) = pK_{R^{\cdot}}(S_0) - \frac{\Delta E_{R^{\cdot}} - \Delta E_{ROH}}{2.3RT} \qquad (4.13)$$

wavelength than the precursor alcohols (i.e., $\Delta E_{R^{\cdot}} - \Delta E_{ROH} < 0$), ROH$^{\cdot}$ should more readily ionize in S_1 than S_0. However, this predicted behaviour has not been observed for ionizations involving C-OH bonds in the excited state, and this discrepancy would imply that excited state equilibria are not a general feature of the photodehydroxylation process. The Förster cycle treatment has been successfully applied to a number of excited state acid-base reactions (involving proton transfer to and from heteroatoms), where intrinsic barriers are known to be much lower and an equilibrium can be established on the excited state surface.[114] The inability of the forward and reverse reactions in C-OH bond cleavage to compete with deactivational processes is consistent with the larger activation barriers associated with C-X ionizations, where considerable rehybridization at the carbon centre may need to occur.

4.1.2 Rate Constants. In an effort to compare intrinsic reactivities, the rate constants for the heterolytic bond cleavage step have been evaluated. Based on the direct one step cleavage mechanism outlined in Scheme I, the quantum yield expression for the formation of the methyl ether product is given by,

$$\Phi_p = \left(\frac{k_{MeOH}[MeOH]}{k_{MeOH}[MeOH] + k_{H_2O}[H_2O]}\right) \Phi_{R^{\cdot}} = \alpha\, \Phi_{R^{\cdot}} \qquad (4.14)$$

where the parameter α replaces the bracketed term, which arises from the partitioning of the incipient cation between methanol and water, and the rate constants are denoted by k_{MeOH} and k_{H_2O}, respectively. The quantum yield of cation formation is given by,

where k_{Het} is defined in Scheme I and Σk_d is the sum of all other rate constants

$$\Phi_{R^+} = \frac{k_{Het}}{\Sigma k_d + k_{Het}} \qquad (4.15)$$

leading to the depletion of S_1. The denominator in equation 4.15 is simply $1/\tau$. Therefore,

$$\Phi_{R^+} = k_{Het}\tau \qquad (4.16)$$

and,

$$\Phi_p = \alpha\ k_{Het}\ \tau \qquad (4.17)$$

Rearranging this equation yields an expression for the heterolytic rate constants,

$$k_{Het} = \frac{\Phi_p}{\alpha\ \tau} \qquad (4.18)$$

In previous treatments of the data[36,95] we have made the assumption that $k_{MeOH} \approx k_{H_2O}$, which simplifies this expression to,

$$k_{Hot} \approx \frac{\Phi_p}{(0.31)\tau} \qquad (4.19)$$

where the mole fraction of methanol in 50% (v/v) MeOH-H_2O has replaced the partitioning ratio in eq 4.18. However, since the capture ratios determined thus far are clearly not unity, and differ depending on the substrates analyzed, it is unclear how we should proceed at this point. It would be desirable to measure the capture ratios for each of the reactive substrates so that the rate constants k_{Hot} may be calculated with a greater degree of certainty. In the meantime we define another quantity,

$$k_s = \left(\frac{k_{MeOH}[MeOH]}{k_{MeOH}[MeOH] + k_{H_2O}[H_2O]}\right) k_{Hot} = \alpha k_{Hot} \qquad (4.20)$$

such that,

$$k_s = \Phi_p/\tau \qquad (4.21)$$

where k_s is referred to as the observed solvolysis rate constant. With this expression in hand, the observed solvolysis rate constant for each of the reactive substrates can be easily evaluated. Although comparing the k_s values of the various substrates directly will be in error (to the extent that the partitioning ratios differ), the use of eq 4.21 allows us to readily compare the intrinsic reactivities for a large number of compounds. When more data becomes available on the partitioning ratio for the various compounds, the rate constants can be easily refined with the use of eq 4.20. The results of this treatment for the compounds

investigated in this report are summarized in Table 4.3.

Table 4.3: Observed Photosolvolysis Rate Constants (k_s) for the Series of Diaryl Alcohols.

Compound	k_s (s^{-1})[a]	Relative Reactivity[b]
1	4.6×10^9	460
2	$< 10^5$ [c]	-
3	$< 10^5$ [c]	-
4	$\approx 3.5 \times 10^7$	3.5
5	$\leq 1 \times 10^7$	1
11	4.0×10^9	400
12	5.3×10^9	530
16	8.7×10^9	870
20	1.5×10^8	15
22	$< 6 \times 10^4$ [c]	-
26	$< 10^6$ [c]	-

[a] At pH 7; calculated using equation 4.21 and data presented in Tables 2.10-2.12 and 2.16.
[b] Based on estimated k_s for **5**.
[c] Estimated upper limit.

A similar treatment of some of the earlier work[36] involving photosolvolysis of benzyl alcohols is presented in Table 4.4. Analysis of the data indicates that the 9-fluorenols are the most reactive compounds towards photodehydroxylation, being even more reactive than the dimethoxybenzyl alcohols.

Table 4.4: Observed Photosolvolysis Rate Constants (k_s) for Several Methoxybenzyl Alcohol Compounds.[a]

Compound	k_s (s^{-1})
meta	4.2×10^6
ortho	2.0×10^7
meta, meta	2.5×10^7
ortho, ortho	5.2×10^8

[a] Based on quantum yields and lifetimes quoted in ref. 35.

Acid Catalysis. The observed acid catalyzed product formation and simultaneous quenching of the substrate fluorescence has been taken as direct evidence of a proton assisted cleavage step. That is,

$$k_{Hot} = k_o + k_H[H^+] \qquad (4.22)$$

where k_o and k_H are the water and acid catalyzed rate constants for the dehydroxylation step. In the present series, 11*H*-benzofluorenol (**20**) has been clearly shown to undergo such catalysis. The value of k_H was obtained from a Stern-Volmer treatment of both steady state and transient fluorescence data and found to be $(3.6 \pm 0.4) \times 10^9\ M^{-1}s^{-1}$. Values in the same range $(4 - 14) \times 10^9\ M^{-1}s^{-1}$ have been previously reported for methoxy substituted benzyl alcohols.[36]

The appearance of acid catalysis is governed by the two terms in equation 4.22, k_o and $k_H[H^+]$. Substituting eq 4.22 into the expression for the quantum yield (eq 4.17), it becomes clear that catalysis will be observed only when $k_H[H^+] >> k_o$.

This situation is more likely to arise for those substrates that are less reactive at pH 7, where k_{Het} and hence k_o is small. Under these circumstances the proton concentrations required to observe the onset of catalysis will be relatively low, and product yields should be observed to increase at lower pH's. Although acid catalysis is expected to be a general feature of photodehydroxylations, the acid concentrations required to observe the onset of catalytic behaviour (i.e., $k_H[H^+] >> k_o$) may be inaccessible for very reactive systems (i.e., large k_o), such as **1**, or for systems that undergo rapid thermal ionizations, such as **5**. In the present study, the most reactive system, 9-fluorenol (**1**), which has $k_s \approx 5 \times 10^9 s^{-1}$, displayed acid catalysis only below $H_o \approx 0$. In contrast, the onset of acid catalysis occurred at pH ≈ 2 for 11*H*-benzo[b]fluorenol (**20**), $k_s \approx 2 \times 10^8$ s^{-1}. Wan and Chak[35] have observed similar behaviour for the series of methoxy substituted benzyl alcohols. Whereas the 2,6- and 2,3-dimethoxybenzyl alcohols ($\Phi_p \approx 0.2 - 0.3$) failed to display acid catalysis between pH 7 - 1, the less reactive ortho and meta alcohols ($\Phi_p < 0.06$) experienced acid catalysis below pH ≈ 3. α-Phenyl-2-napthalenemethanol (**22**), which was unreactive at pH 7 ($k_s < 10^5$ s^{-1}), also displayed acid catalyzed photodehydroxylation. Since $k_H[H^+] >> k_o$ at low pH, eq 4.17 can be modified to,

$$\Phi_p \approx \alpha k_H[H^+]\tau \qquad (4.23)$$

and k_H can be estimated, provided that the lifetime and the quantum yields are either known or can be estimated.

$$k_H \approx \frac{\Phi_p}{\alpha[H^+]\tau} \qquad (4.24)$$

Using the product quantum and the fluorescence lifetime of **22** at pH 1, we obtain a value for $k_H \approx 5 \times 10^6\ M^{-1}s^{-1}$. This estimate is in the same range as similar treatments of the related compound α-methyl-2-naphthalenemethanol.[38]

4.2 PHOTODECARBOXYLATION

4.2.1 General

Product Studies. The photolysis of **6 - 9**, **28** and **30** in 30% ACN-H_2O at pH ≥ pK_a led to the formation of the decarboxylated hydrocarbons as the exclusive photoproduct in deoxygenated solution. 1,2-Diphenylcyclopropene-3-carboxylic acid (**10**) did not decarboxylate under these conditions. The isolated product in this reaction was **79** and indicates that cleavage of the cyclopropene ring followed by carbon-oxygen bond formation has occurred. The esters **29** and **32** were unreactive towards photodecarboxylation under the conditions employed. When **6 - 9** were photolyzed in 40% ACN-D_2O, the corresponding mono-deuterated hydrocarbons were isolated in each case. Although water is a good proton donor, the strong O-H (D) bond makes it a poor hydrogen atom source. Thus, carbanions readily abstract H^+ (D^+) in aqueous solution, whereas radicals tend not to abstract $H^\cdot$ ($D^\cdot$) and will usually dimerize or couple with other hydrogen atom donors. Therefore, the incorporation of deuterium in the photoproducts provides strong evidence for an ionic mechanism. Photolysis in oxygen saturated aq ACN solution

gave rise to the corresponding ketones. Molecular oxygen is a trap for carbanions, leading initially to hydroperoxides.[115] When the concentration of carbanion is low, the mechanism involves electron transfer to generate the superoxide ion, which then recombines with the radical as in eq 4.25. The hydroperoxides of secondary carbons are known to readily eliminate water to yield the corresponding ketone products.[115] For photogenerated carbanions generated in protic solvents, oxygen must compete with other decay processes such as protonation.

$$R^{\cdot} + O_2 \longrightarrow R^{\cdot} + O_2^{-\cdot} \longrightarrow R\text{-}O_2^{-} \xrightarrow{H^+} R\text{-}OOH \qquad (4.25)$$

Table 4.5: Hydrocarbon to Ketone Ratios in the Photolysis of 6 - 9 in O_2 Saturated Solution.

Compound	hydrocarbon/ketone
6	1.7:1
7	2.5:1
8	≈ 15:1
9	> 100:1

In the photolysis of 6 - 9 varying amounts of the ketone products were produced because the intermediate carbanions are partitioned between abstraction of a proton from the solvent and bimolecular reaction with molecular oxygen. The data in Table 4.5 indicate that the amount of oxygen trapped product was

correlated with the ground state stability of the corresponding carbanions, and *not* the efficiency of their photogeneration. Thus dibenzosuberenone (**73**), which would arise from the reaction of the destabilized 5-suberenyl anion (antiaromatic in the ground state) with oxygen, was not observed. Conversely, the photolysis of **6**, which generates the 9-fluorenyl anion (aromatic in the ground state), produced the largest amount of fluorenone (**75**). Compounds **7** and **8**, which photogenerate carbanions of intermediate stability, gave rise to intermediate quantities of ketone.

Sensitization. The triplet sensitization experiments carried out on **6** and **9** indicate that the excited singlet state is responsible for the efficient and clean decarboxylation reactions. The sensitized reactions gave low yields of radical coupling products, suggesting that the triplet excited state undergoes a relatively inefficient homolytic fragmentation process. These results are in accord with the photodecarboxylation of other aryl acetates, which proceed via the singlet state.[102] Further evidence that these photodecarboxylations occur from the excited singlet state comes from the fluorescence data. Whereas both **6** and **9** are strongly fluorescent in nonreactive solvents, such as cyclohexane ($\Phi_f \approx 0.4 - 0.5$), **9** becomes essentially non fluorescent ($\Phi_f < 0.001$) in H_2O, where it is highly reactive. Because **6** is considerably less reactive, its fluorescence emission, on the same solvent change, is quenched to a much lesser extent.

pH and Solvent Effects. The effect of the solvent can be an important criterion in

distinguishing between ionic and radical mechanisms. Whereas reactions proceeding through ionic intermediates are greatly affected by the nature of the solvent, radical reactions are generally unaffected. The moderately reactive compounds **6** - **8** ($\Phi_p \approx 0.04$ - 0.2) were unreactive towards photodecarboxylation in their acidic forms, as the product studies in ACN or aqueous solution ($pH < pK_a$) have indicated. This behaviour has been observed for other aryl and diaryl acetic acid derivatives,[64,65,77,102] and is expected for decarboxylations involving heterolytic cleavage involving the carboxylate ion. The most reactive system, 5-suberene-carboxylic acid (**9**), continued to react with the same efficiency in acidic aqueous solution ($\Phi_p \approx 0.6$). The 5-methyl derivative **30** ($\Phi_p \approx 0.4$ at pH 7) displayed some degree of acid quenching, but only at pH's well below those required to protonate the carboxylate ion. In 100% ACN **9** was much less reactive, but continued to photodecarboxylate ($\Phi_p \approx 0.05$). Thus it would appear that the very reactive chromophores do not require the carboxylate anion form to facilitate departure of the carbanion. A close examination of the fluorescence data presented in Figure 3.4 and Table 3.8 show that both **9** and **30** become slightly more fluorescent in their protonated forms. For example, the fluorescence quantum yields of **9** and **30** are both ≤ 0.001 at pH 7, whereas at pH 1 these values increase to ≈ 0.01 and 0.08 respectively. This observation is significant since it suggests that the carboxylates are indeed more reactive, but that the difference is too small to detect by our quantum yield determinations.

Isotope Effects. The effect of solvent isotopic substitution on the quantum yields for decarboxylation was measured in 20% ACN-L_2O (where L = H or D). Compounds **6 - 9** were all less reactive in D_2O, thus displaying a normal solvent isotope effect, $\Phi_{H_2O}/\Phi_{D_2O} \approx 1.2 - 1.7$. To determine the kinetic solvent isotope effect, k_{H_2O}/k_{D_2O}, the fluorescence lifetimes, measured in the same solvent system, were used in eq 4.4. Table 4.6 summarizes these values.

Table 4.6: Kinetic Solvent Isotope Effects for 6 - 9.

Compound	k_{H_2O}/k_{D_2O}
6	1.2
7	1.7
8	1.8
9	≥1.4[a]

[a] Fluorescence lifetimes below the limit of detection, quoted value is Φ_{H_2O}/Φ_{D_2O}.

The kinetic solvent isotope effects are relatively large and in the expected range for a mechanism involving a large degree of solvent association in the transition state.[118]

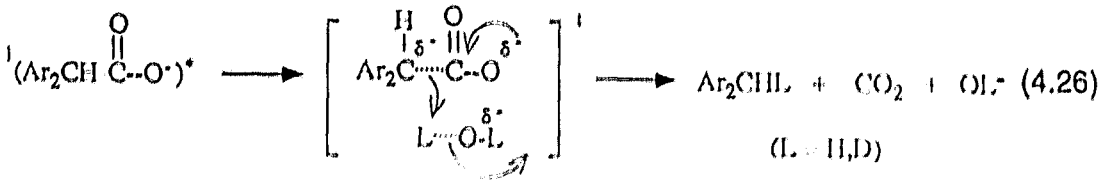

(4.26)

These observations are consistent with an ionic mechanism and also indicate that the C-C bond cleavage may be concerted with protonation from the solvent, (eq. 4.26). The smallest kinetic solvent isotope effect was observed for **6**, which is expected since the carbanion generated in this case is the most stabilized, at least in the ground state. Since the fluorescence lifetimes of **9** were < 0.15 ns in 20% ACN-H_2O, τ_{D_2O}/τ_{H_2O} could not be determined and the entry for **9** in Table 4.5 must be considered a lower limit.

Mechanism. Although numerous reports on the photodecarboxylations of carboxylic acids and esters have established the generality of this reaction, a variety of mechanisms can operate, depending on the substrate and the solvent conditions. It is important to point out that the photochemical decarboxylations in the present study differ from most of the previous examples in two ways. Firstly, the quantum yields of the diaryl acetates **6** - **8** are moderate to high, sharply contrasting most of the previously studied substrates, which are considerably less efficient (Φ_p < 0.1). Secondly, we observe the importance of the carboxylate ion in the efficient photodecarboxylation reactions, since neither the esters nor the acidic form of **6** - **9** displayed this reactivity. Although Miller[82] has outlined 25 possible cleavage modes for the protonated or alkylated carboxyl function, most of these can be eliminated on the basis of our product studies. Therefore, we will consider four primary processes of the excited state carboxylates, as depicted in equations 4.27 - 4.30 below.

$$^1R\text{-}CO_2^- \xrightarrow{k_{dc}} R^- + CO_2 \qquad (4.27)$$

$$^1R\text{-}CO_2^- \xrightarrow{k_h} R\cdot + CO_2^{\cdot-} \xrightarrow{k_{ET}} R^- + CO_2 \qquad (4.28)$$

$$^1R\text{-}CO_2^- \xrightarrow[-e^-]{k_{ec}} R\text{-}CO_2\cdot \xrightarrow{k'_h} R\cdot + CO_2 \qquad (4.29)$$

$$^1R\text{-}CO_2^- \xrightarrow{k_{ISC}} {}^3R\text{-}CO_2^- \xrightarrow[-e^-]{k'_{ec}} R\text{-}CO_2\cdot \xrightarrow{k'_h} R\cdot + CO_2 \qquad (4.30)$$

$$R\cdot + e^- \xrightarrow{k_{cc}} R^- \qquad (4.31)$$

In the first and simplest mechanism, the carboxylate singlet is converted directly to the carbanion as a molecule of CO_2 is ejected. The second process, eq 4.28, involves direct homolytic fragmentation, k_h, of the carboxylate ion to generate the hydrocarbon radical and the radical anion of carbon dioxide. The initially formed radical-radical anion pair then undergoes electron transfer (k_{ET}),to generate the carbanion and CO_2. Although the redox potentials of the various couples are not known, it is not clear why the suberenyl system, which would form the ground state antiaromatic anion, should be the most favoured. In fact the exact opposite trend to that observed might have been expected. Furthermore, the complete absence of radical coupling products, and the large substrate-dependent solvent isotope effects, are inconsistent with this mechanism. A

mechanism in which the excited state carboxylate ejects an electron has been proposed in other photodecarboxylation reactions[116] and is presented in eq 4.29. In this sequence, electron ejection (k_{ee}) is followed by homolytic cleavage (k'_h) to yield the corresponding hydrocarbon radical intermediate. If these radicals are to be converted into the carbanion, as the deuterium incorporation results suggest, they must recapture the initially ejected electrons, eq 4.31. We find this mechanism unreasonable since in the present study no radical coupling products are observed in the direct photolysis experiments. It has been shown that similar radicals produced in this mixed solvent system abstract a hydrogen from ACN and generate products of the form R-H, R-CH_2CN and R-R. It is difficult to imagine that electron capture could compete with these coupling processes so efficiently. The final mechanism involves intersystem crossing to the triplet, followed by electron ejection. Sensitization experiments rule out the involvement of triplets in the direct photolysis, but it should be noted that radical coupling products were observed in the triplet sensitization experiments. This implies that the triplet state may undergo either the direct homolytic fragmentation as in eq 4.28 or the electron ejection process outlined in eq 4.29.

The following observations support an ionic mechanism involving heterolytic carbon-carbon bond cleavage of the carboxylate ions as the primary photochemical event. (1) The incorporation of deuterium in the photoproducts when the reactions are carried out in D_2O implicate the intermediacy of carbanions. The complete

absence of radical coupling products, many of which have been identified in the photosolvolysis work wnere radical intermediates reacted with the solvent, is inconsistent with radical intermediates in the photodecarboxylation reaction. (2) The transient fluorescence data, which displayed a strong dependence on the solvent composition in mixed H_2O-ACN solutions (Table 3.10), indicate that the solvent polarity has a marked affect on the primary photochemical event. The mechanisms shown in eq 4.28 and 4.29 are inconsistent with this observation. (3) The large normal kinetic isotope effect suggests a heterolytic cleavage step which is associated with strong solvent interactions at the transition state. A homolytic fragmentation leading to radical products would be expected to be affected to a much lesser extent.

A working mechanism that is consistent with our observations is presented in Scheme II.

SCHEME II

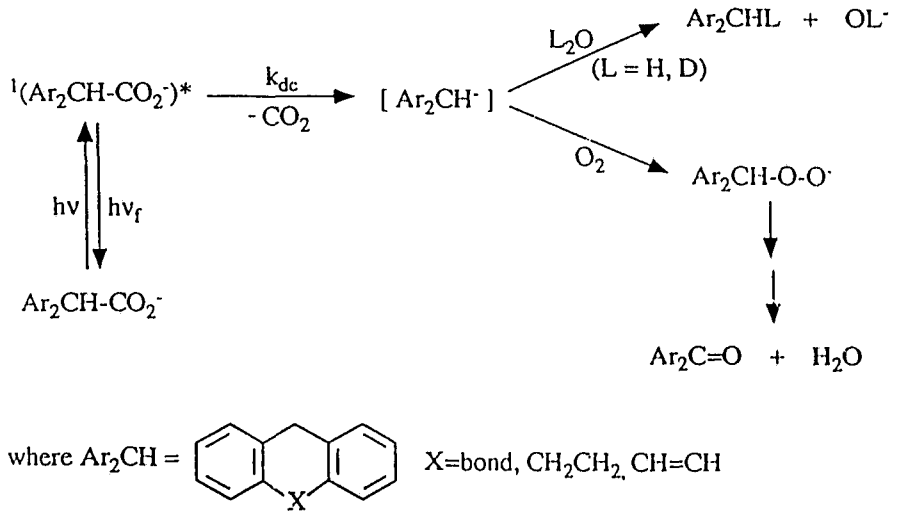

The carbanions produced in the decarboxylation step are many orders of magnitude more basic than the solvent, H_2O. Therefore, the carbanions will be protonated promptly and, in some cases, this is likely concerted with their formation. The only system which produced appreciable amounts of the ketone in oxygenated solution also had the smallest kinetic solvent isotope effect. Since the 9-fluorenyl anion is stabilized by aromaticity in the ground state, it is expected to have the longest lifetime as the "free carbanion".

In ionic ground state decarboxylations it is recognized that electron withdrawing groups that can stabilize the departing carbanion, typically β-carbonyl functions, accelerate the reaction.[69] The tendency of **9** and, to a lesser extent, **30** to decarboxylate in their acidic forms would indicate that in the excited state the departing 5-suberenyl anion has an unusual stabilizing ability.

Adiabaticity. Although heterolytic carbon-carbon bond cleavage is rare in photochemical reactions, a number of recent examples have been reported. There are no known examples of such processes occurring adiabatically. Although photodecarboxylation via eq 4.27 could, in principle, occur on the excited state surface (generating the excited state carbanion), such a process would be remarkable. We have not observed anion fluorescence upon excitation of the carboxylates investigated in this study.

Flash Photolysis. Time-resolved studies on some of the carboxylate ions mentioned here have recently been undertaken by Hilinski and co-workers.[117] Although reports of this work are unavailable at this time, preliminary results have indicated that, upon photolysis in H_2O, 5-suberene carboxylic acid (**9**) produces a short-lived transient with $\lambda_{max} \approx 450$, 800 nm, ($\varepsilon_{450}/\varepsilon_{800} \approx 2$). These absorption characteristics are similar to those we observed on generating the 5-suberenyl anion in THF with n-BuLi ($\lambda_{max} \approx 450$, 800 nm; $\varepsilon_{450}/\varepsilon_{800} \approx 50$). We anxiously await further results from these time-resolved experiments.

4.2.2 Rate Constants.

Using the mechanism presented in Scheme II, the quantum yield expression for decarboxylation is given by,

$$\Phi_p = k_{dc}\tau \qquad (4.32)$$

Combining the product quantum yields and the fluorescence lifetimes (measured in 20% ACN-H_2O) according to eq 4.33 provides rate constants for heterolytic cleavage that can be directly compared in the assessment of the intrinsic excited state reactivity,

$$k_{dc} = \Phi_p/\tau \qquad (4.33)$$

These rate constants for **6** - **9** and **30** are summarized in Table 4.6.

Table 4.7: Rate Constants for Photodecarboxylation (k_{dc}).

Compound	k_{dc} (s^{-1})	Relative Rates
6	8.6×10^6	1
7	1.0×10^8	11
8	1.2×10^8	14
9	$\approx 6 \times 10^9$	680
30	$\approx 4 \times 10^9$	450

The aryl acetates **9** and **30** have exceedingly short fluorescence lifetimes in aqueous solution ($\tau_f \approx 100$ ps) consistent with a high reactivity in this solvent. Compounds **6** - **8**, on the other hand, have lifetimes in the nanosecond range ($\tau_f \approx$ 2-5 ns) and rate constants that are correspondingly much lower than those for **9** and **30**. Notably **6**, which is the most reactive towards decarboxylation in the

ground state, shows the least tendency to react from S_1.

4.3 THE INTERNAL CYCLIC ARRAY

The effect of the ICA in the thermal reactions of **1** - **5** and **6** - **9** is readily understood on the basis of the Hückel *4n+2* rule for aromatic ground states. Thus those systems that proceed via aromatic intermediates (i.e., the 5-suberenyl cation (6 π) and the 9-fluorenyl anion (6 π) are at least three orders of magnitude more reactive than those proceeding through intermediates that are formally antiaromatic, (i.e., the fluorenyl cation (4 π) and the suberenyl anion (8 π). Since systems which do not contain an ICA of π electrons, such as **2** - **4** and **7** - **8**, produce charged intermediates that are neither stabilized nor destabilized by aromaticity, they display reactivities intermediate between these extremes. The relative reactivity for *photodehydroxylation* (Table 4.3) demonstrates a dramatic reversal in the ground state dependence on the ICA. Thus in the photosolvolysis series, which proceed through carbocation intermediates, the most reactive systems, the 9-fluorenols, have an ICA containing 4π electrons. This appears to be a particularly favourable arrangement as the 9-fluorenols (**1**, **12**, **16**) are the most reactive compounds towards photodehydroxylation known to date. Based on their estimated rate constants (k_s), the 9-fluorenols ($k_s \approx 5 \times 10^9$ s^{-1}) are considerably more reactive than 2,6-dimethyoxybenzyl alcohol ($k_s = 5.3 \times 10^8$ s^{-1}). Thus the 4π electron ICA provides a better driving force for dehydroxylation than

two ortho methoxy substituents! The observation that **2** and **3** fail to photodehydroxylate indicates that the unusual reactivity of **1** is not associated with an effect of α-phenyl or 2-phenyl substitution on benzyl alcohol. That **1** reacts more efficiently than 5-suberol (**4**), $k_s(\mathbf{1})/k_s(\mathbf{4}) \approx 10^2$, further suggests that there is a special driving force associated with the ICA. 5-suberenol (**5**), in which the incipient cation has 6π electrons in the ICA, is the least reactive system and is, based on the k_s values, nearly 500 times slower than **1**. That **5** is less reactive than **4** in the excited state is significant since it would indicate that the arrangement of 6 π electrons in the ICA actually decreases the rate of the reaction.

The relative reactivities for photodecarboxylation (Table 4.7) also indicates that the reactivity trends in the photochemically activated process are in opposition to those observed in the ground state.[70] Thus, in the photodecarboxylation series 5-suberene carboxylic acid (**9**), which proceeds through an 8π electron ICA, was the most reactive system. In fact, based on the product quantum yield and the excited state rate constant ($\Phi_p = 0.6$, $k_{dc} \approx 6 \times 10^9 s^{-1}$), **9** is one of the most reactive organic compound towards decarboxylation known to date. In contrast, 9-fluorene carboxylic acid ($k_{dc} \approx 8.8 \times 10^6\ s^{-1}$) is even less reactive towards photodecarboxylation than **7** and **8,** which do not have a conjugated internal cyclic array. This suggests that the presence of a *4n+2* π ICA actually has a retarding effect on the photodecarboxylation rates.

In interpreting the dependence of the excited state reaction rates on structural features, such as the number of π electrons in the ICA, it is tempting to use the same arguments employed for the ground state series. These arguments are essentially thermodynamic and based on the stability of the various charged intermediates, which are known to be either aromatic or antiaromatic on the basis of electron count. Transformations that lead to the highly destabilized *4n* π intermediates (higher ΔG°) will have considerably larger activation barriers (increased $\Delta G^{\ddagger}$). This intuitive argument is based on the Hammond postulate[118], which relates thermodynamic features of an elementary reaction to the structure and energy of the transition state, and hence kinetic behaviour. This approach is presented diagrammatically in Figure 4.3.

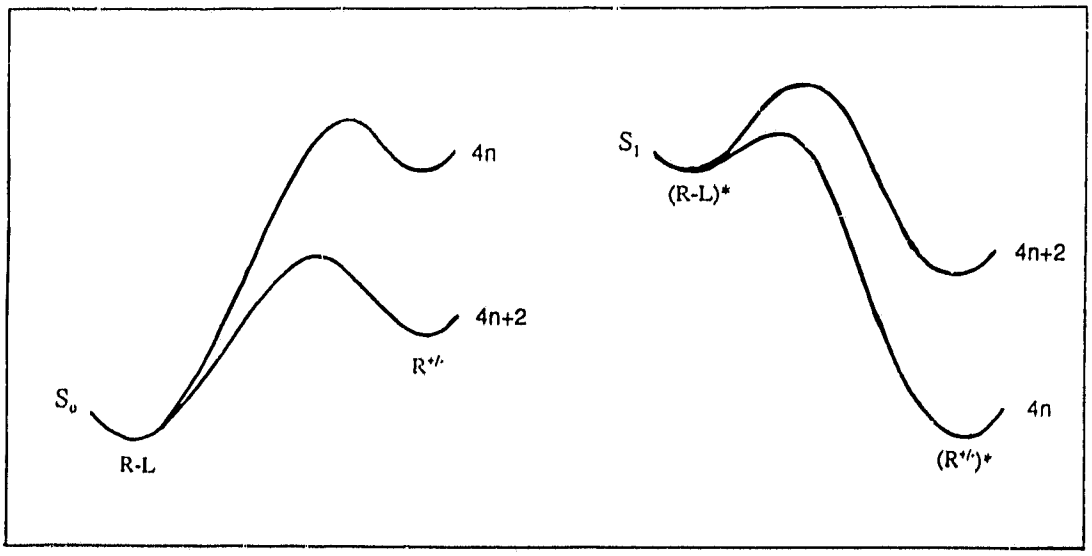

Figure 4.3: Implications of the Hammond Postulate to S_o and S_1 Cleavages.

Application of Förster cycle type calculations to the photogeneration of the

charged intermediates indicates that all the transformations are exothermic in the excited state. If we take the increased photoreactivity of the *4n* systems to imply a lower activation barrier on the S_1 surface, then extension of the Hammond postulate would indicate that the excited state *4n* charged intermediates are indeed more stabilized than their *4n + 2* counterparts. This interpretation is based on two assumptions about the excited state reactions: (1) applicability of the Hammond postulate to the S_1 surface and (2) an adiabatic cleavage step. At present, we have no reason to doubt the former, but the second assumption demands some consideration. If the excited states are "funnelling" down to the ground state potential energy surface, rather than proceeding completely on the S_1 surface, an enhanced stability of the *4n* systems is not required to explain the observed reactivity trends (Case I, Figure 4.4). Instead, one could envisage the *4n* systems being more reactive simply on the basis of the higher thermal activation barriers (known for the ground state reactions), which bring the S_o and S_1 surfaces much closer together and hence increase the rate of internal conversion.

In this case the excited state reactivity is not a function of the S_1 activation barrier, but rather of the S_0 - S_1 energy gap at some critical point along the reaction co-ordinate. However, since the transition state occurs late on the S_o surface (endothermic reaction) and rather early on the S_1 surface (exothermic reaction), it is unclear why internal conversion should occur prior to the S_1 activated complex. In order for diabatic return to the S_o surface to be product forming, it must occur late enough to intercept the S_o transition state. Thus, as

long as internal conversion to S_o follows the rate limiting cleavage step, then the excited state reactivity reflects the S_1 energy barrier.

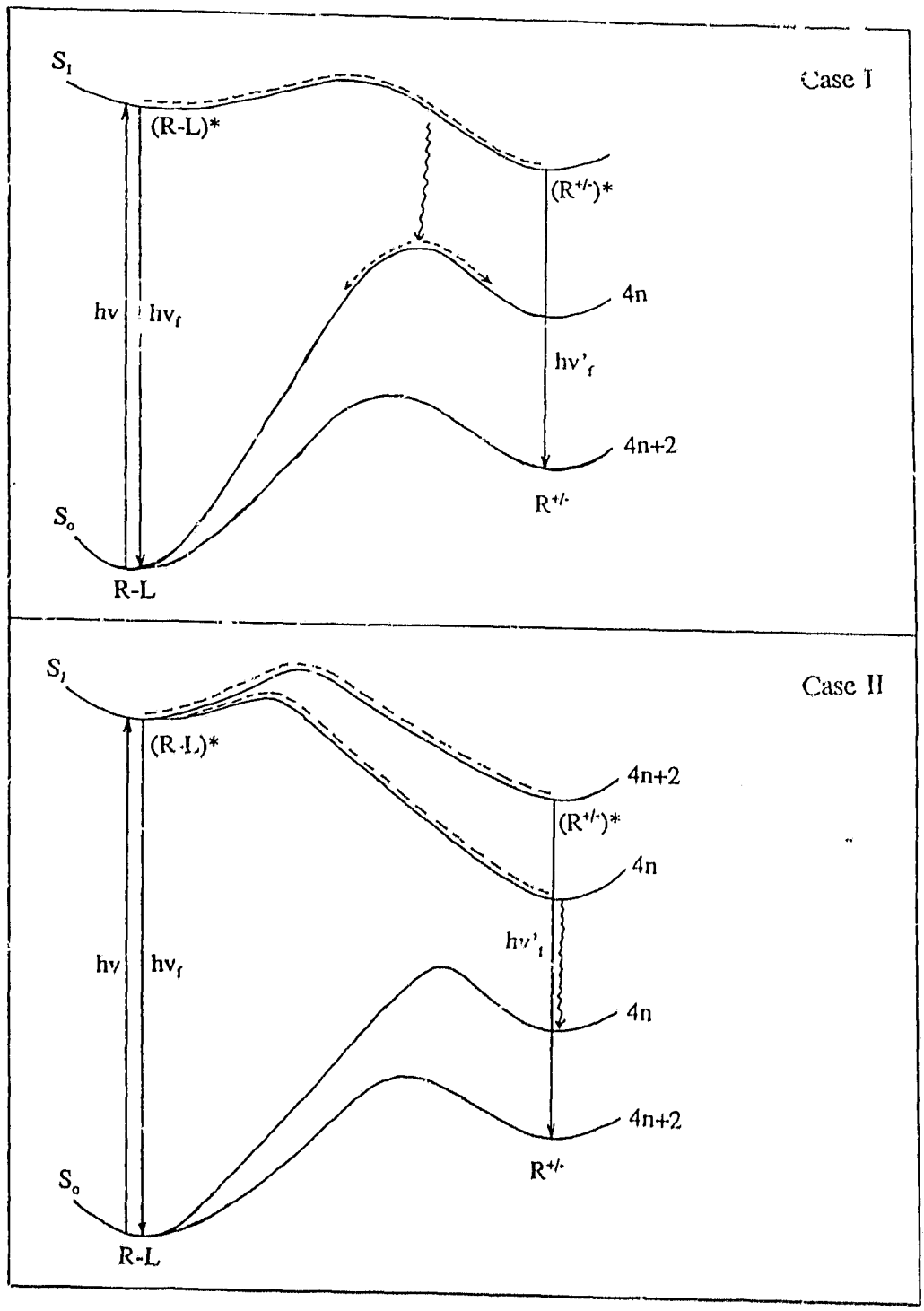

Figure 4.4: Generalized Potential Energy Surface Diagrams for Heterolytic Bond Cleavage Reactions. Case I involves internal conversion to the ground state surface in a diabatic process. Case II involves the adiabatic cleavage step followed by deactivation to the ground state ionic intermediates.

In light of what is known about the ground and excited state reactivities, we have attempted to construct a generalized potential energy surface diagram for the thermal and photochemical reactions leading to *4n* and *4n+2* π electron intermediates. In Case II, the photodehydroxylation or photodecarboxylation steps occur on the excited state surface and give rise to adiabatic fluorescence only for the *4n+2* systems, where the S_o-S_1 energy gap is relatively large. In this scheme, deactivation to the ground state surface occurs at the ionic intermediate stage. Thus, the reactions are adiabatic up to this point. Multiple collisions with the solvent or nucleophilic attack would almost certainly deactivate the charged intermediates to the ground state. At this point, the reaction can proceed toward completion along the S_o surface. Using the 0,0 energies of the precursor alcohols and carboxylic acids, obtained from the absorption and fluorescence spectra, the energy gap for the substrates is in the range of 85-95 kcal mol^{-1}. 5-suberenylium ion and 9-fluorenyl anion, the *4n+2* charged intermediates, have been well characterized in the ground state. Both are known to fluoresce[119,108] and their 0,0 energies can be easily estimated to be in the 54-56 kcal mol^{-1} range. Unfortunately, the electronic spectra for the antiaromatic ions are less well defined.

The calculations of Jug[61] and others have suggested that antiaromatic species have low lying excited states. This may move the transitions beyond the 800 nm cut-off in the optical spectrum. Although Hilinski[117] has recently assigned

absorptions at λ_{max} = 515 nm to Fl^+, it has been suggested that these may arise from S_o - S_2 transitions.[117] We have generated the other *4n* ionic species, 5-suberenyl anion, on treatment of **64** with n-butyllithium in THF solution. It appears to have a weak absorption at ≈ 800 nm. Although our knowledge of the transition energies of the *4n* ionic species is somewhat sketchy, we estimate the energy difference between S_o and S_1 for the *4n* ions is at least 20 kcal mol^{-1} smaller than the corresponding gap for the *4n+2* ions. This is depicted schematically in Case II of Figure 4.4. Hence, the efficient photogeneration of 4π electron carbocations and 8π electron carbanions would suggest that a *4n* stability rule applies in the excited state. These experimental observations corroborate the predictions of Jug and others and support the notion of "excited state aromaticity".[58-62] Experimental evidence of this sort is still scarce but ongoing research, particularly in the excited state carbon acid behaviour of the suberene chromophore (an 8 π system) further supports the findings of this work.

4.4 CONCLUDING REMARKS

The photolysis of various diaryl methanol and diaryl acetates derivatives has led to the photogeneration of a number of charged intermediates in aqueous solution. These reactions are significant in that they provide a means of studying these important intermediates in highly reactive solvent environments by means of laser flash photolysis. The efficient photogeneration of carbocations and carbanions that contain *4n* π electrons in a cyclic array of p-orbitals has demonstrated a dramatic *reversal of the ground state structure-reactivity relationship*. The results demonstrate that reactions leading to intermediates with an electron count of *4n* are enhanced in the excited state. This behaviour suggests that species containing a *4n* ICA are stabilized on the excited singlet state surface. These experimental results provide evidence for the theoretical predictions of "excited state aromaticity" in the *4n* systems.

CHAPTER FIVE

EXPERIMENTAL PROCEDURES

5.1 INSTRUMENTATION

^{1}H NMR spectra were recorded on a Perkin-Elmer R32 (90 MHz) or a Bruker WM-250 (250 MHz) or a Bruker AMX (360 MHz) instrument in $CDCl_3$, unless otherwise noted. Tetramethylsilane (Aldrich gold label) was used as an internal standard for the 90 MHz spectra. UV spectra were obtained on a Perkin-Elmer Lamda 4B or a Pye-Unicam 800 spectrophotometer. IR spectra were recorded on a Perkin-Elmer 283 instrument on NaCl discs and/or solution cells. Mass spectra were taken on a Finnigan 3300 instrument. Melting points were obtained on a Koefler hot stage microscope and are uncorrected. Gas chromatography was performed on a Varian 3700 instrument with a Hewlett-Packard 3390A integrator. Acidites in the pH range were measured on a Corning pH meter 140. Photolyses were carried out in Suprasil quartz cuvettes or 100/200/600 mL quartz tubes using a Rayonet RPR 100 photochemical reactor. An Oriel 200 W Hg light source and an Applied Photophysics monochromator on an optical bench were used for the quantum yield determinations. Fluorescence spectra were taken on a Perkin-Elmer MPF 66 spectrofluorimeter or the Photon Technologies LS-1 in steady state mode. Fluorescence lifetimes were measured using time correlated single photon counting on a Photon Technologies LS-1 instrument in lifetime mode and/or at the Center for Fast Kinetics Research (University of Texas at Austin), using a mode-locked, synch-pumped, cavity-

dumped dye laser, frequency doubled to provide an excitation source at 280 nm (Spectra Physics model 574B dye laser with Spectra Physics series 3000 Nd:YAG as the pump source) and /or in the laboratory of Prof. D. Holden (University of Waterloo), using a Photochemical Research Associates instrument and a standard hydrogen spark lamp.

5.2 COMMON LABORATORY REAGENTS

Dichloromethane (Van Waters and Rogers Ltd.) was distilled before use. Other solvents (A.C.S. reagent grade) were used in reactions, for extraction or for column chromatography without further purification. Deuterated solvents used for NMR spectroscopy were $CDCl_3$ (Aldrich gold label) and acetone-d_6 (MSD Isotopes). The D_2O used for solvent isotope studies, preparatory photolysis and NMR spectroscopy was 99.9% D (MSD Isotopes). Standard buffer solutions (Fisher Scientific), ionic strength 0.05 M unless otherwise noted, were used for product quantum yield experiments and fluorescence work. Solvents for fluorescence studies were of the highest available purity available (H.P.L.C. or Spectral Grade) and checked for spurious emission before use.

5.3 MATERIALS

The following compounds were purchased from Aldrich Chemical Co. for use in synthetic preparations: 9-fluorenone; dibenzosuberenone; dibenzosuberone;

1-indanone; phthalic dicaboxyaldehyde; 2-naphthaldehyde; fluorene; dibenzosuberane; diphenylacetylene. The following compounds were used as secondary standards for fluorescence quantum yield experiments: benzene (spectral grade); naphthalene (recrystallized twice and then sublimed); anthracene (recrystallized three times); fluorene (recrystallized once and then sublimed); 2-aminopyridine (Aldrich, 99%+). The dibenzannelated secondary alcohols were prepared via $NaBH_4$ reduction of the corresponding ketones. The substituted dibenzannelated secondary alcohols were prepared by the addition of the appropriate organometallic reagent to the ketones. The benzo[b]fluorenols were obtained by a similar treatment of 11*H*-benzo[b]fluorenone, which was prepared by the method of Streitwieser and Brown.[120] The related alcohol α-phenyl-2-naphthalenemethanol (**22**) was made by the addition of phenyllithium to 2-naphthaldehyde. Inden-1-ol (**23**) was prepared from indene by the method of Hock and Ernst.[121] The carboxylic acid derivatives were prepared by treating the appropriate hydrocarbons with n-BuLi and quenching with CO_2, except 1,2-diphenylcyclopropene-3-carboxylic acid (**10**) which was prepared by the method of Breslow et al.[122] The dideuterated hydrocarbons were prepared from the reduction of the corresponding ketones with $LiAlD_4/AlCl_3$. The dibenzannelated ethanol derivatives were prepared from the BH_3 reduction of the corresponding carboxylic acids, except 5-suberenylmethanol which was obtained by $LiAlH_4$ reduction of the carboxylic acid.

5.3.1 9-Fluorenol (9*H*-fluoren-9-ol) (1). A solution of 10 g (60 mmol) of fluorenone in 200 mL of methanol was added to 200 mL methanol (made basic with 1 drop of 1 **M** NaOH) containing 0.9 g (30 mmol) of $NaBH_4$, at 0°C. The reaction mixture was stirred at room temperature for 1 h and then poured into 100 g of crushed ice acidified with 10% HCl. The organics were extracted with CH_2Cl_2 (3 x 200 mL), dried over $MgSO_4$, and the solvents removed under reduced pressure to give 9.4 g of a white solid (92% yield), which was recrystallized from ligroin; mp 155-156°C [lit.[123] mp 156°C]; 1H NMR δ 2.2 (boad d, J=6 Hz, 1H) 5.50 (broad s, J=6 Hz, 1H) 7.2-7.7 (m, 8H); mass spectrum (CI) (m/z) 183 (M^++1).

5.3.2 9-Deuterio-9-fluorenol (9-deuterio-9*H*-fluoren-9-ol) (11). To 3.0 g (17 mmol) of fluorenone dissolved in 50 mL of anhydrous ether was added 0.22 g (5.2 mmol) of $LiAlD_4$. After 2 h stirring under reflux, the reaction mixture was poured onto 100 g of an ice/water mixture acidified with 10% HCl and extracted with ether, to yield 2.6 g of a white solid (84% yield), which was recrystallized from ligroin; mp 154°C; ^{1}H NMR δ 1.95 (s, 1H) 7.2-7.7 (m, 8H); mass spectrum (CI) (m/z) 184 (M^++1).

5.3.3 9-Methyl-9-fluorenol (9-methyl-9*H*-fluoren-9-ol) (12). To a solution of 5 g (28 mmol) of fluorenone in 150 mL of anhydrous ether was added 32 mmol of a 1.7 **M** solution of methyl lithium (Aldrich) and refluxed for 2 h. The reaction was worked up by pouring onto 50 g of crushed ice acidified with 10 % HCl. The

organic layer was washed with brine (1 x 100 mL) and H_2O (1 x 100 mL) and then dried over $MgSO_4$,and filtered. The solvent was evaporated at reduced pressure to give 5 g of a white solid (90 % yield), which was recrystallized from hexane; mp 174-176°C; [lit.[124] mp 174-175°C]; ^1H NMR δ 1.65 (s, 3H) 2.0 (s, 1H) 7.2-7.7 (m, 8H); mass spectrum (CI) (m/z) 197 (M^++1).

5.3.4 9-Vinyl-9-fluorenol (9-vinyl-9*H*-fluoren-9-ol) (13). A solution of fluorenone was treated with 1.5 equivalents of vinyl magnesium bromide (Aldrich) and worked up in the usual manner to yield the carbinol as a white solid, which was recrystallized from hexane; mp 91-92°C; ^1H NMR δ 2.15 (br. s, 1H) 5.18 (d of d, J_1 = 9 Hz, J_3 = 2Hz,1H) 5.52 (d of d, J_2 = 16 Hz, J_3 = 2Hz, 1H) 5.98 (d of d, J_1 = 9 Hz, J_2 = 16 Hz, 1H) 7.2-7.7 (m, 8H).

5.3.5 9-*iso*-Propyl-9-fluorenol (9-*iso*-propyl-9*H*-fluoren-9-ol) (14). To a solution of 10 g (56 mmol) of fluorenone in 300 mL of anhydrous ether was added 62 mmol of a 2.0 **M** solution of isopropyl magnesium chloride (Aldrich) via syringe. The solution was heated to reflux for 2 hours and then quenched by pouring into 200 mL of a saturated aqueous NH_4Cl. The organic layer was separated and washed with H_2O (2 x 200 mL), dried on $MgSO_4$, filtered, and reduced under vacuum to yield 10 g of a viscous orange oil. Chromatography on silica gel, eluted with CH_2Cl_2 gave 6 g (50% yield) of a white crystalline, which was recrystallized from hexane; mp 85-88°C [lit.[124] mp 99-101°C]; ^1H NMR δ 0.90 (d, J = 6 Hz, 6H) 2.2

(br. s, 1H) 2.45 (sept., J = 6 Hz, 1H) 7.2-7.8 (m, 8H); mass spectrum (EI) (m/z) 206 (M^+-18).

5.3.6 9-*t*-Butyl-9-fluorenol (9-*t*-butyl-9*H*-fluoren-9-ol) (15). To a solution of 50 g (30 mmol) of fluorenone in 100 mL of dry THF at 0°C under nitrogen was added drop wise a 2.0 **M** solution of t-butyl magnesium chloride (Aldrich) via syringe. The reaction was refluxed for 10 h and then poured into an aqueous ammonium chloride solution, and extracted with CH_2Cl_2 (3 x 150 mL). The combined organic layers were dried on $MgSO_4$, filtered and evaporated at reduced pressure to yield 5 g of a crude yellow solid. Separation on silica gel, solvent gradient 10% CH_2Cl_2-hexane to 40% CH_2Cl_2-hexane gave 1 g of the alcohol as a white solid, which was recrystallized from hexane; mp 94-95°C [lit.[125] 96°C]; ^{1}H NMR δ 0.98 (s, 9H) 2.1 (br.s, 1H) 7.2-7.6 (m, 8H).

5.3.7 9-Phenyl-9-fluorenol (9-phenyl-9*H*-fluoren-9-ol) (16). A solution of fluorenone was treated with phenyl magnesium bromide and worked up in the usual manner, to yield the carbinol as a white solid, which was recrystallized from hexane; mp 87-88°C [lit.[126] 85-88°C]; ^{1}H NMR δ 2.36 (s, 1H) 7.1-7.7 (m, 13H); mass spectrum (CI) (m/z) 259 (M^++1).

5.3.8 9-Bromofluorene (9-bromo-9*H*-fluorene) (18). To a solution of 5 g (30

mmol) of fluorene in 100 mL of CCl_4 was added 5.3 g (35 mmol) of N-bromosuccinimide and 0.05 g of benzoyl peroxide. The reaction was refluxed for 24 h before cooling and removing the succinimide by filtration. Removal of the solvent under reduced pressure yielded 6.6 g of 9-bromofluorene as a brown solid (90 % yield), which gave white needles after recrystallization from ligroin; mp 102-105°C [lit.[127] mp 104-105°C]; ^{1}H NMR δ 5.92 (s, 1H) 7.2-7.7 (m, 8H); mass spectrum (CI) (m/z) 245/247 (M^++1).

5.3.9 9-Methoxyfluorene (9-methoxy-9*H*-fluorene) (17). A solution of 0.5 g (2.0 mmol) of 9-bromofluorene in 10 mL of methanol was heated to reflux for 24 h. Removal of the solvent at reduced pressure gave a viscous yellow oil that solidified at -10°C, which was recrystallized from pet. ether; mp 41-43°C [lit.[128] mp 42-43°C]; ^{1}H NMR δ 3.00 (s,3H) 5.52 (s, 1H) 7.2-7.7 (m, 8H); mass spectrum (CI) (m/z) 197 (M^++1).

5.3.10 9-(Trideuteriomethoxy)fluorene (9-trideuteriomethoxy-9*H*-fluorene). To 3.0 mL of MeOH-d_4 (Aldrich NMR grade 99.5 atom % D) was added 250 mg (1.0 mmol) of 9-bromofluorene. After 48 h at reflux, the solvent was evaporated to yield a viscous oil which solidified on standing to give 150 mg (76% yield). The crude product was recrystallized from petroleum ether; mp 38-40°C; ^{1}H NMR δ 5.58 (s, 1H) 7.2-7.7 (m, 8H); mass spectrum (CI) (m/z) 200 (M^++1).

5.3.11 5-Suberol (5*H*-dibenzo[a,d]cycloheptan-5-ol) (4). Treatment of a methanol solution of dibenzosuberone with $NaBH_4$ in the manner described in the preparation of 9-fluorenol, gave 5-suberol as a white solid (90% yield), which was recrystallized from hexane; mp 91-92°C [lit.[129] mp 91-93°C]; ^1H NMR δ 2.4 (br.s, 1H) 2.6-3.6 (mult., 4H) 5.80 (broad s, 1H) 7.0-7.5 (m, 8H); mass spectrum (EI) (m/z) 210 (M^+).

5.3.12 5-Methyl-5-suberol (5-methyl-5*H*-dibenzo[a,d]cycloheptan-5-ol) (24). To a stirred solution of 6.3 g (30 mmol) of dibenzosuberone in 200 mL of dry THF at -10°C was added 32 mmol of a 1.7 **M** solution of methyl lithium (Aldrich) via syringe under nitrogen. The reaction was warmed to room temperature and stirred for one hour. The reaction was worked up by reducing the THF to 10 mL under vacuum, diluting with CH_2Cl_2 (100 mL) and washing with saturated NH_4Cl (100 mL) followed by H_2O (100 mL). The organic fraction was dried over $MgSO_4$, filtered and reduced under vacuum to yield 6 g of a white solid (90% yield), which was recrystallized from hexane; mp 146-147°C(sublimes); ^1H NMR δ 1.84 (s, 3H) 2.2 (broad s, 1H) 3.8-3.4 (m, 4H) 7.0-7.3 (m, 6H) 7.8-8.0 (m, 2H); mass spectrum (EI) (m/z) 224 (M^+).

5.3.13 5-*t*-Butyl-5-suberol (5-*t*-butyl-5*H*-dibenzo[a,d]cycloheptan-5-ol). To a solution of 6 g (29 mmol) of dibenzosuberone in 100 mL of dry THF, stirred at 0°C, was added 30 mmol of o 2.0 **M** solution of t-butyl magnesium chloride (Aldrich) via

syringe. The solution was heated to reflux for one hour, before being concentrated to 20 mL and diluted with 200 mL of CH_2Cl_2. The organic layer was dried on $MgSO_4$, filtered, and reduced under vacuum to yield a viscous yellow oil, which failed to crystallize on standing. Column chromatography on silica gel eluting with 50% (v/v) CH_2Cl_2/hexane gave 2.2 g (30% yield) of white crystalline solid, which was recrystallized from hexane; mp 99-102°C; ^{1}H nmr δ 8.0-8.2 (m, 2H) 7.1-7.3 (m, 6H) 2.7-3.7 (m, 4H) 1.9 (s, 1H), 1.0 (s, 9H); mass spectrum (CI) (m/z) 267 (M^++1).

5.3.14 5-Suberenol (5*H*-dibenzo[a,d]cyclohepten-5-ol) (5). To 10 g (49 mmol) of dibenzosuberenone dissolved in 200 mL of cold MeOH was added 1.0 g (98 mmol) of $NaBH_4$. After 2 h stirring the solution was quenched with 100 mL of a saturated NH_4Cl solution and extracted with CH_2Cl_2 (3 x 200 ml) to give 8.2 g of a solid (80% yield), which was recrystallized from ligroin; mp 122°C [lit.[129] mp 122-124°C]; ^{1}H NMR δ 2.42 (d, J=6 Hz, 1H) 5.34 (d, J=6 Hz, 1H) 7.04 (s, 2H) 7.2-7.7 (m, 8H); mass spectrum (EI) (m/z) 208 (M^+).

5.3.15 5-Deuterio-5-suberenol (5-deuterio-5*H*-dibenzo[a,d]cyclohepten-5-ol) (25). Treatment of dibenzosuberenone with $LiAlD_4$ in anhydrous ether by the procedure outlined in the preparation of 9-deuterio-9-fluorenol, gave a white solid (90% yield), which was recrystallized from ligroin; mp 119-120°C; ^{1}H NMR δ 2.5 (broad s, 1H) 7.04 (s, 2H) 7.2-7.7 (m, 8H); mass spectrum (EI) (m/z) 209 (M^+).

5.3.16 5-Methyl-5-suberenol (5-methyl-5*H*-dibenzo[a,d]cyclohepten-5-ol) (26).

To a prepared solution of methyl magnesium bromide (36 mmol) in 50 mL of anhydrous ether under N_2 and cooled to -5°C, was added 5.0 g (24 mmol) of dibenzosuberenone dissolved in 100 mL ether. After 1 h at reflux the reaction was quenched by diluting with 100 mL of a saturated NH_4Cl solution and then extracted with ether, to give 3.8 g of a white solid (71% yield), which was recrystallized from hexane; mp 118-120°C [lit.[130] mp 113.5-115°C]; ^{1}H NMR δ 1.6 (broad s, 3H) 2.4 (broad s, 1H) 6.96 (s, 2H) 7.2-8.0 (m, 8H); mass spectrum (EI) (m/z) 222 (M^+).

5.3.17 1*H*-Inden-1-ol (1-hydroxyindene) (23).

To 10 g (86 mmol) of indene (freshly distilled) in 200 mL of anhydrous ether was added 38 mL (95 mmol) of a 2.5 M solution of n-BuLi dropwise, at -78°C under a nitrogen atmosphere. After stirring for 20 min, the solution was purged with O_2 gas via syringe though a rubber septum. Purging was continued for 3 h at which time the temperature was raised to -40°C. A solution of 30 g of KI in 50 mL H_2O/75 mL glacial acetic acid was then poured into the reaction mixture and stirred for 1 h. The reaction mixture was then warmed to 5 °C and a solution of $Na_2S_2O_3$ (45 g in 100 mL H_2O) was added dropwise and stirred for an additional h. The reaction was worked up by neutralizing with 100 mL of 1 M NaOH and separating the organic layer. The aqueous portion was washed with ether (2 x 150 mL). The combined organic fractions were dried over $MgSO_4$ and evaporated to yield 10 g of a yellow oil. The crude material was microdistilled under vacuum (≈ 1 torr)

collecting a light yellow oil at 80°C, that solidified on cooling, which was recrystallized from 4:1 hexane/ether gave 4 g of a white solid, (35% yield), stored under nitrogen at -10°C; mp 49-53°C [lit.[131] mp 55-56°C]; ^{1}H nmr ($CDCl_3$) δ 2.3 (broad s, 1H) 5.08 (broad s, 1H) 6.30 (d, J=6 Hz, 1H) 6.65 (d, J=6 Hz) 7.1-7.6 (m, 4H).

5.3.18 9-methylenefluorene (9-methylene-9*H*-fluorene) (45). A number of attempts have been made to isolate and characterize this unstable compound, in order to confirm its formation in the photolysis of 9-methyl-9-fluorenol (**12**). Following the method of Wieland and Krause,[132] 9-methyl-9-fluorenol was treated with HCl (g) in diethyl ether and worked up to give 9-chloro-9-methylfluorene as a yellow oil, which was heated to 80°C in ethanol and rapidly cooled to yield a white solid. Insufficient quantities were obtained to get good quality ^{1}H NMR spectra, however the UV absorption spectra of this compound matches that obtained on photolysis of dilute (10^{-4} M) solutions of 9-methyl-9-fluorenol, (λ_{max} = 246, 255, 306 nm). Alternately, treatment of a stirred solution of 50 mg of 9-methyl-9-fluorenol (**12**) in 10 mL of acetonitrile with an equal volume of 10 **N** H_2SO_4 in argon saturated solutions for one h, gave a mixture of the carbinol and a compound with an ^{1}H NMR signal at δ 6.1 and an upfield aromatic multiplet δ 6.5-7.5. The UV characteristics match those above.

5.3.19 6,6-Dimethyldibenzofulvene (51). A solution of 1 g (45 mmol) of 9-

isopropyl-9-fluorenol in 25 mL of glacial acetic acid containing 0.3 g of p-toluenesulfonic acid monohydrate was refluxed under nitrogen for 12 h. The solution was cooled and poured into 100 mL of H_2O and extracted with CH_2Cl_2 (2 x 100 ml). The combined organic fractions were dried over $MgSO_4$, filtered and the methylene chloride removed under reduced pressure, to give 0.7 g of a yellow solid, (70% yield), which was recrystallized from ethanol; mp 102-108°C [lit.[133] mp 113-116°C]; ^{1}H NMR δ 2.45 (s, 6H) 7.2-7.9 (m, 8H).

5.3.20 5-methylenesuberane (5-methylene-5*H*-dibenzo[a,d]cycloheptane) (61). A solution of 100 mg of 5-methyl-5-suberol dissolved in 40 mL acetonitrile was treated with an equal volume of ≈ 0.1 **M** $HCLO_4$ for one h. After extracting with methylene chloride and evaporating to dryness, 5-methylenesuberane was isolated by preparative thin layer chromatography, (silica/CH_2Cl_2).; mp 64-65 °C; ^{1}H NMR δ 3.10 (s, 4H) 5.40 (s, 2H) 7.1-7.5 (m, 8H); mass spectrum (EI) (m/z) 206 (M^+).

5.3.21 5-methylenesuberene (5-methylene-5*H*-dibenzo[a,d]cycloheptene) (67). 5-Methyl-5-suberenol was readily dehydrated in mildly acidic solution (pH ≈ 2) to yield a white solid which was purified by preparative TLC; mp 96 °C; ^{1}H NMR δ 5.22 (s, 2H) 6.80 (s, 2H) 7.2-7.5 (m, 8H); mass spectrum (EI) (m/z) 204 (M^+).

5.3.22 11*H*-benzo[b]fluorenone. To 20 mL of freshly distilled dry ethanol, was added 0.32 g (14 mmol) of Na. To this was added a solution of 9.35 g (70 mmol)

of phthalic dicarboxaldehyde in 50 mL of ethanol, followed by the dropwise addition of a solution of 8.66 g (66 mmol) of 1-indanone in 150 mL of ethanol. The reaction solution was stirred for 20 h and then heated to reflux for a additional 24 h. After cooling to room temperature, 8 g of a yellow solid was separated by filtration. The filtrate was concentrated and washed with Et_2O and H_2O. The combined organics were dried over $MgSO_4$ to yield a further 4 g of crude product. The crude material was recrystallized from ethanol to yield 8 g of 11*H*-benzo[b]fluorenone, (53% yield) as fine yellow crystals; mp 153 °C, [lit.[134] mp 153-154.5 °C]; ^{1}H NMR δ 7.0-8.3 (m); mass spectrum (EI) (m/z) 230 (M^+).

5.3.23 11*H*-Benzo[b]fluoren-11-ol (20). A solution of 5.0 g (22 mmol) of 11*H*-benzo[b]fluorenone in 100 mL of MeOH and 50 mL of THF was cooled 0°C while a suspension of 0.80 g (11 mmol) of $NaBH_4$ in 20 mL of MeOH was added dropwise. The reaction was warmed to ambient temperature and then refluxed for 12 h. The product was worked-up by concentrating the mixture to 20 mL, diluting with 200 mL of CH_2Cl_2, and then washing with aqueous NH_4Cl (1 x 200 mL) and H_2O (2 x 200 mL). The organic fraction was dried over $MgSO_4$, and evaporated to yield 4.6 g of a light yellow solid (90% yield), which was recrystallized from ligroin to give white plates; mp 184 °C,[lit.[135] mp 185 °C]; ^{1}H NMR δ 1.9 (d, J = 6 Hz, 1H) 5.75 (d, J = 6Hz, 1H) 7.3-8.1 (m, 10H); mass spectrum (EI) (m/z) 232 (M^+).

5.3.24 11-Methyl-11*H*-benzo[b]fluoren 11-ol (21). To a solution of 2.0 g (8.7 mmol) of benzo[b]fluorenone in 100 mL of dry THF cooled to 0°C under nitrogen was added 10 mmol of a 1.4 **M** solution of methyl lithium (Aldrich) via syringe. After warming to reflux for 1 h the volume of THF was reduced to 10 mL under reduced pressure and then diluted with 100 mL of CH_2Cl_2. After washing with a saturated NH_4Cl solution (1 x 100 ml) the combined organics were dried over $MgSO_4$, filtered and evaporated under vacuum to give 1.9 g of a white solid (90% yield), which was recrystallized from hexane; mp 146-147°C; ^1H NMR δ 1.80 (s, 3H) 2.10 (s, 1H) 7.2-8.1 (m, 10H).

5.3.25 11*H*-Benzo[b]fluorene (69). To a stirred suspension of 0.30 g (8 mmol) $LiAlH_4$ in 150 mL of dry THF was added 2.4 g (18 mmol) of $AlCl_3$ in small portions. The mixture was heated to reflux and 1.0 g (4.4 mmol) of benzo[b]fluorenone was extracted from the thimble of a soxhlet extractor into the reaction vessel over a 6 h period. The reaction was worked-up by reducing the THF to 10 mL, diluting with 100 mL CH_2Cl_2 and pouring onto 50 g of ice acidified with 5% H_2SO_4. The organic layer was separated, washed with H_2O, dried over $MgSO_4$, and evaporated to yield 0.88 g of a white solid (90% yield), which was recrystallized from MeOH and sublimed, mp 209-211 °C [lit.[136] mp 208.5-209.5 °C]; ^1H NMR δ 4.05 (s, 2H) 7.3-8.2 (m, 10H); mass spectrum (EI) (m/z) 216 (M^+).

5.3.26 α-Phenyl-2-naphthalenemethanol (22). To a solution of 5.0 g (32 mmol)

of β-naphthaldehyde in dry THF under nitrogen was added 35 mmol of a 1.8 **M** solution of phenyl lithium (Aldrich) via syringe. The solution was refluxed for 4 h and worked-up as follows. The solution was concentrated to about 20 mL, diluted with 200 mL CH_2Cl_2, and washed H_2O (2 x 200 mL). The combined organic fractions were dried over $MgSO_4$, and evaporated to yield 6.5 g of a white solid (85% yield), which was recrystallized from pet. ether; mp 87-88 °C, [lit.[1,7] mp 87-88 °C]; ^1H NMR δ 2.45 (d, J = 5 Hz, 1H) 5.92 (d, J = 5Hz, 1H) 7.2-7.9 (m, 12H); mass spectrum (EI) (m/z) 232 (M^+).

5.3.27 5-Suberenylmethanol (5*H*-dibenzo[a,d]cycloheptenylmethanol). To a solution of 0.25 g (1.0 mmol) of 5-carboxmethoxy suberene in 50 mL of dry THF at room temperature, was added 0.08 g (2.0 mmol) of $LiAlH_4$. The reaction was refluxed for 5 h and then worked up by reducing the THF to 10 mL under reduced pressure, diluting with 50 mL of CH_2Cl_2 and washing with 5% HCl (1 x 100 mL) followed by H_2O (1 x 100 mL). The organic layer was dried over $MgSO_4$, filtered, and reduced under vacuum to yield a clear oil which solidified on standing, and was recrystallized from hexane; mp 78-81°C; ^1H NMR δ 1.6 (br.s, 1H) 3.70 (d, J = 8 Hz, 2H) 4.12 (t, J = 8 Hz, 1H) 6.80 (s, 2H) 7.1-7.3 (m, 8H); mass spectrum (EI) (m/z) 204 (M^+-18).

5.3.28 9-Fluorenylmethanol (35). A THF solution of 9-fluorene carboxylic acid was treated with BH_3 in a manner similar to that employed for 5-suberane

carboxylic acid. The compound was prepared in 80% yield and recrystallized from hexane; mp 100-101°C [lit. mp 102-104°C]; ^{1}H NMR δ 2.2 (broad s, 1H) 3.6-4.0 (m, 3H) 7.1-7.8 (m, 8H); mass spectrum (EI) (m/z)

5.3.29 5-Suberene carboxylic acid (5*H*-dibenzo[a,d]cycloheptene-5-carboxylic acid) (9). A solution of 1.0 g (5.2 mmol) dibenzosuberene in 100 mL of dry THF under nitrogen was cooled to 0°C and 5.7 mmol of a 2.5 **M** solution of n-BuLi (Aldrich) was added dropwise via syringe. The solution was heated to reflux for one h and then cooled to room temperature before purging with dry CO_2 (g) via syringe. The reaction was worked up by reducing the THF to 10 ml, diluting with 100 mL CH_2Cl_2, and then extracting with a 0.1 **M** NaOH solution (3 x 100 mL). The combined aqueous fractions were acidified and the cloudy precipitate extracted into CH_2Cl_2 (2 x 100 mL). The organic layer was dried over $MgSO_4$, filtered and reduced under vacuum to yield 0.7 g of a white solid (65% yield), which was recrystallized from 1:1 $CHCl_3$/hexane; mp 218-238°C sublimes [lit.[127] mp 241-242°C]; ^{1}H NMR (acetone-d_6) δ 3.8 (broad s, 1H) 5.16 (s, 1H) 7.05 (s, 2H) 7.2-7.6 (m, 8H); mass spectrum (CI) (m/z) 237 (M^++1).

5.3.30 5-Deuterio-5-suberene carboxylic acid (5-deuterio-5*H*-dibenzo[a,d]cycloheptene-5-carboxylic acid) (28). A solution of 5,5-dideuterio-dibenzosuberene was treated n-BuLi and CO_2(g) in the manner outlined above, to give white needles after recrystallization from ethanol; mp 226-239°C; ^{1}H NMR

(acetone-d_6) δ 5.8 (broad s, 1H) 7.05 (s, 2H) 7.2-7.6 (m, 8H); mass spectrum (CI) (m/z) 238 (M^++1).

5.3.31 9-Fluorene carboxylic acid (6). To a solution of 2.0 g (12 mmol) of fluorene in 100 mL of dry THF cooled to 0°C under a nitrogen atmosphere was added 20 mmol of a 1.7 **M** solution of n-BuLi (Aldrich) via syringe. The reaction was warmed to room temperature and stirred for one h. before pouring onto crushed solid carbon dioxide. The mixture was worked up by diluting with 200 mL of H_2O acidified with 10% HCl and extracting with CH_2Cl_2, (2 x 200 mL). The organic fractions were then extracted with 0.1 M NaOH (2 x 200 mL). The combined aqueous layers were cooled on ice and then acidified. Filtration of the precipitate gave 1.6 g of a white solid (60% yield), which was recrystallized from 95% ethanol; mp 202-210°C [lit.[127] mp 230-232°C]; ^{1}H NMR (acetone-d_6) δ 4.2 (broad s, 1H) 4.80 (s, 1H) 7.2-7.8 (m, 8H); mass spectrum (CI) (m/z) 213 (M^++1).

5.3.32 Diphenylacetic acid (7). Treatment of diphenylmethane with n-BuLi and CO_2(s) by the procedure outlined for 9-fluorene carboxylic acid (**6**) gave a white solid that was recrystallized from ethanol/H_2O; mp 148-150°C [lit.$_{127}$ mp 149°C]; ^{1}H NMR (acetone-d_6) δ 4.8 (broad s, 1H) 5.05 (s, 1H) 7.1-7.6 (m, 10H); mass spectrum (CI) (m/z) 215 (M^++1).

5.3.33 5-Suberane carboxylic acid (5*H*-dibenzo[a,d]cycloheptane-5-carboxylic

acid) (8). Treatment of dibenzosuberane with n-BuLi and CO_2(s) by the procedure outlined for 9-fluorene carboxylic acid (**6**) gave a solid material that was recrystallized from ethanol/H_2O; mp 205-211°C; ^{1}H NMR (acetone-d_6) δ 3.6-4.6 (m, 4H) 4.6 (broad s, 1H) 4.90 (s, 1H) 7.0-7.5 (m, 8H); mass spectrum (CI) (m/z) 239 (M^++1).

5.3.34 5-Methyl-5-suberene carboxylic acid (5-methyl-5*H*-dibenzo[a,d]cycloheptene-5-carboxylic acid) (30). To a solution of 0.25 g (1.06 mmol) of suberene carboxylic acid in 40 mL of dry THF cooled to -78°C under a nitrogen atmosphere was added 2.6 mmol of a 1.5 **M** solution of lithium diisopropylamide (Aldrich) via syringe. The solution was stirred for one h and warmed to reflux for an additional one h. A solution of 0.30 g (2.1 mmol) of methyl iodide in 20 mL of THF was added slowly via a dropping funnel. After stirring overnight, the reaction mixture was worked up by evaporating the THF to 10 ml, diluting with CH_2Cl_2 (100 mL) and extracting with aqueous sodium hydroxide (3 x 100 mL, 0.01 **M** NaOH). The aqueous fraction was acidified and extracted with CH_2Cl_2 (3 x 100 mL) to yield 150 mg of a white solid (55% yield); mp 190-210°C sublimes; ^{1}H NMR (acetone-d_6) δ 2.24 (s, 3H) 5.9 (broad s, 1H) 7.06 (s, 2H) 7.2-7.7 (m, 8H); mass spectrum (CI) (m/z) 251 (M^++1).

5.3.35 1,2-Diphenylcyclopropene-3-carboxylic acid (10). A solid mixture of 17 g (95 mmol) of diphenylacetylene and 1.0 g of copper powder (electrolytically

purified) in a three neck flask fitted with a reflux condenser, was heated to 135°C on an oil bath. Upon melting, 5.0 g (50 mmol) of diazoacetate was slowly added through a dropping funnel over a 2 h period, keeping the temperature between 130-140°C. After the addition was complete the mixture was cooled and diluted with 100 mL of ether and filtered. The ether was then removed under vacuum and the crude material was refluxed in alkaline methanol (30 g KOH in 200 mL MeOH) for 90 min. The reaction mixture was washed with CH_2Cl_2 (2 x 200 mL) to recover unreacted diphenylacetylene. The aqueous fraction was acidified and again extracted with CH_2Cl_2 (2 x 200 mL) to yield 2.5 g of a crude yellow solid (20% yield), which was recrystallized from acetone; mp 208-210°C [lit.[122] mp 209-211°C]; ^{1}H NMR (acetone-d_6) δ 2.78 (s, 1H) 7.2-7.8 (m, 10 H) 9.4 (broad s, 1H); mass spectrum (EI) (m/z) 220 (M^+).

5.3.36 5-Carbomethoxy suberene (5-carbomethoxy-5*H*-dibenzo[a,d]cycloheptene) (29). To a solution of 0.05 g (2.1 mmol) of suberene carboxylic acid (**9**) in 50 mL of methanol was added 1 mL of conc. H_2SO_4. The solution was refluxed for 12 hours and then evaporated to 10 ml, and diluted with 100 mL of CH_2Cl_2. This solution was washed with cold 0.1 **M** NaOH solution, (1 x 100 mL) followed by H_2O (1 x 100 mL). The organic fraction was dried over $MgSO_4$, and evaporated to yield 450 mg of a crude white solid (90% yield), which was recrystallized from methanol; mp 108-113°C; ^{1}H NMR δ 3.45 (s, 3H) 4.85 (s, 1H) 7.2-7.4 (m, 8H);

5.3.37 9-Carbomethoxy fluorene (32). To a solution of 1.5 g (7.0 mmol) of 9-fluorene carboxylic acid (**6**) in 100 mL of methanol was added 1.0 mL of conc. H_2SO_4. After refluxing overnight the reaction was worked up in the normal manner, (back washing with aqueous base to remove unreacted carboxylic acid), to give 1.4 g of a light yellow solid, (90% yield), which was recrystallized from methanol; mp 63-64 °C [lit.[127] mp 63°C]; ^{1}H NMR δ 3.70 (s, 3H) 4.85 (s, 1H) 7.2-7.8 (m, 8H); mass spectrum (EI) (m/z) 224 (M^+).

5.3.38 5-Methyl-5-carboethoxy-suberene (5-methyl-5-carboethoxy-5*H*-dibenzo[a,d]cycloheptene) (31). To a solution of 0.5 g (1.9 mmol) of 5-carboethoxysuberene in 50 mL of dry THF at 0°C was added 2.0 mmol of a 1.5 **M** solution of lithium diisopropylamide (Aldrich) via syringe under a nitrogen atmosphere. The solution was heated to reflux for 1 h and 0.50 g (3.6 mmol) of methyliodide was added from a dropping funnel. Stirring was continued for 12 h and then the volume of THF was reduced to 10 mL under vacuum. The residues were taken up in 100 mL of CH_2Cl_2 and washed with brine (2 x 100 mL) and H_2O (1 x 100 mL). The methylene chloride layer was dried over $MgSO_4$, filtered, and evaporated under reduced pressure to yield 0.5 g of gummy solid which was dissolved in a minimum volume of CH_2Cl_2, loaded on a preparative silica gel plate and developed in CH_2Cl_2. The highest band was removed and recrystallized from ethanol; mp °C; ^{1}H NMR δ 1.02 (t, J = 7 Hz, 3H) 2.18 (s, 3H) 3.94 (q, J = 7 Hz, 2H) 7.02 (s, 2H) 7.2-7.6 (m, 8H); mass spectrum (EI) (m/z) 278 (M^+).

5.3.39 5,5-Dideuterosuberene (5,5-dideuterio-5*H*-dibenzo[a,d]cycloheptene). To a suspension of 2.0 g (50 mmol) of $LiAlD_4$ and 6.4 g (48 mmol) of $AlCl_3$ in 40 mL of anhydrous ether under nitrogen was added a solution of 10 g (48 mmol) of dibenzosuberenone in 200 mL of dry ether via a dropping funnel. The addition took 1 h and the reaction was heated to reflux for an additional 3 h. The reaction was quenched by pouring onto 50 g of crushed ice acidified with 10% HCl. After extracting with CH_2Cl_2 (3 x 100 mL) the combined organic layers were dried over $MgSO_4$, filtered, and reduced under vacuum to yield 7 g of white solid (75% yield), which was recrystallized from ethanol; mp 132-133°C; ^1H NMR δ 7.04 (s, 2H) 7.2-7.5 (m, 8H); mass spectrum (EI) (m/z) 194 (M^+).

5.4 PHOTODEHYDROXYLATION

5.4.1 Product Studies.

5.4.1.1 Dark Reactions. None of the 9-fluorenol compounds studied in this work showed any tendency to react thermally under the conditions employed to investigate their photochemistry.The suberols thermally solvolyze at pH < 2, whereas the suberenols displayed some thermal solvolysis at pH < 5. However, at neutral pH, and the typically short irradiation times employed, these compounds exhibited no thermal reactivity. The photosolvolytic behaviour of 11*H*-benzo[b]fluoren-11-ol (**20**) and α-(phenyl)-2-naphthalenemethanol (**22**) were investigated at acidities as high as 0.10 **M** H_2SO_4 where there were no concurrent dark reactions. In more concentrated sulfuric acid solutions, 1.5 **M** and 0.5 **M**,

respectively, thermal solvolysis reactions became significant. A typical experimental procedure for a preparative dark reaction follows. A solution of 100 mg of compound dissolved in 100 mL of MeOH was diluted with 100 mL of water. The solution was stirred in the dark with a cold water circulator (≈ 12°C) for the appropriate irradiation time (usually less than 1 h). The reactions were worked up by saturating the aqueous solution with NaCl and extracting with CH_2Cl_2. The isolated materials were analyzed by ^1H NMR spectroscopy.

5.4.1.2 Relative Reactivity in the Ground State. Solutions consisting of ≈ 100 mg of 9-fluorenol (**1**), 5-suberol (**4**) and 5-suberenol (**5**), were prepared in 100 mL of MeOH and diluted with 100 mL of the appropriate acid solution (ranging from pH 7 to ≈ 40% H_2SO_4). The solutions were stirred in the dark for ≈ 1-2 h, and then extracted with CH_2Cl_2. The extent of reaction was determined by ^1H NMR. At pH 1, both **4** and **5** solvolyzed, the latter being the more reactive. On the other hand, **1** failed to react until much more strongly acidic solutions were used, e.g., 30-40% H_2SO_4.

5.4.1.3 Preparative Photolysis in methanol-water mixtures. In a typical preparative study 200 mg of substrate was dissolved in 100 mL of MeOH and then diluted with 100 mL H_2O. The solution was then transferred to a quartz vessel fitted with a cooling finger (≈ 12°C) and deaerated with a continuous steam of

nitrogen or argon. The solution was then irradiated at 254 nm. After photolysis, the solution was worked up by saturating with NaCl followed by extraction with of CH_2Cl_2 (3 x 100 mL). The photosolyate was then analyzed by ^1H NMR and gas chromatography from which the identity and ratios of various products was determined. Product mixtures were separated by preparative TLC. In each case, the methyl ethers were isolated and characterized by ^1H NMR and mass spectroscopy or by comparison with authentic samples. The ^1H NMR data for the isolated methyl ethers are presented below.

9-Methoxyfluorene (9-methoxy-9H-fluorene) (17).

^1H NMR δ 3.00 (s, 3H) 7.1-7.8 (m, 8H); mp 41-43°C [lit.[128] mp 42-43°C]; mass spectrum (EI) (m/z) 196 (M^+).

9-Methyl-9-methoxyfluorene (46).

^1H NMR δ 1.68 (s, 3H) 2.70 (s, 3H) 7.2-7.8 (m, 8H); mp 86-89°C; mass spectrum (CI) (m/z) 211 (M^++1).

9-Vinyl-9-methoxyfluorene (49).

^1H NMR δ 2.78 (s, 3H) 5.10 (d of d, 1H) 5.40 (d of d, 1H) 6.00 (d of d, 1H) 7.2-7.7 (m, 8H).

9-*i*-Propyl-9-methoxyfluorene (52).

^1H NMR δ 0.85 (d, J = 6 Hz, 6H) 2.48 (septet, J = 6 Hz, 2.84 (s, 3H) 7.2-7.7 (m, 8H)

9-*t*-Butyl-9-methoxyfluorene (54).

^1H NMR δ 0.92 (s, 9H) 2.76 (s, 3H) 7.1-7.7 (m, 8H).

9-Phenyl-9-methoxyfluorene (56).

^{1}H NMR δ 2.90 (s, 3H) 7.1-7.8 (m, 13H) [lit.[138] mp 91-94°C].

5-Methoxysuberane (5-methoxy-5*H*-dibenzo[a,d]cycloheptane) (58).

^{1}H nmr δ 3.30 (s, 3H) 2.7-3.7 (m, 4H) 5.20 (s, 1H) 7.1-7.5 (m, 8H); oil [lit.[139] bp 142-143.5°C (0.35 torr)]; mass spectrum (CI) (m/z) 225 (M^++1).

The photolysis of the 5-suberenols at pH > 7 led to recovery of the starting material. On extended photolysis of 5-suberenol (**5**), the ketone dibenzosuberone (**64**) was isolated and characterized by comparison with authentic material. For comparison purposes, the methyl ethers of **5** and **26** were prepared thermally, by stirring the alcohol for 1 h in methanol made acidic with a few drops of conc. H_2SO_4. The ^{1}H NMR data are presented below.

5-Methoxysuberene (5-methoxy-5*H*-dibenzo[a,d]cycloheptene) (63).

^{1}H NMR δ 3.3 (broad s, 3H) 4.85 (broad s, 1H) 7.00 (s, 2H) 7.1-7.7 (m, 8H).

5-Methoxy-5-methyl-suberene (5-methoxy-5-methyl-5*H*-dibenzo[a,d]cycloheptene) (66).

^{1}H NMR δ 1.6 (s, 3H) 3.36 (s, 3H) 7.00 (s, 2H) 7.2-8.0 (m, 8H).

The photolysis of 5-methyl-5-suberol (**24**) in 50% MeOH-H_2O produced no methyl ether product. The starting material was recovered even after extended photolysis (60 min). The methyl ether was solvolyzed thermally for comparison purposes and the data are presented below.

5-Methoxy-5-methyl-suberane (5-methoxy-5-methyl-5*H*-dibenzo[a,d]cycloheptane) (62).

^{1}H NMR δ 1.80 (s, 3H) 2.95 (s, 3H) 3.08 (s, 4H) 7.0-7.4 (m, 6H) 7.7-7.9 (m, 2H)

The hydrocarbon products that arose from the secondary photolysis of the methyl ethers were isolated and characterized by ^{1}H NMR, mass spectroscopy, and by comparison with authentic materials. This data is summarized below.

Fluorene (33).

^{1}H NMR δ 3.80 (s, 2H) 7.2-7.7 (m, 8H); mp 110-112°C [lit.[129] mp 112-115°C]; mass spectrum (EI) (m/z) 166 (M^+).

9-Methylfluorene (47).

^{1}H NMR δ 1.50 (d, J=6Hz, 3H), 3.92 (q, J=6 Hz, 1H) 7.2-7.8 (m, 8H) [lit.[140]].

9-Phenylfluorene (57).

^{1}H NMR δ 5.02 (s, 1H) 7.1-7.8 (m, 13 H) [lit.[141]].

The dimeric product 9,9'-bifluorene was observed in the photolysis of **1**, whereas the 9,9'-disubstituted-9,9'-bifluorene analogues for the various 9-substituted-9-fluorenols were not observed in sufficient quantity for full characterization.

9,9'-Bifluorene (34).

^{1}H NMR δ 4.78 (s, 2H) 6.8-7.6 (mult., 16 H) [lit.[142]]; mp 242-245°C.

5.4.1.4 Preparative Photolysis of 9-vinyl-9-fluorenol (13). In addition to 9-methoxy-9-vinyl fluorene, two other major products were identified. Their ^{1}H NMR data appear below.

Hydroxyethylidenefluorene (α-(hydroxymethyl)-dibenzofulvene) (48).

^{1}H NMR δ 2.3 (br.s, 1H) 4.85 (d, J=6 Hz, 2H) 6.72 (t, J=6 Hz, 1H) 7.2-7.7 (m, 8H)

Methoxyethylidenefluorene (α-(methoxymethyl)-dibenzofulvene) (50).

^{1}H NMR δ 3.40 (s, 3H) 4.62 (d, J=6 Hz, 2H) 6.76 (t, J=6 Hz, 1H) 7.2-7.7 (m, 8H)

5.4.1.5 Preparative Photolysis of 9-(trideuteriomethoxy)-fluorene (17-d_3). A solution of 50 mg of substrate was dissolved in 50 mL of MeOH and diluted with 100 mL of H_2O. After treating in the normal manner, the solution was photolyzed for 10 min at 254 nm. Recovery of the fluorene fraction from the photolysate was accomplished by preparative TLC (silica/CH_2Cl_2). Analysis of the 250 MHz ^{1}H NMR indicates that deuterium has been 100% incorporated; the partially resolved 1:1:1 triplet at δ 3.84, $J_{H\text{-}D}$ = 2 Hz, integrates as 1:8 with respect to the aromatic signal. This observation was confirmed by the mass spectral data.

9-Deuteriofluorene

^{1}H NMR δ 3.84 (t, J = 2 Hz, 1H) 7.2-7.7 (m, 8H); mass spectrum (EI) (m/z) 167 (M^+).

5.4.1.6 Preparative Photolysis of 1 with External Nucleophiles. A solution of 100 mg of substrate in 30 mL of ACN was diluted with 70 mL of a 0.5 **M** aq. NaCN

or NaBr solution. This was treated in the normal manner and photolyzed for times ranging from 2-60 mins at 254 nm. Neither the cyano or the bromo substituted fluorene derivatives were observed in these photolyses. Photolysis of 9-xanthenol (**39**) in the presence of NaCN under similar conditions produced two cyanide trapped products, which were isolated on preparative TLC (silica/CH_2Cl_2) and identified as 9-cyanoxanthene (**40**) and a ring substituted cyanoxanthene (**41**).

9-cyanoxanthene (40): ^{1}H NMR δ 5.3 (s, 1H) 7.1-7.5 (m, 8H); IR (cm^{-1}) 2225 (w); mass spectrum (CI) (m/z) 208 (M^++1).

41: ^{1}H NMR δ 4.20 (s, 2H) 7.0-7.5 (m, 7H); IR (cm^{-1}) 2200 (m); mass spectrum (CI) (m/z) 208 (M^++1).

5.4.1.7 Preparative Photosolvolysis of 1 in Other Alcohols. The same procedure was employed as in 50% MeOH-H_2O, the following ethers were isolated by preparative TLC (silica/CH_2Cl_2-hexanes) and characterized by their ^{1}H NMR, as follows:

9-Ethoxyfluorene

^{1}H NMR δ 1.13 (t, J=7 Hz, 3H) 3.25 (q, J=7 Hz, 2H) 5.58 (s, 1H) 7.2-7.7 (m, 8H); mp 50-52°C

9-(i-Propyloxy)fluorene

^{1}H NMR δ 1.18 (d, J=7 Hz, 6H) 3.80 (m, 1H) 5.56 (s, 1H) 7.2-7.8 (m, 8H); mp 101-104°C.

9-(t-Butyloxy)fluorene

^{1}H NMR δ 1.20 (s, 9H) 5.50 (s, 1H) 7.2-7.7 (m, 8H); mp 103-104°C.

5.4.1.8 Preparative Photolysis of 1 in pure ACN and CH_3OH. Photolysis of 100 mg of substrate in pure ACN for 30 min gave essentially 100% conversion to a mixture of products which were characterized by GC/MS and by the ^{1}H NMR of the photolysate mixture. The major products were separated by preparative TLC (silica/ CH_2Cl_2), and identified as follows:

9-Fluorenylacetonitrile (43); ^{1}H NMR δ 2.65 (d, J=7 Hz, 2H) 4.10 (t, J=7 Hz, 1H) 7.0-7.5 (m, 8H); IR (cm^{-1}) 2250 (m); mass spectrum (EI) (m/z) 205 (M^+)

N-(9-Fluorenyl)acetamide (44); ^{1}H NMR δ 1.78 (s, 3H) 7.0-7.5 (m, 8H); IR (cm^{-1}) at 1670; mass spectrum (EI) (m/z) 223 (M^+).

Photolysis of 100 mg of substrate in pure CH_3OH gave 9-fluorenylmethanol (**35**) in addition to the expected methyl ether product. It was identified by comparison of its ^{1}H NMR spectra and GC retention time with authentic material.

5.4.1.9 Preparative Photolysis of 11*H*-Benzo[b]fluorenol Derivatives. In a typical photolysis 50 mg of substrate was dissolved in 50 mL of MeOH and diluted with 50 mL of H_2O. (Due to its low solubility in aqueous solutions, 60% MeOH-H_2O was often employed in the preparatory photolysis of **20**). The solution was placed in a quartz tube fitted with a cold finger, (≈ 12 °C), and deaerated with a

continuous stream of argon. The solution was then irradiated at 254 nm. After photolysis, the solution was worked-up by saturating with NaCl followed by extraction with CH_2Cl_2 (2 x 100 mL). The identity and yields of the photosolyate products were determined by ^1H NMR and gas chromatography. Product mixtures were separated by preparative TLC. The ethers of **20** and **22** were characterized by ^1H NMR and mass spectroscopy, as presented below.

11-Methoxy-11*H*-benzo[b]fluorene (67).

^1H NMR δ 3.05 (s, 3H) 5.75 (s, 1H) 7.3-8.1 (m, 10H); mp 90-92°C; mass spectrum (EI) (m/z) 246 (M+).

11-Ethoxy-11*H*-benzo[b]fluorene

^1H NMR δ 1.18 (t, 3H) 3.35 (q, 2H) 5.85 (s, 1H) 7.2-8.1 (m, 10H).

11-n-Propyloxy-11*H*-benzo[b]fluorene

^1H NMR δ 0.90 (t, 3H) 1.56 (sextet, 2H) 3.20 (t, 2H) 5.85 (s, 1H) 7.2-8.1 (m, 10H).

11-i-Propyloxy-11*H*-benzo[b]fluorene

^1H NMR δ 1.24 (d, 6H) 3.94 (septet, 1H) 5.80 (s, 1H) 7.2-8.1 (m, 10H).

α-(Methoxy)-α-(phenyl)-2-methylnaphthalene (71).

^1H NMR δ 3.38 (s, 3H) 5.38 (s, 1H) 7.2-7.5 (m, 8H) 7.7-7.9 (m, 4H); mass spectrum (EI) (m/z) 248 (M+).

11-Methoxy-11-methylbenzo[b]fluorenol (72).

^1H NMR acetone-d_6 δ 1.68 (s, 3H) 2.68 (s, 3H) 7.3-8.2 (m, 10H).

5.4.1.10 Triplet sensitization experiments. The photolysis of 50 mg of 9-

fluorenol (**1**), ($E_T \approx 68$ kcal mol^{-1})[90] was carried out in 100 mL of 50% MeOH-H_2O in the presence of 3.0 g of sodium 4-acetylbenzene sulfonate ($E_T \approx 74$ kcal mol^{-1}).[90] The argon saturated solution was irradiated at 350 nm for 1 h and worked up by extracting with CH_2Cl_2 (5 x 100 mL) and backwashing the organic fraction with brine (1 x 300 mL). The ^1H NMR indicated that no methyl ether had formed. 9-Fluorenol (**1**) was also photolyzed in the presence of a triplet quencher, 5,6-dicarboxylate-1,3-cyclohexadiene ($E_T \approx 52$ kcal mol^{-1}).[90] An argon saturated 50% MeOH-H_2O solution containing 50 mg of **1** and 500 mg of the triplet quencher was adjusted to pH ≈ 6 with a NaOH stock solution and irradiated for 15 mins at 300 nm. The photolsylate was worked up in the usual manner except that CH_2Cl_2 was back washed with a saturated bicarbonate solution (2 x 100 mL). The products were analyzed by ^1H NMR spectroscopy.

Triplet sensitization experiments were also carried out for the photosolvolysis reaction of 11*H*-benzo[b]fluoren-11-ol (**20**) using 2-benzoyl benzoic acid. In these photolyses, 50 mg of substrate ($E_T \approx 57$ kcal mol^{-1})[90] was dissolved in 120 mL of MeOH and diluted with 80 mL of H_2O containing 2.5 g of **70** ($E_T \approx 69$ kcal mol^{-1})[90], adjusted to pH ≈ 8. The solution was purged with argon for 10 min and irradiated for 10 min at 350 nm through a Pyrex vessel. The ^1H NMR indicated 15% conversion to the methyl ether. A UV absorption spectrum of the substrate/sensitizer solution indicated that the substrate was absorbing some of the incident light, accounting for the small amount of methyl ether product. An earlier run using only 1.5 g of the sensitizer produced more of the methyl ether.

Thus, as the amount of sensitizer increased, the production of methyl ether decreased, indicative of competitive absorption by the substrate as opposed to energy transfer to the substrate triplet state.

5.4.1.11 GC scale product studies. Once preparative scale photolysis had been performed to identify and characterize photoproducts, GC scale studies were sometimes carried out to monitor time dependent product distributions or pH dependent product yields. In a typical GC scale reaction a stock solution of substrate was prepared in the appropriate organic solvent (usually ACN or MeOH). Then an aliquot of stock solution was transferred to a quartz UV cuvette and diluted with the appropriate amount of aqueous solution. The substrate concentrations were sufficient to give absorbances greater than 2 (ca. 5×10^{-4} - 5×10^{-5} **M**). The solutions were purged with a stream of argon for 10 min and then irradiated in a merry-go-round apparatus in an RPR 100 Rayonet Photochemical Reactor. For reactions in which a cloudy precipitate formed, the solutions were photolyzed individually on the optical bench with a continuous steam of argon to effect stirring. The reactions were worked up by transferring into 10 mL test tubes, saturating with NaCl, and extracting with CH_2Cl_2 (3 x 3 mL). The organic fractions were then dried over $MgSO_4$, and evaporated to ≈ 0.1 mL before being injected into a GC for analysis. The GC detector response was compared to ^1H NMR integrations after preparative scale photolysis. For more accurate quantitative work, standard solutions were employed to generate correction factors that were

applied to the integrated peak areas.

5.4.2 UV Absorption Studies. A number of photochemical reactions were followed by the change in the UV absorption spectrum. In these experiments, a few μL of an ACN stock solution of the substrate was injected in a UV quartz cuvette containing 3 mL of H_2O to yield solutions with absorbances between 0.5 - 1.0. After dearating the solution, a UV spectrum was recorded. The solution was then irradiated in a merry-go-round apparatus in a RPR 100 Rayonet Photochemical Reactor for an appropriate length of time (typically 10-60 sec) and the UV spectrum was recorded again. The spectra were overlaid and this was repeated until no further changes in the UV occurred.

5.4.3 Steady-State and Transient Fluorescence Behaviour. Fluorescence spectra were measured in 1.00 cm Suprasil quartz cuvettes at 10^{-5}-10^{-4} **M** after 10 min argon purging. Time-correlated single photon counting fluorescence lifetimes were measured at optical densities of 0.03-0.30 at the exciting wavelength (see appendix A). Fluorescence quantum yields (Φ_f) were determined by comparing the integrated corrected emission bands of the substrates with those of secondary standards according to equation 5.1.[143]

$$\Phi_f^u = \Phi_f^s\left(\frac{I_f^u\ \eta_u^2}{I_f^s\ \eta_s^2}\right) \qquad (5.1)$$

where I_f^u and I_f^s are the total fluorescence intensities of the unknown sample and a standard, and where η is the refractive index of the solvent. For these purposes each set of solutions was absorption matched with optical densities less than 0.1 at the exciting wavelength. Standards were choosen to maximize their spectral overlap with the emission bands of the various samples. Naphthalene was the standard of choice for α-(phenyl)-naphthalenemethanol whereas 2-aminopryridine provided a better overlap of the emission bands for benzo[b]fluorene chromophore. All solutions were purged with argon for at least 10 min prior to measurement.

5.4.4 Product Quantum Yields. Quantum yields for the methyl ether formation of **1**, **11**, **20**, and **22** at a number of different pH's and in neutral solution were measured on an optical bench at 280 nm (5 nm slit width). The quantum yields for methyl ether formation for the other 9-fluorenol derivatives were determined using either **1** or 2,6-dimethoxybenzyl alcohol[35] as secondary actinometers. Argon purged solutions (6.0×10^{-3} **M**) were photolyzed in quartz cuvettes in a merry-go-round apparatus at 254 nm in a Rayonet Photochemical Reactor and worked up by transferring the sample to a test tube, saturating with NaCl and extracting with CH_2Cl_2. The conversions were determined by GC. The GC analysis of **4** and **5** were complicated by a thermal decomposition on the column and so the product

quantum yields were estimated based on preparative scale reactions. ^{1}H NMR integrations were used to determine the extent of reaction and the reaction of **1** was employed as a secondary standard. For these purposes consecutive photolysis were carried out under identical conditions; conversions were kept below 25%. In a typical experiment, 0.50 mL of a stock solution of substrate in MeOH (4×10^{-3} **M**) was transferred to a quartz cuvette, diluted with 1.0 mL of MeOH followed by 1.5 mL of H_2O. The solutions were argon purged for 10 min prior to and during the photolysis (usually 1-20 min). Conversions were kept below 20% in all cases. After irradiation the photosolyate was transferred to a test tube, saturated with NaCl, and extracted with CH_2Cl_2 (3 x 3 mL). The organic fractions were separated using a pipette, and then dried over $MgSO_4$, filtered and evaporated to ca. 100 uL before being injected onto a capillary column (220 °C) for analysis. Control experiments indicated that material is not lost during the work-up procedures. Conversions were determined by the relative peak areas of ether and alcohol, using a Hewlett-Packard integrator. Conversions determined this way are in agreement with those obtained from integration of ^{1}H NMR signals. Light intensity measurements were determined by irradiating a 0.006 **M** aqueous solution of potassium ferrioxalate under identical conditions and working up according to the method of Hatchard and Parker,[144] (see appendix B).

5.5 PHOTODECARBOXYLATION

5.5.1 Product Studies.

5.5.1.1 Dark reactions. None of the compounds in this study underwent any decarboxylation in the dark under the conditions employed to study the photochemistry. Control experiments were performed by treating 50 mg of each substrate in exactly the same manner as the photolyzed samples except that they were stirred in the dark for one hour. The samples were analyzed by ^{1}H NMR after being worked-up in the normal way.

5.5.1.2 Relative reactivity in the ground state.

Thermal decarboxylation reactions were carried out by dissolving 50 mg of substrate in 30 mL of acetonitrile and diluting with 70 ml of 0.01 **M** aqueous NaOH. After stirring for one hour each solution was acidified and extracted with CH_2Cl_2. The product mixture was analyzed by ^{1}H NMR.

5.5.1.3 Preparative photolysis of 6 - 10 and 28 - 32 in ACN-H_2O mixtures. In a typical preparative study 100 mg of substrate was dissolved in 30 mL of acetonitrile and then diluted with 70 mL of H_2O. The solution was adjusted to a pH ≥ 8 with the aid of a pH meter, by adding dropwise a stock solution of ≈ 1 **M** NaOH. The solution was then transferred to a quartz vessel fitted with a cooling finger and deaerated with a continuous stream of argon. The solution was then irradiated at 254 nm (1,2-diphenylcyclopropene-3-carboxylic acid (**10**) irradiated at 300 nm). After photolysis the solution was worked up by saturating with NaCl,

acidifying to pH ≈ 1 with 10% HCl, and extracting with CH_2Cl_2 (2 x 100 mL). The photosolyate was analyzed by ^1H NMR and conversions determined by the integrated peak areas. These reactions were very clean giving rise to only one photoproduct. The photoproducts were separated from the carboxylic acid starting material by extracting the crude mixture with bicarbonate solution. The ^1H NMR and mass spectral data were compared with authentic materials.

5.5.1.4 Preparative photolysis of 6 - 9 ACN-D_2O mixtures. In a typical preparative study 50 mg of substrate was dissolved in 20 mL of ACN and diluted with 30 mL of D_2O. After adjusting the pD ≥ 8 with ≈ 1 **M** NaOD the solutions were photolyzed and worked-up in the usual manner. Conversions were determined by ^1H NMR integrations and the monodeuterated photoproducts were then isolated by extracting the crude mixture with a bicarbonate solution. The ^1H NMR and mass spectral data for the isolated monodeuterated products are presented below.

5-Deuterio-suberene (5-deuterio-5*H*-dibenzo[a,d]cycloheptene)

^1H NMR δ 3.73 (t, J=2 Hz, 1H) 7.02 (s, 2H) 7.1-7.5 (m, 8H); mass spectrum (EI) (m/z) 193 (M+).

5-Deuterio-suberane (5*H*-dibenzo[a,d]cycloheptane)

^1H NMR δ (t, J=2 Hz, 1H) (s, 4H) (m, 8H); mass spectrum (EI) (m/z) (197).

α-Deuterio-diphenylmethane

^1H NMR δ (t, J=2 Hz, 1H) (m, 10H); mass spectrum (EI) (m/z) (169).

9-deuterio-fluorene

1H NMR δ 3.80 (t, 2Hz, 1H), 7.2-7.7 (m, 8H).

5.5.1.5 Preparative photolysis of 6 - 9, 29 and 32 in oxygen saturated solution. Photolysis were carried out as before but under a continuous stream of oxygen instead of argon. The conversions were determined by analysis of the crude ^{1}H NMR signals. The ketone photoproducts were identified by comparison of their ^{1}H NMR and GC retention times with authentic materials. The ratio of ketone to hydrocarbon were determined by GC.

5.5.1.6 Preparative photolysis of 10. The preparative photolysis of 1,2-diphenyl cyclopropene-3-carboxylic acid (**10**) were carried out and worked up in the normal manner. Extended photolysis in 30% ACN-H_2O lead to new signals in ^{1}H NMR δ 6.6 (broad s) 6.7 (broad s). An attempted separation of the crude mixture gave only the α,β-unsaturated-γ-lactone (**79**), assigned on the following basis. ^{1}H NMR δ 6.31 (d, J = 1.5 Hz, 1H) 6.53 (d, J = 1.5 Hz, 1H) 7.2-7.4 (m, 10H); ^{13}C NMR δ (84.3, 114.7, 127.5, 127.8, 128.9, 129.1, 129.5, 129.8, 131.2, 135.0, 165.8, 172.4); IR (cm^{-1}) 1725; mass spectrum (CI) (m/z) 237 (M^+ +1); uv λ_{max} (CH_3OH) 274 nm [lit.[145]].

When 1,2-diphenylcyclopropene-3-carboxylic acid (**10**) was photolyzed in 100% ACN or 40% ACN-H_2O (pH ≈ 1), another product which was tentatively

assigned to the unconjugated γ-lactone (**80**) based on the ^{1}H NMR signal δ 3.8 (s). However, this compound also rearranged on attempted separation on silica gel to give **79**.

5.5.2 Steady-State and Transient Fluorescence Behaviour. Fluorescence quantum yields were measured on a PTI LS-1 instrument using equation 5.1 and the procedure outlined in section 5.4.3. Benzene was employed for diphenylacetic acid (**7**) and 5-suberane carboxylic acid (**8**); 2-amniopyridine was employed for compounds with the suberene chromophore (**9, 28 - 31**); and fluorene was used for substrates with the fluorene chromophore (**6, 32**). Solutions were absorbance matched at optical densities less than 0.1 and deaerated with argon for 10 min prior to measurement. Fluorescence lifetimes were measured using time correlated single photon counting, (see appendix A). Solutions (O.D. < 0.3) were deaerated with argon before measurement.

5.5.3 Product Quantum Yields. Quantum yields for formation of the hydrocarbons for **6**, **9** and **28 - 30** were measured in a number of solvents on an optical bench (λ_{ex} = 280 nm). In a typical experiment, 0.6 mL of a stock solution of substrate in ACN (6 x 10^{-3} **M**) was transferred to a quartz cuvette and diluted with 2.4 mL of H_2O (pH 7 buffer). The solutions were purged with a stream of argon for 10 min prior to and during the photolysis (usually 1-20 mins). Conversions were kept below 10% in all cases. After irradiation the photolysate

was transferred to a test tube, saturated with NaCl, and extracted with CH_2Cl_2 (3 x 3 mL). The organic fractions were then extracted with a saturated $NaHCO_3$ solution (1 x 5 mL), separated by pipette, dried over $MgSO_4$ and filtered. Each solution was then injected with 50 μL of a stock solution of 9-fluorenol (**1**) (3.01 x 10^{-2} **M**) and evaporated to ca. 100 μL before being injected onto to a capillary column (180°C) for analysis. The number of moles of product was determined by comparing integrated peak areas employing a correction factor to compensate for the GC detector response. Correction factors were generated by injecting solutions of the authentic photoproduct and 9-fluorenol (**1**) in known molar ratios and checking the response. Light intensity measurements were determined by irradiating a 0.006 **M** aqueous solution of potassium ferrioxalate under identical conditions and working up according to the method of Hatchard and Parker,[144] (see appendix B). Quantum yield determinations for **7** and **8** were determined at 254 nm in the Rayonet reactor using a merry-go-round apparatus and 9-fluorene carboxylic acid (**6**) as a secondary standard (Φ_p = 0.045). In a typical experiment, 0.6 mL of a stock solution of substrate in acetonitrile (ca. 4 x 10^{-2} **M**), was transferred into a quartz cuvette and diluted with 2.4 mL of H_2O (pH 7 buffer). Each solution was purged with a stream of argon for 10 min prior to photolysis, and placed in a merry-go-round. Solutions were irradiated at 30 sec intervals to allow for manual agitation (usual total irradiation time 2 - 10 min). Solutions were worked up and products analyzed as before. Quantum yields were also determined at various pH's using buffer solutions. Quantum yield determinations

in D_2O were basicified with 10 - 80 μL of a ≈ 0.1 **M** NaOD stock solution.

APPENDIX A

SINGLE PHOTON COUNTING EQUIPMENT

Fluorescence lifetimes were measured using a technique known as time correlated single photon counting (SPC). This method measures the time delay between the absorption and and emission of individual photons in a fluorescent sample. This measurement can be repeated up to 1000 s^{-1} and each event can be temporally sorted and counted in the form of a histogram. The lifetimes reported in this thesis were recorded at one of the three locations as outlined in section 5.1. The key components of a SPC instrument are shown in Figure A-1. It consists of a pulsed excitation light source, a start photomultiplier tube (PMT), a stop PMT, a time-to-amplitude converter (TAC), and a multichannel analyzer (MCA). The start pulse triggers the TAC to initiate a time sweep that is terminated by the arrival of the *first* photon to reach the stop PMT. In this way the amplitude of the TAC output is proportional to the time delay between the start and stop pulse. Both the start and the stop pulses are fed to discriminators and must be suitably delayed by a delay generator before reaching the TAC. It is a fundamental assumption in the SPC method that no more than one stop pulse arrives during the sweep of the TAC. Because the TAC detects only the first stop signal, longer time data will be lost and the observed decay will be inherently biased towards shorter times. This problem is known as pile-up and leads to non exponential decay functions. Pile up can be avoided if less than 5% of start pulses result in generating a stop pulse.[89] Since the LS-1 hydrogen spark lamp flashes

with a frequency of ca. 20 kHz, counting rates of up to 1000 per second can be tolerated without pile up distortions.

The output from the TAC is fed to the MCA which acts as a pulse height analyzer. In this mode each of the 512 channels of the MCA corresponds to an certain time interval, Δt (in nanoseconds). Each TAC pulse is then sorted according to height and counted in the appropriate channel. In this fashion a histogram is built up which corresponds to the observed decay curve. The bias level control on the TAC may be used as a zero shift. The TAC is calibrated by replacing the start and stop signals with lines from a time calibrator. These signals appear on the MCA as spikes with a time period (p) determined by the settings on the time calibrator. The width of each channel (Δt) in the MCA is given by the time separation between two spikes (np, where n is the number of period intervals) divided by the number channels separating the first and last spike.

The lifetime data was typically collected until there were 6000 counts in the channel with the maximum counts. The LS-1 SPC instrument also records the temporal distribution of the instrument (governed largely by the lamp profile) known as the instrument response function (IRF). Both the observed decay and the IRF are downloaded and stored on a microcomputer (NEC 8086 processor). The true decay function can be extracted from the above data by an iterative reconvolution procedure. Initial parameters are input as guesses and in a least squares fitting routine each parameter is varied in order to minimize χ^2. The iterative process is self terminating when further variation in the parameters no longer improves the

fit.

All of the instruments employed to measure the fluorescence lifetimes presented in this thesis employed the same principles of operation . They differed only in the manner in which the pulsed excitation light source was generated. The pulse width at half height (HHPW) largely determines the instrument response function (IRF) which in turn affects the detection limit of that particular single photon counter. The pulsed laser excitation source available at the Centre for Fast Kinetics Research had a HHPW of ca. 300 ps at optimum performance. Lifetimes could be readily measured down to 0.50 ns with accuracy and a reproducibility of ±5%. Experimental lifetimes down to 0.10 ns could be reproducibly deconvoluted from the observed sample decay curves with somewhat larger errors of uncertainty. The thyratron hydrogen flash lamp used in the other SPC instruments operates by supplying a high voltage (8 kV) between two tungsten electrodes in a hydrogen filled cavity. Using an electrode gap of 2-3 mm and a gas pressure of 11-13 inches of Hg, the HHPW could be optimized at 1.6-1.8 ns. With this set-up, lifetimes can be routinely measured down to 1 ns and reasonably estimated in the 0.5-1.0 ns range.

The instrument response function (also referred to as the lamp profile) was collected by placing a scatter in the sample beam and recording the temporal data as one would for an emitting sample (i.e., at emission wavelength). Diffuse glass or similar material can be used to scatter the light beam, but a dilute suspension

of milk in distilled water was most convenient. The LS-1 SPC automatically alternates between the sample and scattering solutions during the course of the data acquisition. The concentration of the scattering solution was adjusted to give approximately the same number of stop counts per second. In this way, the observed decay curves and the instrument response function are collected over similar periods of time. Furthermore, since the instrument response function was acquired intermittently over the period of sample collection, any temporal drift in the lamp and/or optical components, will be recorded in the IRF.

Occasionally, scattered light from the sample chamber reached the stop PMT giving rise to poor calculated fits, particularly over the rising edge and early portions of the observed decay curve. The scattered excitation light has the same temporal distribution as the IRF and often appears to contribute a fast decay portion to a non-exponential fit. This source of error was generally not a problem, but does occur for weakly emitting species which are not significantly Stoke's shifted, (i.e., derivatives of diphenylmethane and dibenzosuberane in the present study). This is because the data is collected at the maximum slit width with the excitation and emission wavelengths only marginally separated. To deal with this problem, the separation between the excitation and emission monochromator settings were maximized. Cut-off filters in the emission beam were also employed to eliminate the detection of scattered light.

Having generated the best fit parameters, the quality of the calculated curve can be judged by a number of means. Invariably a combination of visual and

mathematical methods provide the safest and most reliable technique. A visual comparison of the calculated and observed decay curves provides an immediate, if only cursory, means of evaluation. In addition this comparison often suggests possible sources of error either of instrumental, (i.e., radio frequency noise) or sample origin, (i.e., impurity). Another method involves the examination of the weighted residual and autocorrelation functions. Both of these functions are displayed on the output from the LS-1 SPC. The evolution of the weighted residuals with time displays the discrepancies between the calculated best fit, F(t), and the observed decay data, D(t) by the following relation,[89]

$$R_{wi} = w_i R_i = \frac{R_i}{\sigma_i^2} = \frac{R_i}{D(t_i)} \qquad \text{(A-1)}$$

where,

$$R_i = F(t_i) - D(t_i) \qquad \text{(A-2)}$$

The w_i and σ_i are the normal weighting factors and standard deviations of the ith point and $\sigma_i = D(t)^{1/2}$ since SPC data obey Poisson statistics.[89] A good best fit curve should display randomly distributed residuals. The autocorrelation function is also used to evaluate the calculated curve, (eq A-3). For random noise, $C(t_j)$ will be randomly distributed.

$$C(t_j) = \frac{\frac{1}{m}\sum_{i=1}^{m} R_i R_{i+j}}{\frac{1}{N}\sum_{i=1}^{N} R_i^2} \qquad \text{(A-3)}$$

The most common mathematical test involves the use of chi-squared, χ^2, which is calculated according to equation A-4.[89] The reduced chi-squared, $\chi_r^2=\chi^2/\upsilon$, where υ is the number of degrees of freedom in fitting N points with P parameters. If the calculated function is correct, the value of χ_r^2 tends towards unity. The experimental reduced chi-squared values are reported as part of the normal output from the LS-1 SPC. These numbers can be evaluated by comparison to probability tables[89] to test for the statistical likelihood that a value exceeding this quantity would occur. The SPC data is typically collected over 512 channels and analyzed over approximately 400 data points. With this information in hand, there is less than a 5% chance that a value of χ_r^2 will exceed 1.2. Thus a calculated fit that yields a value of $\chi_r^2 > 1.2$ is suspect. Data that could not be fit to better than $\chi_r^2 < 1.4$ were automatically rejected.

$$\chi^2 = \sum_{I=1}^{N} w_I R_I^2 \qquad \text{(A-4)}$$

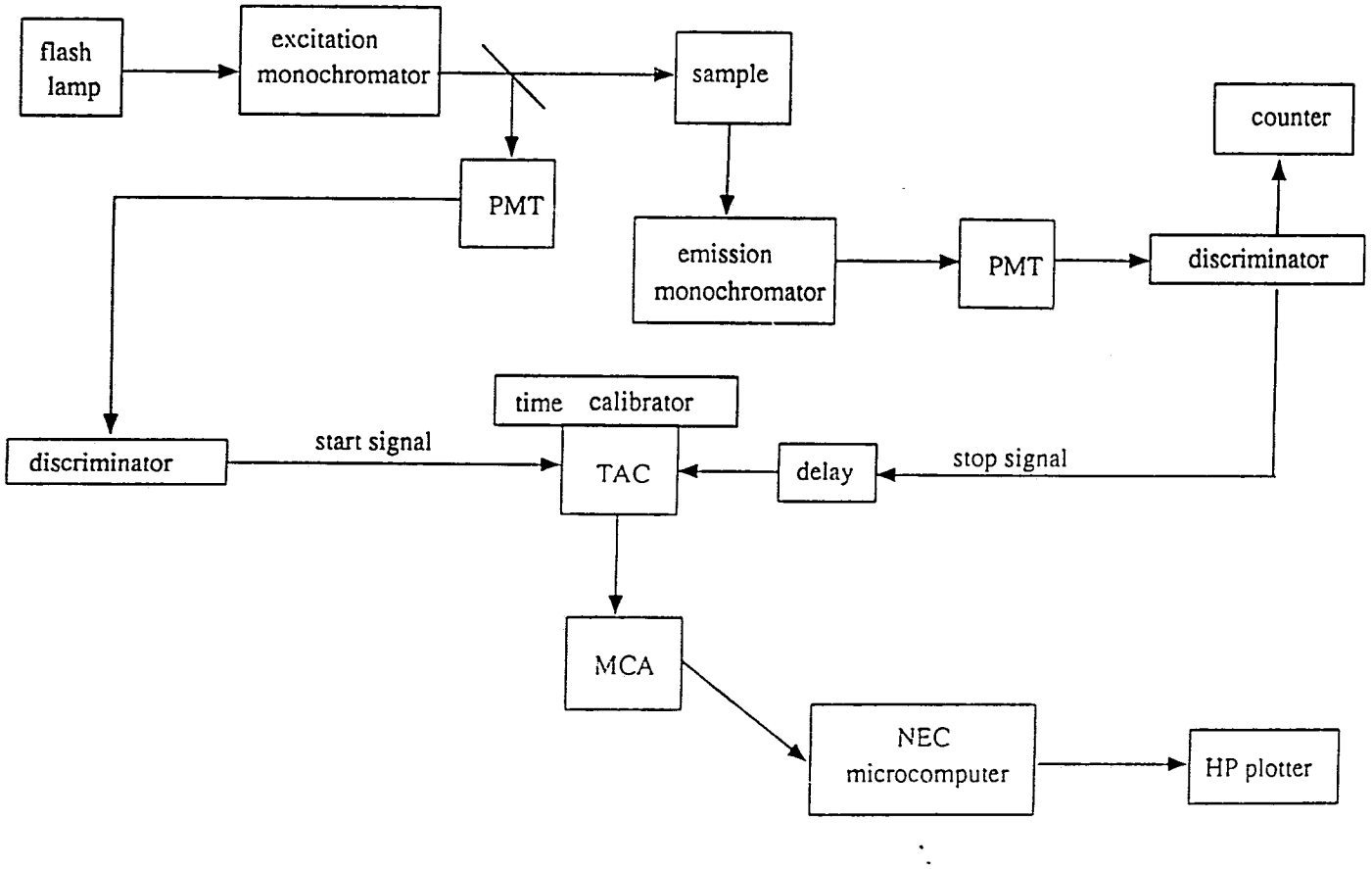

Figure A-1: Block Diagram of the LS-1 Time Correlated Single Photon Counter.

APPENDIX B

LIGHT INTENSITY MEASUREMENTS

The solution phase chemical actinometer based on the reaction of potassium ferrioxalate was developed by Parker and Hatchard.[144] This system was used in this thesis to measure the number of incident photons during the product quantum yield determinations.

When solutions of $K_3Fe(C_2O_4)_3$ in dilute sulfuric acid are irradiated, the iron is efficiently reduced to Fe^{2+} with the simultaneous oxidation of an oxalate ion. Quantum yields for this reaction range from 1.25 to 0.90 over the wavelength range 250 - 500 nm and have been accurately determined at a number of excitation wavelengths.[144] The relatively small dependence of these quantum yields on reactant and product concentration, intensity of the incident light, and temperature make this an convenient actinometer system. The product ferrous ion is transparent to the incident radiation and is analyzed by forming the highly coloured $Fe(phen)_3^{2+}$ complex (where phen = 1,10-phenanthroline) in a work up procedure.

Solutions of 0.006 **M** $K_3Fe(C_2O_4)_3$ in 0.1 **N** are made up from the solid in the absence of light and stored in the dark. All subsequent solution transfers are carried out under a red photographic safelight. To determine the light intensity of a given photochemical irradiation, 3.0 mL (V_1) of the stock solution was pipetted into two uv cuvettes. One of these was photolyzed for the appropriate time (Δt was typically 5.0 min at 280 nm) under a stream of argon which served to stir and

purge the solution. The other cell was handled under the safelight for the same length of time and serves as a blank. Both solutions are worked-up as follows, 1.0 mL (V_2) was pipetted from the cuvette into a 10 mL (V_3) volumetric flask. To this was added 2.0 mL of a 0.1% (weight) solution of 1,10-phenanthroline in water and 0.5 mL of a buffer solution (prepared from 41.0 g $NaOAc{\cdot}3H_2O$ and 5 mL H_2SO_4 in 1 L). The volume was adjusted to 10.0 mL with distilled water and the solutions were mixed and let stand for one hour. The absorbance of the irradiated and blank solutions was then monitored at 510 nm and the difference (ΔA) was used in equation B-1 to calculate the number of einsteins of incident light (where $\varepsilon = 1.11 \times 10^4$ and $\Phi_{Fe2+} = 1.25$ at 280 nm).[144] Since all photolysis were carried out on 3.0 mL of solution, the light intensity was calculated per cuvette per min. The absorbance of the blank (Abs < 0.05) was used to check the quality of the stock solution with respect to photodecomposition.

$$\textit{einsteins/cuvette/min} = \frac{\Delta A \; V_1 \; V_3}{\varepsilon \; \Phi_{Fe^{2+}} \; V_2 \; \Delta t} \qquad \text{B-1}$$

1. Maslak, P.; Narvaez, J.N., *Angew. Chem. Int. Ed. Engl.*, **1990**, 29, 283.

2. Turro, N.J., "Modern Molecular Photochemistry", Benjamin/Cumming, Menlo Park, 1978.

3. Neckers, D.C., "Mechanistic Organic Photochemistry", Reinhold, New York, 1970.

4. Coyle, J.D., "Introduction to Organic Photochemistry", Wiley, New York, 1986.

5. Balzani, V.; Carassiti, V., "Photochemistry of Coordination Compounds", Academic Press, New York, 1970, part II.

6. Streitwieser, A. Jr., "Solvolytic Displacement Reactions", McGraw-Hill Book Co., New York, 1962, p. 42.

7. Lifschitz, J., *Ber.*, **1919**, 52, 1919 as cited in ref 9.

8. Holmes, E.O., *J. Phys. Chem.*, **1958**, 62, 884.

9. Cristol, S.J.; Bindel, T.H. in "Organic Photochemistry"; Padwa, A., Ed.; Marcel Dekker, New York, 1983, Vol. 6, pp. 327-415.

10. Kropp, P.J.; Jones, T.H.; Poindexter, G.S., *J. Am. Chem. Soc.*, **1973**, 95, 5420.

11. Kropp, P.J., *Acc. Chem. Res.*, **1984**, 17, 131.

12. Jaeger, D.A., *J. Am. Chem. Soc.*, **1976**, 98, 6401.

13. Cristol, S.J.; Mahfuza, B.A.; Sankar, I.V., *J. Am. Chem. Soc.*, **1989**, 111, 8207 and references cited therein.

14. Morrison, H., *Rev. Chem. Intermed.*, **1987**, 8, 125 and references cited therein.

15. Sonawane, H.R.; Sethi, S.C.; Merchant, S.N., *Indian J. Chem., Sect. B*, **1984**, 23B, 934.

16. Chow, Y.L.; Marciniak, B.; Misbra, P., *J. Org. Chem.*, **1984**, 49, 1457.

17. Zimmerman, H.E.; Sandel, V.R., *J. Am. Chem. Soc.*, **1963**, 85, 915.

18. Zimmerman, H.E.; Somasekhara, S., *J. Am. Chem. Soc.*, **1963**, 85, 922.

19. Cristol, S.J.; Schloemer, G.C., *J. Am. Chem. Soc.*, **1972**, 94, 5916.

20. Lillis, V.; McKenna, J.; McKenna, J.M.; Smith, M.J.; Taylor, P.S.; Williams, J.H., *J. Chem. Soc., Perkin II*, **1980**, 83.

21. Jaeger, D.A.; Angelos, G.H., *Tetrahedron Lett.*, **1981**, 803.

22. Ivanov, V.B.; Ivanov, V.L.; Kuz'min, U.G., *Mol. Photochem.*, **1974**, 6, 125 and references cited therein.

23. McClelland, R.A.; Banait, N.; Steenken, S., *J. Am. Chem. Soc.*, **1986**, 108, 7023.

24. a) McClelland, R.A.; Kanagasabapathy, V.M.; Steenken, S., *J. Am. Chem. Soc.*, **1988**, 110, 6913.

    b) McClelland, R.A.; Kanagasabapathy, V.M.; Banait, N.; Steenken, S., *ibid*, **1989**, 111, 3966.

25. McClelland, R.A.; Banait, N.; Steenken S., *J. Am. Chem. Soc.*, **1989**, 111, 2929.

26. McClelland, R.A.; Mathivanan, N.; Steenken, S., *J. Am. Chem. Soc.*, **1990**, 112, 4857.

27. Mecklenburg, S.L.; Hilinski, E.F., *J. Am. Chem. Soc.*, **1989**, 111, 5471.

28. Gaillard, B.; Fox, M.A.; Wan, P., *J. Am. Chem. Soc.*, **1989**, 111, 2180.

29. Manning, L.E.; Peters, K.S., *J. Phys. Chem.*, **1984**, 88, 3516.

30. Appleton, D.C.; Bull, D.C.; Givens, R.S.; Lillis, V.; McKenna, J.; McKenna, J.M.; Thackery, S.; Walley, A.R., *J. Chem. Soc., Perkin II*, **1980**, 77.

31. Lin, C.I.; Singh, P.; Ullman, E.F., *J. Am. Chem. Soc.*, **1976**, 98, 6711.

32. Turro, N.J.; Wan, P., *J. Photochem.*, **1985**, 28, 93.

33. Wan, P.; Yates, K.; Boyd, M., *J. Org. Chem.*, **1985**, 50, 2881.

34. Wan, P., *J. Org. Chem.*, **1985**, 50, 2583.

35. Wan,P.; Chak, B., *J. Chem Soc. Perkin Trans 2*, **1986**, 1751.

36. Wan, P.; Chak, B., Krogh, E., *J. Photochem. Photobiol., A:Chem.*, **1989**, 46, 49.

37. Irie, M., *J. Am.Chem. Soc.*, **1983**, 105, 2078.

38. Hall, B.; Wan, P., *J. Photochem. Photobiol. A*, in press.

39. Turro, N.J.; McVey, J.; Ramamurthy, V.; Lechten, P., *Angew. Chem., Int. Ed. Engl.*, **1979**, 18, 572.

40. Minto, R.E.; Das, P.K., *J. Am. Chem. Soc.* **1989**, 111, 8858.

41. Wan, P. personal communication.

42. Cowell, G.W.; Ledwith, A., *J. Chem. Soc. B.*, **1967**, 695.

    Cowell, G.W.; Ledwith, A.; Morrie, D.G., *J. Chem Soc. B.*, **1967**, 697 and 700.

43. Wan, P.; Krogh, E., *J. Chem. Soc. Chem. Comm.*, **1985**, 1207.

44. For a discussion of aromaticity see; Garratt, P.J. "Aromaticity", McGraw-Hill, London, 1971.

45. Strietwieser, A. Jr., "Molecular Orbital Theory for Organic Chemists", Wiley, New York, 1961, pp. 256.

46. Yates, K., "Hückel Molecular Orbital Theory", Academic Press, New York, 1978.

47. Bally, T.; Masamune, S., *Tetrahedron*, **1980**, 36, 343.

48. Jones, A.J., *Rev. Pure Appl. Chem.*, **1968**, 18, 253.

49. Breslow, R., *Acc. Chem. Res.*, **1973**, 6, 393.

50. Olah, G.A.; Schleyer, P.V.R., "Carbonium Ions", Wiley, New York, 1973, Vol. 4.

51. March, J., "Advanced Organic Chemistry", Wiley Eastern Ltd., New Delhi, 1985, pp. 37-64.

52. Lloyd, D., "Non-Benzenoid Conjugated Carbocyclic Compounds", Elsevier, Amsterdam, 1984.

53. Breslow, R., *Top. Nonbenzenoid Arom. Chem.*, **1973**, 1, 81.

54. Breslow, R.; Mazur, S., *J. Am. Chem. Soc.*, **1973**, 95, 584.

55. Woodward, R.B.; Hoffmann, R., "The Conservation of Orbital Symmetry", Verlag-Chemie, Weinheim, 1970.

56. Zimmerman, H.E., *Acc. Chem. Res.*, **1971**, 4, 272.

57. Dewar, M.J.S., *Angew. Chem., Int. Ed. Engl.*, **1971**, 10, 761.

58. Frater, F.; Monev, V.; Janoschek, R., *Tetrahedron*, **1982**, 38, 2929.

59. Nanda, D.N.; Jug, K., *Theor. Chim. Acta*, **1980**, 57, 95.

60. Malar, E.J.P.; Jug, K., *J. Phys. Chem.*, **1984**, 88, 3508.

61. Malar, E.J.P.; Jug, K.; *Tetrahedron*, **1986**, 42, 417.

62. Chak, B.; Dingle, T.; Wan, P., unpublished results.

63. Jug, K., *J. Org. Chem.*, **1983**, 48, 1344.

64. a) Wan, P.; Muralidharan, S., *J. Am. Chem. Soc.* **1988**, 110, 4336.

    b) Wan, P.; Muralidharan, S., *Can. J. Chem.*, **1986**, 64, 1949.

65. McAuley, I.; Krogh, E.; Wan, P., *J. Am. Chem. Soc.*, **1988**, 110, 600.

66. Krogh, E.; Wan, P., *Tetrahedron Lett.*, **1986**, 27, 823.

67. Stowell, J.C., "Carbanions in Organic Synthesis", Wiley, New York, 1979.

68. Hanson, R.W., *J. Chem. Ed.*, **1987**, 64, 591.

69. Artamkina, G.A.; Beletskaya, I.P., *Russ. Chem. Rev.*, **1987**, 56, 983.

70. Toussaini, O.; Capdeville, P.; Maumy, M., *Tetrahedron*, **1984**, 40, 3229.

71. Kuhn, H.J.; Görner, H., *J. Phys. Chem.*, **1988**, 92, 6208.

72. Closs, G.L.; Miller, R.J., *J. Am. Chem. Soc.*, **1978**, 100, 3483.

73. Davidson, R.S.; Goodwin, D.; Pratt, J.E., *J. Chem. Soc. Perkin Trans II*, **1983**, 1729.

74. Sawaki, Y.; Ogata, Y., *J. Am. Chem. Soc.*, **1981**, 103, 6455.

75. Okada, K.; Okamota, K.; Oda, M., *J. Am. Chem. Soc.*, **1988**, 110, 8736.

76. Ahmad, I.; Tollin, G., *Photochem. Photobiol.*, **1981**, 34, 441.

77. Margerum, J.D.; Petrusis, C.T., *J. Am. Chem. Soc.*, **1969**, 91, 2467.

78. Stermitz, F.R.; Huang, W.H., *J. Am. Chem. Soc.*, **1971**, 93, 3427.

79. Epling, G.A.; Lopes, A., *J. Am. Chem. Soc.*, **1977**, 99, 2700.

80. Craig, B.B.; Weiss, R.G.; Atherton, S.J., *J. Phys. Chem.*, **1987**, 91, 5906.

81. Givens, R.S.; Matuszewski, B.; Levi, N.; Leung D., *J. Am. Chem. Soc.*, **1977**, 99, 1896.

82. Meiggs, T.D.; Grossweiner, L.I.; Miller, S.I., *J. Am. Chem. Soc.*, **1972**, 94, 7981.

83. Steenken, S.; Warren, C.J.; Gilbert, B.G., *J. Chem. Soc. Perkin Trans 2*, **1990**, 335.

84. See for example:

Costanzo, L.L.; Guidi, G.De; Condorelli, G.; Cambria, A.; Fama, M., *Photochem. Photobiol.*, **1989**, 50, 359.

Castell, J.V.; Gomez-L, M.J.; Miranda, M.A.; Morera, I.M., *Photochem. Photobiol.*, **1987**, 46, 991.

85. See ref. 2, p. 105.

86. See ref. 2, p. 92.

87. Wayne, R.P., "Principles and Applications of Photochemistry", Oxford University Press, Oxford, 1988.

88. Werner, T.C., "Modern Fluorescence Spectroscopy"; Wehry, E.L., Ed., Plenum Press, New York, 1976, Vol. 2, Chap. 7.

89. Demas, J.N., "Excited State Lifetime Measurements", Academic Press, New York, 1983.

90. Murov, S.L. "Handbook of Photochemistry", Marcel Dekker, New York, 1973

91. Wan, P. unpublished result.

92. Tomioka, H.; Nakamura, H.; Izawa, Y., *J. Chem. Soc., Chem. Commun.*, **1983**, 1070.

93. Burr, J.G., *J. Am. Chem. Soc.*, **1952**, 74, 1717.

94. Mende, U.; Laseter, J.L.; Griffin, G.W., *Tetrahedron Lett.*, **1970**, 3747.

95. Wan, P.; Krogh, E., *J. Am. Chem. Soc.*, **1989**, 111, 4887.

96. Wan, P.; Budac, D.; Krogh, E., *J. Chem. Soc.,Chem. Commun.*, **1989**, 255.

97. Wan, P.; Krogh, E.; Chak, B., *J. Am. Chem. Soc.*, **1988**, 110, 4073.

98. Wan, P.; Budac, D.; Earle, M.; Shukla, D., *J. Am. Chem. Soc.*, **1990**, 112, 8048.

99. Berlman, I.B.; "Handbook of Fluorescence Spectra of Aromatic Compounds", Academic Press, New York, 1971.

100. Olah, G.A.; Prakash, G.K.S.; Liang, G.; Westerman, P.W.; Kunde, K.; Chandrasekhar, J.; Schleyer, P.V.R., *J. Am. Chem. Soc.*, **1980**, 102, 4485.

101. Wan,P.; Xu, X., *Tetrahedron Lett.*, **1990**, 31, 2809.

102. Xu, X., M.Sc. Thesis, University of Victoria, 1990.

103. Ritchie, C.D., *Acc. Chem. Res.*, **1972**, 5, 348.

104. Meot-Ner, M., *J. Am. Chem. Soc.*, **1986**, 108, 6189.

105. Anderson, S.W.; Yates, K., *Can. J. Chem.*, **1988**, 66, 2412.

106. Weast, R.C., (Ed.), "Handbook of Chemistry and Physics", 64th Ed., CRC Press, Boca Raton, 1983.

107. Bethell, D.; Gold, V., "Carbonium Ions", Academic Press, London, 1967.

108. Feldman, M.R.; Thame, N.G., *J. Org. Chem.*, **1979**, 44, 1863.

109. Deno, N.C.; Jaruzelski, J.J.; Schriesheim, A., *J. Org. Chem.*, **1954**, 19, 155.

110. Olah, G.A.; Prakash, G.K.S.; Liang, G.; Westerman, P.W.; Kunde, K.; Chandrasekhar, J.; Schleyer, P.V.R., *J. Am. Chem. Soc.*, **1980**, 102, 4485.

111. Shukla, D., unpublished result.

112. Freedman, H.H. in "Carbonium Ions, Vol IV"; Olah, G.A. and Schleyer, P.v.R., Ed; Wiley, New York, 1973, pp. 1501.

113. Weller, A., Progr. React. Kinet., **1961**, 1, 188.

114. Ireland, J.F.; Wyatt, P.A.H., *Adv. Phys. Org. Chem.*, **1976**, 12, 131.

115. Guthrie, R.D., "Comprehensive Carbanion Chemistry", Buncel, E.; Durst, T. (Eds.), Elsevier, New York, 1980.

116. Coyle, J.D. *Chem. Rev.*, **1978**, 78, 97.

117. Hilinski, E., personal communication.

118. Lowry, T.H.; Richardson, K.S., "Mechanism and Theory in Organic Chemistry", Harper and Row, New York, 1987.

119. Fox, M.A., *Chem. Rev.*, **1979**, 79, 253.

120. Streitwiesser, A.Jr.; Brown, S.M., *J. Org. Chem.*, **1988** 53, 904.

121. Hock, H.; Ernst, H., *Chem. Abs.*, **1960**, 54, 54216.

122. Breslow, R.; Winter, R.; Battistle, M., *J. Org. Chem.*, **1959**, 24, 415.

123. Kliegel, A., *Ber.*, **1929**, 62, 1327.

124. Kice, J.L., *J. Am. Chem. Soc.*, **1958**, 80, 348.

125. Arcus, C.L.; Lucken, E.A., *J. Chem. Soc.*, **1955**, 1634.

126. Stiles, M.; Sisti, A.J., *J. Org. Chem.*, **1961**, 26, 3639.

127. Dictionary of Organic Compounds, 5th ed., Chapman and Hall, New York, 1982.

128. Hennion, G.F.; Fleck, B.R., *J. Am. Chem. Soc.*, **1955**, 77, 3253.

129. Aldrich Catalog Handbook of Fine Chemicals, 1988-89, Aldrich Chemical Company, Milwauke, 1988.

130. Lamanec, T.R.; Bender, D.R.; DeMarco, A.M.; Karady, S; Reamer, R.A.; Weinstock, L.M., *J. Org. Chem.*, **1988**, 53, 1768.

131. Friedrich, E.C.; Taggart, D.B., *J. Org. Chem.*, **1975**, 40, 720.

132. Wieland, H.; Krause, E., *Ann.*, **1925**, 443, 129.

133. Maitland, P.; Tucker, S.H., *J. Chem. Soc.*, **1929**, 2559.

134. Blum, J.; Ashenasy, M.; Pickholtz, Y., *Synthesis*, **1974**, 352.

135. Badder, F.G.; Fleitel, A.M.; Sherif, S., *J. Chem. Soc.*, **1959**, 1009.

136. Streitwieser, A.Jr.; Hammons, J.H.; Cuiffarin, E.; Brauman, J.I., *J. Am. Chem. Soc.*, **1967**, 89, 59.

137. Osman, A.M., Badr, M.Z.A.; Aly, M.M.; El-Sherief, H.A.H., *J. Appl. Chem. Biotechnol.*, **1974**, 24, 319.

138. Bassolier, J.J.; Caumartin, F.; LeRoux, J.P.; Cherton, J.C., *Bull. Soc. Chim. Fr.*, **1974**, 12, 2935.

139. Seidlova, V.; Protiva, M.; *Coll. Czech. Chem. Comm.*, **1967**, 32, 2826.

140. Ohashi, M.; Furukawa, Y.; Tsujimoto, K., *J. Chem. Soc., Perkin Trans 1*, **1980**, 2613.

141. Mathieu, A., *Bull. Chem. Soc. Fr.*, **1971**, 1540.

142. Minabe, M.; Suzuki, K., *J. Org. Chem.*, **1975**, 40, 1298.

143. Eaton, D.F., *Pure Appl. Chem.*, **1988**, 60, 1107.

144. Hatchard, C.G.; Parker, C.A., *Proc. R. Soc. (London)*, **1958**, A235, 518.

145. Krauser, S.F.; Watterson, A.C.Jr., *J. Org. Chem.*, **1978**, 43, 3400.